frontiers | Research Topics

Treatment of brain metastases from non-small cell lung cancer: preclinical, clinical, and translational research

Edited by
Lin Zhou, Jianxin Xue and Lei Deng

Published in
Frontiers in Oncology

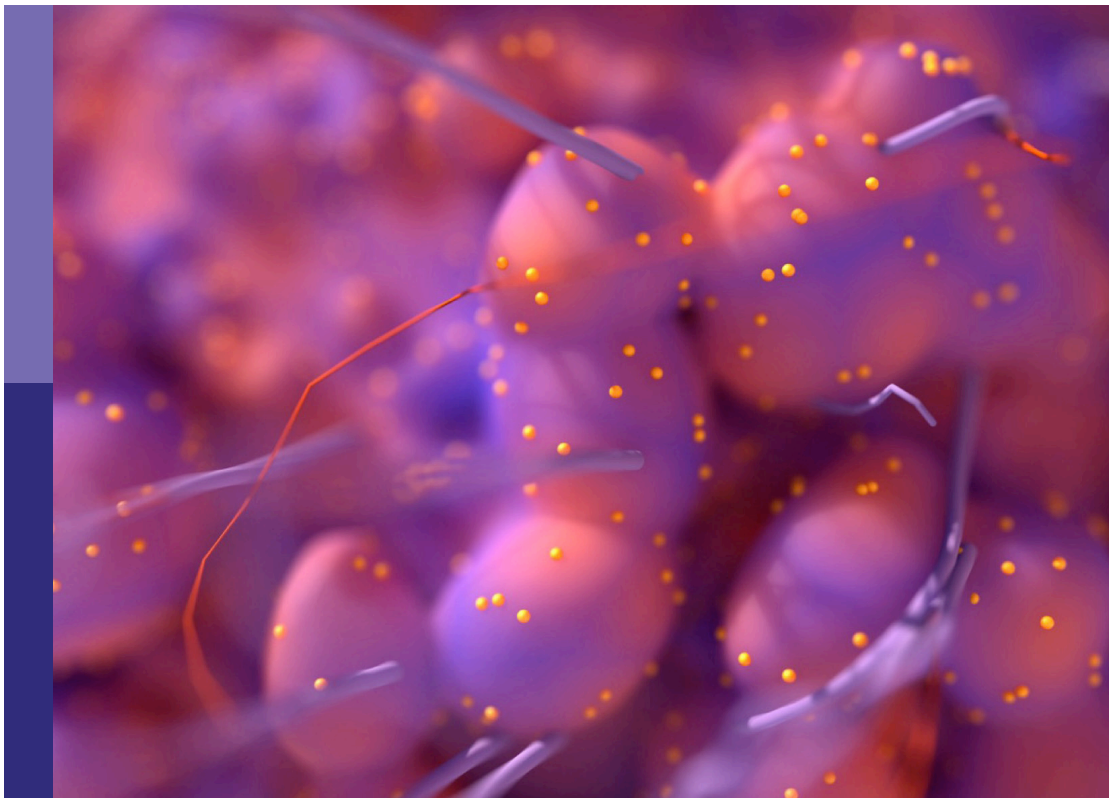

ISSN 1664-8714
ISBN 978-2-8325-6247-5
DOI 10.3389/978-2-8325-6247-5

About Frontiers

Frontiers is more than just an open access publisher of scholarly articles: it is a pioneering approach to the world of academia, radically improving the way scholarly research is managed. The grand vision of Frontiers is a world where all people have an equal opportunity to seek, share and generate knowledge. Frontiers provides immediate and permanent online open access to all its publications, but this alone is not enough to realize our grand goals.

Frontiers journal series

The Frontiers journal series is a multi-tier and interdisciplinary set of open-access, online journals, promising a paradigm shift from the current review, selection and dissemination processes in academic publishing. All Frontiers journals are driven by researchers for researchers; therefore, they constitute a service to the scholarly community. At the same time, the *Frontiers journal series* operates on a revolutionary invention, the tiered publishing system, initially addressing specific communities of scholars, and gradually climbing up to broader public understanding, thus serving the interests of the lay society, too.

Dedication to quality

Each Frontiers article is a landmark of the highest quality, thanks to genuinely collaborative interactions between authors and review editors, who include some of the world's best academicians. Research must be certified by peers before entering a stream of knowledge that may eventually reach the public - and shape society; therefore, Frontiers only applies the most rigorous and unbiased reviews. Frontiers revolutionizes research publishing by freely delivering the most outstanding research, evaluated with no bias from both the academic and social point of view. By applying the most advanced information technologies, Frontiers is catapulting scholarly publishing into a new generation.

What are Frontiers Research Topics?

Frontiers Research Topics are very popular trademarks of the *Frontiers journals series*: they are collections of at least ten articles, all centered on a particular subject. With their unique mix of varied contributions from Original Research to Review Articles, Frontiers Research Topics unify the most influential researchers, the latest key findings and historical advances in a hot research area.

Find out more on how to host your own Frontiers Research Topic or contribute to one as an author by contacting the Frontiers editorial office: frontiersin.org/about/contact

Treatment of brain metastases from non-small cell lung cancer: preclinical, clinical, and translational research

Topic editors
Lin Zhou — Sichuan University, China
Jianxin Xue — Sichuan University, China
Lei Deng — University at Buffalo, United States

Citation
Zhou, L., Xue, J., Deng, L., eds. (2025). *Treatment of brain metastases from non-small cell lung cancer: preclinical, clinical, and translational research*. Lausanne: Frontiers Media SA. doi: 10.3389/978-2-8325-6247-5

Table of contents

frontiers | Frontiers in Oncology

TYPE Editorial
PUBLISHED 04 April 2025
DOI 10.3389/fonc.2025.1598159

OPEN ACCESS

EDITED AND REVIEWED BY
Lizza E. L. Hendriks,
Maastricht University Medical Centre,
Netherlands

*CORRESPONDENCE
Lin Zhou
drzhoulin@163.com
Jianxin Xue
killercell@163.com
Lei Deng
ldeng1@fredhutch.org

RECEIVED 22 March 2025
ACCEPTED 24 March 2025
PUBLISHED 04 April 2025

CITATION
Liu J, Zhou P, Deng L, Xue J and Zhou L (2025) Editorial: Treatment of brain metastases from non-small cell lung cancer: preclinical, clinical, and translational research. *Front. Oncol.* 15:1598159. doi: 10.3389/fonc.2025.1598159

Editorial: Treatment of brain metastases from non-small cell lung cancer: preclinical, clinical, and translational research

Jia Liu[1], Pengfei Zhou[2], Lei Deng[3]*, Jianxin Xue[4]* and Lin Zhou[4]*

[1]Department of Oncology, Chengdu First People's Hospital, Chengdu, Sichuan, China, [2]Department of Thoracic Oncology, Meishan Cancer Hospital, Meishan, Sichuan, China, [3]Roswell Park Comprehensive Cancer Center, University at Buffalo, Buffalo, NY, United States, [4]Division of Thoracic Tumor Multimodality Treatment, Cancer Center and State Key Laboratory of Biotherapy, West China Hospital, Sichuan University, Chengdu, Sichuan, China

KEYWORDS

brain metastases, non-small cell lung cancer, prognosis, treatment, genetic mutation detection

Editorial on the Research Topic
Treatment of brain metastases from non-small cell lung cancer: preclinical, clinical, and translational research

Non-small cell lung cancer (NSCLC) is the most common malignancy worldwide, with up to 50% of patients developing brain metastases (BMs) in their disease course and 70% of BMs developing multiple lesions (1). BMs have a significant negative impact on both survival and quality of life for patients with NSCLC. The Research Topic, which included 15 articles, aims to present new evidence for preclinical, translational, and clinical studies in NSCLC with BMs.

Sampat et al. comprehensively reviewed BMs in NSCLC, focusing on epidemiology, diagnosis, treatment strategies, and prognosis. Generally, local treatments, including surgery/stereotactic radiosurgery (SRS)/stereotactic radiotherapy (SRT), are effective for limited BMs, and whole-brain radiotherapy (WBRT) is used for more extensive disease. For patients with driver gene positive, BMs have shown excellent responses to small molecule tyrosine kinase inhibitors (TKIs). Furthermore, immunotherapies, such as checkpoint inhibitors, also demonstrate some effectiveness.

The pathological subtypes of NSCLC may be correlated with the occurrence and prognosis of BMs. Zhou et al. investigated the prognostic characteristics of BMs originating from invasive lung adenocarcinomas of distinct pathological subtypes. Clinical data from 156 patients were collected and analyzed. Patients were classified into two groups on the basis of pathological subtype: moderately to highly differentiated and poorly differentiated. The median overall survival (mOS) for the poorly differentiated group was 14.67 months (95% CI: 11.80–17.53 months), whereas it was 25.00 months (95% CI: 19.55–30.45 months) for the moderately to highly differentiated group (hazard ratio [HR] of 1.55, 95% CI: 1.06–2.25; $p = 0.023$). However, this study did not provide data on driver gene mutations or programmed death-ligand 1 (PD-L1) expression, which are established prognostic factors

for NSCLC with BMs, and the prevalence of gene mutations and PD-L1 may vary across different pathological subtypes and influence the therapeutic effect (2–4). Wu et al. reported that pathological subtypes, together with sex, leukocyte count, and fibrinogen stage, were independent risk factors for predicting BMs in lung cancer patients. However, this study also did not provide data on driver gene mutations, which have been reported as risk factors for BMs in NSCLC (5).

TKIs serve as the cornerstone of treatment for driver gene-positive, such as epidermal growth factor receptor (EGFR)-mutant and anaplastic lymphoma kinase (ALK) rearrangement, NSCLC with BMs. In particular, new-generation TKIs exhibit high blood–brain barrier permeability and demonstrate superior efficacy against BMs (6, 7). As a result, brain metastases are no longer a critical prognostic factor for this patient population. Li et al. compared the prognoses of synchronous and metachronous BMs from NSCLC and reported that synchronous BMs (HR: 1.335, 95% CI: 1.076–1.657, $p = 0.009$), squamous carcinoma (HR: 1.361, 95% CI: 1.018–1.820, $p = 0.037$), and KPS score < 80 (HR: 1.392, 95% CI: 1.124–1.724, $p = 0.002$) were risk factors for OS. Interestingly, for patients with EGFR mutations, there was no significant difference in OS between synchronous and metachronous BMs ($p = 0.270$), which might indicate that the timing of BMs does not affect the prognosis of patients with EGFR mutations.

There have been numerous studies on the application of radiomics in NSCLC patients with BMs. Radiomics models based on multiparametric MRI can effectively predict the primary origin of brain metastases, clinical benefit, and progression-free survival (PFS) of immunotherapy for NSCLC patients with BMs (8, 9), and bimodal radiomics with CT and MRI (combining primary and BMs) achieves 86.7% accuracy in predicting the EGFR status (10). Similarly, Jiang et al. used CT perfusion imaging to predict pathological types of NSCLC with BMs, and reported that adenocarcinoma and squamous carcinoma patients presented significant differences in cerebral blood flow (CBF) and mean transit time (MTT) ($p < 0.001$, $p = 0.012$). For patients with difficulty to obtain pathological specimens and who are diagnosed with lung cancer clinically, it can assist in determining the pathological type. Xu et al. developed an MRI-based nomogram to predict immunotherapy effectiveness for NSCLC patients with BMs. The nomogram integrated intratumoral and peritumoral radiomic and clinical features and showed high accuracy in predicting the intracranial response and PFS.

Circulating tumor DNA (ctDNA) in cerebrospinal fluid (CSF) is more sensitive in reflecting the genetic features of BMs, especially in patients with leptomeningeal metastasis (LM) (11, 12). Similarly, Liu et al. investigated the utility of CSF and plasma ctDNA in detecting genetic mutations, including LM and brain parenchyma metastases (BPM) in NSCLC patients. The results revealed that CSF ctDNA had greater sensitivity than did plasma ctDNA for detecting mutations in LM patients, with all CSF ctDNA samples testing positive compared with 46.4% positivity in plasma ctDNA. In contrast, CSF ctDNA tests were negative in BPM patients. CSF ctDNA detected by next-generation sequencing can reflect the molecular characteristics and heterogeneity of NSCLC with LM, aiding in early LM detection. Furthermore, Abdulhaleem et al. explored the use of comprehensive genomic profiling via ctDNA to identify biomarkers for predicting clinical outcomes in NSCLC patients with BMs, and identified 72 genes significantly associated with clinical outcomes, with 14 genes linked to unfavorable outcomes and 36 to favorable outcomes.

It has been reported that peritumoral brain edema is correlated with prognosis, with extensive or prolonged edema duration generally associated with poorer outcomes (13, 14). Arrieta et al. investigated the predictive value of perilesional edema diameter (PED) associated with BMs for radiotherapy response in NSCLC patients, and reported that minor PED was independently associated with a better intracranial objective response rate (78.8% vs. 50%, OR 3.71, $p = 0.018$), longer median iPFS (11.8 vs. 6.9 months, HR 2.9, $p < 0.001$), and longer median OS (18.4 vs. 7.9 months, HR 2.1, $p = 0.001$). Cerebral radiation necrosis (CRN) is a relatively common late toxicity that severely influences patients' quality of life following radiotherapy for BMs. The incidence rate of CRN after brain SRT/SRS for BMs has been reported to be 6.3–34% (15–17). Several studies have indicated that bevacizumab alleviates inflammatory responses and clinical symptoms in patients with CRN by inhibiting vascular endothelial growth factor (VEGF), thereby reducing vascular permeability and cerebral edema (18, 19). Zhang et al. explored whether bevacizumab could prevent CRN in NSCLC patients with BMs undergoing SRT, and reported that bevacizumab significantly reduced the incidence of CRN and/or symptomatic edema before ($p = 0.036$) and after ($p = 0.015$) inverse probability of treatment weighting (IPTW) adjustment.

The phase III FLAURA2 trial demonstrated that, compared with first-line osimertinib monotherapy, first-line osimertinib plus chemotherapy improved PFS (HR=0.62, 95% CI 0.49–0.79, $p < 0.001$) and CNS-PFS (HR=0.58, 95% CI 0.33–1.01) (20, 21). Chen et al. performed a meta-analysis to compare the efficacy and safety of combining chemotherapy with EGFR-TKIs (ETC) versus EGFR-TKIs monotherapy for EGFR-mutated NSCLC patients with BMs; the meta-analysis included seven studies based on five randomized clinical trials with 550 patients, and revealed that the ETC group had better OS (HR: 0.64 [0.48, 0.87]), PFS (HR: 0.42 [0.34, 0.52]), and central nervous system PFS (HR: 0.42 [0.31, 0.57]). However, the patients in the ETC group experienced more grade 3-5/serious adverse events. The previous meta-analysis suggested that immunotherapy combined with chemotherapy yielded a better objective response rate (ORR), PFS, and OS than immunotherapy alone for PD-L1-negative and driver-gene-negative nonsquamous NSCLC (22). Brown et al. assessed first-line chemoimmunotherapy and immunotherapy in NSCLC patients with BMs via data from the Australian Registry and biObank of Thoracic Cancers (AURORA), and reported that chemoimmunotherapy was associated with an improved intracranial objective response rate (iORR) (58% vs. 31%, p=0.01) and longer OS (HR 0.35; 95% CI 0.14–0.86, p=0.01), even quite more patients with PD-L1 > 50% in the immunotherapy alone group (95% vs. 27%).

The Research Topic contains three case reports. Xie et al. presented a case report of a 67-year-old male with pulmonary

giant cell carcinoma, which is a rare subtype of NSCLC, and BMs were treated with penpulimab and anlotinib combined with cranial radiotherapy. The patient showed a significant reduction in both lung and brain lesions. Zhong et al. presented a case report of a 52-year-old female with EGFR-mutated NSCLC with LM. After treatment with high-dose aumolertinib (165 mg/day) and intrathecal pemetrexed via the Ommaya reservoir, the patient achieved significant remission, with LM progression-free survival exceeding 20 months. Chen et al. presented a case report of the efficacy of high-dose furmonertinib in treating LM from NSCLC. A 48-year-old man with EGFR-mutated NSCLC experienced rapid neurological symptom relief and 6-month survival post-LM diagnosis after receiving 160 mg/day furmonertinib.

In conclusion, this Research Topic presents new evidence on treatment, prognosis, radiomics analysis, ctDNA detection, and treatment-related adverse event management for NSCLC patients with BMs. However, several areas require further investigation to gain deeper insights into the mechanisms of BMs development, enhance treatment efficacy, and prolong patient survival. These include the tumor microenvironment in BMs from NSCLC, the mechanisms behind varying incidence across pathological/driver gene subtypes, optimal radiotherapy modalities/timing, and therapies for refractory BMs/LM after multiline treatments, etc.

Author contributions

JL: Writing – original draft. PZ: Writing – original draft. LD: Writing – review & editing. JX: Writing – review & editing. LZ: Writing – review & editing, Funding acquisition.

Funding

The author(s) declare that financial support was received for the research and/or publication of this article. This study was supported by the Natural Science Foundation of Sichuan Province (No. 2025ZNSFSC0547), the Sichuan Science and Technology Program (No. 2019YFS0323), and the National Natural Science Foundation of China (No. 81872466).

Conflict of interest

The authors declare that the research was conducted in the absence of any commercial or financial relationships that could be construed as potential conflicts of interest.

Generative AI statement

The author(s) declare that no Generative AI was used in the creation of this manuscript.

Publisher's note

References

1. Iuchi T, Shingyoji M, Itakura M, Yokoi S, Moriya Y, Tamura H, et al. Frequency of brain metastases in non-small-cell lung cancer, and their association with epidermal growth factor receptor mutations. *Int J Clin Oncol.* (2015) 20(4):674–9. doi: 10.1007/s10147-014-0760-9

2. Roman M, Baraibar I, Lopez I, Nadal E, Rolfo C, Vicent S, et al. Kras oncogene in non-small cell lung cancer: clinical perspectives on the treatment of an old target. *Mol Cancer.* (2018) 17:33. doi: 10.1186/s12943-018-0789-x

3. Batra U, Biswas B, Prabhash K, Krishna MV. Differential clinicopathological features, treatments and outcomes in patients with exon 19 deletion and exon 21 L858r Egfr mutation-positive adenocarcinoma non-small-cell lung cancer. *BMJ Open Respir Res.* (2023) 10(1):e001492. doi: 10.1136/bmjresp-2022-001492

4. Liu LU, Xie B, Zhu W, He Q, Zhou J, Liu S, et al. High expression of Pd-L1 mainly occurs in non-small cell lung cancer patients with squamous cell carcinoma or poor differentiation. *Oncol Res.* (2023) 31:275–86. doi: 10.32604/or.2023.028227

5. Tan AC, Itchins M, Khasraw M. Brain metastases in lung cancers with emerging targetable fusion drivers. *Int J Mol Sci.* (2020) 21(4):1416. doi: 10.3390/ijms21041416

6. Lu S, Dong X, Jian H, Chen J, Chen G, Sun Y, et al. Central nervous system efficacy of aumolertinib versus gefitinib in patients with untreated, Egfr-mutated, advanced non-small cell lung cancer: data from a randomized phase iii trial (Aeneas). *Cancer Commun (Lond).* (2024) 44:1005–17. doi: 10.1002/cac2.12594

7. Solomon BJ, Liu G, Felip E, Mok TSK, Soo RA, Mazieres J, et al. Lorlatinib versus crizotinib in patients with advanced Alk-positive non-small cell lung cancer: 5-year outcomes from the phase iii crown study. *J Clin Oncol.* (2024) 42:3400–9. doi: 10.1200/JCO.24.00581

8. Cao G, Zhang J, Lei X, Yu B, Ai Y, Zhang Z, et al. Differentiating primary tumors for brain metastasis with integrated radiomics from multiple imaging modalities. *Dis Markers.* (2022) 2022:5147085. doi: 10.1155/2022/5147085

9. Roh YH, Park JE, Kang S, Yoon S, Kim SW, Kim HS. Prognostic value of Mri volumetric parameters in non-small cell lung cancer patients after immune checkpoint inhibitor therapy: comparison with response assessment criteria. *Cancer Imaging.* (2023) 23:102. doi: 10.1186/s40644-023-00624-0

10. Ouyang Z, Zhang G, He S, Huang Q, Zhang L, Duan X, et al. Ct and Mri bimodal radiomics for predicting Egfr status in Nsclc patients with brain metastases: A multicenter study. *Eur J Radiol.* (2025) 183:111853. doi: 10.1016/j.ejrad.2024.111853

11. Li YS, Lai WP, Yin K, Zheng MM, Tu HY, Guo WB, et al. Lipid-associated macrophages for osimertinib resistance and leptomeningeal metastases in Nsclc. *Cell Rep.* (2024) 43:114613. doi: 10.1016/j.celrep.2024.114613

12. Zheng MM, Zhou Q, Chen HJ, Jiang BY, Tang LB, Jie GL, et al. Cerebrospinal fluid circulating tumor DNA profiling for risk stratification and matched treatment of central nervous system metastases. *Nat Med.* (2025). doi: 10.1038/s41591-025-03538-5

13. Zhao S, Li Y, Ning N, Liang H, Wu Y, Wu Q, et al. Association of peritumoral region features assessed on breast Mri and prognosis of breast cancer: A systematic review and meta-analysis. *Eur Radiol.* (2024) 34:6108–20. doi: 10.1007/s00330-024-10612-y

14. Wen J, Yu JZ, Liu C, Ould Ismail AAO, Ma W. Exploring the molecular tumor microenvironment and translational biomarkers in brain metastases of non-small-cell lung cancer. *Int J Mol Sci.* (2024) 25(4):2044. doi: 10.3390/ijms25042044

15. Lai J, Liu J, Zhao J, Li A, Liu S, Deng Z, et al. Effective method to reduce the normal brain dose in single-isocenter hypofractionated stereotactic radiotherapy for multiple brain metastases. *Strahlenther Onkol.* (2021) 197(7):592–600. doi: 10.1007/s00066-021-01757-6

16. Liang S, Liu X, Liu J, Na F, Lai J, Du L, et al. Optimal timing of hypofractionated stereotactic radiotherapy for epidermal growth factor receptor-mutated non-small-cell

lung cancer patients with brain metastases. *Asia Pac J Clin Oncol*. (2023) 19:731–8. doi: 10.1111/ajco.13957

17. Le Rhun E, Dhermain F, Vogin G, Reyns N, Metellus P. Radionecrosis after stereotactic radiotherapy for brain metastases. *Expert Rev Neurother*. (2016) 16:903–14. doi: 10.1080/14737175.2016.1184572

18. Dashti SR, Kadner RJ, Folley BS, Sheehan JP, Han DY, Kryscio RJ, et al. Single low-dose targeted bevacizumab infusion in adult patients with steroid-refractory radiation necrosis of the brain: A phase ii open-label prospective clinical trial. *J Neurosurg*. (2022) 137:1676–86. doi: 10.3171/2022.2.JNS212006

19. Hua YC, Gao DZ, Wang KY, Ding XS, Xu WR, Li YB, et al. Bevacizumab reduces peritumoral brain edema in lung cancer brain metastases after radiotherapy. *Thorac Cancer*. (2023) 14:3133–9. doi: 10.1111/1759-7714.15106

20. Janne PA, Planchard D, Kobayashi K, Cheng Y, Lee CK, Valdiviezo N, et al. Cns efficacy of osimertinib with or without chemotherapy in epidermal growth factor receptor-mutated advanced non-small-cell lung cancer. *J Clin Oncol*. (2024) 42:808–20. doi: 10.1200/JCO.23.02219

21. Planchard D, Janne PA, Cheng Y, Yang JC, Yanagitani N, Kim SW, et al. Osimertinib with or without chemotherapy in Egfr-mutated advanced Nsclc. *N Engl J Med*. (2023) 389:1935–48. doi: 10.1056/NEJMoa2306434

22. Chai Y, Wu X, Zou Y, Zhang X, Bai H, Dong M, et al. Immunotherapy combined with chemotherapy versus chemotherapy alone as the first-line treatment of pd-L1-negative and driver-gene-negative advanced nonsquamous non-small-cell lung cancer: an updated systematic review and meta-analysis. *Thorac Cancer*. (2022) 13:3124–32. doi: 10.1111/1759-7714.14664

frontiers | Frontiers in Oncology

TYPE Original Research
PUBLISHED 19 June 2023
DOI 10.3389/fonc.2023.1092721

OPEN ACCESS

EDITED BY
Lin Zhou,
Sichuan University, China

REVIEWED BY
Liu Xiaoqin,
First People's Hospital of Jintang County, China
Jialong Han,
Sichuan University, China

*CORRESPONDENCE
Yong Yang
yangyong@gdph.org.cn
Dong Zhou
zhoudong5413@163.com

RECEIVED 19 April 2023
ACCEPTED 31 May 2023
PUBLISHED 19 June 2023

CITATION
Wu B, Zhou Y, Yang Y and Zhou D (2023) Risk factors and a new nomogram for predicting brain metastasis from lung cancer: a retrospective study. *Front. Oncol.* 13:1092721. doi: 10.3389/fonc.2023.1092721

Risk factors and a new nomogram for predicting brain metastasis from lung cancer: a retrospective study

Bo Wu[1,2], Yujun Zhou[1,2], Yong Yang[2]* and Dong Zhou[1,2]*

[1]The Second School of Clinical Medicine, Southern Medical University, Guangzhou, China, [2]Department of Neurosurgery, Guangdong Provincial People's Hospital (Guangdong Academy of Medical Sciences), Southern Medical University, Guangzhou, Guangdong, China

Objective: This study aims to establish and validate a new nomogram for predicting brain metastasis from lung cancer by integrating data.

Methods: 266 patients diagnosed as lung cancer between 2016 and 2018 were collected from Guangdong Academy of Medical Sciences. The first 70% of patients were designated as the primary cohort and the remaining patients were identified as the internal validation cohort. Univariate and multivariable logistics regression were applied to analyze the risk factors. Independent risk factors were used to construct nomogram. C-index was used to evaluate the prediction effect of nomogram.100 patients diagnosed as lung cancer between 2018 and 2019 were collected for external validation cohorts. The evaluation of nomogram was carried out through the distinction and calibration in the internal validation cohort and external validation cohort.

Results: 166 patients were diagnosed with brain metastasis among the 266 patients. The gender, pathological type (PAT), leukocyte count (LCC) and Fibrinogen stage (FibS) were independent risk factors of brain metastasis. A novel nomogram has been developed in this study showed an effective discriminative ability to predict the probability of lung cancer patients with brain metastasis, the C-index was 0.811.

Conclusion: Our research provides a novel model that can be used for predicting brain metastasis of lung cancer patients, thus providing more credible evidence for clinical decision-making.

KEYWORDS

lung cancer, brain metastasis, risk factors, nomogram, gender, pathological type, leukocyte count, fibrinogen stage

Introduction

With the supreme morbidity and mortality, lung cancer is still the most malignant growth at present. The cumulative incidence of brain metastasis (BMs) in lung cancer in 1 year and 5 years is 14.8% and 16.3% (1), respectively, which is the first incidence of all types of tumors. In addition, 80-85% of lung cancer patients are diagnosed as non-small cell lung cancer(NSCLC) (2), so NSCLC is the most familiar primary neoplasm in brain metastasis. We found in some research that the rate of brain metastasis with NSCLC is about 10% to 20% (3–5), and the rate is even higher in advanced NSCLC, about 30% to 50% (4, 6–8). The median survival of brain metastasis is about 6 to 30 months, but early diagnosis is propitious to prolong the survival time (3, 4). Therefore, it's positive for patients if clinicians can determine the probability of brain metastasis early.

At present, a great many essays have been issued to analyze the risk factors for brain metastasis of lung cancer (9, 10). However, their assessment criteria are more complex. In this study, we aimed to analyze the risk factors for brain metastasis in lung cancer patients and establish an effective and noninvasive nomogram for the possibility of brain metastasis in lung cancer patients by adopting advanced statistical analysis. In our nomogram, we can speculate the possibility of brain metastasis through simple blood routine and pathological type, and this nomogram is easier to apply to clinical practice than others of the same type.

Materials and methods

Clinical data of all patients was uninterruptedly enrolled and this study was ratified by the Guangdong Provincial People's Hospital. All enrolled patients were carefully screened according to the following inclusion criteria: Group of primary lung cancer:(a) Patients diagnosed with pathological results;(b) Patients diagnosed only primary neoplasms without brain metastasis;(c) Patients diagnosed between 2016 and 2018;(d) Patients with completely clinical characteristics. Group of brain metastasis:(a) Patients diagnosed with pathological results;(b) Patients diagnosed between 2016 and 2018;(c) Patients with completely clinical characteristics. Finally, a total of 100 patients with primary lung cancer and 166 patients with brain metastasis who were diagnosed at the Department of Neurosurgery, the Guangdong Provincial People's Hospital from 2016 to 2018 were enrolled in this retrospective study.

All patients were randomly arranged. The first 70% of patients were designated as the primary cohort, and the remaining patients were identified as the internal validation cohort. The verification of the nomogram was also assessment in an independent external validation cohort which included 100 patients from 2018 to 2019 who was diagnosed with primary lung cancer and brain metastasis.

Clinical characteristics

As shown in Table 1, the clinical characteristics include gender, age, pathological type (PAT), location of primary tumor, smoke, drunk, blood routine tests, glucose count, protein count, albumin count, electrolyte and coagulation indicators were obtained from medical records. The blood routine tests include erythrocyte count, leukocyte count (LCC), platelet, eosinophil ratio count, lymphocyte ratio count, monocyte ratio count and neutrophil ratio count, basophil ratio count. The electrolyte including kalium count, natrium count, chlorine count, calcium count, magnesium count,

TABLE 1 Detail of patients' characteristics.

characteristics	primary lung cancer (mean±SD/no.%)	brain metastasis (mean±SD/no.%)
Total(n)	70(37.6%)	116(62.4%)
gender		
Male	42 (22.6%)	43 (23.1%)
Female	28 (15.1%)	73 (39.2%)
age	51.07±10.472	57.49±9.574
AS		
low	17(9.1%)	9(4.8%)
middle	40(21.5%)	56(30.1%)
high	13(7.0%)	51(27.4%)
PAT		
squamous carcinoma	8(4.3%)	12(6.5%)
Adenocarcinoma	53(28.5%)	92(49.5%)
Neuroendocrine tumors	3(1.6%)	2(1.1%)
Lymphoepithelioma-like carcinoma	2(1.1%)	2(1.1%)

(Continued)

TABLE 1 Continued

characteristics	primary lung cancer (mean±SD/no.%)	brain metastasis (mean±SD/no.%)
others	4(2.2%)	8(4.3%)
drunk		
yes	1(0.5%)	10(5.4%)
no	69(37.1%)	106(57.0%)
LCC	6.56±2.238	8.43±3.297
LCS		
low	39(20.1%)	23(12.4%)
middle	20(10.8%)	45(24.2%)
high	11(6.0%)	48(25.8%)
PLTC	254.59±70.729	282.64±71.682
PLTS		
low	32(17.2%)	26(14.0%)
middle	19(10.2%)	40(21.5%)
high	19(10.2%)	50(26.9%)
NRS	0.59±0.101	0.66±0.976
LRC	0.31±0.108	0.23±0.838
LRS		
low	14(7.5%)	48(25.8%)
middle	21(11.3%)	45(24.2%)
high	35(18.8%)	23(12.4%)
ERS		
low	16(8.6%)	43(23.1%)
middle	29(15.6%)	40(21.5%)
high	25(13.4%)	33(17.7%)
ALBS		
low	19(10.2%)	50(26.9%)
middle	31(16.7%)	30(16.1%)
high	20(10.8%)	36(19.4%)
GLUS		
low	32(17.2%)	37(19.9%)
middle	20(10.8%)	41(22.0%)
high	18(9.7%)	38(20.4%)
KC	3.83±0.297	3.95±0.413
KS		
low	27(14.5%)	36(19.4%)
middle	30(16.1%)	33(17.7%)
high	13(7.0%)	47(25.3%)
ClC	105.43±5.097	103.59±3.322

(Continued)

TABLE 1 Continued

characteristics	primary lung cancer (mean±SD/no.%)	brain metastasis (mean±SD/no.%)
ClS		
low	19 (10.2%)	47(25.3%)
middle	24(13.0%)	42(22.6%)
high	27(14.5%)	27(14.5%)
FibC	3.47±1.269	4.43±1.127
FibS		
low	40(21.5%)	14(7.5%)
middle	20(10.8%)	46(24.7%)
high	10(5.4%)	56(30.1%)
TTC	16.56±0.889	16.09±1.130
TTS		
low	17(9.1%)	47(25.3%)
middle	20(10.8%)	41(22.0%)
high	33(17.7%)	28(15.1%)
T		
T1	57(30.6%)	48(25.8%)
T2	6(3.2%)	36(19.4%)
T3	5(2.7%)	21(11.3%)
T4	2(1.1%)	11(6.0%)
N		
N0	55(30.0%)	45(24.2%)
N1	15(8.1%)	71(38.2%)

phosphorus count. And the coagulation indicators including Activates partial thromboplastin time (APTT), Fibrinogen count (FibC), Thrombin time (TT), International normalized ratio (INR), Prothrombin activity (PTA) and Plasma prothrombin time determination (PT). This study divides all the continuous variables into low, medium, and high groups with the third point as the dividing line.

Variables selection

Univariate analysis was performed by SPSS (v26.0). The meaningful variables of single factor analysis(p<0.1) were introduced into logistic regression for multivariate analysis, p< 0.05 was statistically significant. The independent risk factors were included By R Studio (v4.2.1) to construct nomogram. C-index was used to judge the predictive capacity of nomogram. We then verified the appropriate calibration in the primary cohort and validation cohorts. The ROC curve was used to assess the nomogram. Furthermore, the DCA analysis shows that the model possesses favourable clinical practice value.

Result

Univariate and multivariate analysis of risk factors

Univariate analysis showed that the factors affecting brain metastasis included the following factors (Table 2): gender (P=0.001, B=-1.009), pathological type (PAT) (P=0.074, B=-0.253), leukocyte count (LCC) (P<0.001, B=0.005), Fibrinogen stage (FibS) (P<0.001, B=1.396).

Introducing the significant factors of single factor analysis into Logistic regression for multivariate analysis and then we got independent risk factors as follows: gender (P=0.033 HR=2.692,95% CI 1.085-6.677), PAT(P=0.009), LCC (P=0.008 HR=1.339,95% CI 1.078-1.661), Fibs(P<0.001) (Table 2).

Development of final prediction model

Based on the results of multivariate analysis, we constructed a nomogram (Figure 1). The risk factors introduced in the model

10.3389/fonc.2023.1092721

TABLE 2 Univariate and Multivariate analysis of risk factors.

Univariate analysis of risk factors									
		B	S.E.	Wald	df	Sig.	Exp(B)	95% CI for Exp(B)	
								Lower	Upper
gender		-1.009	0.312	10.477	1	0.001	0.364	0.198	0.672
age		0.044	0.015	8.854	1	0.003	1.045	1.015	1.076
AS		0.74	0.233	10.094	1	0.001	2.096	1.328	3.308
PAT		-0.253	0.142	3.19	1	0.074	0.777	0.588	1.025
drunk		1.873	1.06	3.122	1	0.077	6.509	0.815	51.993
LCC		0.378	0.087	18.894	1	0	1.459	1.23	1.73
LCS		1.047	0.215	23.69	1	0	2.849	1.869	4.344
PLTC		0.005	0.002	6.826	1	0.009	1.005	1.001	1.009
PLTS		0.541	0.187	8.389	1	0.004	1.718	1.191	2.479
NRS		0.835	0.207	16.236	1	0	2.305	1.536	3.46
LRC		-9.191	1.93	22.678	1	0	0	0	0.004
LRS		-0.887	0.208	18.227	1	0	0.412	0.274	0.619
ERS		-0.351	0.196	3.223	1	0.073	0.704	0.48	1.033
ALBS		-0.365	0.195	3.494	1	0.062	0.694	0.473	1.018
GLUS		0.415	0.192	4.696	1	0.03	1.515	1.04	2.205
KC		0.96	0.419	5.246	1	0.022	2.611	1.148	5.936
KS		0.468	0.186	6.3	1	0.012	1.596	1.108	2.3
ClC		-0.183	0.059	9.653	1	0.002	0.833	0.742	0.935
ClS		-0.524	0.194	7.323	1	0.007	0.592	0.405	0.866
FibC		0.673	0.143	22.173	1	0	1.96	1.481	2.594
FibS		1.396	0.228	37.332	1	0	4.038	2.58	6.318
TTC		-0.354	0.148	5.745	1	0.017	0.702	0.525	0.937
TTS		-0.556	0.191	8.424	1	0.004	0.574	0.394	0.835
T		0.917	0.221	17.168	1	0	2.502	1.621	3.861
N		1.755	0.348	25.431	1	0	5.785	2.924	11.445
Multivariate analysis of risk factors									
		B	S.E.	Wald	df	Sig.	Exp(B)	95% C.I.for EXP(B)	
								Lower	Upper
Step 4[d]	gender	0.99	0.464	4.562	1	0.033	2.692	1.085	6.677
	Pathological type			15.448	5	0.009			
	Squamous cell cancer	0.361	1.017	0.126	1	0.723	1.435	0.196	10.528
	small cell carcinoma	-2.23	1.174	3.606	1	0.058	0.108	0.011	1.074
	adenosquamous carcinoma	-0.972	1.431	0.461	1	0.497	0.378	0.023	6.255
	other types	-24.185	27193.07	0	1	0.999	0	0	.
	neuroendocrine carcinoma	-1.488	1.57	0.899	1	0.343	0.226	0.01	4.897
	Leukocyte count	0.292	0.11	6.992	1	0.008	1.339	1.078	1.661

(Continued)

TABLE 2 Continued

Multivariate analysis of risk factors									
		B	S.E.	Wald	df	Sig.	Exp(B)	95% C.I.for EXP(B)	
								Lower	Upper
Step 4[d]	gender	0.99	0.464	4.562	1	0.033	2.692	1.085	6.677
	Pathological type			15.448	5	0.009			
	Squamous cell cancer	0.361	1.017	0.126	1	0.723	1.435	0.196	10.528
	small cell carcinoma	-2.23	1.174	3.606	1	0.058	0.108	0.011	1.074
	adenosquamous carcinoma	-0.972	1.431	0.461	1	0.497	0.378	0.023	6.255
	other types	-24.185	27193.07	0	1	0.999	0	0	.
	neuroendocrine carcinoma	-1.488	1.57	0.899	1	0.343	0.226	0.01	4.897
	Leukocyte count	0.292	0.11	6.992	1	0.008	1.339	1.078	1.661
	Fib grade			30.594	2	0			
	Fib middle grade	-2.888	0.587	24.173	1	0	0.056	0.018	0.176
	Fib high grade	-0.571	0.544	1.102	1	0.294	0.565	0.194	1.641
	Constant	-0.97	1.495	0.421	1	0.516	0.379		

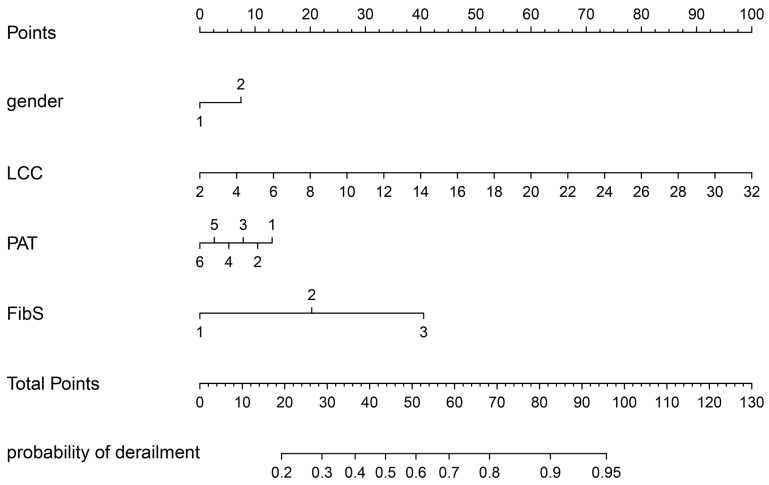

FIGURE 1
BMs-related nomogram prediction score. BMs-related nomogram was constructed to predict BMs for lung cancer patients, with the gender, PAT, LCC and FibS. The nomogram showed the probability of brain metastasis in patients with a pathological diagnosis of lung cancer. PAT, pathlogicl type; LCC, leukocyte count; FibS, Fibrinogen stage.

were given various weights in conformity with the degree of influence, and received different scores according to the individual information of patients. The scores are added together to obtain the ultimate scores, and the forecast results could be found in the nomogram. The C-index in this study was 0.811, showing a good prediction effect. Figure 2 shows the receiver operating characteristic (ROC) curves of these independent risk factors for predicting the risk of brain metastasis. These factors are quite accurate in predicting brain metastasis (the area under the curve [AUCs] of those factors were 0.768, 0.746, 0.446, 0.377). Afterwards, we verified a appropriate calibration in the primary cohort and validation cohorts (Figure 3).

Clinical usage

Figure 4 showed that if the threshold probability of a patient or a doctor is in the range from 0 to 0.85, the net benefit is equivalent, in accordance with DCA. The y-axis shows the net benefit, which is the different value between the ratio of false positive patients and the ratio of

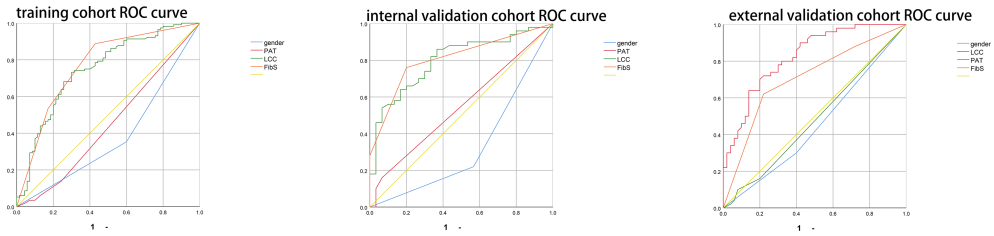

FIGURE 2
Figure 2 shows the receiver operate characteristic (ROC) curves of these risk factors for predicting the risk of brain metastasis.

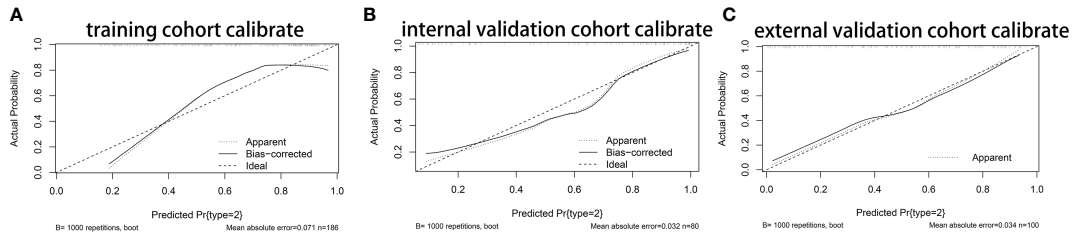

FIGURE 3
The Calibration curves of nomogram. **(A)** The Calibration curves of nomogram in primary cohort. **(B)** The Calibration curves of nomogram in internal validation cohort. **(C)** The Calibration curves of nomogram in primary cohort in external cohort.

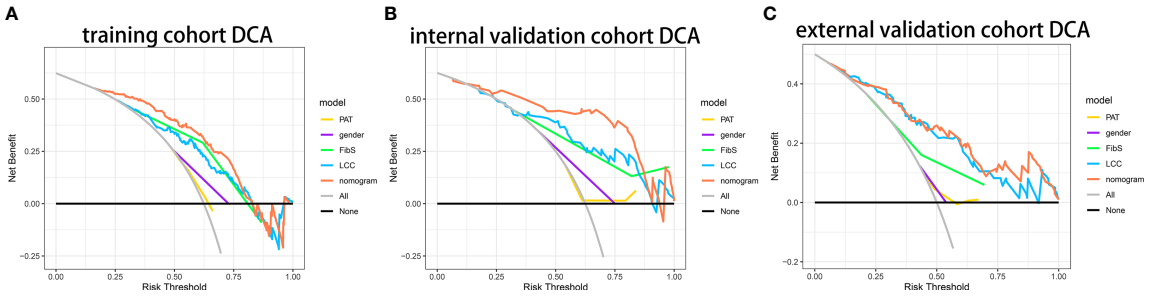

FIGURE 4
Decision curve analysis of nomogram. **(A)** The DCA curves of nomogram in primary cohort. **(B)** The DCA curves of nomogram in internal validation cohort. **(C)** The DCA curves of nomogram in primary cohort in external cohort.

true positive patients, weighted by the relative harm of forgoing treatment and the negative effects of unnecessary treatment (11). The sloping glossy full line stand for the assumption that all patients have BMs. The horizontal glossy full line stands for the assumption that all patients have no BMs. The sloping dashed lines stand for all patients considered to be BMs according to the nomogram. The decision curves in cohorts shows that if the threshold probability is between 0 and 0.80, then the use of the integrated nomogram predicts that BMs will yield more benefits than treating all patients or none, while the perfect model is the model with the highest net benefit under any threshold probability.

Discussion

In our study, the rate of brain metastasis in female is higher than that of male. To understand this situation, we must know that gender differences in human growth, development, disease, and death are so common that people almost acquiesce to gender differences as reasonable. Understanding these differences needs comprehensive analysis at the molecular, cellular, and tissue level. In recent years, this relationship has attracted more and more attention, with researchers investigating the role of gender-related molecular patterns. Thus, this adds to the understanding of fundamental gender differences, identifying mutational (12) and methylation profiles (13), followed by transcriptomes (14) and tumor metabolism (15). Analysis of cellular immanent mechanisms, central to the biology of human cancer cells, is the devitalization of RB1 and p53 functions (16). The change of p53 function may engender differential effects on males and females in multiple species. This partly explains the conclusions of our study. Preliminary characterization of mice with complete loss of p53 function suggests that they develop normally but have an increased rate of spontaneous tumor formation (17). It reflects the effect of

P53 on the tumor. By using astrocytes as the cell of origin in a mouse model of glioblastoma, the loss of p53 function was found to result in significantly increased in growth *in vitro* and tumorigenesis *in vivo* of male astrocytes (18); when RB1 and p53 function are used up, both male and female astrocytes put up analogical tumor-forming potential. This evidence suggests that when P53 and RB1 are intact, gender differences in their regulation have a significant impact on malignant transformation. Both male and female astrocytes differ in cAMP synthesis and degradation, leading to differences in basal cAMP levels (19). The connection between intra-cellular cAMP and tumor growth has been established for decades (20). Analysis of non-intracellular mechanisms, first, there are tremendous differences in immunologic function between males and females, especially in autoimmune diseases. Multiple sclerosis (MS) and rheumatoid arthritis (RA) are twice as common in females compared to males (21, 22), and more than 90% of SLE cases are in females (23, 24); second, another significant and possibly cancer-related gender discrepancy is the effect of gender on vascular function. Cardiovascular disease occurs more frequently in males than females (25). The mechanistic basis for these maturing observations is dimness and may include gender discrepancy in responses to early environmental stressors and acute vascular effects of gender hormones. Possible hormone-dependent mechanisms include estrogen-irritative vasodilatory effects of nitric oxide and prostacyclin, and anti-inflammatory and antioxidant effects of estrogen (26). As mentioned earlier, P53, RB1 and cAMP have important roles in tumor growth and reproduction. The significant difference in basal cAMP between males and females contributes to the difference in the incidence of brain metastases in males and females. The specific mechanisms of P53, RB1 and cAMP affect tumor growth and reproduction need to be further investigated experimentally. In addition, the effect of gender on vascular function is evident. It is well known that the occurrence of brain metastases requires several steps: the shedding of tumor cells at the original site, entering the blood vessels, penetrating the blood-brain barrier with the blood vessels, entering the fixed value site in brain, extravasating to the brain parenchyma, and completing brain metastases. Therefore, blood vessels play a very important role in brain metastasis. As we all know, brain metastases usually occur in areas with rich blood vessels. And the difference of vascular function between male and female can explain to some extent why there are gender differences in brain metastasis.

A retrospective analysis based on the SEER database revealed that the occurrence of BM in non-small cell lung cancer was 9%, and the lowest incidence of squamous cell carcinoma in NSCLC histology was 6% (27). This conclusion is consistent with our research. Adenocarcinoma is a risk factor for brain metastasis in lung cancer. Meanwhile, another study noted that squamous cell carcinoma was significantly related to low BM occurrence in patients with non-small cell lung cancer (28).

Ekaterina Friebel et al. performed a high-parameter single-cell mapping of the tumor microenvironment of patients with brain metastasis, and the results showed that metastasis favored T cell and monocyte-derived macrophage invasion (29). Besides, inflammatory mediators are also involved in several steps of tumor metastasis. EMT,the first step of metastasis, makes migration possible (30). EMT can be enhanced by activating the NF-kB/STAT3 pathway and producing inflammatory cytokines (31). The extracellular matrix (ECM) is then modified, particularly through inflammatory mediators, to allow cancer cells to enter blood vessels and lymphatic vessels (32). Finally, extravasation of cancer cells is induced by chemokines (a family of pro-inflammatory mediators) (33). Then, the process of BMs is completed. Neutrophils accounts for 50-70% of all leukocytes (34) and can mirror the condition of host inflammation, a hallmark of cancer (16). The influence of neutrophils in cancer is multifactorial and still not know it inside out. They can participate in different periods of the carcinogenic process, including tumor origination, growth, propagation, or metastatic spread (35, 36). The release of reactive oxygen species (ROS), reactive nitrogen species (RNS) or proteases from neutrophils can promote tumorigenesis and metastasis (37). Neutrophils can promote tumor propagation and metastasis by destroying the immune system. Moreover, insulin receptor substrate 1 (IRS1) activation of PI3K signaling also mediates tumor propagation as neutrophil elastase metastasizes to cancer cells (38). Ultimately, neutrophils can also promote metastatic spread by repressing natural killer function and promoting exosmosis of tumor cells (39, 40). As seen here, the role of neutrophils in cancer spread is complicated.

Fibrinogen, the most ample plasma coagulation factor, is synthesized by hepatocytes. Animal experiments have proved that increasing local coagulation function will lead to an increase in BMs. This is the same with our conclusion (41). Fibrinogen has been revealed to have prognostic implications in a variety of cancers, including lung cancer (42–45). There is increasing evidence of a correlation between fibrinogen and metastatic spread (46, 47). The process of BMs is divided into: tumor cells oozing from the primary site, tumor cells entering the vasculature, tumors reaching the brain with the vasculature and tumor cells oozing from the vasculature to the brain parenchyma to complete the BMs. Elevated serum fibrinogen concentrations alter blood viscosity, rheology, and endothelial function, which may increase the probability of tumor cells exuding from the vasculature to the brain parenchyma and thus promote BMs. Fibrinogen can enhance brain tumor-initiating cells (BTICs) intercellular adhesion and improve the motility of BTIC, thereby increasing the invasiveness of BTIC (48). Clinical studies have shown that prophylactic anticoagulation in lung cancer patients does not increase the risk of bleeding (49–51). Can lung cancer patients use anticoagulation prophylactically to reduce the BMs? More basic and clinical studies are needed to confirm our conjecture.

Even though our nomogram displays encouraging results among the cohorts, there are still certain shortcomings. Due to the retrospective method is adopted in this study, inherent deviations such as selection deviation and detection deviation is inevitably occur. Furthermore, continuous monitoring of changes in certain parameters cannot be completed. In addition, molecular mechanism researches and large-scale and multi-center clinical trials are required to revise the model.

Conclusion

This research provided a better understanding of the risk factors for brain metastases among lung cancer patients. Besides, we have developed a new pragmatic nomogram, which immensely extends the range of clinical practice to calculate the characteristics of patients with brain metastases from lung cancer.

Data availability statement

The original contributions presented in the study are included in the article/supplementary material. Further inquiries can be directed to the corresponding authors.

Ethics statement

This study was approved by the Guangdong Provincial People's Hospital. Written informed consent from the patients was not required to participate in this study in accordance with the national legislation and the institutional requirements.

Author contributions

All authors listed have made a substantial, direct, and intellectual contribution to the work and approved it for publication.

Funding

This research was supported by GuangDong Basic and Applied Basic Research Foundation: 2022A1515012540 and Guangzhou Basic and Applied Basic Research Foundation: 202201011639.

Acknowledgments

Alafate Wahafu, Zhige Guo, and Zongtai Zheng also contributed to our research.

Conflict of interest

The authors declare that the research was conducted in the absence of any commercial or financial relationships that could be construed as a potential conflict of interest.

Publisher's note

References

1. Schouten LJ, Rutten J, Huveneers HA, Twijnstra A. Incidence of brain metastasis in a cohort of patients with carcinoma of the breast, colon, kidney, and lung and melanoma. *Cancer* (2002) 94:2698–705. doi: 10.1002/cncr.10541

2. Saad AG, Yeap BY, Thunnissen FB, Pinkus GS, Pinkus JL, Loda M, et al. Immunohistochemical markers associated with brain metastasis in patients with nonsmall cell lung carcinoma. *Cancer* (2008) 113:2129–38. doi: 10.1002/cncr.23826

3. Smith DR, Bian Y, Wu CC, Saraf A, Tai CH, Nanda T, et al. Natural history, clinical course and predictors of interval time from initial diagnosis to developmalet of subsequent NSCLC brain metastasis. *J Neurooncol* (2019) 143:145–55. doi: 10.1007/s11060-019-03149-4

4. Waqar SN, Samson PP, Robinson CG, Bradley J, Devarakonda S, Du L, et al. Non-small-cell lung cancer with brain metastasis at presentation. *Clin Lung Cancer* (2018) 19:e373–9. doi: 10.1016/j.cllc.2018.01.007

5. Bajard A, Westeel V, Dubiez A, et al. Multivariate analysis of factors predictive of brain metastasis in localised non-small cell lung carcinoma. *Lung Cancer* (2004) 45:317–23. doi: 10.1016/j.lungcan.2004.01.025

6. Ceresoli GL, Reni M, Chiesa G, Carretta A, Schipani S, Passoni P, et al. Brain metastasis in locally advanced nonsmall cell lung carcinoma after multimodality treatmalet:risk factors analysis. *Cancer* (2002) 95:605–12. doi: 10.1002/cncr.10687

7. Robnett TJ, Machtay M, Stevenson JP, Algazy KM, Hahn SM. Factors affecting the risk of brain metastasis after definitive chemoradiation for locally advanced non-small-cell lung carcinoma. *J Clin Oncol* (2001) 19:1344–9. doi: 10.1200/JCO.2001.19.5.1344

8. Chen AM, Jahan TM, Jablons DM, Garcia J, Larson DA. Risk of cerebral metastasis and neurological death after pathological complete response to neoadjuvant therapy for locally advanced non-small-cell lung cancer: clinical implications for the subsequent managemalet of the brain. *Cancer* (2007) 109:1668–75. doi: 10.1002/cncr.22565

9. Davis FG, Dolecek TA, McCarthy BJ, Villano JL. Toward determining the lifetime occurrence of metastatic brain tumors estimated from 2007 united states cancer incidence data. *Neuro-Oncology* (2012) 14(9):1171–7. doi: 10.1093/neuonc/nos152

10. Lee DS, Kim YS, Jung SL, Lee KY, Kang JH, Park S, et al. The relevance of serum carcinoembryonic antigen as an indicator of brain metastasis detection in advanced non-small cell lung cancer. *Tumour Biol* (2012) 33(4):1065–73. doi: 10.1007/s13277-012-0344-0

11. Zhang GH, Liu YJ, De Ji M. Risk factors, prognosis, and a new nomogram for predicting cancer-specific survival among lung cancer patients with brain metastasis: a retrospective study based on SEER. *Lung* (2022) 200(1):83–93. doi: 10.1007/s00408-021-00503-0

12. Vickers AJ, Cronin AM, Elkin EB, Gonen M. Extensions to decision curve analysis, a novel method for evaluating diagnostic tests, prediction models and molecular markers. *BMC Med Inform Decis Mak* (2008) 8:53. doi: 10.1186/1472-6947-8-53

13. Zhang H, Liao J, Zhang X, Zhao E, Liang X, Luo S, et al. Gender difference of mutation clonality in diffuse glioma evolution. *Neuro Oncol* (2019) 21:201–13. doi: 10.1093/neuonc/noy154

14. Yang W, Warrington NM, Taylor SJ, Whitmire P, Carrasco E, Singleton KW, et al. Gender differences in GBM revealed by analysis of patient imaging, transcriptome, and survival data. *Sci T ransl Med* (2019) 11(473):eaao5253. doi: 10.1126/scitranslmed.aao5253

15. Ippolito JE, Yim AK, Luo J, Chinnaiyan P, Rubin JB. Genderual dimorphism in glioma glycolysis underlies gender differences in survival. *JCI Insight* (2017) 2. doi: 10.1172/jci.insight.92142

16. Hanahan D, Weinberg RA. Hallmarks of cancer: the next generation. *Cell* (2011) 144(5):646–74. doi: 10.1016/j.cell.2011.02.013

17. Donehower LA, Harvey M, Slagle BL, McArthur MJ, Montgomery CAJr, Butel JS, et al. Mice deficient for p53 are developmaletally normal but susceptible to spontaneous tumours. *Nature* (1992) 356(6366):215–21. doi: 10.1038/356215a0

18. Sun T, Warrington NM, Luo J, Brooks MD, Dahiya S, Snyder SC, et al. Genderually dimorphic RB inactivation underlies mesenchymal glioblastoma prevalence in males. *J Clin Invest* (2014) 124(9):4123–33. doi: 10.1172/JCI71048

19. Warrington NM, Sun T, Luo J, McKinstry RC, Parkin PC, Ganzhorn S, et al. The cyclic AMP pathway is a gender-specific modifier of glioma risk in type I neurofibromatosis patients. *Cancer Res* (2015) 75(1):16–21. doi: 10.1158/0008-5472.CAN-14-1891

20. Racagni G, Pezzotta S, Giordana MT, Iuliano E, Mocchetti I, Spanu G, et al. Cyclic nucleotides in experimaletal and human brain tumors. *J Neurooncol* (1983) 1 (1):61–7. doi: 10.1007/BF00153643

21. Sellner J, Kraus J, Awad A, Milo R, Hemmer B, Stüve O. The increasing incidence and prevalence of female multiple sclerosis–a critical analysis of potential environmaletal factors. *Autoimmun Rev* (2011) 10(8):495–502. doi: 10.1016/j.autrev.2011.02.006

22. van Vollenhoven RF. Gender differences in rheumatoid arthritis: more than meets the eye. *BMC Med* (2009) 7:12. doi: 10.1186/1741-7015-7-12

23. Hamilton A, Sibson NR. Role of the systemic immune system in brain metastasis. *Mol Cell Neurosci* (2013) 53:42–51. doi: 10.1016/j.mcn.2012.10.004

24. Weckerle CE, Niewold TB. The unexplained female predominance of systemic lupus erythematosus: clues from genetic and cytokine studies. *Clin Rev Allergy Immunol* (2011) 40(1):42–9. doi: 10.1007/s12016-009-8192-4

25. Lehto HR, Lehto S, Havulinna AS, Salomaa V. Does the clinical spectrum of incident cardiovascular disease differ between male and female? *Eur J Prev Cardiol* (2014) 21(8):964–71. doi: 10.1177/2047487313482284

26. Resanovic I, Rizzo M, Zafirovic S, Bjelogrlic P, Perovic M, Savic K, et al. Anti-atherogenic effects of 17β-estradiol. *Horm Metab Res* (2013) 45(10):701–8. doi: 10.1055/s-0033-1343478

27. Goncalves PH, Peterson SL, Vigneau FD, Shore RD, Quarshie WO, Islam K, et al. Risk of brain metastasis in patients with nonmetastatic lung cancer: analysis of the metropolitan Detroit surveillance, epidemiology, and end results (SEER) data. *Cancer* (2016) 122(12):1921–7. doi: 10.1002/cncr.30000

28. Sun DS, Hu LK, Cai Y, Li XM, Ye L, Hou HY, et al. A systematic review of risk factors for brain metastasis and value of prophylactic cranial irradiation in non-small cell lung cancer. *Asian Pac J Cancer Prev* (2014) 15(3):1233–9. doi: 10.7314/APJCP.2014.15.3.1233

29. Friebel E, Kapolou K, Unger S, Núñez NG, Utz S, Rushing EJ, et al. Single-cell mapping of human brain cancer reveals tumor-specific instruction of tissue-invading leukocytes. *Cell* (2020) 181(7):1626–42.e20. doi: 10.1016/j.cell.2020.04.055

30. Kalluri R, Weinberg RA. The basics of epithelial mesenchymal transition. *J Clin Invest* (2009) 119:1420e8. doi: 10.1172/JCI39104

31. Grivennikov SI, Karin M. Inflammation and oncogenesis: a vicious connection. *Curr Opin Genet Dev* (2010) 20:65e71. doi: 10.1016/j.gde.2009.11.004

32. Nguyen DX, Bos PD, Massague J. Metastasis: from dissemination to organ specific colonization. *Nat Rev Cancer* (2009) 9:274e84. doi: 10.1038/nrc2622

33. Mantovani A, Allavena P, Sica A, Balkwill F. Cancer-related inflammation. *Nature* (2008) 454:436e44. doi: 10.1038/nature07205

34. Bronte V, Brandau S, Chen SH, Colombo MP, Frey AB, Greten TF, et al. Recommaledations for myeloid-derived suppressor cell nomaleclature and characterization standards. *Nat Commun* (2016) 7:12150. doi: 10.1038/ncomms12150

35. Swierczak A, Mouchemore KA, Hamilton JA, Anderson RL. Neutrophils: important contributors to tumor progression and metastasis. *Cancer Metastasis Rev* (2015) 34(4):735–51. doi: 10.1007/s10555-015-9594-9

36. Coffelt SB, Wellenstein MD, de Visser KE. Neutrophils in cancer: neutral no more. *Nat Rev Cancer* (2016) 16(7):431–46. doi: 10.1038/nrc.2016.52

37. Antonio N, Bønnelykke-Behrndtz ML, Ward LC, Collin J, Christensen IJ, Steiniche T, et al. The wound inflammatory response exacerbates growth of pre-neoplastic cells and progression to cancer. *EMBO J* (2015) 34(17):2219–36. doi: 10.15252/embj.201490147

38. Houghton AM, Rzymkiewicz DM, Ji H, Gregory AD, Egea EE, Metz HE, et al. Neutrophil elastase-mediated degradation of IRS-1 accelerates lung tumor growth. *Nat Med* (2010) 16(2):219–23. doi: 10.1038/nm.2084

39. Welch DR, Schissel DJ, Howrey RP, Aeed PA. Tumor-elicited polymorphonuclear cells, in contrast to "normal" circulating polymorphonuclear cells, stimulate invasive and metastatic potentials of rat mammary adenocarcinoma cells. *Proc Natl Acad Sci U S A* (1989) 86(15):5859–63. doi: 10.1073/pnas.86.15.5859

40. Spiegel A, Brooks MW, Houshyar S, Reinhardt F, Ardolino M, Fessler E, et al. Neutrophils suppress intraluminal NK cell-mediated tumor cell clearance and enhance extravasation of disseminated carcinoma cells. *Cancer Discovery* (2016) 6(6):630–49. doi: 10.1158/2159-8290.CD-15-1157

41. Feinauer MJ, Schneider SW, Berghoff AS, Robador JR, Tehranian C, Karreman MA, et al. Local blood coagulation drives cancer cell arrest and brain metastasis in a mouse model. *Blood* (2021) 137(9):1219–32. doi: 10.1182/blood.2020005710

42. Buccheri G, Ferrigno D, Ginardi C, Zuliani C. Haemostatic abnormalities in lung cancer: prognostic implications. *Eur J Cancer* (1997) 33(1):50–5. doi: 10.1016/S0959-8049(96)00310-3

43. Pavey SJ, Hawson GA, Marsh NA. Impact of the fibrinolytic enzyme system on prognosis and survival associated with non-small cell lung carcinoma. *Blood Coagul Fibrinolysis* (2001) 12:51–8. doi: 10.1097/00001721-200101000-00008

44. Seitz R, Rappe N, Kraus M, Immel A, Wolf M, Maasberg M, et al. Activation of coagulation and fibrinolysis in patients with lung cancer: relation to tumour stage and prognosis. *Blood Coagul Fibrinolysis* (1993) 4:249–54. doi: 10.1097/00001721-199304000-00006

45. Wojtukiewicz MZ, Zacharski LR, Moritz TE, Hur K, Edwards RL, Rickles FR, et al. Prognostic significance of blood coagulation tests in carcinoma of the lung and colon. *Blood Coagul Fibrinolysis* (1992) 3:429–37. doi: 10.1097/00001721-199203040-00010

46. Jones JM, McGonigle NC, McAnespie M, Cran GW, Graham AN. Plasma fibrinogen and serum c-reactive protein are associated with non-small cell lung cancer. *Lung Cancer* (2006) 53:97–101. doi: 10.1016/j.lungcan.2006.03.012

47. Zhao J, Zhao M, Jin B, Yu P, Hu X, Teng Y, et al. Tumor response and survival in patients with advanced non-small-cell lung cancer: the predictive value of chemotherapy-induced changes in fibrinogen. *BMC Cancer* (2012) 12:330. doi: 10.1186/1471-2407-12-330

48. Dzikowski L, Mirzaei R, Sarkar S, Kumar M, Bose P, Bellail A, et al. Fibrinogen in the glioblastoma microenvironmalet contributes to the invasiveness of brain tumor-initiating cells. *Brain Pathol* (2021) 31(5):e12947. doi: 10.1111/bpa.12947

49. Ek L, Gezelius E, Bergman B, Bendahl PO, Anderson H, Sundberg J, et al. Swedish Lung cancer study group (SLUSG). randomized phase III trial of low-molecular-weight heparin enoxaparin in addition to standard treatmalet in small-cell lung cancer: the RASTEN trial. *Ann Oncol* (2018) 29(2):398–404. doi: 10.1093/annonc/mdx716

50. Wood P, Boyer G, Mehanna E, Cagney D, Lamba N, Catalano P, et al. Intracerebral haemorrhage in patients with brain metastasis receiving therapeutic anticoagulation. *J Neurol Neurosurg Psychiatry* (2021) 9:jnnp–2020-324488. doi: 10.1136/jnnp-2020-324488

51. Leader A, Hamulyák EN, Carney BJ, Avrahami M, Knip JJ, Rozenblatt S, et al. Intracranial hemorrhage with direct oral anticoagulants in patients with brain metastasis. *Blood Adv* (2020) 4(24):6291–7. doi: 10.1182/bloodadvances.2020003238

frontiers | Frontiers in Oncology

TYPE Original Research
PUBLISHED 20 September 2023
DOI 10.3389/fonc.2023.1225170

OPEN ACCESS

EDITED BY
Lin Zhou,
Sichuan University, China

REVIEWED BY
Tao Hai,
Sichuan University, China
Feifei Na,
Sichuan University, China

*CORRESPONDENCE
Yunqiang Wang
wangyqzyy@163.com

†These authors have contributed equally to this work

RECEIVED 18 May 2023
ACCEPTED 31 August 2023
PUBLISHED 20 September 2023

CITATION
Jiang C, Liu X, Qu Q, Jiang Z and Wang Y (2023) Prediction of adenocarcinoma and squamous carcinoma based on CT perfusion parameters of brain metastases from lung cancer: a pilot study. *Front. Oncol.* 13:1225170. doi: 10.3389/fonc.2023.1225170

Prediction of adenocarcinoma and squamous carcinoma based on CT perfusion parameters of brain metastases from lung cancer: a pilot study

Chuncheng Jiang[1†], Xin Liu[2†], Qianqian Qu[2], Zhonghua Jiang[1] and Yunqiang Wang[1*]

[1]Department of Radiology, Yantai Hospital of Traditional Chinese Medicine, Yantai, Shandong, China, [2]Department of Oncology, Yantai Hospital of Traditional Chinese Medicine, Yantai, Shandong, China

Objectives: Predicting pathological types in patients with adenocarcinoma and squamous carcinoma using CT perfusion imaging parameters based on brain metastasis lesions from lung cancer.

Methods: We retrospectively studied adenocarcinoma and squamous carcinoma patients with brain metastases who received treatment and had been pathologically tested in our hospital from 2019 to 2021. CT perfusion images of the brain were used to segment enhancing tumors and peritumoral edema and to extract CT perfusion parameters. The most relevant perfusion parameters were identified to classify the pathological types. Of the 45 patients in the study cohort (mean age 65.64 ± 10.08 years; M:F = 24:21), 16 were found to have squamous cell carcinoma. Twenty patients were with brain metastases only, and 25 patients were found to have multiple organ metastases in addition to brain metastases. After admission, all patients were subjected to the CT perfusion imaging examination. Differences in CT perfusion parameters between adenocarcinoma and squamous carcinoma were analyzed. The receiver operating characteristic (ROC) curves were used to predict the types of pathology of the patients.

Results: Among the perfusion parameters, cerebral blood flow (CBF) and mean transit time (MTT) were significantly different between the two lung cancers (adenocarcinoma vs. squamous cell carcinoma: $p < 0.001$, $p = 0.012$.). Gender and tumor location were identified as the clinical predictive factors. For the classification of adenocarcinoma and squamous carcinoma, the model combined with CBF and clinical predictive factors showed better performance [area under the curve (AUC): 0.918, 95% confidence interval (CI): 0.797–0.979). The multiple organ metastasis model showed better performance than the brain metastasis alone model in subgroup analyses (AUC: 0.958, 95% CI: 0.794–0.999).

Conclusion: CT perfusion parameter analysis of brain metastases in patients with primary lung cancer could be used to classify adenocarcinoma and squamous carcinoma.

KEYWORDS

CT perfusion, brain metastasis, adenocarcinoma, squamous carcinoma, pathological type

Introduction

The most prevalent kind of cancer to spread to the brain is lung cancer, which affects 7%–10% of non-small cell lung cancer (NSCLC) patients at diagnosis and 20%–40% of NSCLC patients over time (1–3). Similar to primary lung cancer, the treatment plan for brain metastases should be chosen based on the pathological type. However, primary lung cancer often presents with faint borders and internal necrosis. Furthermore, brain metastases are often tiny and could spread throughout the brain. As a result, invasive biopsy or surgical excision for molecular testing is not always feasible (4). Therefore, developing a noninvasive imaging-based approach to assess the pathological type in patients with brain metastases from lung cancer is advisable.

CT perfusion imaging is a noninvasive functional imaging technique that reflects the hemodynamic changes in tumors with the foundation of enhanced CT (5, 6). In comparison to magnetic resonance imaging (MRI) perfusion imaging, it is insensitive to paramagnetic susceptibility artifacts, is more accessible, has shorter examination times, and has better patient tolerance. Moreover, in clinical practice, we have found that some patients undergo cranial CT scans first due to headaches, which subsequently reveal intracranial metastasis accompanied by lung lesions. Despite the generation of rays during use, CT perfusion imaging can provide higher image resolution and more perfusion parameters than MRI perfusion imaging. Previous studies based on different subtypes of primary lung cancer lesions had shown differences between CT perfusion parameters (7–9). Therefore, CT perfusion analysis is a potentially valuable approach that could be applied to identify pathological types.

However, studies on CT perfusion imaging of lung cancer had mainly focused on primary lung lesions, with fewer relevant studies on brain metastases. Moreover, overcoming or reducing the artifacts caused by respiratory movements had been a problem for us. For these purposes, we extracted perfusion parameters from brain metastasis CT images and aimed to establish a model based on perfusion parameters and clinical features to identify adenocarcinoma and squamous carcinoma.

Materials and methods

Patients

This study was approved by the ethics committee of Yantai Hospital of Traditional Chinese Medicine, Affiliated to Shandong University of Traditional Chinese Medicine. A total of 175 patients underwent CT perfusion examination from December 2019 to December 2021. The inclusion criteria included 1) primary NSCLC metastasis to the brain without a prior history of other tumors, 2) the patient's pathological type and immunohistochemistry are determined after surgery or biopsy, and 3) no neoadjuvant radiotherapy or chemotherapy specifically targeting brain metastases was performed prior to the CT perfusion examination. The exclusion criteria included 1) multiple primary tumors or other types of lung cancer, 2) no pathological type and immunohistochemical testing was performed, and 3) neoadjuvant radiotherapy or chemotherapy specifically targeting brain metastases was performed before the CT perfusion examination. Finally, 45 patients (mean age 65.64 ± 10.08 years) were enrolled in this study, including 29 cases of lung adenocarcinoma patients and 16 cases of lung squamous cell carcinoma patients (Figure 1).

Pathological type

All patients in this study underwent pathological tests for primary lung cancer. Lung biopsy or lung surgery was used to acquire tissue samples, which were then analyzed using a variety of therapeutically applicable molecular detection technologies, including immunohistochemistry and next-generation sequencing. The study included 29 patients with adenocarcinoma and 16 patients with squamous cell carcinoma.

CT perfusion image acquisition

We collected the CT perfusion images of lung adenocarcinoma and squamous cell carcinoma patients who were first diagnosed

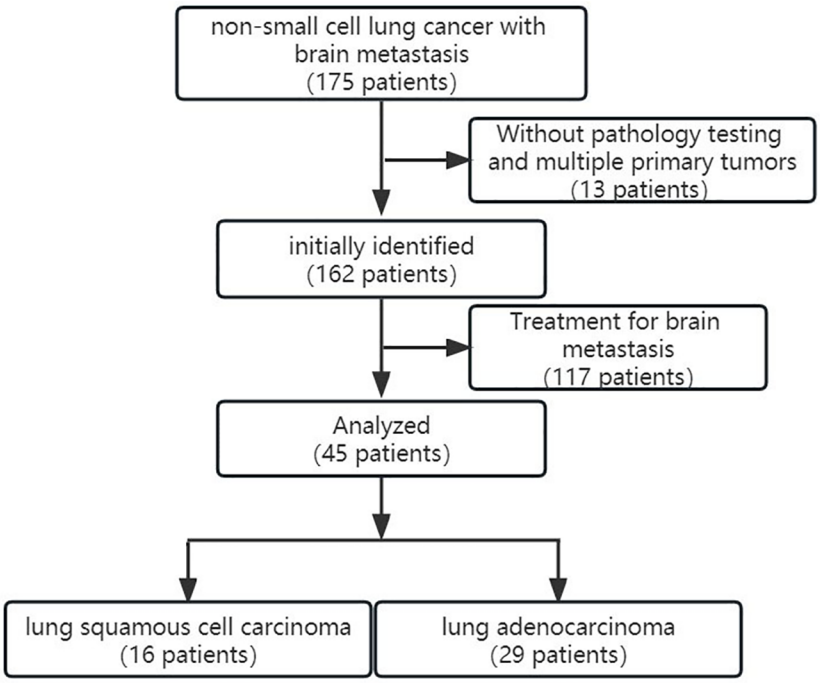

FIGURE 1
The inclusion and exclusion criteria and the patient enrollment flowchart.

with brain metastasis in our hospital. All patients were scanned by a 128-row 256-slice CT scanner (Brilliance iCT, Philips, Netherlands) for CT perfusion imaging. The high-pressure injector was MEDTRON (Germany). The CT perfusion imaging scheme was Philips jog mode. In this study, 70 mL of contrast agent (iopamidol 370 mgI/mL produced by Beilu Pharmaceutical Co., Ltd.) was injected by a high-pressure syringe through the median elbow vein. Injection flow rate 5 mL/s (4 mL/s for patients with poor vascular elasticity). The CT protocol included 15 spiral acquisitions in succession over the entire tumor before (first acquisition) and after (acquisitions 2–15) the delivery of the contrast material. The total perfusion scanning time was about 61.6 s. The following parameters were used for all acquisitions: tube voltage 80 kV, tube current 100 mAs, collimation 128 × 0.625 mm, and slice thickness 5 mm. The images were reconstructed to 2-mm thickness.

CT perfusion postprocessing

All images were processed using the Philips CT perfusion software (IntelliSpace Portal v6.0.5.02900). The processing flow was as follows: 1) Browsed all brain images to ensure the integrity of the collected data; 2) Adjusted the position of the mask midline to the brain midline; 3) Selected and adjusted the mask to cover all brain tissues; 4) Removed the mask, and the region of interest (ROI) was selected on the artery and vein (arterial: basilar artery as the reference standard; venous: sagittal sinus/transverse sinus as the reference standard); 5) ROIs were selected on brain metastasis.

Extraction of CT perfusion parameters

Two independent radiologists outlined the ROIs. One intracranial maximal metastasis was selected for each patient, and ROIs were outlined at the largest level of the metastases and its two consecutive layers above and below. Cases with significant discrepancies in certain subjective outlines were reviewed jointly by the supervising physician until an agreement was reached. Finally, the ROIs outlined by one of the radiologists were selected, and perfusion parameters are obtained by machine operations, including cerebral blood volume (CBV), cerebral blood flow (CBF), mean transit time (MTT), and time to peak (TTP). The averages of the three layers of perfusion parameters for each metastasis were used as the final valid parameters. Figure 2 demonstrated a case of lung adenocarcinoma brain metastasis with CT perfusion images and ROI outlined. To observe the reproducibility of perfusion parameter extraction, we randomly selected 10 patients to perform the intraclass correlation coefficient (ICC) test on the ROI outlined by two radiologists, and ICC ≥0.8 was considered as better reproducibility.

Data analysis

Statistical analysis was performed with SPSS (version 23.0); GraphPad Prism (version 8.0.2). The independent-sample t-test or Mann–Whitney U test was used to compare perfusion parameters. Measurement data were expressed as $\bar{x} \pm s$. The count data were

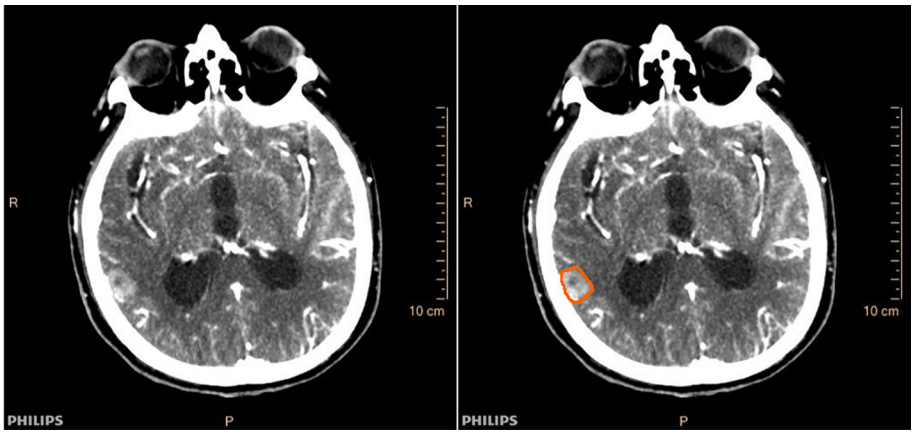

FIGURE 2
Cranial CT perfusion imaging (left) and region of interest (ROI) outline of intracranial metastases (right) in a patient (male, 78 years old) with brain metastases from lung adenocarcinoma.

expressed as n (%), and the chi-square test or Fisher's exact test was used. The ROC and AUC were used to assess the predicted energy efficiency of CT perfusion parameters. The DeLong test was used to compare the differences between different prediction models. $p < 0.05$ was considered statistically significant.

Results

Clinical features

Table 1 summarized the clinicopathological characteristics of 45 patients from the hospital archive electronic information system. Statistical analysis showed that age, smoking, metastasis number, maximum diameter of metastases, maximum diameter of tumor, T staging, N staging, and treatment were not significantly correlated with the pathological type. However, there were significant differences between adenocarcinoma and squamous carcinoma patients in terms of gender and location of the tumor ($p = 0.005$, $p = 0.017$).

Classification of NSCLC

The ICC of perfusion parameter extraction had achieved 0.83 between the two different radiologists. The CBF of brain metastasis in adenocarcinoma was significantly higher than that of squamous cell carcinoma ($p < 0.001$, Mann–Whitney U test), while the MTT of brain metastasis in adenocarcinoma was significantly lower ($p = 0.012$, independent-sample t-test) (Figure 3). The ROC curve analysis showed that the AUCs of CBF, MTT, clinical model, and clinical-CBF model in predicting pathological types were 0.845 [95% confidence interval (CI): 0.706–0.935], 0.722 (95% CI: 0.568–0.845), 0.792 (95% CI: 0.645–0.898), and 0.918 (95% CI: 0.797–0.979), respectively (Table 2, Figure 4). The DeLong test showed that there was a significant difference between the clinical-CBF model and MTT, clinical model ($p = 0.017$, $p = 0.018$) but showed no significant difference between the clinical-CBF model and CBF ($p = 0.112$). In subgroup analyses, the AUCs of the multiple organ metastasis model and the brain metastasis alone model were 0.958 (95% CI: 0.794–0.999) and 0.846 (95% CI: 0.617–0.966) (Table 3, Figure 5).

Discussion

In this study, we collected perfusion parameters from CT images of brain metastatic lesions. Subsequently, we used the perfusion parameters to build models for the classification of pathological types of the two most common cancers in NSCLC patients, namely, adenocarcinoma and squamous cell carcinoma. Our findings suggested that CT imaging-based perfusion parameters of brain metastases could be used as a noninvasive tool to distinguish pathological types of NSCLC.

Currently, the pathologic type of NSCLC remains an important basis for patient treatment and prognosis. With the progress of lung cancer treatment and research, some therapies and drugs, such as immune checkpoint inhibitors and targeted therapies, had shown better results in providing longer survival and better quality of life for patients with brain metastases of lung cancer. The prerequisite for these precise treatments is the clarification of the pathologic type.

Our study originally used a perfusion parameter approach to analyze CT images of brain metastatic lesions to classify adenocarcinoma and squamous carcinoma, whereas previous studies concentrated on using perfusion parameters of primary cancers. For example, Tacelli et al. (10) proved that CT perfusion imaging technology may, to some extent, reflect the creation of pulmonary capillaries and the ability of tumor metastasis and dispersion. Bevilacqua et al. (8) found that the BF of adenocarcinoma was significantly higher than that of squamous cell carcinoma, which may be used to guide treatment strategy. Chen et al. (7) used perfusion parameters from low-dose CT images of primary lesions to differentiate adenocarcinoma and squamous cell carcinoma. However, no significant difference was found.

TABLE 1 The clinicopathological characteristics of the 45 patients.

Characteristics	Type of lung cancer		*p*
	Lung adenocarcinoma (n =29)	Lung squamous cell carcinoma (n =16)	
Age, years[a]	65.24±10.25	66.38±10.04	0.722
Metastasis maximum diameter,cm[a]	1.45±0.31	1.52±0.27	0.704
Metastasis number,n(%)			0.509
1≤n≤3	21(72.41%)	13(81.25%)	
n>3	8(27.59%)	3(18.75%)	
Sex, n (%)			0.005*
Male	11(37.93%)	13(81.25%)	
Female	18(62.07%)	3(18.75%)	
Smoking, n (%)			0.373
Yes	13(44.83%)	11(68.75%)	
No	16(55.17%)	5(31.25%)	
Tumor maximum diameter,cm[a]	5.02±1.42	5.79±1.27	0.075
Location of tumor n (%)			0.017*
Central	11(37.93%)	12(75.00%)	
Peripheral	18(62.07%)	4(25.00%)	
T staging n (%)			0.492
T1+T2	6(20.69%)	2(12.50%)	
T3+T4	23(79.31%)	14(87.50%)	
N staging n (%)			0.372
N0+N1	9(31.03%)	3(18.75%)	
N2+N3	20(68.97%)	13(81.25%)	
Treatment n (%)			
None	22(75.86%)	13(81.25%)	0.561
Radiotherapy and/or Chemotherapy	5(17.24%)	3(18.75%)	
Targeted therapies	2(6.90%)	0	

[a]Mean ± SD.
*$p < 0.05$.

CT perfusion imaging plays an important role in evaluating patients with acute ischemic stroke (11–13). And there are still many challenges in diagnosing brain tumors. However, we believe that there are still clues to follow in distinguishing between intracranial metastases and intracranial primary tumors. First, CT perfusion imaging is based on contrast-enhanced CT scans, which can easily distinguish brain metastases that are more commonly located in the cerebral cortex and the cortical–subcortical junction. Second, brain metastases not only have a history of primary lung cancer but also exhibit characteristics such as small nodular lesions and significant edema, which can be easily differentiated on CT perfusion images. Recent research had shown that perfusion imaging has the ability to differentiate between brain metastases and intracranial primary tumors (14). Our CT perfusion imaging of brain metastases was based on two considerations. On one hand, primary lesions and metastases showed high consistency in pathological type. On the other hand, we believed that this approach can avoid lung breathing artifacts on perfusion parameters. Despite the fact that the pathology samples of the patients were collected from primary lung cancer, our CT perfusion analysis of brain metastases should still have merit. At first, approximately 10% of NSCLC patients have brain metastases diagnosed before lung cancer (15). A CT perfusion examination of their brain metastases prior to the primary lung cancer biopsy or resection specimen may provide significant information on the pathological type of their primary lung cancer. Second, in actual practice, the pathology of lung cancer may not always be available (16). In contrast to invasive biopsy or surgery for either the original lung cancer

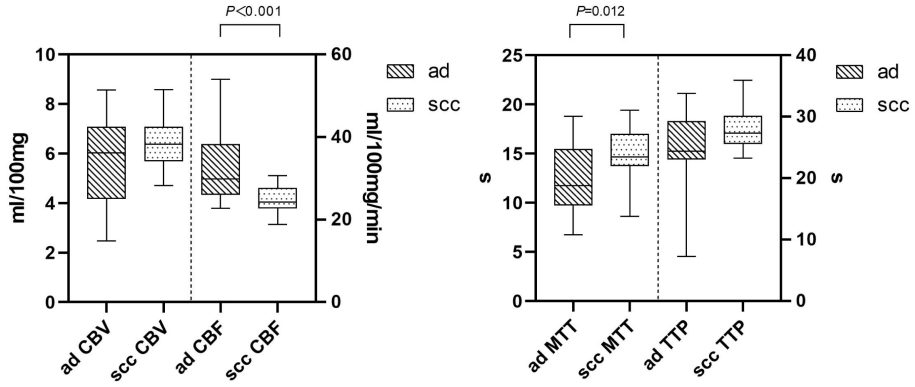

FIGURE 3
Comparison in CT perfusion parameters of brain metastases. The y-axis represents the unit, while the x-axis represents the perfusion parameters. The CBF of the brain metastasis in adenocarcinoma was significantly higher than that of squamous cell carcinoma (left). CBV stands for cerebral blood volume, and its unit is mL/100 mg. CBF stands for cerebral blood flow, and its unit is mL/100 mg/min. The MTT of the brain metastasis in adenocarcinoma was significantly lower than that of squamous cell carcinoma (right). MTT stands for mean transit time, and its unit is seconds (s). TTP stands for time to peak, and its unit is seconds (s). "ad" stands for adenocarcinoma of the lung, while "scc" stands for squamous cell carcinoma of the lung.

TABLE 2 Predictive performance of the four models.

	AUC (95% CI)	Sensitivity	Specificity
CBF	0.845 (0.706 - 0.935)	0.563	0.966
MTT	0.722 (0.568 - 0.845)	0.813	0.724
Clinical model	0.792 (0.645 - 0.898)	0.813	0.621
Clinical-CBF model	0.918 (0.797 - 0.979)	1.000	0.759

AUC, area under the curve; CBF, cerebral blood flow; CI, confidence interval; MTT, mean transit time.

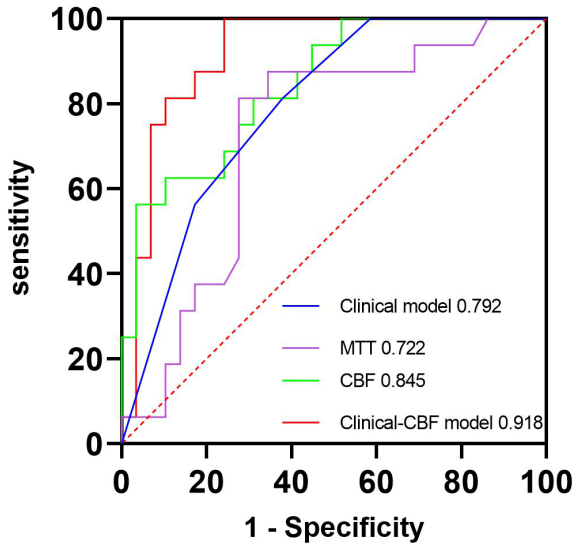

FIGURE 4
ROC curves of the clinical model, MTT, CBF, and clinical-CBF model. The blue line represents the clinical model, and its AUC is 0.792. The purple line represents the MTT parameter model, and its AUC is 0.722. The green line represents the CBF parameter model, and its AUC is 0.845. The red line represents the clinical combined with CBF model, and its AUC is 0.918. AUC, area under the curve; CBF, cerebral blood flow; MTT, mean transit time; ROC, receiver operating characteristic.

TABLE 3 Predictive performance of brain metastasis alone and multiple organ metastasis models.

	AUC (95% CI)	Sensitivity	Specificity
Brain metastasis alone model	0.846 (0.617 - 0.966)	0.714	0.923
Multiple organ metastasis model	0.958 (0.794 - 0.999)	1.000	0.875

AUC, area under the curve; CI, confidence interval.

or the brain metastases, brain CT perfusion scans are noninvasive and considerably easier to get. Third, in contrast to relying merely on primary lung cancer to predict the pathological type, the CT perfusion analysis of the brain metastases not only avoids the interference of respiratory movement but also serves as a helpful addition.

Our results were not directly comparable to previous correlative studies due to different perfusion approaches. However, some similar perfusion parameters could be used for reference, such as our study found that the CBF of adenocarcinoma was significantly higher than that of squamous cell carcinoma, which was similar to the study by Bevilacqua et al. (8) and suggested that adenocarcinoma patients would most benefit from antiangiogenic therapies. Our subgroup study showed that the multiple organ metastasis model exhibited a higher AUC than the brain metastasis alone model, which we believed may be due to the fact that multiple organ metastases imply a greater invasive capacity of the tumor and higher blood flow. Although adding clinical factors, our highest AUC for predicting pathological types showed no significant difference with the CBF model (0.918 vs. 0.845, $p = 0.112$), which may be caused by the small sample size. We believed that further studies with a larger sample size will surely make the prediction model more reliable.

Several limitations of our research should be noted. First, this study was retrospective, and we collected CT perfusion parameters from lung cancer brain metastases. Some confounding variables could not be sufficiently controlled. For example, patients who had good vascular elasticity arranged the 5 mL/s flow rate of contrast administration, while those with poor vascular elasticity patients arranged 4 mL/s. Furthermore, patients in our research cohort may have received different treatments for primary lung cancer before brain metastases. We lacked the statistical capacity to account for the impact of various treatment regimens on predictive modeling. Second, our results were based on a limited number of samples in a single center, and our models had not been validated with external data, which may lead to bias; therefore, conclusions driven by the potential predictive value of CT parameters should be taken with caution. Third, we delineated ROIs with larger brain metastases for the reason that tiny or cystic metastases may lead to unreliable results. Nevertheless, the results reported in this paper may be used as preliminary data to support prospective studies using CT perfusion parameters to classify pathological types in patients with brain metastases.

In summary, our study showed that CT perfusion parameters based on brain metastasis can be used as a noninvasive approach to classify adenocarcinoma and squamous carcinoma. To validate our

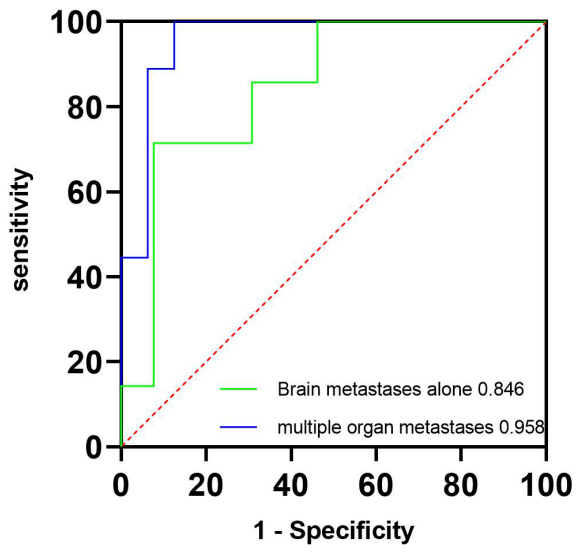

FIGURE 5
ROC curves of the multiple organ metastasis model and the brain metastasis alone model. The green line represents the brain metastasis alone model, and its AUC is 0.846. The blue line represents the multiple organ metastasis model, and its AUC is 0.958. AUC, area under the curve; ROC, receiver operating characteristic.

findings, future research should be carried out with a larger sample size, multicenter, and multiple clinical features.

Data availability statement

The raw data supporting the conclusions of this article will be made available by the authors, without undue reservation.

Ethics statement

The studies involving humans were approved by ethical committee of Yantai Hospital of Traditional Chinese Medicine Yantai Hospital of Traditional Chinese Medicine. The studies were conducted in accordance with the local legislation and institutional requirements. The ethics committee/institutional review board waived the requirement of written informed consent for participation from the participants or the participants' legal guardians/next of kin because accordance with the national legislation and the institutional requirements.

Author contributions

CJ, ZJ, and YW: study design. CJ, XL, and QQ: data collection. CJ, XL, and QQ: data processing. CJ and XL: manuscript writing. YW, ZJ: funding acquisition. All authors contributed to the article and approved the submitted version.

Funding

This study was supported by the Science and Technology Plan Project of Yantai (2022YD091, 2020YD053).

Conflict of interest

The authors declare that the research was conducted in the absence of any commercial or financial relationships that could be construed as a potential conflict of interest.

Publisher's note

All claims expressed in this article are solely those of the authors and do not necessarily represent those of their affiliated organizations, or those of the publisher, the editors and the reviewers. Any product that may be evaluated in this article, or claim that may be made by its manufacturer, is not guaranteed or endorsed by the publisher.

References

1. Franchino F, Rudà R, Soffietti R. Mechanisms and therapy for cancer metastasis to the brain. *Front Oncol* (2018) 8:161. doi: 10.3389/fonc.2018.00161

2. Jünger ST, Schödel P, Ruess D, Ruge M, Brand JS, Wittersheim M, et al. Timing of development of symptomatic brain metastases from non-small cell lung cancer: impact on symptoms, treatment, and survival in the era of molecular treatments. *Cancers (Basel).* (2020) 12(12):3618. doi: 10.3390/cancers12123618

3. Cacho-Díaz B, Cuapaténcatl LD, Rodríguez JA, Garcilazo-Reyes YJ, Reynoso-Noverón N, Arrieta O, et al. Identification of a high-risk group for brain metastases in non-small cell lung cancer patients. *J Neurooncol* (2021) 155(1):101–6. doi: 10.1007/s11060-021-03849-w

4. Cabibi D, Bellavia S, Giannone AG, Baracco N, Cipolla C, Martorana A, et al. TTF-1/p63-positive poorly differentiated NSCLC: A histogenetic hypothesis from the basal reserve cell of the terminal respiratory unit. *Diagnost (Basel).* (2020) 10(1):25. doi: 10.3390/diagnostics10010025

5. Huang C, Liang J, Lei X, Xu X, Xiao Z, Luo L. Diagnostic performance of perfusion computed tomography for differentiating lung cancer from benign lesions: A meta-analysis. *Med Sci Monit* (2019) 25(5):3485–94. doi: 10.12659/MSM.914206

6. Yue X, Dong X, Huang M, Yang H, Qian K, Yi C, et al. Early assessment of response to radiofrequency ablation with CT perfusion imaging in rabbit VX2 liver tumor model. *Front Oncol* (2021) 11:728781. doi: 10.3389/fonc.2021.728781

7. Chen ML, Wei YY, Li XT, Qi LP, Sun YS. Low-dose spectral CT perfusion imaging of lung cancer quantitative analysis in different pathological subtypes. *Transl Cancer Res* (2021) 10(6):2841–8. doi: 10.21037/tcr-20-3479

8. Bevilacqua A, Gavelli G, Baiocco S, Barone D. CT perfusion in patients with lung cancer: squamous cell carcinoma and adenocarcinoma show a different blood flow. *BioMed Res Int* (2018) 2018:6942131. doi: 10.1155/2018/6942131

9. Shi J, Schmid-Bindert G, Fink C, Sudarski S, Apfaltrer P, Pilz LR, et al. Dynamic volume perfusion CT in patients with lung cancer: baseline perfusion characteristics of different histological subtypes. *Eur J Radiol* (2013) 82 (12):e894–900. doi: 10.1016/j.ejrad.2013.08.023

10. Tacelli N, Remy-Jardin M, Copin MC, Scherpereel A, Mensier E, Jaillard S, et al. Assessment of non-small cell lung cancer perfusion: pathologic-CT correlation in 15 patients. *Radiology* (2010) 257(3):863–71. doi: 10.1148/radiol.10100181

11. Krishnan P, Murphy A, Aviv RI. CT-based techniques for brain perfusion. *Top Magn Reson Imag* (2017) 26(3):113–9. doi: 10.1097/RMR.0000000000000129

12. Wannamaker R, Buck B, Butcher K. Multimodal CT in acute stroke. *Curr Neurol Neurosci Rep* (2019) 19(9):63. doi: 10.1007/s11910-019-0978-z

13. Kim-Tenser M, Mlynash M, Lansberg MG, Tenser M, Bulic C, Jagadeesan B, et al. CT perfusion core and ASPECT score prediction of outcomes in DEFUSE 3. *Int J Stroke* (2021) 16(3):288–94. doi: 10.1177/1747493020915141

14. Yeung TP, Bauman G, Yartsev S, Fainardi E, Macdonald D, Lee TY, et al. Dynamic perfusion CT in brain tumors. *Eur J Radiol* (2015) 84(12):2386–92. doi: 10.1016/j.ejrad.2015.02.012

15. Nolan C, Deangelis LM. Overview of metastatic disease of the central nervous system. *Handb Clin Neurol* (2018) 149:3–23. doi: 10.1016/B978-0-12-811161-1.00001-3

16. Chen BT, Jin T, Ye N, Mambetsariev I, Daniel E, Wang T, et al. Radiomic prediction of mutation status based on MR imaging of lung cancer brainmetastases. *Magn Reson Imag* (2020) 69:49–56. doi: 10.1016/j.mri.2020.03.002

frontiers | Frontiers in Oncology

TYPE Original Research
PUBLISHED 17 October 2023
DOI 10.3389/fonc.2023.1251620

OPEN ACCESS

EDITED BY
Lin Zhou,
Sichuan University, China

REVIEWED BY
Raees Tonse,
Baptist Hospital of Miami, United States
Hongmin Chen,
Sichuan University, China

*CORRESPONDENCE
Oscar Arrieta
ogarrieta@gmail.com

RECEIVED 31 July 2023
ACCEPTED 18 September 2023
PUBLISHED 17 October 2023

CITATION
Arrieta O, Bolaño-Guerra LM, Caballé-Pérez E, Lara-Mejía L, Turcott JG, Gutiérrez S, Lozano-Ruiz F, Cabrera-Miranda L, Arroyave-Ramírez AM, Maldonado-Magos F, Corrales L, Martín C, Gómez-García AP, Cacho-Díaz B and Cardona AF (2023) Perilesional edema diameter associated with brain metastases as a predictive factor of response to radiotherapy in non-small cell lung cancer. *Front. Oncol.* 13:1251620. doi: 10.3389/fonc.2023.1251620

Perilesional edema diameter associated with brain metastases as a predictive factor of response to radiotherapy in non-small cell lung cancer

Oscar Arrieta[1*], Laura Margarita Bolaño-Guerra[1], Enrique Caballé-Pérez[1], Luis Lara-Mejía[1], Jenny G. Turcott[1], Salvador Gutiérrez[1], Francisco Lozano-Ruiz[2], Luis Cabrera-Miranda[1], Andrés Mauricio Arroyave-Ramírez[3], Federico Maldonado-Magos[4], Luis Corrales[5], Claudio Martín[6], Ana Pamela Gómez-García[1], Bernardo Cacho-Díaz[7] and Andrés F. Cardona[8]

[1]Thoracic Oncology Unit, Department of Thoracic Oncology, Instituto Nacional de Cancerología (INCan), México City, Mexico, [2]Radioncology Department, Hospital Medica Sur, México City, Mexico, [3]Medical Oncology Department, Hospital Medica Sur, México City, Mexico, [4]Radiotherapy Unit, Instituto Nacional de Cancerología (INCan), México City, Mexico, [5]Oncology Department, Hospital San Juan de Dios, San José, Costa Rica, [6]Thoracic Oncology Unit, Alexander Fleming Institute, Buenos Aires, Argentina, [7]Neuro-oncology Unit, Instituto Nacional de Cancerología (INCan), México City, Mexico, [8]Direction of Research and Education, Luis Carlos Sarmiento Angulo Cancer Treatment and Research Center - Cancer Treatment and Research Cente (CTIC), Bogotá, Colombia

Background: Different prognostic scales exist in patients with brain metastasis, particularly in lung cancer. The Graded Prognostic Assessment for lung cancer using molecular markers (Lung-molGPA index) for brain metastases is a powerful prognostic tool that effectively identifies patients at different risks. However, these scales do not include perilesional edema diameter (PED) associated with brain metastasis. Current evidence suggests that PED might compromise the delivery and efficacy of radiotherapy to treat BM. This study explored the association between radiotherapy efficacy, PED extent, and gross tumor diameter (GTD).

Aim: The aim of this study was to evaluate the intracranial response (iORR), intracranial progression-free survival (iPFS), and overall survival (OS) according to the extent of PED and GT.

Methods: Out of 114 patients with BM at baseline or throughout the disease, 65 were eligible for the response assessment. The GTD and PED sum were measured at BM diagnosis and after radiotherapy treatment. According to a receiver operating characteristic (ROC) curve analysis, cutoff values were set at 27 mm and 17 mm for PED and GT, respectively.

Results: Minor PED was independently associated with a better iORR [78.8% vs. 50%, OR 3.71 (95% CI 1.26–10.99); p = 0.018] to brain radiotherapy. Median iPFS was significantly shorter in patients with major PED [6.9 vs. 11.8 months, HR 2.9

(95% CI 1.7–4.4); $p < 0.001$] independently of other prognostic variables like the Lung-molGPA and GTD. A major PED also negatively impacted the median OS [18.4 vs. 7.9 months, HR 2.1 (95% CI 1.4–3.3); $p = 0.001$].

Conclusion: Higher PED was associated with an increased risk of intracranial progression and a lesser probability of responding to brain radiotherapy in patients with metastatic lung cancer. We encourage prospective studies to confirm our findings.

KEYWORDS

central nervous system, tumor diameter, perilesional edema, lung adenocarcinoma, lung cancer, local therapy, radiation therapy

1 Introduction

Lung cancer (LC) is the leading cause of cancer-related mortality worldwide, with 1.8 million deaths in 2020 and an estimated incidence of 2.2 million (1). Non-small cell lung cancer (NSCLC) represents 85% of LC cases and is the leading cause of brain metastases (BM) (2). Patients with oncogenic driver alterations own the highest cumulative incidences of BM, with a lifetime prevalence between 46% and 80% (3, 4). Other factors associated with a higher BM incidence are the adenocarcinoma subtype, solid predominant tumors (5), disease burden, and carcinoembryonic antigen (CEA) levels (6).

In patients with LC, BM is associated with significant morbidity, mortality, reduced quality of life, and a substantial economic burden (7–9). Some Latin American regions have barriers to LC attention, increasing the mortality of patients with BM (10). Whole-brain radiation therapy (WBRT) has been the standard approach for local control in LC patients, and it remains the preferred modality in case of multiple lesions or symptomatic disease, with a significant improvement in symptom relief, local and distant recurrences, and response rates of 70%–93% (11–13). Nevertheless, WBRT is associated with detrimental effects on cognitive function, no overall survival (OS) benefit, and a median OS of 3–6 months (14).

Stereotactic radiosurgery (SRS) has emerged as a radiation modality for a limited number and size of BM, with high rates of local control comparable with WBRT, lower incidence of neurocognitive effects, and increased overall quality of life (11). Despite the broad introduction of target therapy and immunotherapy in actionable and non-actionable driver gene NSCLC, WBRT remains the most common upfront radiotherapy modality with extremely heterogeneous clinical outcomes (14–16). However, considering the current high effectiveness of CNS-penetrant systemic treatments and novel radiotherapy techniques, selecting patients suitable for local therapy has become controversial.

Extensive efforts have focused on predicting survival outcomes for NSCLC with BM. In this context, several prognostic indexes, such as Recursive Partitioning Analysis (RPA), Graded Prognostic Assessment (GPA) (17, 18), and recently an update of the Disease-Specific GPA using molecular markers (Lung-molGPA index), which introduced EGFR, ALK, and PD-L1 status (19, 20), have been developed to estimate survival and guide clinical decision-making. Nevertheless, limited advances in clinical predictors of radiation therapy response in patients with BM-NSCLC have been studied (11).

The PED has been linked to hypoxia, and HIF1α production promotes pro-angiogenic pathways and the induction of neovascularization, which limits response to radiation therapy (21). In this regard, perilesional edema diameter (PED) has been associated with worse radiological responses and increased risk of new brain lesions in patients with NSCLC (22, 23). A clinical surrogate marker of a radioresistant phenotype might represent a potential predictive factor associated with treatment failure that could help to design highly effective strategies at a central nervous system (CNS) level, minimizing toxicity and extending survival. This study aimed to evaluate the impact of PED on the intracranial response (iORR) and their association with survival outcomes in NSCLC patients with BM receiving radiation therapy.

2 Materials and methods

2.1 Patient selection

An institutional research committee reviewed and approved the study under project 2021/054.

A retrospective cohort study was conducted between 2014 and 2021. The clinical characteristics, histopathological diagnostic, molecular status, and systemic treatment details were examined through shared medical records. Eligible patients were those with recurrent or metastatic histologically proven NSCLC and measurable intracranial disease according to the Response Assessment in Neuro-oncology (RANO) working group criteria (24), and those who underwent radiation therapy after BM diagnosis. The RANO criteria define measurable disease as bidimensional contrast-enhancing lesions with defined margins,

with two perpendicular diameters of at least 10 mm, visible on ≥2 axial slices. Patients with previous local BM-directed treatment (including surgical resection or former radiation treatment), meningeal carcinomatosis, and lack of baseline MRI were omitted.

2.2 MRI acquisition and measurements

All MRI scans were performed on a 1.5-T Signa HDxt scanner (GE Healthcare). Routine MRI pulse sequences included axial T1-, T2-weighted, and fluid-attenuated inversion recovery (FLAIR). A radiation oncologist evaluated baseline neuroimaging features before local therapy. The most representative images were selected based on tumor maximum diameter and maximum edema extent on midplane axial, sagittal, or coronal sections. GT was established as the sum of the maximum diameter (mm) of the three most representative T1-weighted gadolinium-enhanced lesions. In contrast, PED was defined as the sum of the maximum diameter (mm) of the perilesional hyperintense area on a T2-weighted or FLAIR MRI sequence. The PED/GT ratio was calculated by dividing the PED maximum extent by the maximum tumor diameter. Figure 1 provides guidance on how clinicians performed the measuring method in this study, which could help to incorporate PED in further treatment decisions.

2.3 Radiation treatment

Treatment decisions were made on a case-by-case basis by a multidisciplinary tumor board. SRS was performed on the Gamma Knife Radiosurgery platform (Elekta, Stockholm, Sweden). Treatment plans were generated from thin-slice MRI merged with a stereotactic computed tomography scan. SBRT was delivered in cases with up to four intra-axial metastatic lesions, and the regimen was a single dose of 18–24 Gy, resulting in an equivalent dose (EQD2) of 42–68 Gy. The prescription could vary on tumor size and location according to the RTOG-90-05 protocol (25).

Whole brain radiation therapy (WBRT) was delivered as a palliative therapy with a conventional megavoltage external beam radiotherapy administered with a linear accelerator (energy 6 MV). According to the institutional protocol, for all patients treated with WBRT, the regimen was 30 Gy in 10 fractions, resulting in an EQD2 of 32.5 Gy and a biologically effective dose (BED) of 39 Gy, estimated with an alpha/beta ratio of 10. An expert radio-oncologist prescribed hippocampal avoidance, corticosteroid dose, and duration courses.

2.4 Outcome measures

The main outcome was the intracranial objective response rate (iORR), defined as the proportion of patients who achieved complete response (CR) and partial response (PR) according to the RANO criteria. Secondary outcomes included the intracranial clinical benefit rate (iCBR) determined as the sum of CR, PR, and stable disease (SD); intracranial duration of response (iDoR) defined as the time from radiation therapy to intracranial progression or death; and depth of response (iDpR) defined as the percentage of maximal tumor reduction from the baseline of intracranial target lesions. Patients were grouped into four quartiles based on the most significant proportion of reduction in intracranial target lesions from the baseline. They were compared with patients with no tumor reduction (NTR). A brain contrast-enhanced MRI was performed at baseline and 8 to 12 weeks after radiation therapy, then every 4 to 6 months or as clinically indicated. An independent radiation oncologist reviewed all response assessments. Intracranial progression-free survival (iPFS) was defined as the time from radiation therapy until intracranial progression or death. OS was defined as the time from radiation treatment until death from any cause.

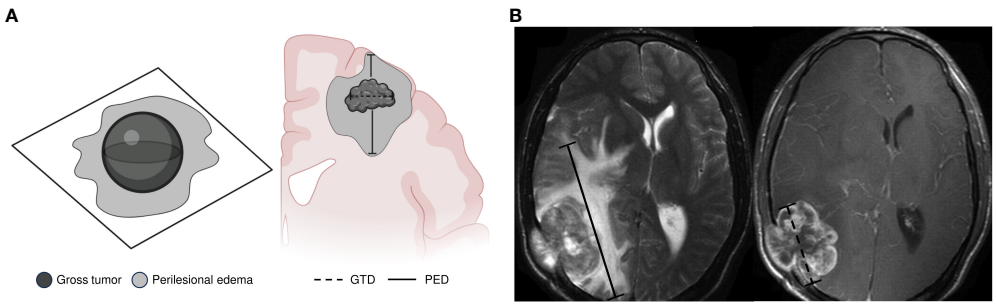

FIGURE 1
Method used for measuring peritumoral edema extent. We selected the most representative images based on the tumor's maximum diameter and maximum edema extent on midplane axial, sagittal, or coronal sections. **(A)** Gross tumor (GT) was established as the sum of the maximum diameter (mm) of the three most representative T1-weighted gadolinium-enhanced lesions. Perilesional edema (PE) was defined as the sum of the maximum diameter (mm) at the perilesional hyperintense area on a T2-weighted or FLAIR MRI sequence. **(B)** Examples of perilesional edema diameter (PED) measurement on MRI FLAIR sequences (axial) and gross tumor diameter (GTD) measurement on MRI T1 gadolinium-enhanced scans (axial). GT was established as the sum of the maximum diameter of the three most representative lesions. PED was defined as the sum of the maximum diameter of the perilesional hyperintense area. Dotted black lines indicate the maximum GTD in millimeters (mm). Solid black lines indicate the maximum PED in mm. The PED/GT ratio was calculated by dividing the PED maximum extent by the maximum tumor diameter. GT, gross tumor; GTD, gross tumor diameter; PED, perilesional edema diameter.

2.5 Statistical analysis

Continuous variables were summarized as arithmetic means with standard deviations or medians with their respective interquartile range. Categorical variables were reported as numbers and percentages. Comparisons between two independent groups were made using the Student's *t*-test or nonparametric Mann–Whitney *U*-test, according to data distribution determined by the Kolmogorov–Smirnov test. The chi-square test (χ^2) and the Fisher exact test assessed the differences between the categorical variables as a function of the size of the groups within the comparisons. The quantitative variables were defined as pre-established dichotomous variables and were modeled using bivariate and multivariate logistic regression. The performance of PED and GT diameters to discriminate iORR was assessed by receiver operating characteristic (ROC) curve analyses. Cutoff values were optimal when the product of sensitivity and specificity was maximal. Cutoff point values discriminate between major and minor lesions (mm) related to the edema and tumor. The results were presented as odds ratios (ORs) with corresponding 95% confidence intervals (CIs) and *p*-values and were modeled using bivariate and multivariate logistic regression. Progression-free survival and OS results were analyzed using the Kaplan–Meier estimate, whereas the log-rank test was used to estimate differences among subgroups. All variables were dichotomized for the survival analysis. Predefined variables were chosen for the adjusted multivariate Cox regression model. Hazard ratios (HRs) and their corresponding 95% CIs were calculated to measure association. Statistical significance was set at a p-value ≤ 0.05, two-tailed. All statistical analyses were conducted using Stata/MP 14.0 for Mac (Stata Corp LP, 2015), and GraphPad Prism 9.0.1 for macOS (GraphPad Software, 2021) was used for plotting.

3 Results

A total of 114 patients with NSCLC and BM diagnosis were identified and eligible for the analysis (Figure S1). Patients' baseline clinical and pathological characteristics and the Lung-molGPA index are summarized in Table 1. The mean age was 57.5 ± 12.4 years, and 62 (54.4%) were men. At BM diagnosis, 70 (61.4%) patients had a Karnofsky Performance Status (KPS) of ≤80. The most common histological subtype was adenocarcinoma [98 (86.0%)]; 33 (28.9%) patients harbored a sensitive EGFR mutation (del exon 19 or L858R) or an ALK rearrangement. Only 51 (44.7%) patients had a Lung-molGPA score ranging from 1.5 to 2. Additionally, 83 (72.8%) had multiple lesions in brain MRI, with a median of 2 (1–5) brain lesions. Among these, 43 (37.7%) had five or more BM at diagnosis, and 79 (69.3%) were in the supratentorial compartment. Steroids were employed in 48 (42.1%) of the 114 cases at baseline MRI evaluation. At the MRI response assessment, 28 (43.1%) of the 65 patients used steroids. WBRT was used in 103 (90.4%) patients and SRS in 11 (9.6%). The median prednisone dose did not significantly affect the entire court or between the two groups.

3.1 Discriminating values of gross tumor diameter and perilesional edema diameter as potential predictive factors

The best discriminating GTD cutoff value was 17 mm, with a sensitivity of 26.1% and a specificity of 76.2% [AUC = 0.658 (0.44–0.73)] (Figure S2A). The best discriminating PED cutoff value for iORR was 27 mm, with a sensitivity of 34.8% and a specificity of 73.8% [AUC = 0.60 (0.46–0.75)] (Figure S2B).

3.2 Major perilesional edema diameter and clinical characteristics

A major PED (≥27 mm) was identified in 63 (55.2%) patients and was significantly associated with male patients, KPS ≤ 80, multiple brain lesions located in the supratentorial compartment, and more use of steroids at diagnosis. From patients with major PED, 61 (59.2%) were treated mainly with WBRT, and 11 (44.4%) had a Lung-MolGPA score of 0–1. Patients with a PED ≥27 mm had a median GTD larger than those with PED < 27 mm (40.6 vs. 17.0 mm) (Table 1).

3.3 Intracranial objective response rate

The iORR was assessed by a post-RT MRI within 8–12 weeks, and post-radiation therapy was available in 65 (57.0%) cases of the entire cohort. The investigator-assessed iORR was 64.6%. The iORR was significantly higher among patients with minor PED [78.8% vs. 50.0%, OR 3.71 (1.26–10.99; $p = 0.018$)]; however, the GTD showed no significant association (Figures 2A, B). In the bivariate analysis, only a minor PED was associated with better intracranial responses [OR 3.71, (95% CI 1.26–10.99); $p = 0.018$) (Figure 2C).

Partial response was reached in 35 (53.8%) patients and showed no significant difference between PED subgroups. Patients who responded utterly belonged to the minor PED subgroup (21.2%, $p < 0.006$). The median iDoR was 9.5 (4.5–14.5) months, with 36 (55.4%) patients achieving a durable response ≥ 6 months. When PED subgroups were compared, the median iDoR was longer in those with a minor PED [13.3 (5.9–20.7) vs. 4.5 (1.2–7.9); $p < 0.001$]. The proportion of patients with a durable response ≥ 6 months favored the subgroup with a minor PED [24 (72.7%) vs. 12 (37.5%), $p = 0.004$]. In patients with any reduction of tumor diameter, DpR was more pronounced among cases with a minor PED. A tumor reduction ≥ 75% was only observed in the subgroup with a minor PED [8(24.2%); $p = 0.006$] (Table 2). The maximum percentage change in target lesion size after radiotherapy according to the PED size at baseline is summarized in Figure 3A.

3.4 Intracranial progression-free survival

At the data cutoff (22 July 2022), the median follow-up time was 10.2 [3.2–18.9] months. The median iPFS was 8.9 months [7.3–10.5], and the 6-month iPFS rate was 57.0% for the entire cohort ($n = 114$).

10.3389/fonc.2023.1251620

TABLE 1 Demographic and histological characteristics of patients.

		Overall	Perilesional edema diameter (PED), mm		*p*-value
			Minor PED <27	Major PED ≥27	
Patients		*n* = 114	*n* = 51	*n* = 63	
Age, years	<65	78 (68.4)	36 (70.6)	42 (66.7)	
	≥65	36 (31.6)	15 (29.4)	21 (33.3)	
		57.5 ± 12.4	56.8 ± 12.3	58.1 ± 12.5	0.581
Sex	Female	52 (45.6)	32 (62.7)	20 (31.7)	
	Male	62 (54.4)	19 (37.3)	43 (68.3)	**0.001**
KPS at BM diagnosis	90–100	44 (38.6)	31 (60.8)	13 (20.6)	
	≤80	70 (61.4)	20 (39.2)	50 (79.4)	**<0.001**
BM occurrence	Synchronous	77 (67.5)	31 (60.8)	46 (73.0)	
	Metachronous	37 (32.5)	20 (39.2)	17 (27.0)	0.165
Smoking status	Present	58 (50.9)	20 (39.2)	38 (60.3)	
	Absent	56 (49.1)	31 (60.8)	25 (39.7)	0.025
Histology	Adenocarcinoma	98 (86.0)	48 (94.1)	50 (79.4)	
	Squamous cell carcinoma	7 (6.1)	1 (2.0)	6 (9.5)	
	Other	9 (7.9)	2 (4.0)	7 (8.3)	0.236
Adenocarcinoma classification	Lepidic	9 (7.9)	5 (10.4)	4 (8.0)	
	Acinar	34 (29.8)	18 (37.5)	16 (32.0)	
	Papillary	13 (11.4)	7 (14.6)	6 (12.0)	
	Micropapillary	4 (3.5)	1 (2.1)	3 (6.0)	
	Solid	35 (30.7)	16 (33.3)	19 (38.0)	
	NOS	3 (2.6)	1 (2.1)	2 (4.0)	0.869
Mutation status	Wild type/Unknown	81 (71.1)	27 (52.9)	54 (85.7)	
	EGFR/ALK-positive	33 (28.9)	24 (47.1)	9 (14.3)	**<0.001**
Lung-molGPA index	0.0–1.0	33 (28.9)	5 (9.8)	28 (44.4)	
	1.5–2.0	51 (44.7)	26 (51.0)	25 (39.7)	
	2.5–3.0	26 (22.8)	16 (31.4)	10 (15.9)	
	3.5–4.0	4 (7.8)			**<0.001**
Number of BM	1	31 (27.2)	20 (39.2)	11 (17.5)	
	2–4	40 (35.1)	17 (33.3)	23 (36.5)	
	≥5	43 (37.7)	14 (27.5)	29 (46.0)	**0.023**
BM location	Supratentorial	79 (69.3)	41 (80.4)	38 (60.3)	
	Infratentorial	35 (30.7)	10 (19.6)	25 (39.7)	**0.021**
Steroids at baseline MRI evaluation	Present	48 (42.1)	12 (23.5)	36 (57.1)	
	Absent	66 (57.9)	39 (76.5)	27 (42.9)	**<0.001**
Steroids at MRI response assessment (*n* = 65)	Present	28 (43.1)	11 (33.3)	17 (53.1)	
	Absent	37 (59.9)	22 (66.7)	15 (46.)	**0.087**

(Continued)

10.3389/fonc.2023.1251620

TABLE 1 Continued

		Overall	Perilesional edema diameter (PED), mm		*p*-value
			Minor PED <27	Major PED ≥27	
Median dose of prednisone at MRI response assessment (*n* = 65)		15.0 [5.0–25.0]	20.0 [5.0–45.0]	5.0 [5.0–20.0]	**0.578***
RT modality	WBRT	103 (90.4)	42 (40.8)	61 (59.2)	
	SRS	11 (9.6)	9 (17.6)	2 (3.2)	**0.012‡**
Median gross tumor diameter (GTD), mm		28.1 [15.7–49.1]	17.0 [9.1–26.2]	40.6 [27.5–60.6]	**<0.001***

Data are reported as numbers and percentages, n (%), otherwise as mean ± standard deviation or median with interquartile range [IQR]. Normal distribution was tested by Kolmogorov–Smirnoff. Normal distribution assuming not equal variances was analyzed using independent-samples Student´s t-test; otherwise, *Mann–Whitney U-test was applied. Nominal variables were analyzed by the Pearson Chi-Square test, except where a small size (n < 5) was required using ‡ Fisher's exact test. Two-tailed significance was set at p ≤ 0.05 (bold values). ALK, anaplastic lymphoma kinase; BM, brain metastases; EGFR, epidermal growth factor receptor; KRAS, Kirsten rat sarcoma viral oncogene homolog; KPS, Karnofsky performance status; Lung-molGPA, Graded Prognostic Assessment for NSCLC using molecular markers; RT, radiotherapy; WBRT, whole-brain radiotherapy; SRS, stereotactic radiosurgery. SD, standard deviation. IASLC/ATS/ERS Lung Adenocarcinoma classification (n = 98).

According to the extension of PED, median PFS was 11.8 (8.3–15.3) months in the group with a minor PED versus 6.9 (3.5-10.2) months in those with a major PED [HR 2.9 (1.7–4.4); $p < 0.001$] (Figure 3B).

The 6-month iPFS rate was also higher in the minor PED subgroup, 73.5% versus 41.5%, p <0.001, respectively. On bivariate analysis, factors associated with a higher hazard for intracranial progression or death were male patients, a Lung-molGPA index of 0–1 and 1.5–2.0, infratentorial lesions, major PED, and no tumor response to radiotherapy (Table 3).

Multivariate analysis showed that only the Lung-mol GPA and the PED were significant factors associated with the risk of intracranial progression. After the adjustment for significant factors in model 1, a major PED remained a negative risk factor for intracranial progression [HR 3.3 (95% CI 1.6–5.8)] independently of Lung-molGPA [Index of 0–1 HR 34.8 (95% CI 3.9–31.0); and 1.5–2.0 HR 9.9 (95% CI 1.24–79.6)]. In contrast, the GTD <17 mm became a protective factor for intracranial progression [HR 0.51 (95% CI 0.27–0.96)] after the adjustment (Table 3). A second multivariate model was built for progression and survival with the components of the Lung-molGPA displayed separately in Table S1. The major PED continued to be a negative factor for intracranial progression.

3.5 Overall survival

The median OS was 11.8 [95% CI 7.9–15.7] months, with a 6-month OS rate of 64.9% for the entire population. According to

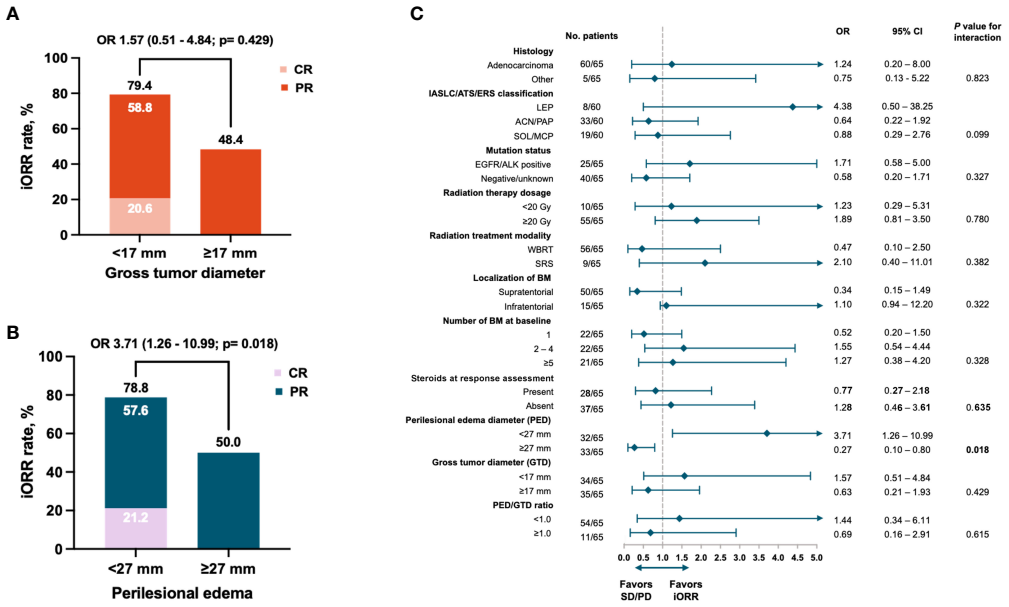

FIGURE 2
Intracranial response rate according to **(A)** gross tumor diameter, **(B)** Perilesional edema diameter, and **(C)** Forest plot of odds ratios random effects for ICR. Black diamonds and horizontal lines correspond to the ORs and 95% confidence intervals. The two-way solid arrow at the bottom of the graph represents the combined odds ratio and 95% confidence interval. The dotted vertical line corresponds to no effect of response to treatment (odds ratio 1.0). Two-tailed P values ≤ 0.05 were considered statistically significant (Bold values). CR, complete response; PR, partial response; SD, stable disease; PD, progressive disease; PED, perilesional edema diameter; GTD, gross tumor diameter.

10.3389/fonc.2023.1251620

TABLE 2 Intracranial response in evaluable population.

	Overall	Perilesional edema diameter (PED)		*p*-Value
		<27 mm	≥27 mm	
Patients	*N* = 65	*N* = 33	*N* = 32	
Investigator-assessed response				
Intracranial objective response (iORR)	42 (64.6)	26 (78.8)	16 (50.0)	**0.015**
Complete response (CR)	7 (10.7)	7 (21.2)		**0.006**
Partial response (PR)	35 (53.8)	19 (57.6)	16 (50.0)	0.540
Stable disease (SD)	15 (23.0)	5 (15.2)	10 (31.3)	0.124
Progressive disease (PD)	8 (12.3)	2 (6.1)	6 (18.8)	0.120
Intracranial disease control rate (iDCR)	57 (87.7)	31 (93.9)	26 (81.3)	0.120
iDoR median (95% IC), mo	9.5 [4.5–14.5]	13.3 [5.9–20.7]	4.5 [1.2–7.9]	**<0.001**
Durable response (CR + PR) ≥6 mo	36 (55.4)	24 (72.7)	12 (37.5)	**0.004**
Depth of response (DpR) category				
NTR	8 (12.3)	3 (9.1)	5 (15.6)	0.423
Q1 > 0% to 25%	10 (15.4)	3(9.1)	7 (21.9)	0.153
Q2 > 25% to 50%	23 (35.4)	8 (24.2)	15 (46.9)	0.056
Q3 > 50% to 75%	16 (24.6)	11 (33.3)	5 (15.6)	0.098
Q4 > 75% to 100%	8 (12.3)	8 (24.2)		**0.003**

Data are reported as numbers and percentages, n (%). Two-tailed significance was set at p ≤ 0.05 (bold values). CNS, central nervous system; iORR, intracranial objective response rate; CBR, clinical benefit rate; BOR, best overall response rate; iDoR, duration of intracranial response; DpR, depth of response; NTR, no tumor reduction; mo, month.

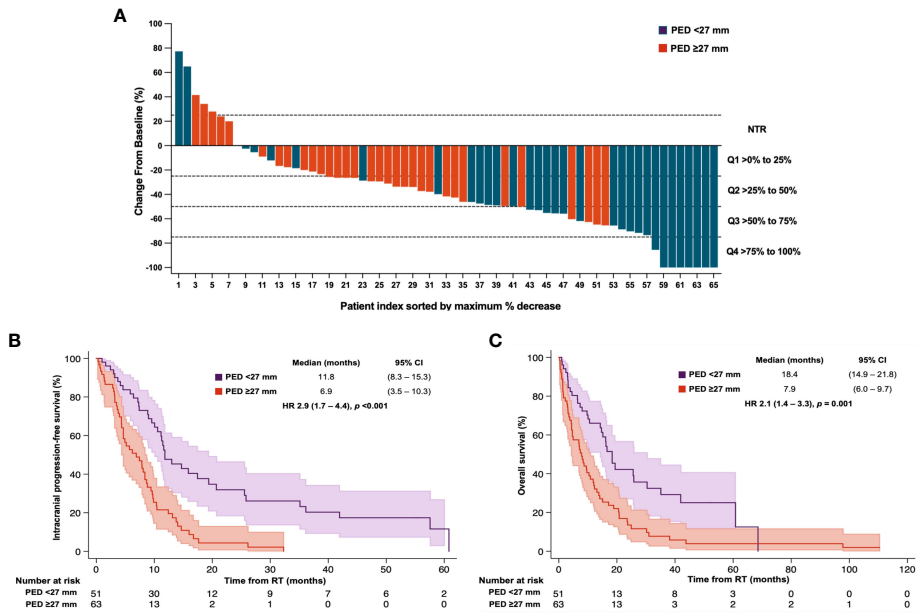

FIGURE 3
Intracranial responses according to the perilesional edema diameter. **(A)** CNS depth of intracranial responses according to the PED diameter. The Kaplan-Meier plot assessed the PED after radiotherapy according to **(B)** progression-free survival and **(C)** overall survival. MV analysis: PED (>27 mm) remained significant for 8 CNS PFS after the adjustment for sex, Lung-molGPA score, and gross tumor diameter. Cut Off PED was set at <27mm and ≥27mm. Two-tailed P values ≤ 0.05 were considered statistically significant (Bold values). PED, perilesional edema diameter; GTD, gross tumor diameter.

10.3389/fonc.2023.1251620

TABLE 3 Bivariate and multivariate analysis (model 1) of progression-free and overall survival.

	Progression-free survival						Overall survival					
	Bivariate analysis			Multivariate analysis			Bivariate analysis			Multivariate analysis		
	HR	95 CI%	*p*	HR	95 CI%	*p*	HR	95 CI%	*p*	HR	95 CI%	*p*
Sex												
Female	0.47	0.30–0.72		0.646	0.37-1.10	0.111	0.55	0.36–0.85		1.0		
Male	2.15	1.37–3.36	**0.001**	1.0			1.81	1.18–2.77	**0.006**	1.21	0.70–2.08	0.486
IASLC/ATS/ERS adenocarcinoma subtype												
LEP	0.64	0.29–1.40					0.69	0.30–1.60		1.0		
ACI/PAP	1.01	0.64–1.60					0.78	0.49–1.23		0.869	0.50–1.48	0.607
SOL/MIP	1.20	0.75–1.89	0.265				1.49	0.94–2.38	0.089	1.56	0.59–4.09	0.364
Lung-molGPA index												
0.0–1.0	3.81	2.25–6.45		34.85	3.91-310.6	**0.001**	5.27	3.26–8.54		11.89	2.27–62.2	**0.003**
1.5–2.0	1.56	1.02–2.41		9.93	1.24-79.6	**0.031**	1.32	0.86–2.02		3.61	0.80–16.2	0.95
2.5–3.0	0.39	0.23–0.64		3.16	0.39-25.1	0.277	0.23	0.13–0.42		0.727	0.15–3.4	0.685
3.5–4.0	0.11	0.09–0.77	**<0.001**	1.0			0.29	0.07–1.19	**<0.001**	1.0		
Radiation treatment modality												
WBRT	1.84	0.95–3.58		1.27	0.61-2-61	0.514	1.70	0.88–3.30				
SRS	0.51	0.24–1.06	0.071	1.0			0.32	0.13–0.77	**0.012**			
BM location												
Supratentorial	0.59	0.38–0.93					0.63	0.41–0.96				
Infratentorial	1.69	1.08–2.66	**0.022**				1.60	1.04–2.48	**0.034**			
Perilesional edema diameter (PED), mm												
≥27 <27	2.88 0.35	1.83-4.55 0.22–0.55	**<0.001**	3.13 1.0	1.68-5.84	**<0.001**	2.23 0.47	1.34-3.27 0.31–0.73	**0.001**	1.85 1.0	0.93–3.66	0.76
Gross tumor diameter (GTD), mm												
<17	0.78	0.50–1.23		0.518	0.278-0.968	**0.039**	0.88	0.56–1.39		0.471	0.23–0.95	**0.036**
≥17	1.28	0.82–2.00	0.287	1.00			1.13	0.72–1.78	0.593	1.00		
PED/GTD ratio												
<1.0	0.61	0.15–2.52					0.90	0.29–2.89				
≥1.0	1.61	0.40–2.82	0.503				1.09	0.35–3.49	0.872			
Best overall response												
CR + PR	0.57	0.33–0.99					0.52	0.29–0.92				
SD + PD	1.74	1.00–3.02	0.050				1.93	1.08–3.45	**0.026**			
DpR category												
NTR	3.68	1.67–8.16					3.54	1.60–7.88				
Q1	0.89	0.43–1.88					1.06	0.51–2.22				
Q2	1.28	0.72–2.26					0.81	0.44–1.52				
Q3	0.83	0.46–1.56					0.76	0.37 -1.59				
Q4	0.46	0.20–1.07	**0.007**				0.77	0.32–1.81	**0.034**			

DpR, depth of response; PS, performance status; WBRT, whole brain radiotherapy; SRS, stereotactic radiosurgery; CR, complete response; PR, partial response; SD, stable disease; PD, progressive disease; IASLC, International Association of the Study of Lung Cancer; ATS, American Thoracic Society; ERS, European Respiratory Society. Histological grading of differentiation provides a simple architectural grading system, most applicable to resection specimens, with grade 1 (well differentiated; lepidic [LEP] predominant), grade 2 (moderately differentiated; acinar or papillary [ACI/PAP] predominant), and grade 3 (poorly differentiated; solid or micropapillary [SOL/MIP] predominant). Two-tailed significance was set at $p \leq 0.05$ (bold values).

PED, median OS was 18.4 (95% CI 14.9–21.8) versus 7.9 (95% CI 6.0–9.7) months [HR 2.1, (95% CI 1.4–3.3); $p = 0.001$] in the minor versus major PED subgroup, respectively (Figure 3C). The 6-month OS rate was 72.5% vs. 45.9%, $p = 0.007$, favoring those patients with a minor PED.

On bivariate analysis, factors associated with a higher hazard for death were male patients, Lung-molGPA index of 0–1, infratentorial brain lesions, a major PED, and stable or progressive disease as a best intracranial response. In contrast, protective factors for death were using SRS as the chosen radiation modality. On the multivariate analysis in model 1, only the Lung-mol GPA score of 0–1 increased the risk of death [HR 11.8 (95% CI 2.2–62.2)]. In contrast, a GTD < 17 mm was associated with a better OS [HR 0.47 (95% CI 23–0.95); $p = 0.036$]. PED ≥ 27 mm only showed a tendency to increase the risk of death [HR 1.85 (95% CI 0.93–3.66); $p = 0.76$] (Table 3).

The PED was not a significant factor for death in the multivariate analysis in model 2. However, a GTD <17 mm continued to be a protective factor for death [HR 0.38 (95% CI 0.15–0.93), $p < 0.035$] after the adjustment by the individual components of the Lung-molGPA score (Table S1).

4 Discussion

This retrospective single-center study highlights the relevance of PED as a potential biomarker for intracranial response to radiation therapy in patients with NSCLC and BM. Our results strongly indicate a negative predictive role of PED on response and risk of progression. Peritumoral vasogenic cerebral edema is a significant cause of morbidity and mortality in patients with CNS tumors, including NSCLC BM. This condition is associated with blood–brain barrier (BBB) disruption, leakage of plasma fluid and proteins, increased interstitial fluid pressure (IFP), poor tissue perfusion, and inefficient delivery of oxygen, which results in a hypoxic tumor microenvironment (26).

Hypoxia-mediated radioresistance in CNS tumors is mediated by multiple mechanisms related to cell survival, accelerated tumor proliferation, and repopulation ability (27). Hypoxia-inducible factors (HIFs) play a critical role in regulating genes enabling cell survival in hypoxic environments, including those involved in glycolysis, angiogenesis, and expression of growth factors that promote tumor regrowth (28). Hypoxic tumor microenvironment also drives genomic instability and downregulates DNA repair, leading to cancer progression and radioresistance (29). Furthermore, tumor hypoxia is strongly associated with acquired stem cell phenotype expression in which cancer stem cells (CSCs) are characterized by a reduced accumulation of radiation-induced DNA damage, an increased capacity of DNA Damage Response (DDR) pathway repair, and the activation of anti-apoptotic signaling (29). In addition, CSCs also have lower levels of reactive oxygen species (ROS) and tend to overexpress ROS scavengers, which limits the extent of ROS-dependent damage induced by ionizing radiation (30). Such hypothesis would be supported by the observations of a significantly decreased proportion of tumor shrinkage among patients with greater PED extent.

In the response analysis dataset, a negative association was found between PED and iORR, where patients with a higher PED have a decreased likelihood of achieving intracranial response, consistent with previously published reports (22, 23, 31). Moreover, the study showed a significant association between iDpR and long-term outcomes, which clarifies the significant role of intracranial tumor reduction for survival. Additional studies may further evaluate the role of iDpR as a surrogate endpoint for treatment efficacy in BM.

Measurement of PED represents a simple and accessible potential tool for predicting intracranial response following radiation therapy. Furthermore, it could be easily integrated into clinical practice to identify high-risk patients suitable for treatment intensification strategies. It could also support the rationale to combine anti-angiogenesis agents with radiation therapy to reduce peritumoral vasogenic edema and improve outcomes.

In preclinical and clinical models, agents that target the VEGF signaling pathway have the potential to normalize tumor vasculature, decrease permeability, alleviate edema, lower IFP, improve tissue oxygen levels, and enhance the efficacy of cytotoxic therapies like radiation, chemotherapy, or immunotherapy (32–34). Vascular normalization facilitates the delivery of exogenous agents (35) and enhances DNA damage and cell death through increased ROS after irradiation (35). Additionally, it activates tumor immune response by promoting the maturation and activity of dendritic cells and infiltration of T cells (36, 37), minimizing steroid use and facilitating immunotherapy. Few studies have explored the efficacy and safety of radiotherapy (WBRT or SRS) combined with anti-VEGF, especially bevacizumab, demonstrating encouraging response rates and acceptable safety profile but without consistent survival benefit (38–40).

In the survival analysis, the crucial prognostic role of PED for survival outcome was confirmed; however, it did not remain significant after the adjustment for other relevant prognostic factors. Noteworthy, the PED remained significantly associated with iPFS when adjusted by the other clinical–pathological variables. Notably, PED remained independently associated with poorer outcomes even in the presence of robust prognostic indexes, such as Lung-molGPA. Thus, it is worthwhile to explore the addition of PED to established graded predictive assessment models to improve the accuracy of prognosis for NSCLC patients with BM.

The limitations of this study are the retrospective nature design and the limited number of patients, which prevent us from applying more advanced statistical methods to diminish potential bias. Also, the heterogeneity of the analyzed population, including many oncogene-addictive tumors and various therapies involving target therapy, makes our results difficult to generalize. However, despite the fact that one-third of our cohort harbored an oncogene addictive alteration, the EGFR-TKIs employed were first and second generation in most cases; thus, we did not expect that this factor would affect intracranial response and progression-free outcomes due to the limited brain penetration of these drugs. Moreover, our population received different radiotherapy modalities, which can introduce significant biases to drive

definitive conclusions. Of note, WBRT was the chosen radiation modality in 90%, which limits driving conclusions in those patients treated with SRS. Finally, the PED measurement was a fundamental difference between prior studies that might compromise the reproducibility of results.

5 Conclusion

PED is a strong predictor of response to radiation therapy in NCSCLC BM. Identification of PED might help better tailor therapy in this context and identify candidates for intensification strategies to improve intracranial response. PED could be a user-friendly tool to predict the survival of patients. It is worthwhile to explore the addition of PED to established graded prognostic assessment models. Further studies are needed to validate these findings. The potential efficacy of anti-angiogenic agents in high-risk patients needs further examination through phase III randomized controlled trials.

Data availability statement

The data analyzed in this study is subject to the following licenses/restrictions: Institutional Data Protection laws. Requests to access these datasets should be directed to ogarrieta@gmail.com.

Ethics statement

The studies involving humans were approved by Research committee under the project 2021/054. The studies were conducted in accordance with the local legislation and institutional requirements. Written informed consent for participation was not required from the participants or the participants' legal guardians/next of kin in accordance with the national legislation and institutional requirements.

Author contributions

Conceptualization and project administration: OA. Methodology, validation, investigation, and resources: All authors. Formal analysis and data curation: EC-P, LL-M, AG-G, and OA. Writing—review and editing the original draft: All authors. Visualization: All authors. All authors contributed to the article and approved the submitted version.

Funding

The author(s) declare that no financial support was received for the research, authorship, and/or publication of this article.

Conflict of interest

The authors declare that the research was conducted in the absence of any commercial or financial relationships that could be construed as a potential conflict of interest.

Publisher's note

Supplementary material

The Supplementary Material for this article can be found online at: https://www.frontiersin.org/articles/10.3389/fonc.2023.1251620/full#supplementary-material

References

1. Sung H, Ferlay J, Siegel RL, Laversanne M, Soerjomataram I, Jemal A, et al. Global Cancer Statistics 2020: GLOBOCAN estimates of incidence and mortality worldwide for 36 cancers in 185 countries. *CA Cancer J Clin* (2021) 71:209–49. doi: 10.3322/caac.21660

2. Lamba N, Wen PY, Aizer AA. Epidemiology of brain metastases and leptomeningeal disease. *Neuro Oncol* (2021) 23:1447–56. doi: 10.1093/neuonc/noab101

3. Drilon A, Lin JJ, Filleron T, Ni A, Milia J, Bergagnini I, et al. Frequency of brain metastases and multikinase inhibitor outcomes in patients with RET-rearranged lung cancers. *J Thorac Oncol* (2018) 13:1595–601. doi: 10.1016/J.JTHO.2018.07.004

4. Rangachari D, Yamaguchi N, VanderLaan PA, Folch E, Mahadevan A, Floyd SR, et al. Brain metastases in patients with EGFR-mutated or ALK-rearranged non-small-cell lung cancers. *Lung Cancer* (2015) 88:108–11. doi: 10.1016/J.LUNGCAN.2015.01.020

5. Arrieta O, Salas AA, Cardona AF, Díaz-García D, Lara-Mejía L, Escamilla I, et al. Risk of development of brain metastases according to the IASLC/ATS/ERS lung adenocarcinoma classification in locally advanced and metastatic disease. *Lung Cancer* (2021) 155:183–90. doi: 10.1016/j.lungcan.2021.01.023

6. Cacho-Díaz B, Cuapaténcatl LD, Rodríguez JA, Garcilazo-Reyes YJ, Reynoso-Noverón N, Arrieta O. Identification of a high-risk group for brain metastases in non-small cell lung cancer patients. *J Neurooncol* (2021) 155:101–6. doi: 10.1007/s11060-021-03849-w

7. Burudpakdee C, Wong W, Seetasith A, Corvino FA, Yeh W, Gubens M. Economic impact of preventing brain metastases with alectinib in ALK-positive non-small cell lung cancer. *Lung Cancer* (2018) 119:103–11. doi: 10.1016/J.LUNGCAN.2018.03.008

8. Walker MS, Wong W, Ravelo A, Miller PJE, Schwartzberg LS. Effect of brain metastasis on patient-reported outcomes in advanced NSCLC treated in real-world community oncology settings. *Clin Lung Cancer* (2018) 19:139–47. doi: 10.1016/J.CLLC.2017.10.003

9. Roughley A, Damonte E, Taylor-Stokes G, Rider A, Munk VC. Impact of brain metastases on quality of life and estimated life expectancy in patients with advanced non-small cell lung cancer. *Value Health* (2014) 17:A650. doi: 10.1016/J.JVAL.2014.08.2364

10. Werutsky G, Barrios CH, Cardona AF, Albergaria A, Valencia A, Ferreira CG, et al. Perspectives on emerging technologies, personalised medicine, and clinical research for cancer control in Latin America and the Caribbean. *Lancet Oncol* (2021) 22:e488–500. doi: 10.1016/S1470-2045(21)00523-4

11. Brown PD, Ballman KV, Cerhan JH, Anderson SK, Carrero XW, Whitton AC, et al. Postoperative stereotactic radiosurgery compared with whole brain radiotherapy for resected metastatic brain disease (NCCTG N107C/CEC·3): a multicentre, randomised, controlled, phase 3 trial. *Lancet Oncol* (2017) 18:1049–60. doi: 10.1016/S1470-2045(17)30441-2

12. Maldonado F, Gonzalez-Ling A, Oñate-Ocaña LF, Cabrera-Miranda LA, Zatarain-Barrón ZL, Turcott JG, et al. Prophylactic cranial irradiation in patients with high-risk metastatic non-small cell lung cancer: quality of life and neurocognitive analysis of a randomized phase II study. *Int J Radiat Oncol Biol Phys* (2021) 111:81–92. doi: 10.1016/j.ijrobp.2021.04.017

13. Arrieta O, Maldonado F, Turcott JG, Zatarain-Barrón ZL, Barrón F, Blake-Cerda M, et al. Prophylactic Cranial Irradiation Reduces Brain Metastases and Improves Overall Survival in High-Risk Metastatic Non-Small Cell Lung Cancer Patients: A Randomized phase 2 Study (PRoT-BM trial). *Int J Radiat Oncol Biol Phys* (2021) 110:1442–50. doi: 10.1016/j.ijrobp.2021.02.044

14. Loganadane G, Hendriks L, Le Péchoux C, Levy A. The current role of whole brain radiation therapy in non–small cell lung cancer patients. *J Thorac Oncol* (2017) 12:1467–77. doi: 10.1016/j.jtho.2017.07.006

15. Ashworth AB, Senan S, Palma DA, Riquet M, Ahn YC, Ricardi U, et al. An individual patient data metaanalysis of outcomes and prognostic factors after treatment of oligometastatic non-small-cell lung cancer. *Clin Lung Cancer* (2014) 15:346–55. doi: 10.1016/J.CLLC.2014.04.003

16. Le Rhun E, Guckenberger M, Smits M, Dummer R, Bachelot T, Sahm F, et al. EANO–ESMO Clinical Practice Guidelines for diagnosis, treatment and follow-up of patients with brain metastasis from solid tumours ☆. *Ann Oncol* (2021) 32:1332–47. doi: 10.1016/j.annonc.2021.07.016

17. Gaspar L, Scott C, Rotman M, Asbell S, Phillips T, Wasserman T, et al. Recursive Partitioning Analysis (RPA) of prognostic factors in three Radiation Therapy Oncology Group (RTOG) brain metastases trials. *Int J Radiat Oncol Biol Phys* (1997) 37:745–51. doi: 10.1016/S0360-3016(96)00619-0

18. Sperduto PW, Kased N, Roberge D, Xu Z, Shanley R, Luo X, et al. Summary report on the graded prognostic assessment: an accurate and facile diagnosis-specific tool to estimate survival for patients with brain metastases. *J Clin Oncol* (2012) 30:419–25. doi: 10.1200/JCO.2011.38.0527

19. Sperduto PW, De B, Li J, Carpenter D, Kirkpatrick J, Milligan M, et al. Graded prognostic assessment (GPA) for patients with lung cancer and brain metastases: initial report of the small cell lung cancer GPA and update of the non-small cell lung cancer GPA including the effect of programmed death ligand 1 and other prognostic factors. *Int J Radiat Oncol Biol Phys* (2022) 114:60–74. doi: 10.1016/j.ijrobp.2022.03.020

20. Sperduto PW, Yang TJ, Beal K, Pan H, Brown PD, Bangdiwala A, et al. Estimating survival in patients with lung cancer and brain metastases an update of the graded prognostic assessment for lung cancer using molecular markers (Lung-molGPA). *JAMA Oncol* (2017) 3:827–31. doi: 10.1001/jamaoncol.2016.3834

21. Spanberger T, Berghoff AS, Dinhof C, Ilhan-Mutlu A, Magerle M, Hutterer M, et al. Extent of peritumoral brain edema correlates with prognosis, tumoral growth pattern, HIF1a expression and angiogenic activity in patients with single brain metastases. *Clin Exp Metastasis* (2013) 30:357–68. doi: 10.1007/S10585-012-9542-9

22. Nardone V, Nanni S, Pastina P, Vinciguerra C, Cerase A, Correale P, et al. Role of perilesional edema and tumor volume in the prognosis of non-small cell lung cancer (NSCLC) undergoing radiosurgery (SRS) for brain metastases. *Strahlenther Onkol* (2019) 195:734–44. doi: 10.1007/S00066-019-01475-0

23. Tini P, Nardone V, Pastina P, Battaglia G, Vinciguerra C, Carfagno T, et al. Perilesional edema in brain metastasis from non-small cell lung cancer (NSCLC) as predictor of response to radiosurgery (SRS). *Neurol Sci* (2017) 38:975–82. doi: 10.1007/S10072-017-2876-Y

24. Lin NU, Lee EQ, Aoyama H, Barani IJ, Barboriak DP, Baumert BG, et al. Response assessment criteria for brain metastases: proposal from the RANO group. *Lancet Oncol* (2015) 16:e270–8. doi: 10.1016/S1470-2045(15)70057-4

25. Shaw E, Scott C, Souhami L, Dinapoli R, Kline R, Loeffler J, et al. Single dose radiosurgical treatment of recurrent previously irradiated primary brain tumors and brain metastases: Final report of RTOG protocol 90- 05. *Int J Radiat Oncol Biol Phys* (2000) 47:291–8. doi: 10.1016/S0360-3016(99)00507-6

26. Gerstner ER, Duda DG, di Tomaso E, Ryg PA, Loeffler JS, Sorensen AG, et al. VEGF inhibitors in the treatment of cerebral edema in patients with brain cancer. *Nat Rev Clin Oncol* (2009) 6:229–36. doi: 10.1038/nrclinonc.2009.14

27. Price JM, Prabhakaran A, West CML. Predicting tumour radiosensitivity to deliver precision radiotherapy. *Nat Rev Clin Oncol* (2023) 20(2):83–98. doi: 10.1038/s41571-022-00709-y

28. Harris AL. Hypoxia — a key regulatory factor in tumour growth. *Nat Rev Cancer* (2002) 2:38–47. doi: 10.1038/nrc704

29. Peitzsch C, Kurth I, Kunz-Schughart L, Baumann M, Dubrovska A. Discovery of the cancer stem cell related determinants of radioresistance. *Radiother Oncol* (2013) 108:378–87. doi: 10.1016/j.radonc.2013.06.003

30. Diehn M, Cho RW, Lobo NA, Kalisky T, Dorie MJ, Kulp AN, et al. Association of reactive oxygen species levels and radioresistance in cancer stem cells. *Nature* (2009) 458:780–3. doi: 10.1038/nature07733

31. Alemany M, Domènech M, Argyriou AA, Vilariño N, Majós C, Naval-Baudin P, et al. Perilesional edema in brain metastases as predictive factor of response to systemic therapy in non-small cell lung cancer patients: a preliminary study. *Ann Transl Med* (2021) 9:648–8. doi: 10.21037/atm-20-6497

32. Lee C-G, Heijn M, di Tomaso E, Griffon-Etienne G, Ancukiewicz M, Koike C, et al. Anti-Vascular endothelial growth factor treatment augments tumor radiation response under normoxic or hypoxic conditions. *Cancer Res* (2000) 60(19):5565–70.

33. Winkler F, Kozin SV, Tong RT, Chae S-S, Booth MF, Garkavtsev I, et al. Kinetics of vascular normalization by VEGFR2 blockade governs brain tumor response to radiation. *Cancer Cell* (2004) 6:553–63. doi: 10.1016/j.ccr.2004.10.011

34. Batchelor TT, Sorensen AG, di Tomaso E, Zhang W-T, Duda DG, Cohen KS, et al. AZD2171, a pan-VEGF receptor tyrosine kinase inhibitor, normalizes tumor vasculature and alleviates edema in glioblastoma patients. *Cancer Cell* (2007) 11:83–95. doi: 10.1016/j.ccr.2006.11.021

35. Shang B, Cao Z, Zhou Q. Progress in tumor vascular normalization for anticancer therapy: challenges and perspectives. *Front Med* (2012) 6:67–78. doi: 10.1007/s11684-012-0176-8

36. Osada T, Chong G, Tansik R, Hong T, Spector N, Kumar R, et al. The effect of anti-VEGF therapy on immature myeloid cell and dendritic cells in cancer patients. *Cancer Immunol Immunother* (2008) 57:1115–24. doi: 10.1007/s00262-007-0441-x

37. Terme M, Pernot S, Marcheteau E, Sandoval F, Benhamouda N, Colussi O, et al. VEGFA-VEGFR pathway blockade inhibits tumor-induced regulatory T-cell proliferation in colorectal cancer. *Cancer Res* (2013) 73:539–49. doi: 10.1158/0008-5472.CAN-12-2325

38. Besse B, le Moulec S, Mazières J, Senellart H, Barlesi F, Chouaid C, et al. Bevacizumab in patients with nonsquamous non–small cell lung cancer and asymptomatic, untreated brain metastases (BRAIN): A nonrandomized, phase II study. *Clin Cancer Res* (2015) 21:1896–903. doi: 10.1158/1078-0432.CCR-14-2082

39. Berghoff AS, Breckwoldt MO, Riedemann L, Karimian-Jazi K, Loew S, Schlieter F, et al. Bevacizumab-based treatment as salvage therapy in patients with recurrent symptomatic brain metastases. *Neurooncol Adv* (2020) 2:1–9. doi: 10.1093/noajnl/vdaa038

40. Lévy C, Allouache D, Lacroix J, Dugué AE, Supiot S, Campone M, et al. REBECA: a phase I study of bevacizumab and whole-brain radiation therapy for the treatment of brain metastasis from solid tumours. *Ann Oncol* (2014) 25:2351–6. doi: 10.1093/annonc/mdu465

frontiers | Frontiers in Oncology

TYPE Case Report
PUBLISHED 18 October 2023
DOI 10.3389/fonc.2023.1233198

OPEN ACCESS

EDITED BY
Lin Zhou,
Sichuan University, China

REVIEWED BY
Xiaqin Cheng,
Sichuan University, China
Shasha Zeng,
Sichuan University, China

*CORRESPONDENCE
Jie Chen
cjid119@qq.com

†These authors have contributed equally to this work and share first authorship

RECEIVED 01 June 2023
ACCEPTED 04 September 2023
PUBLISHED 18 October 2023

CITATION
Chen T, Chen J, Liu D-s, Shu Y-l, Fu M-y, Gou H-j, Lei K-j and Jia Y-m (2023) Successful therapy using high-dose furmonertinib for non-small cell lung cancer with leptomeningeal metastasis: a case report and literature review. *Front. Oncol.* 13:1233198. doi: 10.3389/fonc.2023.1233198

Successful therapy using high-dose furmonertinib for non-small cell lung cancer with leptomeningeal metastasis: a case report and literature review

Ting Chen[1†], Jie Chen[1*†], De-sheng Liu[2], Yan-ling Shu[1], Mao-yue Fu[1], Hai-jun Gou[3], Kai-jian Lei[1] and Yu-ming Jia[1]

[1]Department of Oncology, Second People's Hospital of Yibin, Yibin, Sichuan, China, [2]Department of Thoracic and Cardiovascular Surgery, Second People's Hospital of Yibin, Yibin, Sichuan, China, [3]Department of Oncology, People's Hospital of Junlian County, Yibin, Sichuan, China

Background: Lung cancer is the second most common form of malignant tumor and has the highest mortality rate worldwide. Among its subtypes, lung adenocarcinoma is the most prevalent. Leptomeningeal metastasis (LM) is rare and is characterized by a dismal prognosis, with overall survival periods typically spanning 4 to 6 weeks without treatment. However, in specific cases, survival can be extended to 4 to 6 months with appropriate therapy. The recent approval of third-generation tyrosine kinase inhibitors (TKIs), such as osimertinib, aumolertinib, and furmonertinib, has introduced promising treatment options for individuals with non-small cell lung cancer (NSCLC) who develop LM after developing resistance to first- and second-generation TKIs. These third-generation TKIs exhibit an enhanced ability to penetrate the blood–brain barrier (BBB), opening up new avenues for managing this challenging condition.

Case summary: We report the case of a 48-year-old Chinese man diagnosed with advanced NSCLC harboring an epidermal growth factor receptor (*EGFR*) mutation. Following a pulmonary lobectomy and postoperative adjuvant therapy with gefitinib, the patient was diagnosed with LM, which was confirmed by his neurologic symptoms, cerebrospinal fluid cytologic analysis, and cranial enhancement magnetic resonance imaging. Subsequently, he received oral treatment in the form of 160 mg of furmonertinib daily. After 5 days of furmonertinib therapy, the patient recovered from lethargy, with an obvious improvement in cognitive function. Follow-up visits revealed a 6-month survival period following the LM diagnosis. Patients with NSCLC and LM typically present with severe symptoms, and the efficacy of systemic treatment, intrathecal chemotherapy, and radiotherapy remains unsatisfactory. We hope that this specific case provide valuable insights into the management of patients with *EGFR* mutation-associated NSCLC with LM.

Conclusion: Furmonertinib, a third-generation *EGFR* TKI with notable BBB penetration, shows promise in LM control and the rapid alleviation of intracranial symptoms. Further investigations into appropriate dosage and toxicity management are imperative.

KEYWORDS

NSCLC, *EGFR*, furmonertinib, leptomeningeal metastasis, target therapy

Introduction

Lung cancer is the second most common form of malignant tumor worldwide, and it also has the highest mortality rate worldwide (1). Among the various subtypes, adenocarcinoma emerges as the most prevalent. Notably, gene mutations within the epidermal growth factor receptor (*EGFR*) represent the most prevalent driver mutations, with *EGFR*-activating mutations being detected in approximately 10% of Caucasians and 30% to 40% of East Asians (2). For patients with advanced non-small cell lung cancer (NSCLC) and *EGFR* mutations, first- and second-generation *EGFR* tyrosine kinase inhibitors (TKIs) have been approved as the first-line treatment. However, acquired resistance is inevitable in most cases, as a result of the *EGFR* T790M mutation, among patients who benefit from these *EGFR* TKIs. The central nervous system (CNS) is a common site of metastasis, including brain metastasis (BM) and leptomeningeal metastasis (LM), partly because of the limited blood–brain barrier (BBB) penetration of the first- and second-generation TKIs (3). The incidence of LM is 3.8% among all patients and can increase to 10% in those with NSCLC and *EGFR* mutations (4). Prior to the advent of TKIs and immunotherapy, the treatment of LM showed limited improvement in overall survival (OS); this treatment involved intrathecal chemotherapy (ITC), whole-brain radiation therapy (WBRT), and systemic chemotherapy. Although LM is relatively rare and bears a poor prognosis, with OS of only 4–6 weeks without therapy, a subset of patients can experience an extension in survival to 4–6 months with treatment (5). Recent years have seen the approval of third-generation TKIs, such as osimertinib, aumolertinib, and furmonertinib, targeting both *EGFR*-activating mutations and the T790M mutation, and with improved ability to diffuse through the BBB. These agents have offered promising treatment options for NSCLC with LM. However, despite the growing interest in CNS metastases in the modern era, most controlled clinical trials have excluded patients with LM due to their grim prognosis and poorer performance status. In addition, although a recent increase in incidence has occurred, LM is a rare complication of NSCLC and patient numbers remain limited, posing significant challenges for the implementation of random clinical trials. Moreover, previous studies have demonstrated significant genomic divergence between the primary tumor and intracranial metastases (6). Consequently, providing individualized therapy for patients with LM remains an exceptionally challenging task for clinical physicians.

Furmonertinib, developed in China, is a newly designed third-generation *EGFR* TKI with a trifluoroethoxypyridine-based molecule structure. The efficacy of furmonertinib in treating NSCLC with LM remains unclear. Herein we present the case of a patient with NSCLC who developed LM and underwent high-dose furmonertinib treatment. We aim to provide insights and valuable experience for the management of NSCLC patients with LM.

Case presentation

A 48-year-old Chinese man with a long-term history of smoking was diagnosed with stage IIB lung cancer in June 2020 (Figure 1). Preoperative chest computed tomography (CT) revealed the presence of a 25 mm × 20 mm mass in the upper lobe of the left lung, deemed resectable upon surgical evaluation (Figure 2A). Thereafter, he underwent thoracoscopic-assisted pulmonary radical lobectomy and lymph node dissection. Pathologic examination identified adenocarcinoma with positive staining for Napsin A, TTF-1, p53, and CK7 and negative staining for p63, CK5/6, and Ki-67 (30%). Parabronchial lymph nodes (2/4) showed negative staining for CK5/6 and P63. Pleural invasion and vascular cancer embolism were observed (pT2aN1M0 stage IIB; AJCC 8th edition) (Figure 2B). The patient declined postoperative chemotherapy and radiotherapy. The surgical specimen was analyzed using next-generation sequencing (NGS) to identify possible targetable molecular alterations. The findings revealed a mutation in exon 19 of *EGFR*, with no other gene mutations detected.

Subsequently, the patient received adjuvant targeted therapy with the first-generation TKI gefitinib (250 mg orally) every day for 15 months, during which time no recurrence was noted. However, due to transaminase elevation (grade 2, common terminology criteria for adverse events), dyspepsia (grade 2), and rash (grade 2), the patient temporarily withdrew without medical permission.

Abbreviations: LM, leptomeningeal metastasis; TKI, tyrosine kinase inhibitor; NSCLC, non-small cell lung cancer; *EGFR*, epidermal growth factor receptor; BBB, blood–brain barrier; CNS, central nervous system; OS, overall survival; CT, computed tomography; NGS, next-generation sequencing; ECOG, Eastern Cooperative Oncology Group; PS, performance status; MRI, magnetic resonance imaging; ORR, objective response rate; PFS, progression-free survival; ITC, intrathecal chemotherapy; WBRT, whole-brain radiation therapy; BM, brain metastasis; CSF, cerebrospinal fluid.

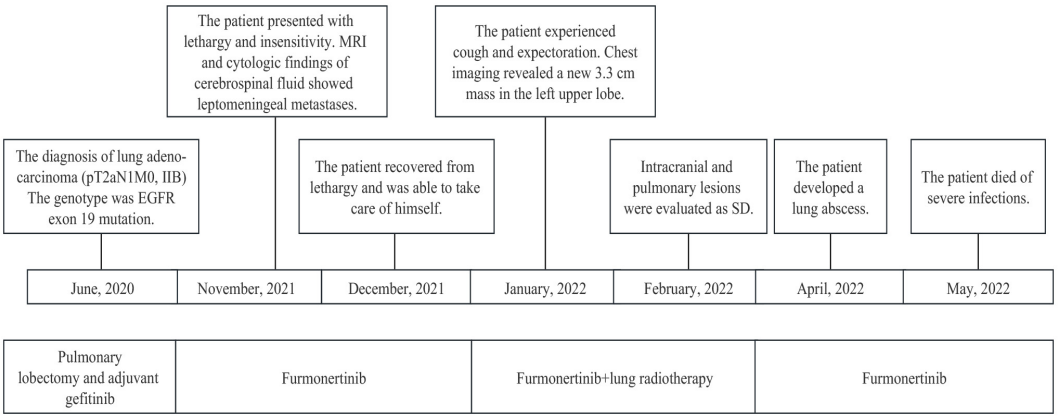

FIGURE 1
Summary of the diagnosis and treatment process.

In November 2021, the patient experienced rapid disease progression, with an Eastern Cooperative Oncology Group (ECOG) performance status (PS) of 3. He exhibited a series of symptoms, including nausea, vomiting, dizziness, lethargy, insensitivity, and an inability to provide accurate answers to questions. Brain enhancement magnetic resonance imaging (MRI) examination revealed mild hydrocephalus and slightly swollen meninges without parenchyma metastases (Figure 3). No extracranial recurrence was detected following a comprehensive examination. A second round of NGS using peripheral blood confirmed an *EGFR* exon 19 mutation, with no evidence of acquired T790M, *KRAS*, *ALK*, *ROS1*, *RET*, or *MET* mutations. Cytologic findings from cerebrospinal fluid (CSF) obtained by lumbar puncture revealed adenocarcinoma cells (Figure 2E). Furmonertinib is a novel third-generation *EGFR* TKI that targets both *EGFR*-sensitive mutations and the T790M mutation while sparing wild-type *EGFR*. Furmonertinib has been shown to be more effective than gefitinib in treating the CNS in patients with *EGFR*-mutated NSCLC and CNS metastases. Therefore, our patient was administered high-dose furmonertinib (160 mg/day). Mannitol was administered to alleviate cerebral edema. Remarkably, within 5 days of receiving furmonertinib, the patient, who had been admitted with lethargy, showed significant improvement in physical and cognitive function. After discharge, the patient continued oral furmonertinib at a daily dose of 160 mg. Imaging studies were not performed until January 2022, following 2 months of furmonertinib administration, when the patient developed symptoms of cough, expectoration, and dyspnea. A chest examination revealed a new 3.3 cm mass in the left upper lobe hilar region, with right hilar and mediastinal lymphadenopathies (Figure 3). Electronic fiber bronchoscopy revealed complete obstruction of the left upper lobe bronchus, with a neoplasm protruding from the lumen at the opening (Figure 2D). A biopsy was attempted but proved to be challenging, yielding inconclusive pathological results. Re-biopsy was quite difficult to perform. Positron emission tomography/CT (PET/CT) indicated abnormally increased fluorodeoxyglucose metabolism in the left hilar surgical region, left thoracic entrance, mediastinal aortic arch, right lower paratracheal lymph nodes, carina lymph nodes, and right hilar lymph nodes (Figure 2C). While definitive pathological diagnoses were unavailable, a combination of CT, PET/CT, and bronchoscopy findings led us to suspect tumor recurrence in the lungs. Consequently, the patient received intensity-modulated radiotherapy at a total dose of 30 Gy, delivered over a 2-week period at 3 Gy per fraction, in conjunction with 160 mg (daily) of furmonertinib. By February 2022, after 3 months of furmonertinib and radiotherapy, both intracranial and pulmonary lesions were evaluated as stable disease (SD) (Figure 3). The primary adverse events observed were transaminase elevation (grade 2) and nausea (grade 2). In April 2022, following 5 months of furmonertinib administration, the patient was hospitalized due to a left lung abscess, accompanied by fever, cough, dyspnea, and loss of consciousness. Anti-infective therapy was administered for 2 weeks. One month later, in May 2022, the patient died of severe infections. Accordingly, furmonertinib extended the patient's OS by 6 months.

Discussion

LM is primarily diagnosed using cerebrospinal fluid cytology, and brain MRI also exhibits special imaging features in which LM primarily or solely manifests as cranial nerve involvement (7). NSCLC with LM generally presents with serious symptoms, with headaches, nausea, and vomiting being the most common symptoms. LM carries a grim prognosis, often shorter than that of BM. The effectiveness of systemic treatment, ITC, and radiotherapy has been unsatisfactory. Systemic chemotherapy has a clear curative effect in the treatment of NSCLC patients with LM, as it is an independent predictor of survival (5). In the case of ITC, it shows a specific efficacy for NSCLC patients. A pooled analysis, comprising four prospective studies and five retrospective studies, evaluated 552 patients who received multiple interventions (ITC, WBRT, *EGFR* TKI, systemic chemotherapy, and supportive care) and 37 patients who received ITC only. The analysis reported a longer median OS among patients who received ITC only (6.0 months) compared to those who received multiple interventions (3.0–5.0 months) (8). However, given the heterogeneity in the ITC

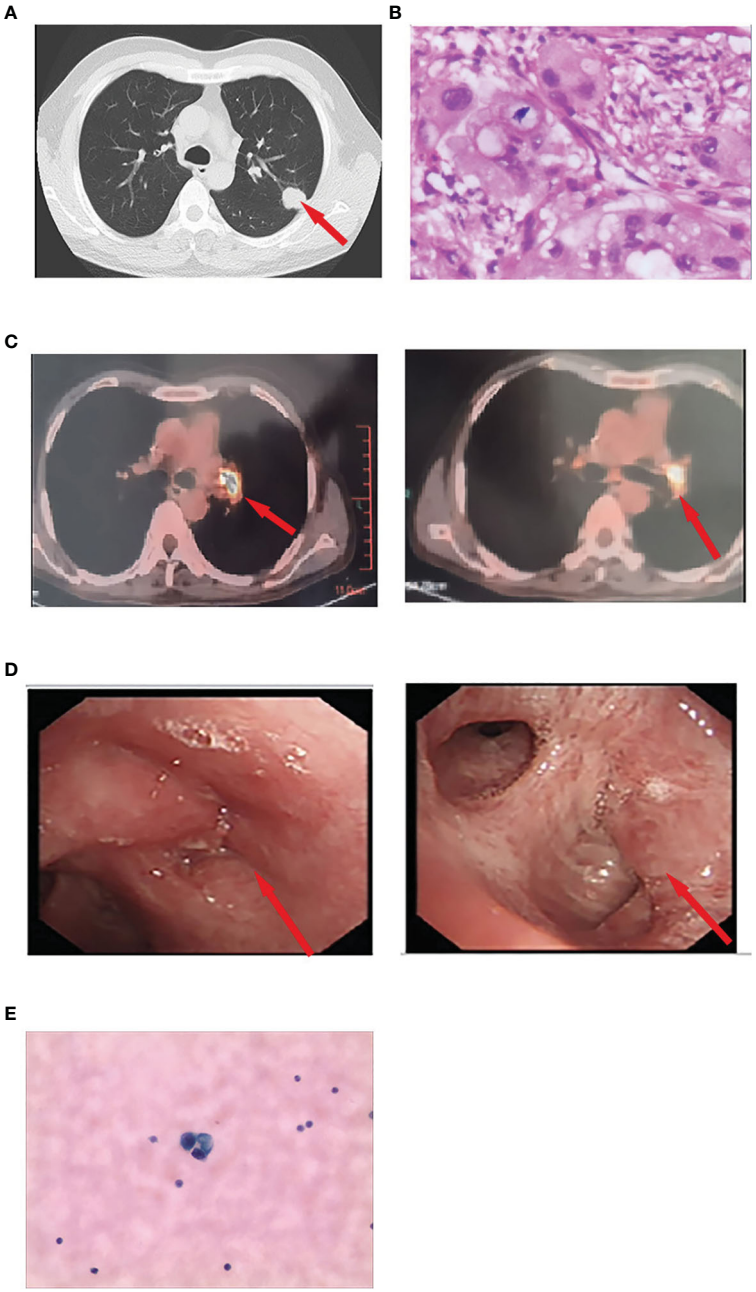

FIGURE 2
(A) Preoperative chest computed tomography revealing a 25 × 20-mm mass in the left upper lobe. **(B)** Pathological diagnosis of the resected specimen was lung adenocarcinoma. **(C)** Positron emission/CT examination showed abnormally increased fluorodeoxyglucose metabolism in the left hilar surgical region and mediastinal lymph nodes. The cytologic findings of CSF by lumbar puncture revealed adenocarcinoma cells. **(D)** An electronic fiber bronchoscopy revealed complete obstruction of the left upper lobe bronchus with a neoplasm protruding from the lumen at the opening and leading to left inferior basal segment external pressure stenosis. **(E)** The cytologic findings of CSF by lumbar puncture revealed adenocarcinoma cells.

treatment and confounding factors, further research is needed to determine the efficacy of ITC. WBRT, on the other hand, has limited efficacy for NSCLC patients with LM. A retrospective study analyzed 51 NSCLC patients with LM and found no significant differences in intracranial objective response rate (ORR) (15.4% vs.16%, $p = 0.952$) or disease control rate (34.7% vs. 28%, $p = 0.611$) between the WBRT group and the non-WBRT group. Survival was also not statistically improved for patients treated with WBRT (9). Another study reached the same conclusion, namely, that receiving WBRT did not confer a survival advantage (10). In clinical practice, WBRT is typically applied for palliative relief, for example to address obstructive lesions causing hydrocephalus (11). In a Phase II clinical trial in which WBRT was combined with ITC for solid tumors in patients with LM, the median OS was only 6.7 months among NSCLC patients (12). Moreover, a significant number of patients (those with a weak physical status) may not

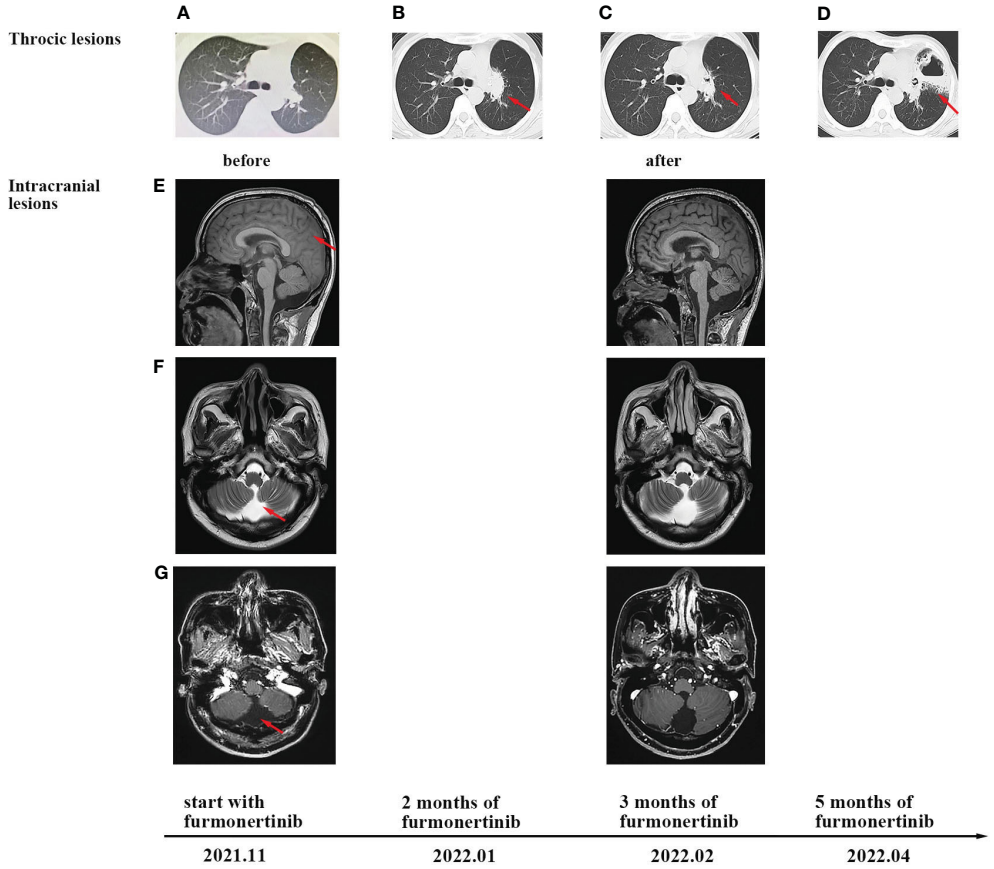

FIGURE 3
CT and MRI scans at different clinical time points, as indicated. **(A)** Chest CT scans before furmonertinib treatment. **(B)** Progression of thoracic lesions was observed after 2 months of furmonertinib. **(C)** The change in lung lesions after 3 months of furmonertinib and lung radiotherapy. **(D)** CT scans after 5 months of furmonertinib revealed a left-lung abscess. **(E)** T1-weighted imaging of brain MRI before and after 3 months of furmonertinib. The coronal plane revealed slightly swollen meninges. **(F)** T2-weighted imaging of brain MRI indicated mild hydrocephalus. **(G)** T1-weighted imaging enhancement scans revealed no leptomeningeal enhancement and no parenchyma metastases.

tolerate conventional chemotherapy and radiotherapy, necessitating individualized therapeutic strategies for LM patients. Previous studies have reported that a good ECOG PS is a significant prognostic factor. In one study, among patients diagnosed with LM who underwent ITC with or without systemic treatment, including cytotoxic chemotherapy and *EGFR* TKIs, the median OS was only 0.7 months in patients with an ECOG PS of 3–4, significantly shorter than the 5.5 months observed in patients with an ECOG PS of 1–2 ($p < 0.001$) (13). Poorer PS significantly impacts the efficacy of therapeutic regimens and limits treatment options for patients.

The National Comprehensive Cancer Network Guidelines recommend the use of osimertinib (regardless of T790M status) for patients with *EGFR*-activating mutations who have progressive CNS disease or leptomeningeal disease, based on the BLOOM clinical trial data (14). We have summarized recent clinical trials of third-generation TKIs on NSCLC patients with LM (Table 1) (15–22). In the previous AURA program studies (AURA extension, AURA2, AURA17, and AURA3), 22 patients with LM with acquired T790M resistance mutation received 80 mg of osimertinib after disease progression on prior TKIs. A retrospective analysis of this dataset showed a LM ORR of 55%, with median progression-free survival (PFS) of 11.1 months and OS of 18.8 months (17). Consequently, in the Phase I BLOOM study, 41 patients with cytologically confirmed LM received 160 mg of osimertinib. The LM ORR was 62%, with PFS of 8.6 months and OS of 11.0 months (19). Compared with 80mg osimertinib, 160 mg osimertinib slightly improved the LM ORR. The findings initially suggest that osimertinib may have promising effects on LM disease control, but further prospective clinical trials are needed to confirm its efficacy in LM and determine the optimal dose. Furmonertinib is a newly designed third-generation *EGFR* TKI with a trifluoroethoxypyridine-based molecule structure, demonstrating promising efficacy in patients with NSCLC having *EGFR* activation or T790M mutation. Preclinical studies have shown higher concentrations of drug-related active substances in the brain than in the plasma, indicating that furmonertinib may be effective in patients with CNS metastases (23). In the phase III FURLONG study, which enrolled 63 *EGFR*-sensitizing mutation-positive, untreated patients with asymptomatic CNS metastases, furmonertinib was associated with longer PFS [18.0 vs. 12.4 months, hazard ratio (HR) 0.50, p=0.0028], CNS PFS (20.8 vs. 9.8 months, HR 0.40, p=0.0011), and CNS ORR (91% vs. 65%, OR=6.82, p=0.0277) compared with gefitinib (24). In a Phase II

TABLE 1 Selected studies of third-generation TKIs in NSCLC patients with LM.

Study	Year	Type	Treatment	Patients (*n*)	*EGFR* status	Rate of T790M positivity	Median PFS (m)	Median OS (m)	LM ORR	LM DCR	Toxicity
Saboundji et al. (15)	2018	R	Osimertinib	20	2 Exon18 7 Exon19 11 Exon21	65%	17.2	18.0	85%	NA	NA
Nanjo et al. (16)	2017	P	Osimertinib 80mg/day	13	10 Eon19 3 Exon21	100%	7.2	NR	15%	NA	G3–4: 0%
Ahn et al. (17)	2020	R	Osimertinib 80mg/day	22	3 Exon18 13 Exon19 8 Exon21	100%	11.1	18.8	55%	91%	G3–4: 45%
Park et al. (18)	2020	II	Osimertinib 160mg/day	40	1 Exon18 23 Exon19 16 Exon21	100%	8.0	13.3	12.5%	92.5%	G3–4: 34%
Yang et al. (19)	2020	I	Osimertinib 160mg/day	41	EGFR mutation	100%	8.6	11.0	62%	95%	G3–4: 66%
Li et al. (20)	2022	R	41 Osimertinib 6 other *EGFR* TKIs 6 non-*EGFR* TKIs	53	1 Exon18 19 Exon19 2 Exon20 26 Exon21	21.4%	NA	13	NA	90%	NA
Xu Y et al. (21)	2021	R	Osimertinib 80mg/day	40	15 Exon19 23Exon21	40%	10	15.1	20%	95%	NA
Xu Z et al. (22)	2023	R	Furmonertinib 160mg/day	16	7 Exon19 6 Exon21	6.3%	4.3	NR	NA	NA	G3–4: 14.3%

LM, leptomeningeal metastasis; PFS, progression-free survival; OS, overall survival; R, retrospective; P, prospective; NSCLC, non-small cell lung cancer; m, months; EGFR, epidermal growth factor receptor; TKI, tyrosine kinase inhibitor; ORR, overall response rate; DCR, disease control rate; NR, not reached; NA, not applicable; G, grade of toxicity.

dose-expansion study enrolling patients with NSCLC harboring the *EGFR* T790M mutation, the CNS efficacy of furmonertinib as a second- or later-line treatment was tested; the results showed promising CNS ORR (60.0% with 80 mg once daily and 84.6% with 160 mg once daily) and CNS PFS (9.7 months with 80 mg once daily and 19.3 months with 160 mg once daily) (25), indicating that a higher dose of furmonertinib may lead to better outcomes in patients with NSCLC having CNS metastases. However, the efficacy of double-dose furmonertinib needs further validation with balancing of baseline characteristics. Prior brain radiotherapy may affect the subsequent response to targeted drugs. In the radiotherapy subgroup analysis of the AURA3 study, the CNS ORR in patients with prior CNS radiotherapy-treated with osimertinib was 64%, which was higher than the 34% observed in radiotherapy-naive patients. Compared with the AURA3 study, the AST2818 study included more patients with *EGFR* L858R mutations (47.8% vs. 38.8%) and fewer patients with previous CNS radiotherapy (13% vs. 28.8%) (26, 27). Based on the data, the efficacy of furmonertinib in reducing intracranial lesions seems not to be inferior to that of osimertinib. Furthermore, previous cases have indicated that a high dose of furmonertinib could reverse osimertinib resistance in patients with NSCLC having BM (28, 29). In our case, the LM PFS was 6 months, and disease control of LM was observed even when the disease progressed in extracranial lesions, indicating the potential of furmonertinib for sustained efficacy in LM.

In the case described here, the patient received gefitinib adjuvant therapy for 15 months after pulmonary radical lobectomy, which was followed by intracranial progression only. Previous studies have revealed that the ability of gefitinib to penetrate the CNS is limited. Preclinical data show that gefitinib is distributed in the brain to a lesser extent than osimertinib (CSF/brain-to-blood ratio of exposure was 0.28 for $^{[11C]}$gefitinib and 2.62 for $^{[11C]}$osimertinib) (30). Several studies have reported that intracranial progression is likely to be associated with the poor ability of TKIs to diffuse through the BBB, resulting in pharmacokinetic failure (31). For the patient mentioned in this case, genetic testing of the surgical specimen in June 2020 revealed an *EGFR* exon 19 mutation. However, after intracranial progression, his plasma samples still tested positive for *EGFR*-activating mutations and negative for the T790M mutation. It has been reported that the frequency of T790M mutation is much lower in CSF lesions than in thoracic lesions (32). Therefore, we consider that the initial disease progression was probably due to the poor ability of gefitinib to penetrate the CNS, leading to the rapid development of intracranial lesions.

After the development of LM, the patient exhibited an ECOG PS of 3 with lethargy and a high intracranial burden. Given the poor prognosis of T790M-negative patients, systemic chemotherapy and ITC were not appropriate choices for the patient. In recent years, TKIs have shown extensive benefits for survival in patients with oncogenic driver mutations. Considering previous studies suggesting that a high dose of furmonertinib may be better in order to deliver a higher dosage to the CNS, we innovatively administered a high dose of furmonertinib to achieve better control of intracranial lesions and rapidly alleviate neurologic symptoms. After 5 days, the neurologic symptoms completely disappeared, and the patient regained self-care abilities. Eventually, the patient experienced an extended lifespan of 6 months, similar to that achieved with conventional therapy. This case implies that third-generation TKIs should be recommended for NSCLC patients with intracranial progression, especially patients with poorer physical status and limited tolerance for cytotoxic chemotherapy after the administration of first- or second-generation TKIs, regardless of T790M status. Given the dismal prognosis of NSCLC patients with LM, high-dose TKIs should be administered to achieve rapid disease control.

In the case described here, extracranial lesions exhibited no response to furmonertinib, while intracranial lesions were better controlled. The heterogeneity of resistance to TKIs in progressive disease is worth further exploration. The efficacy of furmonertinib on extracranial lesions can also be observed in patients treated with third-generation TKIs. Previous studies have indicated that heterogeneity of missense mutations between primary and metastatic lesions in NSCLC is frequent (33, 34). The ORR for extracranial lesions in patients with CNS metastases treated with furmonertinib has been found to be 77% (26), exceeding the ORRs of 56% in patients treated with osimertinib (27) and 61.5% in patients treated with aumolertinib (35). A case series in NSCLC has reported that ineffective TKI treatment could be explained in part by the discordance of molecular genetic profiles in lung adenocarcinoma with intrapulmonary metastases (36). We considered the possibility that extracranial resistance to furmonertinib could be attributed to the coexistence of the T790M mutation with other subclones. The *EGFR* C797S mutation is a common mutation site during progression under first- and second-generation *EGFR*-TKIs. A recent study has further indicated that, when the C797S mutation is in cis with the T790 mutation (i.e., on the same allele), the cancer cells are resistant to all *EGFR* TKIs, alone or in combination (37). In addition, several retrospective studies have observed a better clinical response and longer intracranial PFS in NSCLC and LM patients with T790M-positive CSF than in T790M-negative patients (15, 38). In this article, we have reported on observations of heterogeneity in resistance to third-generation TKIs between intracranial and extracranial lesions, and discussed the clinical implications. Current clinical trials in NSCLC with LM mostly exclude patients without the T790M mutation. For LM patients without acquired T790M mutation, it is important to closely monitor TKI resistance in clinical practice.

There are several limitations to this case study. The genetic status of the thoracic lesions could not be confirmed owing to the absence of re-biopsy of primary lesions, and the lack of CSF genotyping limited further interpretation of the heterogeneity of resistance to furmonertinib. Gene detection of CSF samples should be recommended owing to a perceived difference in genetic sequencing results between the plasma and CSF samples (32). Sequencing of CSF samples can improve diagnostic accuracy and therapeutic monitoring in LM. In this case, it was regrettable that we were not able to sequence the patient's CSF. Because we did not reserve enough CSF for NGS, we would have needed a second lumbar puncture; the alternative option was to use peripheral blood as a replacement. Unfortunately, the patient refused a second lumbar puncture, and we had to sequence the peripheral blood.

Conclusion

In conclusion, furmonertinib, a third-generation *EGFR* TKI with a strong ability to penetrate the BBB, may be effective in controlling LM and rapidly alleviating intracranial symptoms. However, further research is needed to determine the appropriate dosage and toxicity management strategies.

Data availability statement

The original contributions presented in the study are included in the article/supplementary material. Further inquiries can be directed to the corresponding author.

Ethics statement

Written informed consent was obtained from the individual(s) for the publication of any potentially identifiable images or data included in this article.

Author contributions

TC was responsible for the conceptualization of the study, investigations, and writing of the original draft. JC was responsible for writing, reviewing, and editing. D-SL, Y-LS, H-JG, M-YF, and H-JG were responsible for performing the data analyses. K-JL and Y-MJ were responsible for visualization. All authors contributed to and approved the final version of the manuscript.

Acknowledgments

We would like to thank the patient and his family, who consented to the publication of this case.

Conflict of interest

The authors declare that the research was conducted in the absence of any commercial or financial relationships that could be construed as a potential conflict of interest.

Publisher's note

References

1. Sung HA-O, Ferlay J, Siegel RA-O, Laversanne M, Soerjomataram I, Jemal A, et al. Global cancer statistics 2020: GLOBOCAN estimates of incidence and mortality worldwide for 36 cancers in 185 countries. *CA Cancer J Clin* (2021) 71(3):209–49. doi: 10.3322/caac.21660

2. Yamaoka T, Ohba M, Ohmori T. Molecular-targeted therapies for epidermal growth factor receptor and its resistance mechanisms. *Int J Mol Sci* (2017) 18(11):2420. doi: 10.3390/ijms18112420

3. Zhao J, Chen M, Zhong W, Zhang L, Li L, Xiao Y, et al. Cerebrospinal fluid concentrations of gefitinib in patients with lung adenocarcinoma. *Clin Lung Cancer* (2013) 14(2):188–93. doi: 10.1016/j.cllc.2012.06.004

4. Liao BC, Lee JH, Lin CC, Chen YF, Chang CH, Ho CC, et al. Epidermal growth factor receptor tyrosine kinase inhibitors for non-small-cell lung cancer patients with leptomeningeal carcinomatosis. *J Thorac Oncol* (2015) 10(12):1754–61. doi: 10.1097/JTO.0000000000000669

5. Cheng H, Perez-Soler R. Leptomeningeal metastases in non-small-cell lung cancer. *Lancet Oncol* (2018) 19(1):e43–55. doi: 10.1016/s1470-2045(17)30689-7

6. Brastianos PK, Carter SL, Santagata S, Cahill DP, Taylor-Weiner A, Jones RT, et al. Genomic characterization of brain metastases reveals branched evolution and potential therapeutic targets. *Cancer Discovery* (2015) 5(11):1164–77. doi: 10.1158/2159-8290.Cd-15-0369

7. Chamberlain M, Junck L, Brandsma D, Soffietti R, Rudà R, Raizer J, et al. Leptomeningeal metastases: a RANO proposal for response criteria. *Neuro Oncol* (2017) 19(4):484–92. doi: 10.1093/neuonc/now183

8. Wu Y-L, Zhou L, Lu Y. Intrathecal chemotherapy as a treatment for leptomeningeal metastasis of non-small cell lung cancer: A pooled analysis. *Oncol Lett* (2016) 12(2):1301–14. doi: 10.3892/ol.2016.4783

9. Yan W, Liu Y, Li J, Han A, Kong L, Yu J, et al. Whole brain radiation therapy does not improve the overall survival of EGFR-mutant NSCLC patients with leptomeningeal metastasis. *Radiat Oncol* (2019) 14(1):168. doi: 10.1186/s13014-019-1376-z

10. Morris PG, Reiner AS, Szenberg OR, Clarke JL, Panageas KS, Perez HR, et al. Leptomeningeal metastasis from non-small cell lung cancer: survival and the impact of whole brain radiotherapy. *J Thorac Oncol* (2012) 7(2):382–5. doi: 10.1097/JTO.0b013e3182398e4f

11. Nayar G, Ejikeme T, Chongsathidkiet P, Elsamadicy AA, Blackwell KL, Clarke JM, et al. Leptomeningeal disease: current diagnostic and therapeutic strategies. *Oncotarget.* (2017) 8(42):73312–28. doi: 10.18632/oncotarget.20272

12. Pan Z, Yang G, He H, Zhao G, Yuan T, Li Y, et al. Concurrent radiotherapy and intrathecal methotrexate for treating leptomeningeal metastasis from solid tumors with adverse prognostic factors: A prospective and single-arm study. *Int J Cancer* (2016) 139 (8):1864–72. doi: 10.1002/ijc.30214

13. Park JH, Kim YJ, Lee JO, Lee KW, Kim JH, Bang SM, et al. Clinical outcomes of leptomeningeal metastasis in patients with non-small cell lung cancer in the modern chemotherapy era. *Lung Cancer* (2012) 76(3):387–92. doi: 10.1016/j.lungcan.2011.11.022

14. Ettinger DS, Wood DE, Aisner DL, Akerley W, Bauman JR, Bharat A, et al. Non-small cell lung cancer, version 3.2022, NCCN clinical practice guidelines in oncology. *J Natl Compr Canc Netw* (2022) 20(5):497–530. doi: 10.6004/jnccn.2022.0025

15. Saboundji K, Auliac J-B, Pérol M, François G, Janicot H, Marcq M, et al. Efficacy of osimertinib in EGFR-mutated non-small cell lung cancer with leptomeningeal metastases pretreated with EGFR-tyrosine kinase inhibitors. *Target Oncol* (2018) 13 (4):501–7. doi: 10.1007/s11523-018-0581-2

16. Nanjo S, Hata A, Okuda C, Kaji R, Okada H, Tamura D, et al. Standard-dose osimertinib for refractory leptomeningeal metastases in T790M-positive EGFR-mutant non-small cell lung cancer. *Br J Cancer* (2017) 118(1):32–7. doi: 10.1038/bjc.2017.394

17. Ahn M-J, Chiu C-H, Cheng Y, Han J-Y, Goldberg SB, Greystoke A, et al. Osimertinib for patients with leptomeningeal metastases associated with EGFR T790M-positive advanced NSCLC: the AURA leptomeningeal metastases analysis. *J Thorac Oncol* (2020) 15(4):637–48. doi: 10.1016/j.jtho.2019.12.113

18. Park S, Lee MH, Seong M, Kim ST, Kang JH, Cho BC, et al. A phase II, multicenter, two cohort study of 160 mg osimertinib in EGFR T790M-positive non-small-cell lung cancer patients with brain metastases or leptomeningeal disease who progressed on prior EGFR TKI therapy. *Ann Oncol* (2020) 31(10):1397–404. doi: 10.1016/j.annonc.2020.06.017

19. Yang JCH, Kim SW, Kim DW, Lee JS, Cho BC, Ahn JS, et al. Osimertinib in patients with epidermal growth factor receptor mutation-positive non-small-cell lung cancer and leptomeningeal metastases: the BLOOM study. *J Clin Oncol* (2020) 38 (6):538–47. doi: 10.1200/JCO.19.00457

20. Li N, Bian Z, Cong M, Liu Y. Survival outcomes of patients with epidermal growth factor receptor mutations in non-small cell lung cancer with leptomeningeal metastasis. *Front Oncol* (2022) 11:723562. doi: 10.3389/fonc.2021.723562

21. Xu H, Chen H, Kong J, Zhang Y, Liu S, Yang G, et al. Osimertinib for the treatment of epidermal growth factor receptor-mutated non-small cell lung cancer patients with leptomeningeal metastases and different T790M status. *Ann Trans Med* (2021) 9(11):937. doi: 10.21037/atm-21-1249

22. Xu Z, Hao X, Wang Q, Yang K, Li J, Xing P. Intracranial efficacy and safety of furmonertinib 160 mg with or without anti-angiogenic agent in advanced NSCLC patients with BM/LM as salvage therapy. *BMC Cancer* (2023) 23(1):206. doi: 10.1186/s12885-023-10676-x

23. Shi Y, Zhang S, Hu X, Feng J, Ma Z, Zhou J, et al. Safety, clinical activity, and pharmacokinetics of alflutinib (AST2818) in patients with advanced NSCLC with EGFR T790M mutation. *J Thorac Oncol* (2020) 15(6):1015–26. doi: 10.1016/j.jtho.2020.01.010

24. Shi Y, Chen G, Wang X, Liu Y, Wu L, Hao Y, et al. Furmonertinib (AST2818) versus gefitinib as first-line therapy for Chinese patients with locally advanced or metastatic EGFR mutation-positive non-small-cell lung cancer (FURLONG): a multicentre, double-blind, randomised phase 3 study. *Lancet Respir Med* (2022) 10 (11):1019–28. doi: 10.1016/S2213-2600(22)00168-0

25. Shi Y, Hu X, Liao W, Zhang S, Wang Z, Yang N, et al. P76.65 CNS efficacy of AST2818 in patients with T790M-positive advanced NSCLC: data from a phase I-II dose-expansion study. *J Thorac Oncol* (2021) 16(3):S616. doi: 10.1016/j.jtho.2021.01.1122

26. Shi Y, Hu X, Zhang S, Lv D, Wu L, Yu Q, et al. Efficacy, safety, and genetic analysis of furmonertinib (AST2818) in patients with EGFR T790M mutated non-small-cell lung cancer: a phase 2b, multicentre, single-arm, open-label study. *Lancet Respir Med* (2021) 9(8):829–39. doi: 10.1016/s2213-2600(20)30455-0

27. Wu YL, Ahn MJ, Garassino MC, Han JY, Katakami N, Kim HR, et al. CNS efficacy of osimertinib in patients with T790M-positive advanced non-small-cell lung cancer: data from a randomized phase III trial (AURA3). *J Clin Oncol* (2018) 36 (26):2702–9. doi: 10.1200/JCO.2018.77.9363

28. Cheng D, Tang S, Li D, Zhao W, Wei W, Fang C, et al. Successful salvage therapy using high-dose furmonertinib (AST2818) for non–small-cell lung cancer after Osimertinib resistance: a case report. *Anti-Cancer Drugs* (2022) 33(8):768–72. doi: 10.1097/cad.0000000000001368

29. Qian C, Zhang Y, Cheng W, Zhang Q, Li M, Fang S. Case report: Rechallenge with EGFR–TKIs after immunotherapy in EGFR–mutated non–small cell lung cancer with leptomeningeal metastasis. *Front Oncol* (2022)12:957661. doi: 10.3389/fonc.2022.957661

30. Ballard P, Yates JWT, Yang Z, Kim D-W, Yang JC-H, Cantarini M, et al. Preclinical comparison of osimertinib with other EGFR-TKIs in EGFR-mutant NSCLC brain metastases models, and early evidence of clinical brain metastases activity. *Clin Cancer Res* (2016) 22(20):5130–40. doi: 10.1158/1078-0432.Ccr-16-0399

31. Oxnard GR, Arcila ME, Chmielecki J, Ladanyi M, Miller VA, Pao W. New strategies in overcoming acquired resistance to epidermal growth factor receptor tyrosine kinase inhibitors in lung cancer. *Clin Cancer Res* (2011) 17(17):5530–7. doi: 10.1158/1078-0432.Ccr-10-2571

32. Li YS, Jiang BY, Yang JJ, Zhang XC, Zhang Z, Ye JY, et al. Unique genetic profiles from cerebrospinal fluid cell-free DNA in leptomeningeal metastases of EGFR-mutant non-small-cell lung cancer: a new medium of liquid biopsy. *Ann Oncol* (2018) 29 (4):945–52. doi: 10.1093/annonc/mdy009

33. Kim EY, Cho EN, Park HS, Kim A, Hong JY, Lim S, et al. Genetic heterogeneity of actionable genes between primary and metastatic tumor in lung adenocarcinoma. *BMC Cancer* (2016) 16. doi: 10.1186/s12885-016-2049-z

34. Ali S, Gorska Z, Duchnowska R, Jassem J. Molecular profiles of brain metastases: A focus on heterogeneity. *Cancers (Basel)* (2021) 13(11):2645. doi: 10.3390/cancers13112645

35. Lu S, Wang Q, Zhang G, Dong X, Yang CT, Song Y, et al. Efficacy of aumolertinib (HS-10296) in patients with advanced EGFR T790M+ NSCLC: updated post-national medical products administration approval results from the APOLLO registrational trial. *J Thorac Oncol* (2022) 17(3):411–22. doi: 10.1016/j.jtho.2021.10.024

36. Ericson-Lindquist K, Johansson A, Leveen P, Elmberger G, Jonsson G, Staaf J, et al. Targeted sequencing may facilitate differential diagnostics of pulmonary tumours: a case series. *Diagn Pathol* (2017) 12(1):31. doi: 10.1186/s13000-017-0621-8

37. Reita D, Pabst L, Pencreach E, Guerin E, Dano L, Rimelen V, et al. Molecular mechanism of EGFR-TKI resistance in EGFR-mutated non-small cell lung cancer: application to biological diagnostic and monitoring. *Cancers (Basel)* (2021) 13 (19):4926. doi: 10.3390/cancers13194926

38. Zheng M-M, Li Y-S, Tu H-Y, Jiang B-Y, Yang J-J, Zhou Q, et al. Genotyping of cerebrospinal fluid associated with osimertinib response and resistance for leptomeningeal metastases in EGFR-mutated NSCLC. *J Thorac Oncol* (2021) 16 (2):250–8. doi: 10.1016/j.jtho.2020.10.008

frontiers | Frontiers in Oncology

TYPE Original Research
PUBLISHED 07 November 2023
DOI 10.3389/fonc.2023.1214126

OPEN ACCESS

EDITED BY
Jianxin Xue,
Sichuan University, China

REVIEWED BY
Timothy F. Burns,
University of Pittsburgh, United States
Yifei Deng,
Chengdu Seventh People's Hospital, China
Zhuoran Yao,
Sichuan University, China

*CORRESPONDENCE
John C. Hunting
jhunting@wakehealth.edu

RECEIVED 28 April 2023
ACCEPTED 10 October 2023
PUBLISHED 07 November 2023

CITATION
Abdulhaleem M, Hunting JC, Wang Y, Smith MR, Agostino RD, Lycan T, Farris MK, Ververs J, Lo H-W, Watabe K, Topaloglu U, Li W, Whitlow C, Su J, Wang G, Chan MD, Xing F and Ruiz J (2023) Use of comprehensive genomic profiling for biomarker discovery for the management of non-small cell lung cancer brain metastases.
Front. Oncol. 13:1214126.
doi: 10.3389/fonc.2023.1214126

Use of comprehensive genomic profiling for biomarker discovery for the management of non-small cell lung cancer brain metastases

Mohammed Abdulhaleem[1], John C. Hunting[1]*, Yuezhu Wang[2], Margaret R. Smith[2], Ralph D' jr. Agostino[3], Thomas Lycan[1], Michael K. Farris[4], James Ververs[4], Hui-Wen Lo[2], Kounosuke Watabe[2], Umit Topaloglu[2], Wencheng Li[5], Christopher Whitlow[6], Jing Su[7], Ge Wang[8], Michael D. Chan[4], Fei Xing[2] and Jimmy Ruiz[1]

[1]Department of Internal Medicine (Hematology & Oncology), Wake Forest School of Medicine, Winston-Salem, NC, United States, [2]Department of Cancer Biology, Wake Forest School of Medicine, Winston-Salem, NC, United States, [3]Department of Biostatistics and Data Science, Wake Forest School of Medicine, Winston-Salem, NC, United States, [4]Department of Radiation Oncology, Wake Forest School of Medicine, Winston-Salem, NC, United States, [5]Department of Pathology, Wake Forest School of Medicine, Winston-Salem, NC, United States, [6]Department of Radiology, Wake Forest School of Medicine, Winston-Salem, NC, United States, [7]Department of Biostatistics and Health Data Science, Indiana University School of Medicine, Indianapolis, IN, United States, [8]Department of Biomedical Engineering, Rensselaer Polytechnic Institute, Troy, NY, United States

Background: Clinical biomarkers for brain metastases remain elusive. Increased availability of genomic profiling has brought discovery of these biomarkers to the forefront of research interests.

Method: In this single institution retrospective series, 130 patients presenting with brain metastasis secondary to Non-Small Cell Lung Cancer (NSCLC) underwent comprehensive genomic profiling conducted using next generation circulating tumor deoxyribonucleic acid (DNA) (Guardant Health, Redwood City, CA). A total of 77 genetic mutation identified and correlated with nine clinical outcomes using appropriate statistical tests (general linear models, Mantel-Haenzel Chi Square test, and Cox proportional hazard regression models). For each outcome, a genetic signature composite score was created by summing the total genes wherein genes predictive of a clinically unfavorable outcome assigned a positive score, and genes with favorable clinical outcome assigned negative score.

Results: Seventy-two genes appeared in at least one gene signature including: 14 genes had only unfavorable associations, 36 genes had only favorable associations, and 22 genes had mixed effects. Statistically significant associated signatures were found for the clinical endpoints of brain metastasis velocity, time to distant brain failure, lowest radiosurgery dose, extent of extracranial metastatic disease, concurrent diagnosis of brain metastasis and NSCLC, number of brain metastases at diagnosis as well as distant brain failure. Some genes were solely associated with multiple favorable or unfavorable outcomes.

Conclusion: Genetic signatures were derived that showed strong associations with different clinical outcomes in NSCLC brain metastases patients. While these data remain to be validated, they may have prognostic and/or therapeutic impact in the future.

Statement of translation relevance: Using Liquid biopsy in NSCLC brain metastases patients, the genetic signatures identified in this series are associated with multiple clinical outcomes particularly these ones that lead to early or more numerous metastases. These findings can be reverse-translated in laboratory studies to determine if they are part of the genetic pathway leading to brain metastasis formation.

KEYWORDS

brain metastasis, non-small cell lung cancer, outcomes, biomarkers, genomic profiling

Highlights

*Among NSCLC brain metastases, seventy-two genes significantly signaled clinical outcomes.

*Unfavorable outcomes only associated with 14 genes while 36 only favorable.

*Genetic signals strongly indicate the ability to predict oligometastatic disease.

Introduction

Nearly 170,000 patients a year in the United States are diagnosed with brain metastases (1), and approximately half of brain metastases derive from NSCLC (2). However, even amongst patients with metastases originating from the same primary cancer type, there is a significant diversity of biological and clinical outcomes. A heterogeneity in clinical outcomes derives from a variability in the size and number of metastases (3), along with differences in histology (4) and health status (5, 6) of each patient. The sensitivity of each patient's cancer to systemic therapy has also been found to be an important variable that contributes to clinical differences between patients (7).

The diversity of the brain metastasis population has made biomarker discovery an important goal. Recent evidence suggests that there may be brain metastasis-specific mutations, and that the genetics of brain metastases may evolve differently from a patient's primary cancer (8). Several attempts have been made to link genetic signatures found in resected brain metastasis samples to clinical outcomes of brain metastases (9, 10). However, thus far, clinically useful predictive biomarkers for brain metastasis outcomes have been generally elusive.

Over the past several years, several commercial platforms have developed for comprehensive genomic profiling of non-small cell lung cancers (11). Methods for such profiling include genetic sequencing of a biopsied tumor sample, as well as sequencing of circulating tumor DNA (12). Circulating tumor DNA has been shown to correlate with tumor mutations both in serum and cerebrospinal fluid (CSF) (13). Sensitivities have varied, among populations, notably with circulating tumor DNA of the CSF having a higher correlation to brain metastases mutations given the blood brain barrier (13–15). Though plasma samples remain valid and are more easily and commonly obtained prior to known diagnosis of brain metastases. These platforms for genomic profiling of lung cancers has helped to identify potential therapeutic targets in patients that are found to have targetable mutations (16–18), or identify populations that are more likely to respond to immunotherapy (16, 19).

Amongst the brain metastasis population, several potential clinical dilemmas exist for which biomarker discovery could potentially change practice. The ability to predict such outcomes as brain metastasis velocity (20), leptomeningeal disease (21), and which patients benefit from whole brain radiation (22) would give practitioners guidance to select proper therapies for each individual. The goal of the present study is to demonstrate the feasibility of using comprehensive genomic profiling to discover biomarkers that predict brain metastasis outcomes in patients with NSCLC. To this end, we used a single institution retrospective review of NSCLC brain metastasis patients receiving stereotactic radiosurgery (SRS) who underwent comprehensive genomic profiling and analyzed whether the genes assessed in genomic profiling were associated with clinical characteristics and patient outcomes.

Methods

Data acquisition, inclusion, and exclusion

The present study was approved by the institutional review board at Wake Forest School of Medicine. Patients were eligible for this study if they had a diagnosis of brain metastasis from NSCLC and had comprehensive genomic profiling performed with at least

one mutation detected. Patients without detectable mutations, whether uninformative test with no ctDNA detected or negative test with no alterations found were excluded. The Wake Forest brain metastasis database which prospectively includes all patients receiving stereotactic radiosurgery for brain metastases was searched for all patients with NSCLC. Clinical characteristics and outcomes were determined via the electronic medical records. Tumor and dosing characteristics were determined using the GammaPlan Treatment Planning System (Elekta AB, Stockholm).

A total of 130 patients who had initial diagnosis of brain metastasis between August 2012 - September 2021 were included in the study. Data collected included age, race, gender, smoking status, number of metastases at initial gamma knife (GK), lowest dose prescribed to a metastasis at SRS, Karnofsky performance scale (KPS), systemic disease burden, time of brain metastasis, number of metastases at first distant brain failure, and time of death. Patient characteristics are summarized in Table 1.

Stereotactic radiosurgery

Patients included in the study were treated with SRS using the GK Perfexion (Elekta AB, Stockholm, Sweden). Patients were immobilized using rigid frame fixation and underwent a same day high resolution stereotactic magnetic resonance imaging (MRI) with contrast (GE Healthcare, Chicago, IL). Treatment planning was performed using the GammaPlan Treatment Planning System. Dose prescription was done per guidelines derived from the RTOG 90-05 study (23).

Comprehensive genomic profiling

Comprehensive genomic profiling was conducted using next generation circulating tumor DNA(Guardant Health, Redwood City, CA). Blood sample of cell free DNA obtained from the patients prior to receiving systemic therapy using a CLIA-certified Next Generation Sequencing test as described by Leighl et al. (24). Sequencing included collections both before and after initiating GK treatment. Time to genomic sequencing is further described in Table 1.

Response assessment, follow-up and definition of clinical outcomes

Patients generally underwent a follow-up MRI with clinical evaluation 6-8 weeks after SRS and then every 3 months thereafter for the first 2 years after radiosurgery. If the patient did not experience tumor progression to that point, the imaging follow-up was done less frequently at that point (every 4-6 months).

Brain metastasis velocity (BMV) was defined as previously published by Farris et al. (7). In brief, BMV was defined as the cumulative number of new brain metastases since SRS divided by the number of brain metastases. Time to distant brain failure was defined as the time to development of new brain metastases that were not previously treated with SRS (3). Lowest GK dose was defined as the lowest prescribed dose to any brain metastasis at time of SRS. This factor has previously been used as a surrogate for treatment volume as the lowest GK dose is inversely proportional to the dose delivered to metastases in a fairly linear relationship (25). Systemic disease burden was defined as none, oligometastatic or widespread (26). If patients had ≤5 non-brain metastases without diffuse involvement of any one organ, the patient was considered to have oligometastatic disease, while having >5 metastases or diffuse distant organ involvement is considered widespread disease (27). Concurrent "Synchronous metastasis" was defined as the diagnosis

TABLE 1 Patient Characteristics.

Total = 130 patients	Median (range).
Primary diagnosis (Adenocarcinoma)	97 (75%)
Gender (Female)	68 (52%)
Age (years)	68 (41–85)
Race (White)	108 (83%)
KPS	78 (60–90)
Smoking status	
Former	83 (64%)
Current	26 (20%)
Never	21 (16%)
Lowest GK	18 (12–24)
Number of metastases at first GK	4 (1–18)
Systemic disease burden (oligometastatic)	51 (39%)
Brain metastasis velocity (n 54/130)	14.2 (0 – 210)
Low (≤4)	21/54
Intermediate (4–13)	21/54
High (>13)	12/54
Number of metastases at distant brain failure (n 54/130)	4 (1–35)
Concurrent diagnosis	88 (68%)
Timing relationship between sequencing and GK (days)	
Patients sequenced first later treated with GK (n 67)	25 (12.5 - 103)
Patients who received sequencing after GK (n 63)	188 (22.5 - 384.5)
Frequency of mutated genes (N=77)	
TP53	70%
KRAS	32%
EGFR	26%
ARID1A, ERBB2, NF1, KTI, STK11, PIK3CA, PDGFRA, AR, MET, BRAF(V600), BRACA1, APC.	10% - 20%
Other genes	< 10%

Categorical variables reported as count (frequency).
Continuous variables reported as median (interquartile range).

of a brain metastasis within a three-month interval of the diagnosis of the primary NSCLC (28).

Statistics

Descriptive statistics (means/medians, standard deviations, ranges, counts and percent) were calculated for all outcomes of interest. Separate genetic signatures were created for each of the nine outcomes of interest (brain metastasis velocity, concurrent diagnosis of brain metastases and primary cancer, time to distant brain failure, performance status, lowest SRS dose, number of metastases at treatment failure, number of metastases at diagnosis, extent of extracranial metastatic disease, and overall survival). The approach consisted of a four-step process. The first step was to screen the seventy-seven genes across each of the nine outcomes to identify any genes that had a modest association ($p<0.1$) with the outcome. For the five continuous outcomes (brain metastasis velocity, performance status, lowest SRS dose, number of metastases at treatment failure, and number of metastases at diagnosis), 2-sample t-tests were used, for the two binary outcomes (concurrent diagnosis of brain metastases and primary cancer and extent of extracranial metastatic disease), Fisher's exact tests were used, for overall survival, Cox proportional hazard's regression was used, and for time to distant brain failure, a competing risk model was used to identify genes for each signature.

Next, for each outcome, the genes identified were separated into "protective" and "harmful" categories based on the direction of the point estimate of each individually assessed mutation with outcome compared to absence of the mutation. (i.e., if the presence of a gene was associated with worse outcome (shorter survival) it was considered "unfavorable" whereas if the presence of a gene was associated with an improved outcome (longer survival) it was considered "favorable"). Favorable clinical outcomes included lower hazard ratio of death, lower mean brain metastasis velocity, lower mean number of brain metastases at first GK or distant brain failure (DBF), lower mean first dose of GK required, longer time to DBF, higher mean KPS, increased frequency of oligometastatic disease pattern, and lower frequency of concurrent diagnosis. Unfavorable outcomes were considered as the converse. For the third step, each unfavorable gene received a score of +1 and each favorable gene received a score of -1. These scores were then summed across genes for each outcome. Finally, the overall gene score was created by transforming the gene scores into 3–level ordinal variables (one for each outcome) as follows: if the gene score for an outcome was negative it was coded as -1, if the gene score was 0 it was coded as 0, and if it was positive it was coded as +1.

These nine gene scores were then evaluated for their ability to predict each of the nine outcomes, respectively. For each of the five continuous outcomes, a general linear model was fit with the gene score included as a class variable. Mean values for each of the 3 levels of the gene score were then compared. For the two binary outcomes, Chi-square tests were performed to assess the gene score. For the time to event outcomes, Cox proportional hazard's regression models were fit and hazard ratios were examined based on the gene scores. For evaluating the success of the gene scores (signatures), $p<0.05$ was used to identify significant scores. Multiple testing corrections was not performed.

Results

Identification of genes for inclusion in gene signatures for profiling brain metastasis related outcomes

Table 2 summarizes the genes identified that had a statistically significant association for each clinical outcome of interest. As can be seen, the number of genes included in each signature ranged from six (for Overall Survival) to twenty-eight (for Brain Metastasis Velocity). Across the different outcomes, more genes were identified as favorable than unfavorable, meaning that for several outcomes, having a gene present was associated with not having the negative outcome (i.e., the presence of the *ATM* gene mutation was associated with a more favorable Brain Metastasis Velocity, fewer metastases at first GK, fewer metastases at DBF and the presence of an oligometastatic disease burden).

As described in the methods above, each patient included in the analysis was given a gene signature for each outcome. These scores took on one of three potential values. Genes predictive of a favorable or unfavorable outcome for each clinical endpoint were assigned a value of -1 or -+1, respectively, and then scores were summed to determine risk profile for each patient. Patients with positive sum were considered unfavorable risk, those with a negative sum were considered favorable risk, and those with zero sum were neutral. For example, for the outcome of overall survival there were 6 genes included in the signature, 2 favorable (*KRAS* and *CDK6*) and 4 unfavorable (*NRAS, RIT1, RAF1 or ALK_EML4*). If a patient had one or both favorable genes (*KRAS* and *CDK4*) and no unfavorable genes, then they would be assigned a -1 and considered to have a favorable gene signature. Likewise, if a patient had no favorable genes, but had at least one or more of the unfavorable genes (*NRAS, RIT1, RAF1 or ALK_EML4*) they would be assigned a +1 for their overall survival gene signature. Finally, if a patient had either an equal number of favorable and unfavorable gene mutations, or had no favorable or unfavorable genes present, then they would be assigned a 0 for their overall survival gene score.

Using this approach for each outcome, Table 3 shows the comparisons of results for each outcome stratified by gene signature. As can be seen, all nine gene signatures were statistically significant for predicting the outcome of interest. In fact, most gene signatures showed a highly statistically and clinically significant difference across values of the signature. Figures 1–3 also display graphically the ability of the gene signatures to differentiate patients for the outcomes of Brain Metastasis Velocity, overall survival and time to distant brain failure (accounting for the competing risk of death).

It should be noted that Karnofsky performance status did not have as strong a statistically significant genomic signature association as other endpoint signatures. The difference between neutral and favorable signatures was KPS of 78 *vs* 80, respectively,

10.3389/fonc.2023.1214126

TABLE 2 Clinical outcomes and their associated genes signature.

Clinical outcomes	Genes Predictive of Favorable Outcome		Genes Predictive of Unfavorable Outcome	
		P-value		P-value
Overall survival	*KRAS* *CDK6*	*.094* *.092*	*NRAS* *RIT1* *RAF1* *ALK_EML4*	*0.128* *0.173* *0.551* *0.10*
BMV	*AKT1* *APC* *AR* *ATM* *CCND1* *CCND2* *CDH1* *CDK6* *CDK12* *CDKN2A* *CTNNB1* *EGFR* *ERBB2* *FGFR1* *GATA3* *HFN1A* *MAP2K2* *MTOR* *NOTCH1* *NTRK3* *PALB2* *SMAD4*	*.0065* *.0263* *.0391* *.0175* *.0046* *.0049* *.0838* *.0778* *.0043* *.0046* *.0171* *.0974* *.0497* *.0197* *.0046* *.0041* *.0507* *.0069* *.0297* *.0046* *.0163* *.0228*	*CDK4* *FGFR2* *KIT* *MYC* *NFE2l2* *PDGFRA*	*.0408* *.0181* *.0925* *.0119* *.0006* *.0442*
Number of metastases at first GK	*APC* *ATM* *BRCA1* *CCND2* *FGFR1* *FGFR3* *FGFR3_TACC3* *GATA3* *HRAS* *MET* *NOTCH1* *NTRK3* *RAF1* *TSC1*	*.0961* *.0527* *.0002* *<.0001* *.0017* *.0373* *.0413* *<.0001* *.0022* *.0720* *.0049* *.0402* *.0003* *.0022*	*BRAF* *EGFR* *NRAS* *PDGFRA* *RAD51D* *RB1*	*.0741* *.0830* *.0423* *.0516* *.0089* *.0815*
Lowest GK dose	*ALK,* *EML4_ALK* *FBXW7* *HRAS* *IDH2* *SMO* *STK11* *TCI1*	*.048* *.0696* *<0.001* *<0.001* *.0696* *<0.001* *.0028* *.002*	*BRCA2* *CCND1* *EGFR* *MAP2K2* *NF1* *NRAS* *RHEB* *SMAD4*	*.02* *.013* *.097* *.018* *.0258* *.0217* *.0109* *.009*
Number of metastases at DBF*	*AKT1* *ATM* *CCND1* *CCND2* *CDH1* *CDK6* *CDK12* *CDKN2A* *CHEK2* *CTNNB1* *FGFR2* *GATA3* *HFN1A* *MET*	*.0013* *.0115* *.0015* *.0015* *.0229* *.0572* *.0015* *.0015* *.0095* *.0657* *.0583* *.0013* *.0013* *.0927*	*KIT* *PDGFRA*	*.008* *.513*

(Continued)

10.3389/fonc.2023.1214126

TABLE 2 Continued

Clinical outcomes	Genes Predictive of Favorable Outcome		Genes Predictive of Unfavorable Outcome	
		P-value		P-value
	MTOR *NOTCH1* *NTRK3* *PALB2* *SMAD4* *SMO*	*.0012* *.0657* *.0013* *.0650* *.0062* *.0095*		
Time for distant brain failure.	*NRAS* *RET* *FGFR3_TACC3* *EML4_ALK* *FBXW7* *KEAP1* *TSC1* *EZH2* *GNA11* *LRIG3_ROS1* *MAP2K1* *ALK_EML4* *RIT1* *FANCA* *ARAF* *NTRK2* *RHEB*	*<.0001* *<.0001* *<.0001* *<.0001* *<.0001* *<.0001* *<.0001* *<.0001* *<.0001* *<.0001* *<.0001* *<.0001* *<.0001* *<.0001* *<.0001* *<.0001* *<.0001*	*PMS2*, *IDH1*, *MAP2K2*, *GNAQ*, *HRAS*, *APC*	*<.001* *<.0001* *.0004* *.0006* *.0032* *.0495*
KPS	*PMS2*	*.0163*	*AKT1* *CDH1* *FBXW7* *GATA3* *GNAS* *HFN1A* *HRAS* *MAP2K2* *MAPK1* *NTRK3* *SMO*	*.0342* *.0342* *.0342* *.0342* *.0342* *.0342* *.0342* *.0342* *.0342* *.0869* *.0342*
Disease burden (Oligometastatic)	*ATM* *JAK2* *MAP2K2* *NTRK1*	*.048* *.058* *.058* *.058*	*ARID1A* *CCNE1*	*.097* *.088*
Concurrent diagnosis (synchronous)	*MYC*, *NTRK1* *PTEN* *RB1* *AKT1* *GATA3*	*.057* *.032* *.036* *.085* *.099* *.099*	*FGFR2*	*.031*

*BMV, Brain Metastasis Velocity; DBF, Distant Brain Failure.

and the unfavorable signature only represented one patient with a KPS of 60.

Genes associated with multiple outcomes

Several genes were associated with multiple clinical outcomes. These are summarized in Table 4. Genes associated with improved clinical outcomes included *AKT1* (greater likelihood of oligometastatic disease, lower number of metastases at first SRS and distant brain failure), *CDK6* (lower BMV and lower number of metastases at distant brain failure), and *GATA3* (better KPS, lower BMV, lower number of metastases at first GK and distant brain failure). Genes associated with a multiple negative clinical outcome include: *NRAS* (lower dose delivered at SRS and greater number of metastases at first SRS), and *PDGFRA* (higher BMV, greater number of metastases at first SRS and at distant brain failure).

Discussion

NSCLC represents a genetically diverse population. In the late 1990's, subpopulations of NSCLC patients who were found to be predominantly female non-smokers were identified and found to have cancers that responded to tyrosine kinase inhibitors (29). The mechanism of this response has been determined to be an activating

TABLE 3 Statical significance of genetic signature in association with the clinical outcomes.

	Favorable*	Neutral**	Unfavorable***	P Value
BMV (mean)	4.75	7.85	51.1	0.0002
Lowest Dose at GK (mean) with corresponding brain metastasis volume	20.7 Gy (1 cc)	19.2 Gy (2 cc)	17.5 Gy (6 cc)	<0.0001
Number Metastases at 1st GK (mean)	2.3	3.7	7.2	<0.0001
Number Brain Metastases at DBF (mean)	1.2	3.2	9.2	0.0007
KPS (mean)	80.4	78.3	60	0.026
Oligometastatic extracranial disease (%Yes)	78%	41%	11.5%	<0.0001
Concurrent Diagnosis of Brain Metastasis and Extracranial Disease (%Yes)	22.7%	75.5%	100%	<0.0001
DBF (% Yes)	0%	43%	83%	<0.0001
OS (median in weeks)	124	65	9	0.0017

*Sum of gene values with predictive ability is a positive integer.
**Sum of gene values with predictive ability is zero.
***Sum of gene values with predictive ability is a negative integer.

mutation in the *EGFR* gene (30). This discovery led to a cascade of subsequent discoveries of various subpopulations of the NSCLC population including the ALK (31), ROS-1 (32), RET (33) and BRAF-mutated (34) populations. While the aforementioned mutations represent activating mutations for which targeted agents have been developed to counter, these may not represent the full story for how genomic analysis may ultimately affect care in NSCLC patients.

Biomarker discovery for brain metastasis behavior has thus far been an elusive process (35). This difficulty derives from several reasons including the histologic heterogeneity of the brain metastasis population (3), and the propensity for continued mutation between a primary tumor and the clonogens that ultimately become brain metastases (8). A preliminary study found that assessing circulating DNA in the serum as done in the present study may better detect mutations not found in a primary colorectal tumor though these findings would need to be validated in lung cancer patients (36). The present study also attempted to address the issue of histologic heterogeneity by using a population of purely NSCLC patients. Future investigations will likely include attempts to use tissue acquired from craniotomy samples in order to ensure that mutations from brain metastases are captured in the genomic analyses (9).

In the present analysis, genetic signatures were discovered for factors that have the potential to affect management. For example, patients with a signature predicting a lower SRS dose represent a population in which a dominant brain metastasis developed that was generally large and/or symptomatic. These brain metastases are ones that historically lead to significant morbidity and mortality (37, 38). Such a signature could yield a population for which surveillance imaging even prior to brain metastasis diagnosis may be useful. In addition, patients with signatures for lower BMV or lower number of brain metastases at distant brain failure may ultimately represent populations for which aggressive use of SRS is justified (39, 40), perhaps even in cases when a greater number of metastases are present than are normally offered SRS (41).

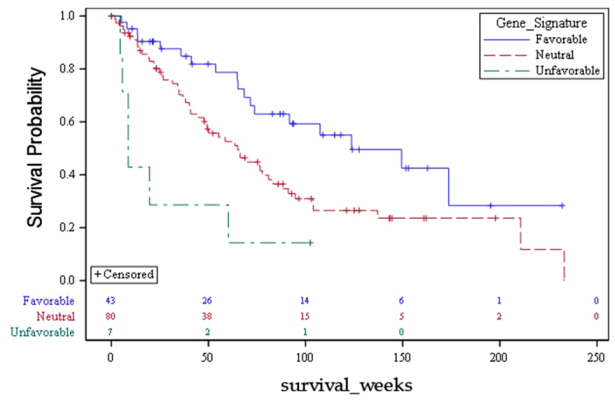

FIGURE 1
Kaplan Meier Plot for genetic signatures associated with Overall Survival.

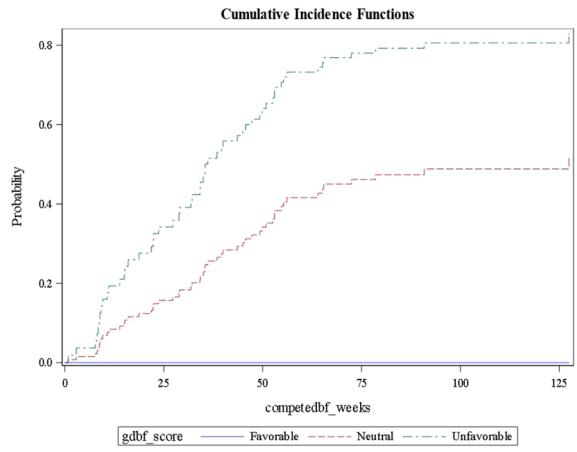

FIGURE 2
Cumulative Incidence Plot for genetic signatures associated with Distant Brain Failure.

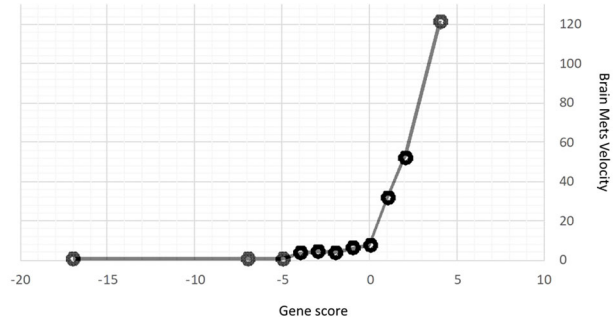

FIGURE 3
Brain Metastasis Velocity by Gene Signature Score.

Clinical outcomes in the present analysis were scored with regards to whether they were favorable or unfavorable in the clinical setting. For example, larger or more numerous brain metastases or higher BMV were considered adverse, whereas smaller or fewer brain metastases were considered protective. This allowed for assessment of whether single genes could be favorable or unfavorable in multiple outcomes. Several gene mutations were identified within the multiple genetic signatures and these genes were found to be more likely to be either favorable or unfavorable (as opposed to discordant) across those multiple outcomes. Ultimately, genetic mutations identified in multiple unfavorable signatures are candidates, particularly in outcomes that lead to early or more numerous metastases, to be reverse-translated in laboratory studies to determine if they are part of the genetic pathway leading to brain metastasis formation.

The meaningful clinical separation between risk strata determined in the present series was quite large. For example, the survival difference between favorable, neutral, and unfavorable strata was 124 weeks, 65 weeks, and 9 weeks respectively (p=0.002). Patients with life expectancy as low as 2 months of survival may choose to have treatments that can be costly and affect quality of life. Moreover, the corresponding tumor volumes predicted for each risk strata by the present analysis based on lowest GK dose are 1 cc (favorable), 2 cc (neutral) and 6 cc (unfavorable). Tumors of the favorable or neutral scores tend to be good candidates for SRS whereas those with unfavorable scores had tumor volumes that are often best managed with surgery. These findings with regards to presenting tumor volume suggest that there may be volumetric phenotypes for brain metastasis presentation (large symptomatic *vs* small asymptomatic) which are driven by biology. Such a hypothesis has significant reverse translational potential.

TABLE 4 Single genes and associated with multiple clinical outcomes.

Genes	Favorable clinical outcomes	Unfavorable clinical outcomes
ATK1	Oligometastatic disease, lower number of metastases at first GK and DBF,	NA
CDK6	Lower BMV, lower number of metastases at DBF	NA
GATA3	Lower KPS, lower number of metastases at first GK and DBF	NA
NRAS	NA	Higher SRS dose, and number of metastases at first GK
PDGFRA	NA	Higher number of metastases at first GK and DBF, and higher BMV

Table notation for associated clinical outcomes with genes identified of interest.
NA (not-applicable) listed for outcomes when the association is understood to be the converse.

That KPS was the single clinical characteristic assessed for which the identified signature demonstrated a weaker statistical association and minimal clinical impact served to strengthen the argument that the other signatures may be valid. Other clinical factors such as BMV, number of brain metastases and size of brain metastases at presentation are factors for which there is a reasonable assumption of a biological phenotype responsible for the size and rate of seeding of the brain with cancer. KPS on the other hand is a complex variable dependent upon multiple factors such as age, burden of systemic disease, comorbidities, and ability to access care (42, 43). Many of these factors are beyond the scope of the genetics of a patient's cancer, and thus it would not be expected that a genetic signature could be found for KPS, but it was significant finding that this was the one variable that could not be predicted by a genomic signature in our dataset, functioning essentially as a negative control.

One of the genetic associations found in the present series was the signature for having oligometastatic extracranial disease. It has been hypothesized that a certain subset of cancers are truly oligometastatic, and thus, limited in their burden of tumor spread (44). As such, these cancers may benefit from local therapies directed towards the few sites of disease. There have been several recently published series that have suggested that such local treatment of extracranial oligometastatic disease can be beneficial for patients with regards to endpoints such as progression free survival, overall survival and need for systemic therapy (45). However, while some patients benefit and truly have a limited burden of metastatic disease, there are others that will experience rapid and diffuse failure, essentially rendering the local therapies non-useful. As with other relevant signatures found in the present series, the true clinical spread between favorable and unfavorable was quite large, as patients with favorable predictive score for oligometastatic disease had a 78% likelihood of having true oligometastatic disease. Conversely, those with unfavorable predictive score only had a 12% risk of having oligometastatic disease. If these genomic signatures for oligometastatic disease are validated, then they will have the potential to help dictate which patients may be candidates for local extracranial therapies.

There are several limitations to the present study. The study is a retrospective analysis and is therefore subject to selection bias. There also exists the issue of circulating DNA sampling as cancers are known to continue to mutate and the mutations found in the circulating DNA may or may not be present in the brain metastases. Additionally, only half the population had ctDNA drawn prior to SRS adding the potential for confounding. Circulating DNA from the CSF has been shown to correlate more

closely to mutations of CNS involvement such as leptomeningeal disease (46) and brain metastases, though remain a more invasive procedure via lumbar puncture and less standardized than blood draw. If validated, however, the identified genomic signatures in this series represent clinically useful data obtained via non-invasive liquid biopsy to help risk stratify patients to potentially inform treatment or surveillance decisions.

Data availability statement

The data analyzed in this study is subject to the following licenses/restrictions: Data will be made available per request to the corresponding author. Requests to access these datasets should be directed to John Hunting, jhunting@wakehealth.edu.

Ethics statement

The studies involving humans were approved by Wake Forest School of Medicine IRB. The studies were conducted in accordance with the local legislation and institutional requirements. Written informed consent for participation was not required from the participants or the participants' legal guardians/next of kin in accordance with the national legislation and institutional requirements.

Author contributions

MA, MC, FX contributed to conception and design of the study. YW, MA, H-WL, KW, UT procured relevant data. RD'A, JS, GW performed the statistical analysis. MA wrote the first draft of the manuscript. All authors contributed to manuscript revision, read, and approved the submitted version.

Funding

MC, MF, and JV are speakers for the Elekta SBRT course, and MC received an honorarium from Monteris for speaking. JS was partially financially supported by the Indiana University Precision Health Initiative and by the Indiana University Melvin and Bren Simon Comprehensive Cancer Center Support Grant from the National Cancer Institute [P30 CA 082709]. Otherwise, no other author has anything to disclose.

Conflict of interest

The authors declare that the research was conducted in the absence of any commercial or financial relationships that could be construed as a potential conflict of interest.

Publisher's note

References

1. Soike MH, Hughes RT, Farris M, McTyre ER, Cramer CK, Bourland JD, et al. Does stereotactic radiosurgery have a role in the management of patients presenting with 4 or more brain metastases? Neurosurgery. *Narnia;* (2019) 84:558–66.

2. Johnson JD, Young B. Demographics of brain metastasis. *Neurosurg Clinics North America* (1996), 337–44. doi: 10.1016/s1042-3680(18)30365-6

3. Ayala-Peacock DN, Peiffer AM, Lucas JT, Isom S, Kuremsky JG, Urbanic JJ, et al. A nomogram for predicting distant brain failure in patients treated with gamma knife stereotactic radiosurgery without whole brain radiotherapy. *Neuro Oncol* (2014) 16:1283–8. doi: 10.1093/neuonc/nou018

4. Kuremsky JG, Urbanic JJ, Petty WJ, Lovato JF, Bourland JD, et al. Tumor histology predicts patterns of failure and survival in patients with brain metastases from lung cancer treated with gamma knife radiosurgery. *Neurosurgery* (2013) 73:641–7. doi: 10.1227/NEU.0000000000000072

5. Alphonse-Sullivan N, Taksler GB, Lycan T, Weaver KE, McTyre ER, Shenker RF, et al. Sociodemographic predictors of patients with brain metastases treated with stereotactic radiosurgery. *Oncotarget* (2017) 8:101005–11. doi: 10.18632/oncotarget.22291

6. LeCompte MC, McTyre ER, Strowd RE, Lanier C, Soike MH, Hughes RT, et al. Impact of diabetes mellitus on outcomes in patients with brain metastasis treated with stereotactic radiosurgery. *J Radiosurg SBRT* (2018) 5:285–91.

7. Farris M, McTyre ER, Cramer CK, Hughes R, Randolph DM 2nd, Ayala-Peacock DN, et al. Brain metastasis velocity: A novel prognostic metric predictive of overall survival and freedom from whole-brain radiation therapy after distant brain failure following upfront radiosurgery alone. *Int J Radiat Oncol Biol Phys* (2017) 98:131–41.

8. Brastianos PK, Carter SL, Santagata S, Cahill DP, Taylor-Weiner A, Jones RT, et al. Genomic characterization of brain metastases reveals branched evolution and potential therapeutic targets. *Cancer Discov* (2015) 5:1164–77.

9. Su J, Song Q, Qasem S, O'Neill S, Lee J, Furdui CM, et al. Multi-omics analysis of brain metastasis outcomes following craniotomy. *Front Oncol* (2021). doi: 10.3389/fonc.2020.615472

10. Soike MH, Logue J, Qasem S, Hughes RT, McTyre E, Su J, et al. CD138 plasma cells may predict brain metastasis recurrence following resection and stereotactic radiosurgery. *Sci Rep* (2019) 9:14385.

11. Tourneau CL, Le Tourneau C, Delord J-P, Gonçalves A, Gavoille C, Dubot C, et al. Molecularly targeted therapy based on tumour molecular profiling versus conventional therapy for advanced cancer (SHIVA): a multicentre, open-label, proof-of-concept, randomised, controlled phase 2 trial. *Lancet Oncol* (2015), 1324–34. doi: 10.1016/s1470-2045(15)00188-6

12. Abbosh C, Birkbak NJ, Wilson GA, Jamal-Hanjani M, Constantin T, Salari R, et al. Phylogenetic ctDNA analysis depicts early-stage lung cancer evolution. *Nature* (2017) 545:446–51. doi: 10.1038/nature22364

13. Schwaederle M, Chattopadhyay R, Kato S, Fanta PT, Banks KC, Is C, et al. Genomic alterations in circulating tumor DNA from diverse cancer patients identified by next-generation sequencing. *Cancer Res* (2017) 77(19):5419–27. doi: 10.1158/0008-5472.CAN-17-0885

14. Aldea M, Hendriks L, Mezquita L, Jovelet C, Planchard D, Auclin E, et al. Circulating tumor DNA analysis for patients with oncogene-addicted NSCLC with isolated central nervous system progression. *J Thorac Oncol* (2020) 15(3):383–91. doi: 10.1016/j.jtho.2019.11.024

15. De Mattos-Arruda L, Mayor R, Ng CKY, Weigelt B, Martínez-Ricarte F, Torrejon D, et al. Cerebrospinal fluid-derived circulating tumour DNA better

represents the genomic alterations of brain tumours than plasma. *Nat Commun* (2015) 6:8839. doi: 10.1038/ncomms9839

16. Planchard D, Smit EF, Groen HJM, Mazieres J, Besse B, Helland Å, et al. Dabrafenib plus trametinib in patients with previously untreated BRAF-mutant metastatic non-small-cell lung cancer: an open-label, phase 2 trial. *Lancet Oncol* (2017) 18:1307–16. doi: 10.1016/S1470-2045(17)30679-4

17. Drilon A, Clark JW, Weiss J, Ou S-HI, Camidge DR, Solomon BJ, et al. Antitumor activity of crizotinib in lung cancers harboring a MET exon 14 alteration. *Nat Med* (2020) 26:47–51. doi: 10.1038/s41591-019-0716-8

18. Gainor JF, Curigliano G, Kim D-W, Lee DH, Besse B, Baik CS, et al. Pralsetinib for RET fusion-positive non-small-cell lung cancer (ARROW): a multi-cohort, open-label, phase 1/2 study. *Lancet Oncol* (2021) 22:959–69. doi: 10.1016/S1470-2045(21)00247-3

19. Strickler JH, Hanks BA, Khasraw M. Tumor mutational burden as a predictor of immunotherapy response: is more always better? *Clin Cancer Res* (2021) 27:1236–41. doi: 10.1158/1078-0432.CCR-20-3054

20. McTyre ER, Soike MH, Farris M, Ayala-Peacock DN, Hepel JT, Page BR, et al. Multi-institutional validation of brain metastasis velocity, a recently defined predictor of outcomes following stereotactic radiosurgery. *Radiother Oncol* (2020) 142:168–74. doi: 10.1016/j.radonc.2019.08.011

21. Huang AJ, Huang KE, Page BR, Ayala-Peacock DN, Lucas JT Jr, Lesser GJ, et al. Risk factors for leptomeningeal carcinomatosis in patients with brain metastases who have previously undergone stereotactic radiosurgery. *J Neurooncol* (2014) 120:163–9. doi: 10.1007/s11060-014-1539-6

22. Ayala-Peacock DN, Attia A, Braunstein SE, Ahluwalia MS, Hepel J, Chung C, et al. Prediction of new brain metastases after radiosurgery: validation and analysis of performance of a multi-institutional nomogram. *J Neurooncol* (2017) 135:403–11. doi: 10.1007/s11060-017-2588-4

23. Shaw E, Scott C, Souhami L, Dinapoli R, Kline R, Loeffler J, et al. Single dose radiosurgical treatment of recurrent previously irradiated primary brain tumors and brain metastases: final report of RTOG protocol 90-05. *Int J Radiat Oncol Biol Phys* (2000) 47:291–8. doi: 10.1016/S0360-3016(99)00507-6

24. Leighl NB, Page RD, Raymond VM, Daniel DB, Divers SG, Reckamp KL, et al. Clinical utility of comprehensive cell-free DNA analysis to identify genomic biomarkers in patients with newly diagnosed metastatic non–small cell lung cancer. *Clin Cancer Res* (2019), 4691–700. doi: 10.1158/1078-0432.ccr-19-0624

25. McTyre ER, Johnson AG, Ruiz J, Isom S, Lucas JT Jr, Hinson WH, et al. Predictors of neurologic and nonneurologic death in patients with brain metastasis initially treated with upfront stereotactic radiosurgery without whole-brain radiation therapy. *Neuro Oncol* (2017) 19:558–66.

26. Harris S, Chan MD, Lovato JF, Ellis TL, Bourland JD, et al. Gamma knife stereotactic radiosurgery as salvage therapy after failure of whole-brain radiotherapy in patients with small-cell lung cancer. *Int J Radiat Oncol Biol Phys* (2012) 83:e53–9.

27. Dingemans A-MC, Hendriks LEL, Berghmans T, Levy A, Hasan B, Faivre-Finn C, et al. Definition of synchronous oligometastatic non–small cell lung cancer—A consensus report. *J Thorac Oncol* (2019), 2109–19. doi: 10.1016/j.jtho.2019.07.025

28. Laubert T, Habermann JK, Hemmelmann C, Kleemann M, Oevermann E, Bouchard R, et al. Metachronous metastasis- and survival-analysis show prognostic importance of lymphadenectomy for colon carcinomas. *BMC Gastroenterol BioMed Central;* (2012) 12:1–8.

29. Kris MG, Natale RB, Herbst RS, Lynch TJ Jr, Prager D, Belani CP, et al. Efficacy of gefitinib, an inhibitor of the epidermal growth factor receptor tyrosine kinase, in symptomatic patients with non-small cell lung cancer: a randomized trial. *JAMA* (2003) 290:2149–58.

30. Paez JG, Jänne PA, Lee JC, Tracy S, Greulich H, Gabriel S, et al. EGFR mutations in lung cancer: correlation with clinical response to gefitinib therapy. *Science* (2004) 304:1497–500.

31. Kwak EL, Bang Y-J, Camidge DR, Shaw AT, Solomon B, Maki RG, et al. Anaplastic lymphoma kinase inhibition in non-small-cell lung cancer. *N Engl J Med* (2010) 363:1693–703.

32. Shaw AT, Ou S-HI, Bang Y-J, Camidge DR, Solomon BJ, Salgia R, et al. Crizotinib in ROS1-rearranged non-small-cell lung cancer. *N Engl J Med* (2014) 371:1963–71.

33. Drilon A, Oxnard GR, Tan DSW, Loong HHF, Johnson M, Gainor J, et al. Efficacy of selpercatinib in fusion-positive non-small-cell lung cancer. *N Engl J Med* (2020) 383:813–24. doi: 10.1056/NEJMoa2005653

34. Marchetti A, Felicioni L, Malatesta S, Grazia Sciarrotta M, Guetti L, Chella A, et al. Clinical features and outcome of patients with non-small-cell lung cancer harboring BRAF mutations. *J Clin Oncol* (2011) 29:3574–9. doi: 10.1200/JCO.2011.35.9638

35. Dohm A, Su J, McTyre ER, Taylor JM, Miller LD, Petty WJ, et al. Identification of CD37, cystatin A, and IL-23A gene expression in association with brain metastasis: analysis of a prospective trial. *Int J Biol Markers* (2019), 1724600818803104. doi: 10.1177/1724600818803104

36. Pectasides E, Stachler MD, Derks S, Liu Y, Maron S, Islam M, et al. Genomic heterogeneity as a barrier to precision medicine in gastroesophageal adenocarcinoma. *Cancer Discov Am Assoc Cancer Res* (2018) 8:37–48. doi: 10.1158/2159-8290.CD-17-0395

37. Devoid H-M, McTyre ER, Page BR, Metheny-Barlow L, Ruiz J, Chan MD. Recent advances in radiosurgical management of brain metastases. *Front Biosci* (2016) 8:203–14. doi: 10.2741/s458

38. Lester SC, Taksler GB, Kuremsky JG, Lucas JT Jr, Ayala-Peacock DN, Randolph DM 2nd, et al. Clinical and economic outcomes of patients with brain metastases based on symptoms: an argument for routine brain screening of those treated with upfront radiosurgery. *Cancer* (2014) 120:433–41. doi: 10.1002/cncr.28422

39. McTyre E, Ayala-Peacock D, Contessa J, Corso C, Chiang V, Chung C, et al. Multi-institutional competing risks analysis of distant brain failure and salvage patterns after upfront radiosurgery without whole brain radiotherapy for brain metastasis. *Ann Oncol* (2018) 29:497–503. doi: 10.1093/annonc/mdx740

40. Johnson AG, Ruiz J, Hughes R, Page BR, Isom S, Lucas JT, et al. Impact of systemic targeted agents on the clinical outcomes of patients with brain metastases. *Oncotarget* (2015) 6:18945–55. doi: 10.18632/oncotarget.4153

41. Hughes RT, Masters AH, McTyre ER, Farris MK, Chung C, Page BR, et al. Initial SRS for patients with 5 to 15 brain metastases: results of a multi-institutional experience. *Int J Radiat Oncol Biol Phys* (2019) 104:1091–8. doi: 10.1016/j.ijrobp.2019.03.052

42. Naik H, Qiu X, Brown MC, Eng L, Pringle D, Mahler M, et al. Socioeconomic status and lifestyle behaviours in cancer survivors: smoking and physical activity. *Curr Oncol* (2016) 23:e546–55. doi: 10.3747/co.23.3166

43. West H, Jin JO. Performance status in patients with cancer. *JAMA Oncol* (2015), 998. doi: 10.1001/jamaoncol.2015.3113

44. Hellman S, Weichselbaum RR. Oligometastases. *J Clin Oncol* (1995) 13:8–10.

45. Petty WJ, Urbanic JJ, Ahmed T, Hughes R, Levine B, Rusthoven K, et al. Long-term outcomes of a phase 2 trial of chemotherapy with consolidative radiation therapy for oligometastatic non-small cell lung cancer. *Int J Radiat Oncol Biol Phys* (2018) 102:527–35.

46. Liu X, Li G, Zhang H, Chang Q, Fang M, Lu C, et al. Molecular characteristics and prognostic factors of leptomeningeal metastasis in non-small cell lung cancer. *Clin Neurol Neurosurg* (2023) 225:107572.

frontiers | Frontiers in Oncology

TYPE Original Research
PUBLISHED 10 January 2024
DOI 10.3389/fonc.2023.1322635

OPEN ACCESS

EDITED BY
Lin Zhou,
Sichuan University, China

REVIEWED BY
Kagaku Azuma,
University of Occupational and Environmental Health Japan, Japan
Xiaojia Sun,
First Affiliated Hospital of Harbin Medical University, China

*CORRESPONDENCE
Guangrui Li
grli@hebmu.edu.cn

RECEIVED 25 October 2023
ACCEPTED 13 December 2023
PUBLISHED 10 January 2024

CITATION
Liu X, Mei F, Fang M, Jia Y, Zhou Y, Li C, Tian P, Lu C and Li G (2024) Cerebrospinal fluid ctDNA testing shows an advantage over plasma ctDNA testing in advanced non-small cell lung cancer patients with brain metastases.
Front. Oncol. 13:1322635.
doi: 10.3389/fonc.2023.1322635

Cerebrospinal fluid ctDNA testing shows an advantage over plasma ctDNA testing in advanced non-small cell lung cancer patients with brain metastases

Xiaocui Liu[1,2], Fengjun Mei[1], Mei Fang[3], Yaqiong Jia[1], Yazhu Zhou[1], Chenxi Li[1], Panpan Tian[1], Chufan Lu[1] and Guangrui Li[4,5]*

[1]Department of Neurology, The Fourth Hospital of Hebei Medical University, Shijiazhuang, Hebei, China, [2]Department of Neurology, North China University of Science and Technology Affiliated Hospital, Tangshan, Hebei, China, [3]Department of Reproductive Medicine, The Fourth Hospital of Hebei Medical University, Shijiazhuang, Hebei, China, [4]Department of Neurology, The First Hospital of Hebei Medical University, Shijiazhuang, Hebei, China, [5]Department of Infectious Diseases, The Third Hospital of Hebei Medical University, Shijiazhuang, Hebei, China

Background: Brain metastases (BM), including brain parenchyma metastases (BPM) and leptomeningeal metastases (LM), are devastating metastatic complications in advanced cancer patients. Next-generation sequencing (NGS) is emerging as a new promising tool for profiling cancer mutation, which could facilitate the diagnosis of cancer. This retrospective study aimed to investigate the molecular genetic characteristics of non-small cell lung cancer (NSCLC) patients with BPM and LM using NGS.

Methods: Cerebrospinal fluid (CSF) samples and paired plasma samples were collected from 37 patients of NSCLC-BM. We profiled genetic mutation characteristics using NGS from NSCLC-BM by comparing CSF circulating tumour DNA (ctDNA) with plasma ctDNA and primary tumour tissues.

Results: Among the 37 patients with NSCLC-BM, 28 patients had LM with or without BPM, while 9 patients only had BPM. Driver and drug-resistant mutations in primary tumours with LM included: *EGFR* L858R (10, 35.7%), *EGFR* 19del (6, 21.4%), *EGFR* L858R+*MET* (1, 3.6%), *EGFR* L858R+S768I (1, 3.6%), *ALK* (2, 7.1%), *ROS1* (1, 3.6%), negative (5, 17.9%), and unknown (2, 7.1%). In patients with NSCLC-LM, the detection rate and abundance of ctDNA in the CSF were significantly higher than those in paired plasma. The main driver mutations of NSCLC-LM remained highly consistent with those of the primary tumours, along with other unique mutations. Circulating tumour DNA was negative in the CSF samples of BPM patients. Patients with BMP had a higher ratio of *EGFR* 19del than L858R mutation (55.6% vs 11.1.%), whereas NSCLC patients with LM had a higher ratio of *EGFR* L858R than 19del mutation (50.0% vs 25.0%). Most patients with positive plasma ctDNA results were male (p = 0.058) and in an unstable state (p = 0.003).

Conclusion: Our study indicated that the CSF ctDNA detected by NGS may reflect the molecular characteristics and heterogeneity of NSCLC-LM. Timely screening of patients with NSCLC for CSF ctDNA, especially for patients with positive plasma ctDNA, may facilitate the early detection of LM. Furthermore, patients with the *EGFR* 19del may have a higher risk of developing BPM.

KEYWORDS

non-small cell lung cancer (NSCLC), leptomeningeal metastases (LM), brain parenchyma metastases (BPM), cerebrospinal fluid circulating tumour DNA (ctDNA), next generation sequencing

Background

Brain metastases (BM), including brain parenchyma metastases (BPM) and leptomeningeal metastases (LM), are devastating complications in advanced cancer patients. Lung cancer is the leading cause of brain metastases (BM). Patients with advanced non-small cell lung cancer (NSCLC) are often present with metastatic disease, including 64.5% with BPM and 35.5% with LM (1). Epidermal growth factor receptor (*EGFR*) mutations occur in 9.4% of NSCLC patients (2). The most common occurrence site of BPM is the cerebral hemisphere, followed by the cerebellum and brainstem (3). LM is defined as cancer cells disseminating to both the leptomeninges (pia and arachnoid) and cerebrospinal fluid (CSF) compartment and often results in significant neurological morbidity. The diagnosis of LM usually relied on magnetic resonance imaging (MRI) with gadolinium enhancement and CSF cytology. Notably, CSF cytology is the gold standard for diagnosing LM. CSF cytological evaluation has high specificity but only moderate sensitivity with a positive rate of the first test was 50% (4). MRI has limited sensitivity, and the sensitivity of this diagnostic modality has not yet been firmly established. Existing treatment options for BM primarily include radiation therapy, systemic chemotherapy, targeted therapy, intrathecal chemotherapy, and immune checkpoint inhibitors, among which targeted therapy can improve the prognosis and quality of life in NSCLC-BM patients with sensitive mutations. However, the prognosis of patients with NSCLC-BM remains poor, with a median overall survival (OS) of 36.3 months for patients with BPM and 26.4 months for patients with LM (1).

Genomic characterisation of NSCLC-BM is crucial for its precise diagnosis and treatments. However, obtaining brain tissues is difficult, which hinders our understanding of BM's genetic status. With the development of liquid biopsy, plasma and CSF circulating tumours (ctDNA) detected by next-generation sequencing (NGS) play an increasingly important role in guiding the management of NSCLC-LM. For metastatic and/or recurrent disease, the advantages of liquid biopsy over tissue biopsy are non-invasive, repeatable, and the possibility to obtain a full overview of the genetic makeup of the disease, overcoming both spatial and temporal heterogeneity (5). However, plasma ctDNA levels do not fully reflect genetic mutations in patients with BM. A previous study indicated that CSF-derived ctDNA detected by NGS shows higher sensitivity than plasma ctDNA and better reflects the genetic profile of patients with LM (6). In this retrospective study, we aimed to investigate the ctDNA molecular genetic characteristics of patients with non-small cell lung cancer patients with BPM and LM by NGS.

Patients and methods

Patients

In total, 28 patients with NSCLC-LM and 9 patients with NSCLC-BPM were enrolled between March 2019 and September 2022 at the Neurology Department of the Fourth Hospital of Hebei Medical University. Inclusion criteria: (1) the primary tumour was confirmed as NSCLC by pathology or cytology; (2) LM was confirmed according to the 2017-ESMO guidelines, including 1) a clear history of tumour, 2) new neurological signs, 3) typical imaging manifestations, 4) cancer cells were found in CSF cytology; (3) the diagnostic criteria for BPM were based on a positive result on brain MRI; and (4) NGS testing of samples, including CSF, plasma, and/or tissues. Exclusion criteria were as follows: (1) CSF and plasma ctDNA were not paired and (2) co-existing primary tumour of the brain or spinal cord (Figure 1).

The research was conducted according to the principles set out in the Declaration of Helsinki 1964. All subsequent revisions and informed consent were obtained and the study was approved by the Institutional Review Board and Ethics Committee of the Fourth Hospital of Hebei Medical University (approval 2022KS004).

Data collection

Data on the initial diagnosis of LM or BPM were collected in the medical records of enrolled patients, including sex, age, Eastern

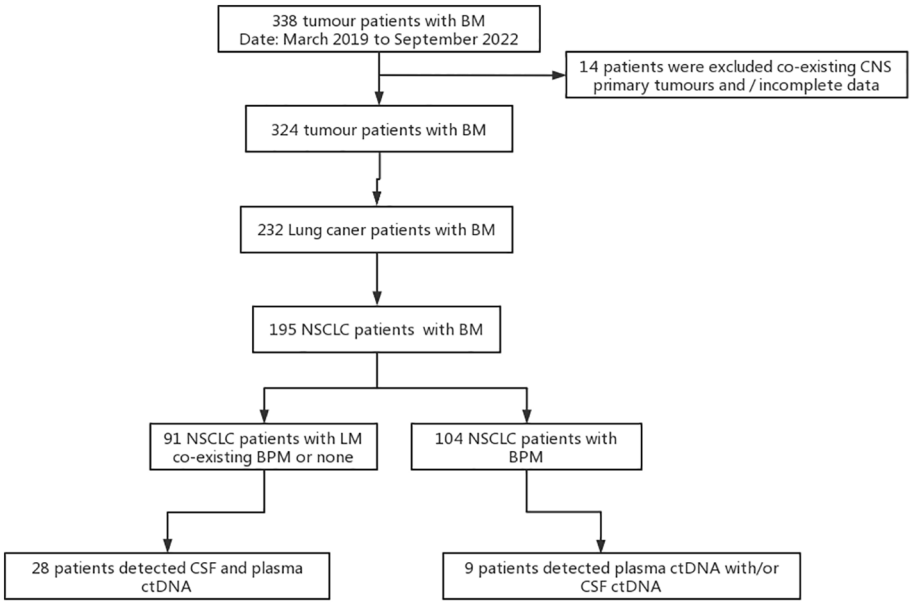

FIGURE 1
Study flowchart. BM, brain metastases; BPM, brain parenchyma metastases; LM, leptomeningeal metastases; CSF, cerebrospinal fluid circulating tumour; ctDNA, circulating tumour DNA; NSCLC, non-small cell lung cancer.

Cooperative Oncology Group Performance Status (ECOG PS) score, extracranial disease status, BPM status, driver and drug-resistant mutations of primary tumours, NGS results, CSF parameters, imaging examination results, and treatment history (Table 1). Extracranial disease progression was defined using the Response Evaluation Criteria in Solid Tumours (RECIST) version 1.1 (7). BPM progression was defined using the Response Assessment in Neuro-oncology Brain Metastases (RANO-BM).

Circulating tumour DNA extraction and library construction

First, 5ml of whole blood was collected by EDTA blood collection tubes and then centrifuged within 1 hour of collection at 1,800×g for 10 minutes at 4≥°C or room temperature to remove the blood cells. The supernatant containing the plasma was removed with special care taken so as to not disturb the buffy coat. This was then centrifuged at 16,000× g for 10 minutes to remove any remaining cells. ctDNA was extracted from 2ml plasma, by digestion in 100µl proteinase K buffer for 10min at 37°C followed by purification with the NucleoSpin Plasma XS kit with modified protocols. The purified ctDNA was quantified by a Picogreen fluorescence assay using the provided lambda DNA standards (Invitrogen). Then, library construction with the KAPA Hyper DNA Library Prep Kit, containing mixes for end repair, dA addition and ligation, was performed in 96-well plates (Eppendorf). Dual-indexed sequencing libraries were PCR amplified for 4-7 cycles.

Hybrid selection and ultra-deep NGS of ctDNA

The 5'-biotinylated probe solution was provided as capture probes, the baits targeted 416 cancer-related genes. Furthermore, 1µg of each ctDNA-fragment sequencing library was mixed with 5µg of human Cot-1 DNA, 5µg of salmon sperm DNA, and 1 unit adaptor-specific blocker DNA in hybridisation buffer, heated for 10 minutes at 95°C, and held for 5 minutes at 65°C in the thermocycler. Within 5 minutes, the capture probes were added to the mixture, and the solution hybridisation was performed for 16-18 hours at 65°C. After hybridisation was complete, the captured targets were selected by pulling down the biotinylated probe/target hybrids using streptavidin-coated magnetic beads, and the off-target library was removed by washing with wash buffer. The PCR master mix was added to directly amplify (6-8 cycles) the captured library from the washed beads. After amplification, the samples were purified by AMPure XP beads, quantified by qPCR (Kapa) and sized on a Bioanalyzer 2100 (Agilent). Libraries were normalised to 2.5nM and pooled. Deep Sequencing was performed on Illumina HiSeq 4000 using PE75 V1 Kit. Cluster generation and sequencing was performed according to the manufacturer's protocol.

Sequence alignment and processing

Base calling was performed using bcl2fastq v2.16.0.10 (Illumina, Inc.) to generate sequence reads in FASTQ format (Illumina 1.8+ encoding). Quality control (QC) was applied with Trimmomatic.

10.3389/fonc.2023.1322635

TABLE 1 Clinical information of non-small cell lung cancer with leptomeningeal metastases.

NO.	Age	Sex	Driver mutation of primary tumour	PS	Metastactic site	Extracranial disease status	BPM status	Therapy before CSF collection	TKIs after LM
1	55	F	(-)	3	BPM/LM	without	PD	None	None
2	47	F	L858R	2	LM	without	without	None	osimertinib
3	57	F	L858R	2	BPM/LM/bone/ Lymph node	PD	SD	gefitinib	osimertinib
4	52	M	ROS1	2	LM/Bone/Lymph node	SD	without	crizotinib	Lorlatinib
5	62	M	L858R	1	BPM/LM	without	SD	None	almonertinib/ osimertinib
6	54	M	(-)	2	LM/Bone	SD	without	almonertinib	Sevatinib/ furmonertinib
7	57	M	19del	1	BPM/LM/Pleural/ Lymph node	SD	PD	gefitinib	osimertinib
8	59	M	(-)	1	BPM/LM	without	SD	None	None
9	64	F	L858R	3	BPM/LM/Lymph node	SD	PD	icotinib	osimertinib
10	65	F	L858R	3	LM/Bone	SD	without	Icotinib/osimertinib	osimertinib
11	62	M	(-)	2	BPM/LM	PD	PD	gefitinib	osimertinib
12	50	F	(-)	3	BPM/LM/Bone/ spinalis/Lymph node	SD	SD	osimertinib	Osimertinib/ crizotinib
13	74	F	L858R	1	BPM/LM/Bone	PD	PD	gefitinib	osimertinib
14	70	F	ALK	1	BPM/LM/Bone/ abdomen/Lymph node	PD	PD	crizotinib	bugatinib
15	53	F	ALK	1	BPM/LM	without	PD	Crizotinib/ceritinib	alectinib
16	66	F	19del	1	BPM/LM/pulmonary	SD	PD	gefitinib	osimertinib
17	70	M	19del	1	BPM/LM/Bone/ Pleural/peritoneum	PD	SD	Icotinib/ gefitinib/almonertinib	almonertinib
18	39	F	19del	0	BPM/LM/Bone/ Lymph node	PD	PD	Gefitinib/erlotinib	erlotinib
19	48	M	L858R	2	LM/bone	PD	without	None	osimertinib
20	67	M	L858R	1	LM	without	without	gefitinib	Almonertinib/ furmonertinib
21	71	M	L858R	2	BPM/LM/Bone/adrenal	PD	PD	osimertinib	Almonertinib
22	72	M	19del	4	LM/Lymph node	SD	without	None	erlotinib
23	54	F	L858R	2	BPM/LM/Bone	PD	SD	icotinib	osimertinib
24	50	M	19del	3	BPM/LM/Bone/ Pleural/adrenal	PD	PD	gefitinib	Erlotinib/ Almonertinib/ osimertinib
25	34	F	L858R/MET	2	LM/Bone/pulmonary	SD	without	Icotinib/osimertinib	osimertinib/ dacomitinib/ crizotinib
26	52	M	unknown	2	LM/Bone	PD	without	Icotinib/osimertinib	afatinib
27	56	F	unknown	3	LM/Bone/spinalis	SD	without	icotinib	None
28	51	M	L858R+ S768I	1	BPM/LM/Lymph node	SD	PD	icotinib	Osimertinib/ afatinib

BPM, brain parenchyma metastases; LM, leptomeningeal metastases; CSF, cerebrospinal fluid circulating tumour; TKIs, tyrosine kinase inhibitors: Disease stability assessment: CR, complete response; PR, partial response; SD, stable disease; PD, progress disease.

High-quality reads were mapped to the human genome (hg19, GRCh37 Genome Reference Consortium Human Reference 37) using modified BWA aligner 0.7.12 with BWA-MEM algorithm and default parameters to create SAM files. Picard 1.119 (http://picard.sourceforge.net/) was used to convert SAM files to compressed BAM files which were then sorted according to chromosome coordinates. The Genome Analysis Toolkit (GATK, version 3.4-0) was modified and used to locally realign the BAM files at intervals with indel mismatches and recalibrate base quality scores of reads in the BAM files.

SNVs/Indels/CNVs detections

Single nucleotide variants (SNVs) and short insertions/deletions (indels) were identified using VarScan2 2.3.9 with the minimum variant allele frequency threshold set at 0.01 and the p-value threshold for calling variants set at 0.05 to generate Variant Call Format (VCF) files. All SNVs/indels were annotated with ANNOVAR, and each SNV/indel was manually checked with the Integrative Genomics Viewer (IGV). Copy number variations (CNVs) were identified using ADTEx 1.0.4. In total, 425 cancer-related genes are listed in Supplementary Table 1.

Statistical analysis

Due to the relatively small sample size, only descriptive statistics were used. Data are presented as numbers and percentages.

Results

Baseline characteristics of NSCLC-BM patients

Among the 37 patients with NSCLC, 28 had LM with or without BPM, while 9 patients had only BPM. Of the 28 patients with LM, 14 (50.0%) were female, and the median age was 57 years (range: 34–74 years). LM was diagnosed either at baseline (n = 3, 10.7%) or during the treatment course (n = 25, 89.3%), with a median interval of 19.0 (1.0–70.0) months. The main driver mutations of primary tumours with LM were determined by NGS, including *EGFR* L858R (10, 35.7%), *EGFR* 19del (6, 21.4%), *EGFR* L858R + *MET* amplification (1, 3.6%), *EGFR* L858R+S768I (1, 3.6%), *ALK* (2, 7.1%), *ROS1* (1, 3.6%), negative (5, 17.9%), and unknown (2, 7.1%) (Figure 2A). The ECOG PS scores at the time diagnosis of LM were as follows: 0 (1, 3.6%), 1 (10, 35.7%), 2 (10, 35.7%), 3 (6, 21.4%), 4

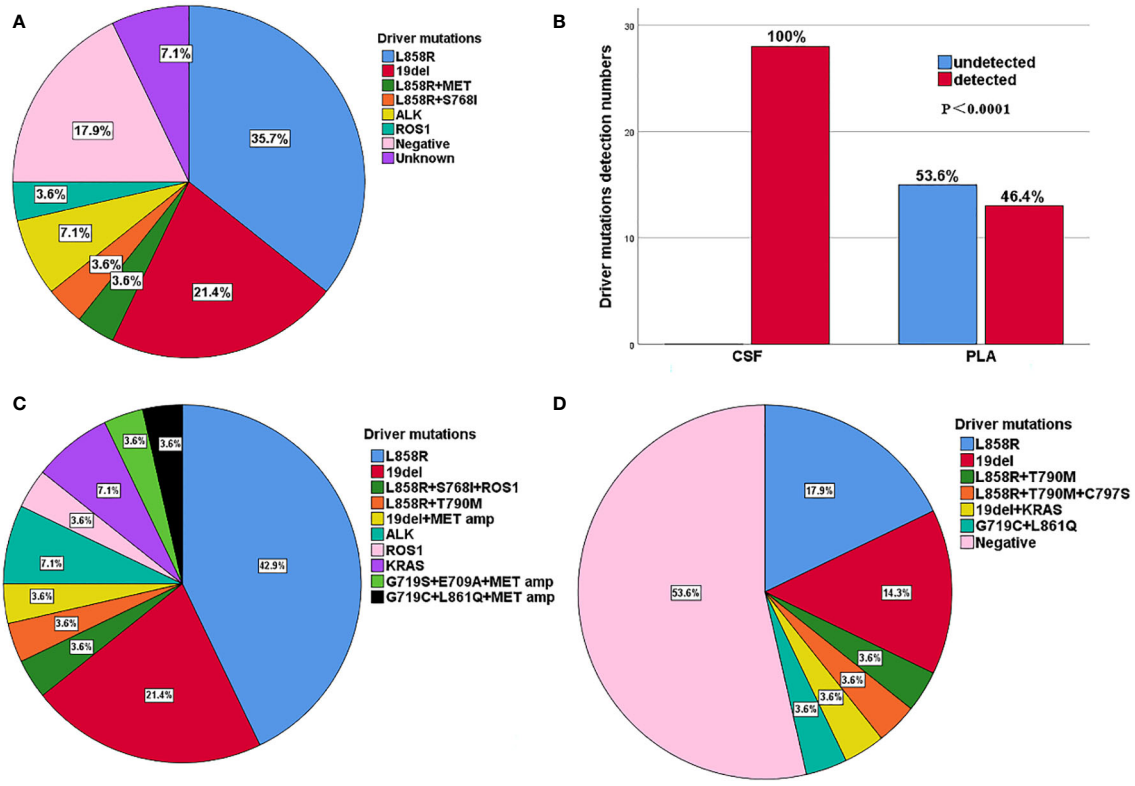

FIGURE 2
(A) Distribution of driver mutations of primary tumour in 28 patients with LM. **(B)** Comparison of driver gene mutations in CSF and plasma of 28 patients with LM. **(C)** Distribution of mainly gene mutations in CSF for 28 patients with LM. **(D)** Distribution of mainly gene mutations in plasma for 28 patients with LM.

(1, 3.6%). Of the 28 patients, 18 (64.3%) had BPM at the initial diagnosis of LM. In total, 22 patients (78.6%) had an extracranial disease. The BPM status was as follows: PD (12, 42.9%), SD (6, 21.4%), and no BPM (10, 35.7%). Extracranial disease status was as follows: PD (11, 39.3%), SD (11, 39.3%), and no extracranial disease (n = 6, 21.4%). Most patients (23 of 28, 82.1%) with driver mutations had a history of targeted therapies and were switched to a different targeted drug upon the disease progression (Table 1).

CSF ctDNA showed a higher sensitivity than plasma ctDNA in NSCLC-LM patients

The results indicated that CSF ctDNA demonstrated higher sensitivity compared to plasma ctDNA in detecting mutations in LM. All CSF ctDNA were positive, while 13 of 28 (46.4%) plasma ctDNA were positive (Figure 2B). The main driver and drug-resistant mutations detected in CSF include *EGFR* L858R (12, 42.9%), *EGFR* 19del (6, 21.4%), *EGFR* L858R+S768I+*ROS1* (1, 3.6%), *EGFR* L858R+T790M (1, 3.6%), *EGFR* 19del+*MET* amplification (1, 3.6%), *ALK* (2, 7.1%), *ROS1* (1, 3.6%), *KRAS* (2, 7.1%), *EGFR* G719S+E709A+*MET* amplification (1, 3.6%), and *EGFR* G719C+L861Q+*MET* amplification (1, 3.6%) (Table 2, Figure 2C). Mutations detected in plasma include *EGFR* L858R (5, 17.9%), *EGFR* 19del (4, 14.3%), *EGFR* L858R+T790M (1, 3.6%), *EGFR* L858R+T790M+C797S (1, 3.6%), *EGFR* 19del+*KRAS* (1, 3.6%), *EGFR* G719C+L861Q (1, 3.6%), and negative (15, 53.6%) (Table 2, Figure 2D). The detection rate and types of ctDNA in the CSF were higher than those in paired plasma samples. The consistency of main mutations between the CSF and the paired plasma was 32.1% (9/28). Most of patients with positive driver mutations in plasma ctDNA were male (M:F = 9:4), and their extracranial disease state was more likely to be at a progressive stage (8/13, 61.5%) (Figure 3A, Supplementary Figure 1). Conversely, the majority of patients without driver mutations in plasma were female (M:F = 5:10), whose extracranial disease state was more likely at a stable stage/without extracranial disease (13/15, 86.7%) (Figure 3A, Supplementary Figure 1). Moreover, 76.9% (10/13) of NSCLC-LM patients, who were positive for plasma ctDNA, had BPM, compared with 53.3% (8/15) of patients without plasma ctDNA (Table 1, Figure 3B). The abundance of CSF ctDNA was significantly higher than that of plasma ctDNA, except in one patient (P24) who had a higher abundance of driver mutations in the plasma sample than CSF sample and his extracranial disease was in progression with new bone metastases at the time of the initial diagnosis of LM (Table 1, Figure 4A).

The consistency of CSF and plasma ctDNA with driver mutations of primary tumours for NSCLC-LM

The main driver mutations observed in NSCLC-LM demonstrated high consistency with those found in primary tumours. Mutations in the CSF samples showed greater concordance with the primary tumour mutations. Among the 21 patients with positive driver mutations in their primary tumours, 19 (90.5%) patients showed driver mutations in the CSF. In two

TABLE 2 The results of gene mutations of non-small cell lung cancer with leptomeningeal metastases.

NO.	Driver mutations of primary tumours	Interval time (month)	Tumour tissues	Abundance (tissues) (%)	CSF ctDNA	Abundance (CSF) (%)	Plasma ctDNA	Abundance (plasma) (%)
1	(-)	1			KRAS	23.7	(-)	
2	L858R	0			L858R	31.1	(-)	
3	L858R	17			L858R	77.1	L858R/ T790M	5.6
4	ROS1	32			ROS1	10.0	(-)	
5	L858R	54			L858R	61.5	L858R	0.1
6	(-)	15			G719C/L861Q/MET	73.7/67.3/3.35	G719C/ L861Q	10.1/11.3
7	19del	28			L858R	40.7	L858R	0.2
8	(-)	19	KRAS	10.13	KRAS	10.9	(-)	
9	L858R	38			L858R/T790M	72.6/9.7	(-)	
10	L858R	45			L858R	44.8	(-)	
11	(-)	19			19del	71.4	19del	8.8
12	(-)	15			19del/MET	64.3/2.09	(-)	
13	L858R	17			L858R	34.6	L858R/ T790M/ C797S	0.5/0.28/0.1

(Continued)

10.3389/fonc.2023.1322635

TABLE 2 Continued

NO.	Driver mutations of primary tumours	Interval time (month)	Tumour tissues	Abundance (tissues) (%)	CSF ctDNA	Abundance (CSF) (%)	Plasma ctDNA	Abundance (plasma) (%)
14	ALK	14			ALK	48.9	(-)	
15	ALK	23	ALK	54.82	ALK	92.6	(-)	
16	19del	6			19del	54.0	(-)	
17	19del	22			19del	55.7	19del/KRAS	8.7/1.46
18	19del	20			19del	78.1	19del	12.9
19	L858R	0			L858R	50.5	L858R	0.3
20	L858R	8			L858R	14.5	(-)	
21	L858R	0	L858R	22.7	L858R	8.4	L858R	4.4
22	19del	35			19del	7.4	19del	0.3
23	L858R	3			L858R	4.6	L858R	0.2
24	19del	12	19del	56.7	19del	8.0	19del	81.4
25	L858R/MET	67	G719S/ E709A	20.85/21.33	G719S/E709A/MET	69.2/69.6/3.14	(-)	
26	unknown	70			L858R	61.8	(-)	
27	unknown	45			L858R	69.6	(-)	
28	L858R+E S768I	17			L858R+S768I+ROS1	66.5/69.5/6.1	(-)	

NSCLC, non-small cell lung cancer; CSF, cerebrospinal fluid circulating tumour; ctDNA, circulating tumour DNA.

patients, who did not show driver mutations in primary tumours, *EGFR* mutations were detected in the CSF, including 19del mutation in patient 7 (which later changed to L858R mutation after 28 months), and L858R+MET amplification in patient 25 (which later changed to G719S+E709A+MET amplification after 67 months). Of these 21 patients, 10 (47.6%) of them were driver mutation positive in plasma samples (Tables 1, 2).

Five of the 28 patients with NSCLC-LM underwent both tumour tissue biopsy and paired CSF NGS, with a high consistency between the two sample types. While driver mutations had been detected in the CSF sample of the five patients, who were driver mutation negative in the primary tumour, only two of them had driver mutations detected in the paired plasma sample. One drug-resistant mutation (*MET*) was also detected in the CSF but not in the tumour tissues (Table 2).

Genomic profiles of NSCLC-LM

Figure 4B displays genomic profiles of the 28 NSCLC-LM cases in both the CSF and paired plasma. The primary driver mutations were observed in the *EGFR* gene. The rare mutations were partially different between CSF and plasma samples. The average number of mutations identified in the CSF was 4.9 (range, 0–12). The most

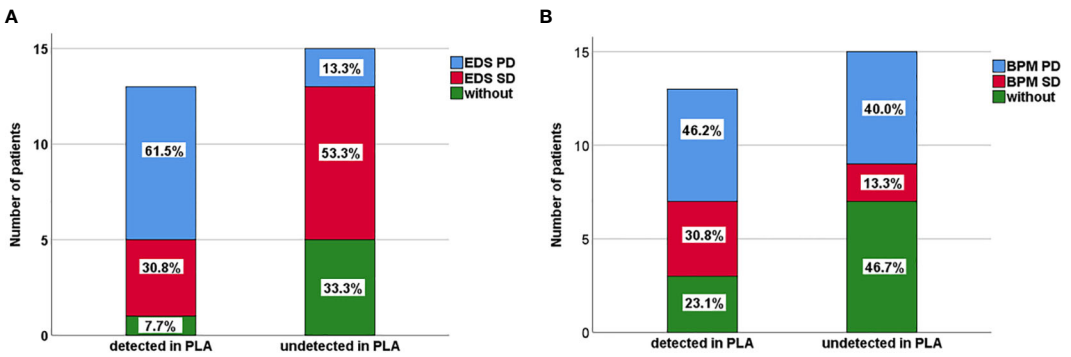

FIGURE 3
(A) Extracranial disease status (EDS) of 13 patients positive with plasma ctDNA and 15 patients negative with plasma ctDNA in NSCLC-LM patients. **(B)** Brain parenchyma metastases (BPM) status of 13 patients positive with plasma ctDNA and 15 patients negative with plasma ctDNA in NSCLC-LM patients.

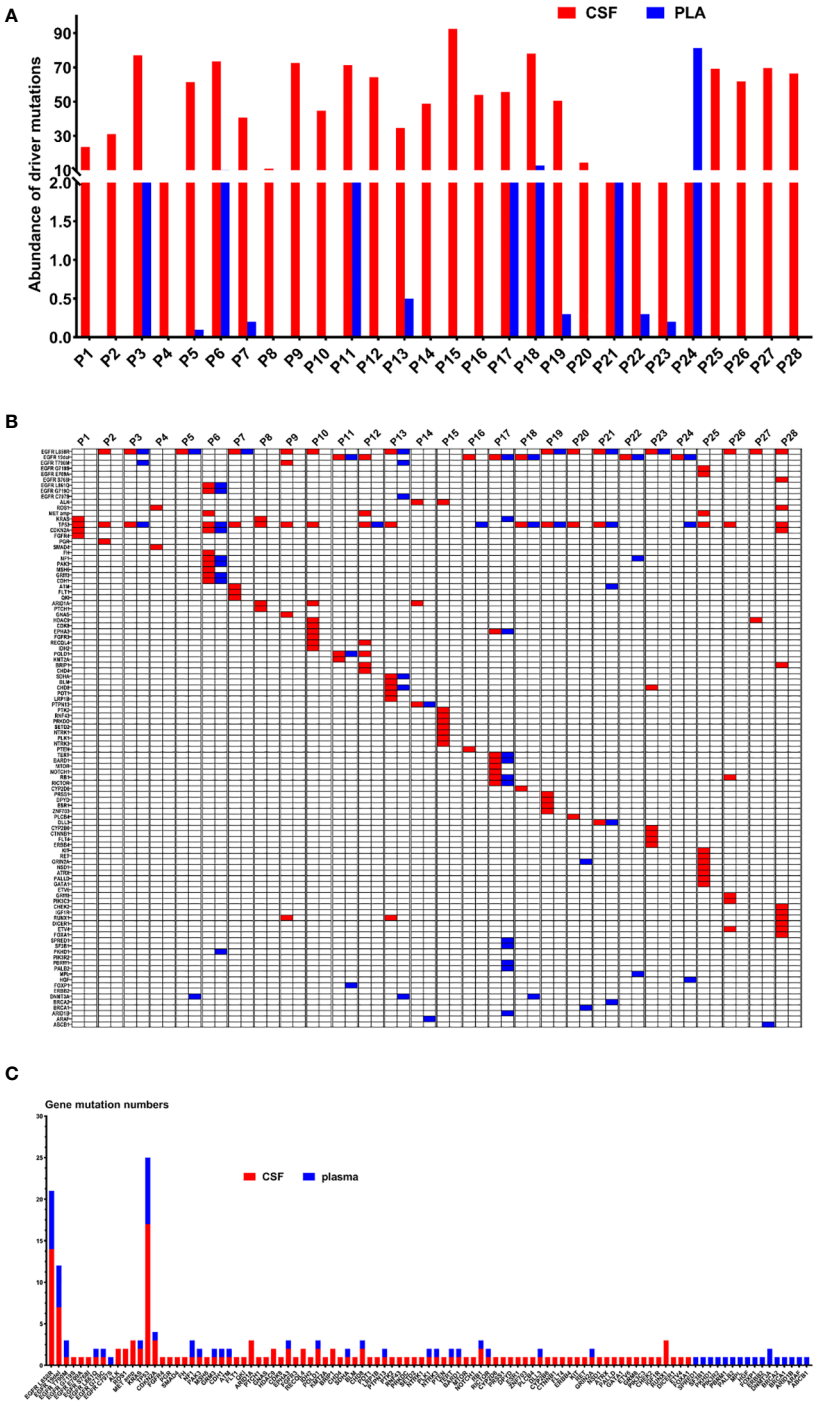

FIGURE 4
(A) The abundance of ctDNA in the CSF and plasma of 28 patients with LM. **(B)** Genetic profiles of 28 LM patients in the CSF and the paired plasma. **(C)** The gene mutation numbers of 28 LM patients in the CSF and the paired plasma. Red: CSF; Blue: plasma.

frequently mutated genes were *TP53* (17, 60.7%), *EGFR* L858R (14, 42.9%), *EGFR* 19del (7, 21.4%), *ARID1A* (3, 10.7%), *CDKN2A* (3, 10.7%), *MET* (3, 10.7%), *RUNX1* (3, 10.7%), *ALK* (2, 7.1%), *ROS1* (2, 7.1%), *CHD8* (2, 7.1%), *HDAC9* (2, 7.1%), *KRAS* (2, 7.1%), *POLD1* (2, 7.1%), *EPHA3* (2, 7.1%), *RECQL4* (2, 7.1%), *BRIP1* (2, 7.1%), and *RB1* (2, 7.1%) (Figures 4B, C). The average number of different mutations identified in the plasma was 2.3 (range 0–12). The frequently altered genes were *TP53* (8, 28.6%), *EGFR* L858R (7, 25.0%), *EGFR* 19del (5, 17.9%), *EGFR* T790M (2, 7.1%), *DNMT3A* (2, 7.1%), and *NF1* (2, 7.1%) (Figures 4B, C). The *EGFR* T790M mutation was detected in two plasma samples (P3 and P13) and one CSF sample (P9). All the patients were treated with first-generation

EGFR-tyrosine kinase inhibitors (TKIs) before testing. *MET* amplification was detected in three CSF samples (P6, P12, and P25), treated with third-generation *EGFR*-TKIs. Additionally, some rare concomitant mutations, including *EGFR* G719C+L861Q+*MET* amplification (1, 3.6%), *EGFR* G719S+E709A+*MET* amplification (1, 3.6%), and *EGFR* L858R+S768I + *ROS1* (1, 3.6%), were also detected in the CSF samples. Furthermore, *EGFR* L858R+C797S +T790M (1, 3.6%) was detected in the plasma samples (Table 2, Figure 4B).

CSF and plasma ctDNA for NSCLC-BPM

Among the nine patients with BPM, driver mutations of primary tumours were determined by NGS, including *EGFR* mutations (5, 55.6%), which include 19del (4, 44.4%), L858R +A871E + *MET* (1, 11.1%), *ALK* (1, 11.1%), *ROS1* (1, 11.1%), *KRAS* (1, 11.1%), and unknown (1, 11.1%). CSF ctDNA tests were performed in seven patients, all of whom tested negative for ctDNA. For the five patients initially diagnosed with BPM, both tissues and paired plasma were tested in four patients, with two of them showing consistency (2/4, 50.0%). In four patients diagnosed with BPM during the course of the disease, three patients had explicit genetic mutations, with one patient's driver mutations being consistent in plasma ctDNA and primary tumour tissues (1/3, 33.3%), along with T790M resistant mutation only detected in the plasma. It is worth noting that while plasma ctDNA may be useful in BPM as a complementary assay for tissue analysis, it cannot be substituted for tissue analysis (Table 3).

Discussion

In our study, the median interval from the NSCLC diagnosis to BM was 18.0 (0.0–70.0) months. BM incidence can increase to 80% in some particular groups, such as patients with anaplastic lymphoma kinase (*ALK*) positive NSCLC patients (8). This is particularly important for Asians, whose prevalence of *EGFR* mutations has been reported to be 63%, much higher than other populations (1, 9). In our study, the most frequently detected driver mutations in BM were *EGFR* mutations (23/37, 62.2%), including L858R (13/37, 35.1%) and 19del (10/37, 27.1%), respectively, which is consistent with the results of previous studies (1, 10).

Genetic mutation profiles are fundamental to precision medicine in patients with tumours (11). With the development of liquid biopsy and sequencing methods, plasma and CSF ctDNA detected by NGS play increasingly important roles in guiding the management of NSCLC-BM. Previous studies have shown that CSF ctDNA can reflect BM's molecular characteristics and heterogeneity, including BPM (12, 13). In our study, the CSF ctDNA positivity rate was high in patients with LM but low in patients with BPM (all tested patients were negative). A previous study indicated that the detection rate of mutations in the CSF was lower in patients with BPM, which might be because tumours are located farther away from the cerebral ventricle, where CSF is generated. Cancer cells may access the leptomeningeal space through four main points of entry: arterial circulation through the choroid plexus, venous circulation through Bateson's plexus, direct invasion along the spinal and cranial nerves, and invasion from parenchymal disease through the glia limitans (14).

The process of tumour cell metastasising to the brain involves a series of steps, including detachment from the primary site, invasion of surrounding tissues and blood vessels, blood transmission, crossing of the blood-brain barrier (BBB), and brain clonal growth (14). In our study, the absence of CSF ctDNA in patients with BPM may be because the tumour cells had not yet crossed the BBB. To some extent, CSF ctDNA combined with imaging manifestations may assist clinicians in determining whether patients with BPM and/or LM require intrathecal chemotherapy. If conditions permit, we suggest that patients with BPM should be simultaneously tested for CSF ctDNA, plasma ctDNA, and tumour tissues for comprehensive evaluation and treatment. Further studies of other sensitive biomarkers and advanced testing methods for BMP are required.

TABLE 3 The results of gene mutations for brain parenchyma metastases.

NO.	Driver mutations of primary tumour	Interval time (month)	Tumour tissues	Abundance (tissues)	Plasma ctDNA	Abundance (plasma)	CSF ctDNA
1	unknown	12			19del	0.3%	(-)
2	19del	132			(-)		(-)
3	19del	0	19del	31.4%	POLE	0.6%	(-)
4	KRAS	0			KRAS	17.3%	(-)
5	L858R/A871E/MET	0	L858R/ A871E/MET	39.5%/ 38.8%/19.2%	L858R/ A871E/MET	0.1%/0.2%/0.1%	Unperformed
6	ROS1	18			DNMT3A	0.5%	Unperformed
7	19del	23			19del/T790M	0.1%/0.2%	(-)
8	19del	0	19del	25.3%	19del	2.3%	(-)
9	ALK	0	ALK	24.2%	(-)		(-)

CSF, cerebrospinal fluid circulating tumour; ctDNA, circulating tumour DNA; NSCLC, non-small cell lung cancer.

The CSF ctDNA levels may reflect the molecular characteristics and heterogeneity of patients with NSCLC-LM and complement the LM diagnosis (15). A previous study showed that the mutation status of NSCLC-LM patients was concordant with the primary tumour and is in approximately 90% of cases (16). In our study, the mutation profile of patients with NSCLC-LM patients in CSF showed high concordance with the primary tumours (90.5%), consistent with the result of a previous study. Many other mutations have also been detected in CSF, reflecting tumour heterogeneity. This result suggested that CSF ctDNA is a reliable biomarker that may guide the management of NSCLC-LM. In particular, plasma ctDNA is the most extensively studied and widely used method for genotyping if tumour tissue is not available (17), which mostly reflects the primary tumours and extracranial disease (13).

As the application time of TKI drugs is extended, the tumour cells develop new mutations, or the non-dominant mutations become dominant mutations, leading to drug resistance (18). In our study, the driver mutations in patients with LM included *EGFR* L858R (12, 42.9%), 19del (6, 21.4%), *ALK* (2, 7.1%), and *ROS1* (2, 7.1%), which are the major drug targets in the clinic. Third-generation TKI drugs with high BBB permeability are recommended for patients with LM even if there is no T790M mutation. In the present study, the most common drug-resistant mutations were *EGFR* T790M (3/28, 10.7%) and *MET* amplification (3/28,10.7%). A previous study showed that the *EGFR* T790M mutation is the main resistance mechanism generated after applying first- and second-generation *EGFR*-TKI drugs, which could be easily detected in the plasma (19). In our study, three patients were *EGFR* T790M mutation positive, of which two cases were detected in the plasma samples and one case in the CSF sample. All three patients were administered first-generation TKIs. To date, osimertinib has been approved for patients harbouring the *EGFR* T790M mutation, which is suitable for LM treatment (20). MET amplification is another mechanism underlying acquired TKI drug resistance (21). Acquired *MET* amplification has been identified in 5%–20% of NSCLC patients with sensitive *EGFR* mutations, who develop resistance to first-, second-, and third-generation *EGFR*-TKIs (22). In our study, three patients treated with third-generation TKIs showed *MET* amplification, all of which were detected in the CSF. The combination of an *EGFR*-TKI and *MET*-TKI remains effective for NSCLC patients with both *EGFR* mutations and *MET* amplification after progression to a prior *EGFR*-TKI, especially for patients with higher levels of *MET* amplification (23).

EGFR G719C, G719S, L861Q, S768I, and C797S were also detected in our study. Previous studies show that the incidence of uncommon *EGFR* mutations accounts for approximately 20% of *EGFR*-mutated NSCLC patients (24). The G719X and L861Q are the main uncommon mutations and are associated with favourable efficacy of *EGFR*-TKIs (25), whereas the S768I mutation is in exon 20 and is associated with a lack of sensitivity to *EGFR*-TKIs (26). The combination of C797S with T790M mutation is a reason for osimertinib resistance (27). A previous study indicated that the prognosis of patients with uncommon mutations was significantly inferior to that of patients with common mutations (including L858R and 19del mutations) (26). Afatinib, a second-generation *EGFR*-TKI, appears to be able to penetrate the CNS at a sufficient concentration to have a clinical effect on CNS metastases and might be the optimal *EGFR*-TKI against these uncommon *EGFR* mutations (28). In addition, most patients with LM not harbouring resistance genes also showed disease progression, suggesting the existence of other resistance mechanisms or the limitations of current detection methods. In our study, many patients with LM harboured *TP53* (17/28, 60.7%) mutations. *TP53* is a tumour suppressor gene and mutations in this gene predict poor prognosis. To date, *TP53* mutations are undruggable (29).

KRAS mutations have been considered a key driver of lung cancer, in which *KRAS* p.G12C accounts for 45% to 50% of *KRAS* mutations (30). In our study, three patients with NSCLC-LM harboured *KRAS* mutations, all of which were p.G12V mutations (3/28, 10.7%), two of which were detected in the CSF and one in the plasma. Despite recent drug developments with some drugs targeting *KRAS* p.G12C mutation, most *KRAS* oncoproteins remain undruggable (31).

Most patients with advanced NSCLC (68.1%) had BPM comorbidities. However, only 32.4% of the patients were simultaneously diagnosed with LM and advanced NSCLC. Most patients with NSCLC are diagnosed with LM onset during the treatment course, which is considered a later event than BPM in advanced NSCLC. In addition, compared to BPM, LM patients are prone to multiple metastases (≥ 2 metastatic sites) and have shorter survival times (1).

Cancers are prone to complications. Melanoma, NSCLC, small-cell lung cancer, and breast cancer are prone to both BPM and LM. Renal cancers often metastasise to the brain parenchyma. In contrast, lymphomas and leukaemia often cause LM. Patients with small-cell lung cancer, adenocarcinoma of the lung, and non–small cell lung cancer have an incidence of brain metastases at diagnosis of >10%. Only 0.4%, 1.5%, and 0.7% of patients with breast cancer, renal cancer, and melanoma, respectively, had brain metastases at diagnosis (32).

The mechanisms underlying these phenomena are unknown, but they may be clinical manifestations of genetic aberrations in different tumours. NSCLC patients with *EGFR* L858R are more likely to develop LM than those with *EGFR* 19del (1). In a BPM study, Takano et al. found that *EGFR* L858R mutation metastases were more likely to occur in the parenchyma (caudate, cerebellum, and temporal lobes) than those with 19del and were located closer to the surface of the brain than those with 19del or wild-type *EGFR* (33).

However, the limited sample size of nine patients with BMP did not allow us to thoroughly compare the characteristics of BPM and LM. Our study showed that 55.6% (5/9) of patients with BMP harboured *EGFR* 19del mutation, whereas only 11.1% (1/9) of them harboured the L858R mutation. In contrast, 50.0% (14/28) of patients with LM harboured *EGFR* L858R, while 25.0% (7/28) of

them harboured *EGFR* 19del mutation. Similar results were reported by Li et al. that NSCLC patients with *EGFR* 19del were more likely to develop BMP than patients with the *EGFR* L858R mutation (1).

We also found that there was a sex difference in the extracranial disease of NSCLS-LM patients. Patients with positive driver mutations in plasma ctDNA were mostly male (M:F = 9:4) and were more likely to be at a progressive stage (8 out of 13, 61.5%), suggesting that male patients had a higher tumour burden (Tables 1, 2, Figure 3A, Supplementary Figure 1). Accumulating evidence shows that the incidence of lung cancer is higher in males than in females; furthermore, male patients had a poorer prognosis than female patients (34). NSCLC female patients are usually non-smokers, and *EGFR* mutation positive. *EGFR* incidence is especially high in Asian NSCLC patients (35). The better outcome for female patients might be because they could be treated with *EGFR* TKIs, which was consistent with clinical practice.

In addition, in LM patients who were ctDNA positive in the plasma, the extracranial disease was more likely to be in a progressive stage compared to negative patients, 61.5% (8/13) versus 13.3% (2/15) (Tables 1, 2, Figure 3A), suggesting that ctDNA in the plasma is a prognostic factor. This may be because a higher tumour burden causes higher ctDNA levels in the plasma. Our results suggest that plasma ctDNA is a prognostic factor for patients with NSCLC-LM (10, 36).

To the best of our knowledge, few studies have used NGS to compare cancer-related genetic profiles of NSCLC-LM and NSCLC-BPM patients (1). Li et al. compared the characteristics of patients with NSCLC-LM and NSCLC-BPM in Sichuan province, located in southeastern China, including *EGFR* mutations, onset time of BPM or LM, proportion of multiple metastases, and survival. They found significant differences in lesion location and *EGFR* mutation subtypes between patients with NSCLC-LM and those with NSCLC-BPM. Our study included patients from the Hebei Province, located in the northern part of China. These two studies represent the characteristics of the Chinese population. Further studies should be conducted in other ethnicities, such as Caucasians and Africans, to determine whether this is a universal phenomenon.

The present study has limitations. Our study was a single-centre retrospective study with a relatively small sample size and case selection was based on the NGS of CSF and paired plasma, which had inevitable bias in case selection. Therefore, future multi-centre, prospective large sample-sized studies are needed to validate our findings.

Conclusions

Our study indicated that the main driver mutations of NSCLC-LM remained highly consistent with those of primary tumours, along with other unique genetic profiles. CSF ctDNA detected by NGS may reflect the molecular characteristics and heterogeneity of NSCLC-LM. Timely screening of NSCLC patients for CSF ctDNA, especially for patients with a mutation in plasma ctDNA, may facilitate early detection of LM. Patients with *EGFR* 19del might be at higher risk of suffering from BPM.

Data availability statement

The raw sequence data reported in this paper have been deposited in the Genome Sequence Archive (37) in National Genomics Data Center (38), China National Center for Bioinformation / Beijing Institute of Genomics, Chinese Academy of Sciences (GSA-Human: HRA006432) that are publicly accessible at https://ngdc.cncb.ac.cn/gsa-human.

Ethics statement

The studies involving humans were approved by The Institutional Review Board and Ethics Committee of the Fourth Hospital of Hebei Medical University. The studies were conducted in accordance with the local legislation and institutional requirements. The participants provided their written informed consent to participate in this study.

Author contributions

XL: Data curation, Investigation, Writing – original draft. FM: Funding acquisition, Methodology, Project administration, Supervision, Writing – original draft, Writing – review & editing. MF: Data curation, Formal Analysis, Funding acquisition, Supervision, Writing – original draft, Writing – review & editing. YJ: Data curation, Formal Analysis, Investigation, Methodology, Writing – original draft. YZ: Data curation, Investigation, Software, Writing – original draft. CXL: Data curation, Formal Analysis, Methodology, Validation, Writing – original draft. PT: Data curation, Formal Analysis, Investigation, Methodology, Writing – original draft. CFL: Data curation, Formal Analysis, Investigation, Software, Validation, Writing – original draft. GL: Conceptualization, Data curation, Formal Analysis, Funding acquisition, Investigation, Methodology, Project administration, Resources, Supervision, Validation, Writing – original draft, Writing – review & editing.

Funding

The author(s) declare financial support was received for the research, authorship, and/or publication of this article. This research was supported by the National Natural Science Foundation of China (NSFC) Program for Young Scientists, No. 82201973; Hebei Provincial Department of Human Resources and Social Security, Hebei Provincial Clinical Medical Excellent Talents Training Project, Jicai Prepayment [2021] No. 379; and Hebei Provincial Department of Human Resources and Social Security Project for Returned Overseas Chinese Talents, No. C20210111; Hebei Provincial Department of Human Resources and Social Security Project for Returned Overseas Chinese Talents, No. C20220109; Health Commission of Hebei Province, Hebei Provincial Research Project for Medical Science, No20210152; Health Commission of Hebei Province, Hebei Provincial Research Project for Medical Science, No20210079.

Conflict of interest

The authors declare that the research was conducted in the absence of any commercial or financial relationships that could be construed as a potential conflict of interest.

Publisher's note

All claims expressed in this article are solely those of the authors and do not necessarily represent those of their affiliated organizations, or those of the publisher, the editors and the reviewers. Any product that may be evaluated in this article, or claim that may be made by its manufacturer, is not guaranteed or endorsed by the publisher.

Supplementary material

The Supplementary Material for this article can be found online at: https://www.frontiersin.org/articles/10.3389/fonc.2023.1322635/full#supplementary-material

References

1. Li Q, et al. Brain parenchymal and leptomeningeal metastasis in non-small cell lung cancer. *Sci Rep* (2022) 12(1):22372. doi: 10.1038/s41598-022-26131-z

2. Li YS, et al. Leptomeningeal metastases in patients with NSCLC with EGFR mutations. *J Thorac Oncol* (2016) 11(11):1962–9. doi: 10.1016/j.jtho.2016.06.029

3. Brenner AW, Patel AJ. Review of current principles of the diagnosis and management of brain metastases. *Front Oncol* (2022) 12:857622. doi: 10.3389/fonc.2022.857622

4. Cheng H, Perez-Soler R. Leptomeningeal metastases in non-small-cell lung cancer. *Lancet Oncol* (2018) 19(1):e43–55. doi: 10.1016/S1470-2045(17)30689-7

5. Vitiello PP, et al. Clinical practice use of liquid biopsy to identify RAS/BRAF mutations in patients with metastatic colorectal cancer (mCRC): A single institution experience. *Cancers (Basel)* (2019) 11(10). doi: 10.3390/cancers11101504

6. Li YS, et al. Unique genetic profiles from cerebrospinal fluid cell-free DNA in leptomeningeal metastases of EGFR-mutant non-small-cell lung cancer: a new medium of liquid biopsy. *Ann Oncol* (2018) 29(4):945–52. doi: 10.1093/annonc/mdy009

7. Eisenhauer EA, et al. New response evaluation criteria in solid tumours: revised RECIST guideline (version 1. *1). Eur J Cancer* (2009) 45(2):228–47. doi: 10.1016/j.ejca.2008.10.026

8. Rangachari D, et al. Brain metastases in patients with EGFR-mutated or ALK-rearranged non-small-cell lung cancers. *Lung Cancer* (2015) 88(1):108–11. doi: 10.1016/j.lungcan.2015.01.020

9. Matsumoto S, et al. Frequent EGFR mutations in brain metastases of lung adenocarcinoma. *Int J Cancer* (2006) 119(6):1491–4. doi: 10.1002/ijc.21940

10. Kapeleris J, et al. Clinical applications of circulating tumour cells and circulating tumour DNA in non-small cell lung cancer-an update. *Front Oncol* (2022) 12:859152. doi: 10.3389/fonc.2022.859152

11. Pinzani P, et al. Updates on liquid biopsy: current trends and future perspectives for clinical application in solid tumors. *Clin Chem Lab Med* (2021) 59(7):1181–200. doi: 10.1515/cclm-2020-1685

12. Bronkhorst AJ, Ungerer V, Holdenrieder S. The emerging role of cell-free DNA as a molecular marker for cancer management. *Biomol Detect Quantif* (2019) 17:100087. doi: 10.1016/j.bdq.2019.100087

13. Ma C, et al. Detection of circulating tumor DNA from non-small cell lung cancer brain metastasis in cerebrospinal fluid samples. *Thorac Cancer* (2020) 11(3):588–93. doi: 10.1111/1759-7714.13300

14. Valiente M, et al. The evolving landscape of brain metastasis. *Trends Cancer* (2018) 4(3):176–96. doi: 10.1016/j.trecan.2018.01.003

15. De Mattos-Arruda L, et al. Cerebrospinal fluid-derived circulating tumour DNA better represents the genomic alterations of brain tumours than plasma. *Nat Commun* (2015) 6:8839. doi: 10.1038/ncomms9839

16. Tonse R, et al. Systematic review and meta-analysis of lung cancer brain metastasis and primary tumor receptor expression discordance. *Discovery Oncol* (2021) 12(1):48. doi: 10.1007/s12672-021-00445-2

17. Rolfo C, et al. Liquid biopsy for advanced NSCLC: A consensus statement from the international association for the study of lung cancer. *J Thorac Oncol* (2021) 16 (10):1647–62. doi: 10.1016/j.jtho.2021.06.017

18. Westover D, et al. Mechanisms of acquired resistance to first- and second-generation EGFR tyrosine kinase inhibitors. *Ann Oncol* (2018) 29(suppl_1):i10–9. doi: 10.1093/annonc/mdx703

19. Wu X, et al. Cerebrospinal fluid cell-free DNA-based detection of high level of genomic instability is associated with poor prognosis in NSCLC patients with leptomeningeal metastases. *Front Oncol* (2022) 12:664420. doi: 10.3389/fonc.2022.664420

20. Song Y, et al. Osimertinib quantitative and gene variation analyses in cerebrospinal fluid and plasma of a non-small cell lung cancer patient with leptomeningeal metastases. *Curr Cancer Drug Targets* (2019) 19(8):666–73. doi: 10.2174/1568009618666181017114111

21. Nanjo S, et al. MET copy number gain is associated with gefitinib resistance in leptomeningeal carcinomatosis of EGFR-mutant lung cancer. *Mol Cancer Ther* (2017) 16(3):506–15. doi: 10.1158/1535-7163.MCT-16-0522

22. Schoenfeld AJ, et al. Tissue-based molecular and histological landscape of acquired resistance to osimertinib given initially or at relapse in patients with EGFR-mutant lung cancers. *J Clin Oncol* (2019) 37:1–2. doi: 10.1200/JCO.2019.37.15_suppl.9028

23. Guo R, et al. MET-dependent solid tumours - molecular diagnosis and targeted therapy. *Nat Rev Clin Oncol* (2020) 17(9):569–87. doi: 10.1038/s41571-020-0377-z

24. Arrieta O, et al. The impact of common and rare EGFR mutations in response to EGFR tyrosine kinase inhibitors and platinum-based chemotherapy in patients with non-small cell lung cancer. *Lung Cancer* (2015) 87(2):169–75. doi: 10.1016/j.lungcan.2014.12.009

25. Keam B, et al. Rare and complex mutations of epidermal growth factor receptor, and efficacy of tyrosine kinase inhibitor in patients with non-small cell lung cancer. *Int J Clin Oncol* (2014) 19(4):594–600. doi: 10.1007/s10147-013-0602-1

26. Shi J, et al. Uncommon EGFR mutations in a cohort of Chinese NSCLC patients and outcomes of first-line EGFR-TKIs and platinum-based chemotherapy. *Chin J Cancer Res* (2017) 29(6):543–52. doi: 10.21147/j.issn.1000-9604.2017.06.09

27. Thress KS, et al. Acquired EGFR C797S mutation mediates resistance to AZD9291 in non-small cell lung cancer harboring EGFR T790M. *Nat Med* (2015) 21 (6):560–2. doi: 10.1038/nm.3854

28. Hoffknecht P, et al. Efficacy of the irreversible ErbB family blocker afatinib in epidermal growth factor receptor (EGFR) tyrosine kinase inhibitor (TKI)-pretreated non-small-cell lung cancer patients with brain metastases or leptomeningeal disease. *J Thorac Oncol* (2015) 10(1):156–63. doi: 10.1097/JTO.0000000000000380

29. Vokes NI, et al. Concurrent TP53 mutations facilitate resistance evolution in EGFR-mutant lung adenocarcinoma. *J Thorac Oncol* (2022) 17(6):779–92. doi: 10.1016/j.jtho.2022.02.011

30. Cox AD, et al. Drugging the undruggable RAS: Mission possible? *Nat Rev Drug Discovery* (2014) 13(11):828–51. doi: 10.1038/nrd4389

31. Awad MM, et al. Acquired resistance to KRAS(G12C) inhibition in cancer. *N Engl J Med* (2021) 384(25):2382–93. doi: 10.1056/NEJMoa2105281

32. Cagney DN, et al. Incidence and prognosis of patients with brain metastases at diagnosis of systemic Malignancy: a population-based study. *Neuro Oncol* (2017) 19 (11):1511–21. doi: 10.1093/neuonc/nox077

33. Takano K, et al. Different spatial distributions of brain metastases from lung cancer by histological subtype and mutation status of epidermal growth factor receptor. *Neuro Oncol* (2016) 18(5):716–24. doi: 10.1093/neuonc/nov266

34. Ragavan M, Patel MI. The evolving landscape of sex-based differences in lung cancer: a distinct disease in women. *Eur Respir Rev* (2022) 31(163). doi: 10.1183/16000617.0100-2021

35. Cheng YI, et al. Potential genetic modifiers for somatic EGFR mutation in lung cancer: a meta-analysis and literature review. *BMC Cancer* (2019) 19(1):1068. doi: 10.1186/s12885-019-6317-6

36. Kapeleris J, et al. Prognostic value of integrating circulating tumour cells and cell-free DNA in non-small cell lung cancer. *Heliyon* (2022) 8(7):e09971. doi: 10.1016/j.heliyon.2022.e09971

37. The genome sequence archive family: toward explosive data growth and diverse data types. *Genomics Proteomics Bioinform* (2021) 19(4):578–86. doi: 10.1016/j.gpb.2021.08.001

38. Database resources of the national genomics data center, China National Center for Bioinformation in 2022. *Nucleic Acids Res* (2022) 50(D1):D27–D38. doi: 10.1093/nar/gkab951

frontiers | Frontiers in Oncology

TYPE Original Research
PUBLISHED 07 February 2024
DOI 10.3389/fonc.2024.1305720

OPEN ACCESS

EDITED BY
Jianxin Xue,
Sichuan University, China

REVIEWED BY
Elizabeth Gaughan,
University of Virginia, United States
Kenji Morimoto,
Kyoto Prefectural University of Medicine, Japan

*CORRESPONDENCE
Benjamin Y. Kong
ben.kong@health.nsw.gov.au

RECEIVED 02 October 2023
ACCEPTED 08 January 2024
PUBLISHED 07 February 2024

CITATION
Brown LJ, Khou V, Brown C, Alexander M, Jayamanne D, Wei J, Gray L, Chan WY, Smith S, Harden S, Mersiades A, Warburton L, Itchins M, Lee JH, Pavlakis N, Clarke SJ, Boyer M, Nagrial A, Hau E, Pires da Silva I, Kao S and Kong BY (2024) First-line chemoimmunotherapy and immunotherapy in patients with non-small cell lung cancer and brain metastases: a registry study. *Front. Oncol.* 14:1305720. doi: 10.3389/fonc.2024.1305720

First-line chemoimmunotherapy and immunotherapy in patients with non-small cell lung cancer and brain metastases: a registry study

Lauren Julia Brown[1,2,3,4], Victor Khou[4,5,6], Chris Brown[7], Marliese Alexander[8,9], Dasantha Jayamanne[4,5,10], Joe Wei[11], Lauren Gray[11], Wei Yen Chan[12,13], Samuel Smith[12], Susan Harden[8,14], Antony Mersiades[7,15], Lydia Warburton[16,17], Malinda Itchins[4,10,11], Jenny H. Lee[12,13], Nick Pavlakis[4,10,11], Stephen J. Clarke[4,10,11], Michael Boyer[4,12], Adnan Nagrial[2,3,4], Eric Hau[1,2,3,4], Ines Pires da Silva[3,4,18], Steven Kao[4,12] and Benjamin Y. Kong[4,11,19,20]*

[1]Translational Radiation Biology and Oncology Group, Westmead Institute for Medical Research, Westmead, NSW, Australia, [2]Crown Princess Mary Cancer Centre, Westmead Hospital, Westmead, NSW, Australia, [3]Blacktown Cancer and Haematology Centre, Blacktown Hospital, Blacktown, NSW, Australia, [4]Faculty of Medicine and Health, The University of Sydney, Sydney, NSW, Australia, [5]Department of Radiation Oncology, Royal North Shore Hospital, St Leonards, NSW, Australia, [6]Department of Radiation Oncology, North Coast Cancer Institute, Coffs Harbour, NSW, Australia, [7]National Health and Medical Research Council (NHMRC) Clinical Trials Centre, The University of Sydney, Sydney, NSW, Australia, [8]Sir Peter MacCallum Department of Oncology, The University of Melbourne, Parkville, VIC, Australia, [9]Pharmacy Department, Peter MacCallum Cancer Centre, Parkville, VIC, Australia, [10]Genesis Care, St Leonards, NSW, Australia, [11]Department of Medical Oncology, Royal North Shore Hospital, St Leonards, NSW, Australia, [12]Department of Medical Oncology, Chris O'Brien Lifehouse, Camperdown, NSW, Australia, [13]Faculty of Medicine and Health Sciences, Macquarie University, Macquarie Park, NSW, Australia, [14]Department of Radiation Oncology, Sir Peter MacCallum Cancer Centre, Parkville, VIC, Australia, [15]Department of Medical Oncology, Northern Beaches Hospital, Frenches Forest, NSW, Australia, [16]Department of Medical Oncology, Fiona Stanley Hospital, Murdoch, WA, Australia, [17]Centre for Precision Health, Edith Cowan University, Joondalup, WA, Australia, [18]Melanoma Institute Australia, Wollstonecraft, NSW, Australia, [19]Department of Medical Oncology, Prince of Wales Hospital, Randwick, NSW, Australia, [20]Sydney Partnership for Health, Education, Research and Enterprise (SPHERE) Cancer Clinical Academic Group, Faculty of Medicine, University of New South Wales (NSW), Sydney, NSW, Australia

Introduction: Brain metastases commonly occur in patients with non-small cell lung cancer (NSCLC). Standard first-line treatment for NSCLC, without an EGFR, ALK or ROS1 mutation, is either chemoimmunotherapy or anti-PD-1 monotherapy. Traditionally, patients with symptomatic or untreated brain metastases were excluded from the pivotal clinical trials that established first-line treatment recommendations. The intracranial effectiveness of these treatment protocols has only recently been elucidated in small-scale prospective trials.

Methods: Patients with NSCLC and brain metastases, treated with first-line chemoimmunotherapy or anti-PD-1 monotherapy were selected from the Australian Registry and biObank of thoracic cancers (AURORA) clinical database covering seven institutions. The primary outcome was a composite time-to-event

(TTE) outcome, including extracranial and intracranial progression, death, or need for local intracranial therapy, which served as a surrogate for disease progression. The secondary outcome included overall survival (OS), intracranial objective response rate (iORR) and objective response rate (ORR).

Results: 116 patients were included. 63% received combination chemoimmunotherapy and 37% received anti-PD-1 monotherapy. 69% of patients received upfront local therapy either with surgery, radiotherapy or both. The median TTE was 7.1 months (95% CI 5 - 9) with extracranial progression being the most common progression event. Neither type of systemic therapy or upfront local therapy were predictive of TTE in a multivariate analysis. The median OS was 17 months (95% CI 13-27). Treatment with chemoimmunotherapy was predictive of longer OS in multivariate analysis (HR 0.35; 95% CI 0.14 – 0.86; p=0.01). The iORR was 46.6%. The iORR was higher in patients treated with chemoimmunotherapy compared to immunotherapy (58% versus 31%, p=0.01). The use of chemoimmunotherapy being predictive of iORR in a multivariate analysis (OR 2.88; 95% CI 1.68 - 9.98; p=0.04).

Conclusion: The results of this study of real-world data demonstrate the promising intracranial efficacy of chemoimmunotherapy in the first-line setting, potentially surpassing that of immunotherapy alone. No demonstrable difference in survival or TTE was seen between receipt of upfront local therapy. Prospective studies are required to assist clinical decision making regarding optimal sequencing of local and systemic therapies.

KEYWORDS

non-small cell lung cancer, brain metastases, immune checkpoint inhibitor, chemoimmunotherapy, stereotactic radiosurgery, whole brain radiotherapy, intracranial therapy

1 Introduction

Brain metastases are an important clinical problem in the treatment of non-small cell lung cancer (NSCLC), occurring in up to 30% of cases at the time of diagnosis (1). The impact of brain metastases on the prognosis of NSCLC is mixed, linked to a poor prognosis in some studies (1), while other reports suggest it can lead to improved outcomes (2). Active, symptomatic or untreated brain metastases are almost universal criteria for exclusion from lung cancer clinical trials, therefore overall survival (OS) estimates from clinical trials do not accurately reflect that of patients with brain metastases.

In patients with driver mutations such as epidermal growth factor receptor (EGFR) mutations or anaplastic lymphoma kinase (ALK) rearrangements, the incidence of brain metastases is higher than those without mutations (3). The intracranial activity of later generation tyrosine kinase inhibitors is high with the intracranial objective response rate (iORR) of EGFR inhibitor, osimertinib reported as 64% (4) and ALK inhibitor, lorlatinib up to 82% (5). Prior studies of combination EGFR inhibitors plus chemotherapy have also shown higher iORR of up to 85% (6).

For patients who test negative for actionable biomarkers, multimodal management with immune checkpoint inhibitors (ICI's) with or without chemotherapy and local therapy is recommended by international guidelines (7). In contrast to the intracranial activity observed with targeted therapy, systemic treatment with chemotherapy alone is estimated to have a 28 – 42% iORR in asymptomatic brain metastases (8–10). However, first-line immunotherapy and chemoimmunotherapy regimens have rapidly become a standard of care for both adenocarcinoma and squamous cell carcinoma in patients with adequate performance status (11–16). A pooled analysis of the KEYNOTE-021, KEYNOTE-189 and KEYNOTE-407 trials, all of which enrolled patients with treated or stable brain metastases, revealed that the addition of immunotherapy to chemotherapy improved overall survival, progression-free survival (PFS) and iORR compared with chemotherapy alone (17). The recently published ATEZO-BRAIN (18) and CAP-BRAIN trials (19) have both demonstrated the

intracranial activity of first-line anti-PD-(L)1 antibodies plus chemotherapy in select patients with non-squamous lung cancer with untreated brain metastases, without the need for upfront local therapy.

The intracranial activity of immunotherapy and chemoimmunotherapy regimens in non-squamous NSCLC has been recently established in small prospective studies. The ideal treatment sequencing between systemic (immunotherapy or chemoimmunotherapy) and local (radiotherapy and/or surgery) therapy remains unknown. In this study we have compared the clinical outcomes of the different treatment approaches for patients with both non-squamous and squamous NSCLC with brain metastases in a real-world setting. These approaches include chemoimmunotherapy versus immunotherapy, both with and without local therapy (comprising radiotherapy, surgery, or a combination of both).

2 Materials and methods

2.1 Patient population

Patients from seven institutions were retrospectively identified via the Australian Registry and biObank of thoracic cancers (AURORA). AURORA is approved by the Peter MacCallum Cancer Centre Human Research Ethics Committee (HREC/17/PMCC/42). All patients had Stage IV NSCLC with brain metastases and received first-line systemic therapy with anti-PD-1 monotherapy or combination chemoimmunotherapy. All patients were negative for EGFR, ROS1, ALK oncogenes by institutional standard-of-care testing. Variables collected included baseline patient demographics, disease characteristics (including sites of extracranial disease, method of brain metastasis assessment, number and symptoms of brain metastases, size of brain metastases and presence or absence of symptoms) and treatment details (including systemic therapy dose, radiotherapy timing and dose and surgical details).

2.2 Outcome measures

Intracranial disease progression may be manifested by asymptomatic radiological findings, symptomatic progression, or death. Thus, a composite time-to-event (TTE) primary endpoint was constructed to capture all progression events regardless of whether intracranial imaging was performed at the time of progression or death. This included investigator-assessed radiological intracranial or extracranial progressive disease (PD), need for local therapy (surgery or radiotherapy) or death due to any cause. Intracranial progression was defined as a ≥20% increase in the sum of the lesions in the brain or the presence of a new lesion as per RECIST 1.1 (20).

Secondary endpoints included OS, iORR and objective response rate (ORR). ORR and iORR were determined by best investigator-assessed extracranial and intracranial responses. ORR and iORR were defined as the proportion of patients who had a partial (PR) or complete response (CR) to treatment by best investigator-assessed response. This was defined as ≥30% reduction in the size of measured lesions or complete resolution of measured lesions, respectively as per RECIST 1.1 (20).

2.3 Statistical analysis

Descriptive statistics were used to summarize patients and disease characteristics, including medians and ranges for continuous variables and proportions for categorical variables. Chi-squared tests were used to examine associations between categorical variables. OS and TTE were calculated from the date of commencement of systemic treatment to the date of death and to the date of an event (either death, intracranial or extracranial PD or salvage radiotherapy). Patients without a clinical event were censored at the last known follow-up date.

Univariate and multivariate logistic and Cox-proportional hazards regression models were used to identify factors associated with the composite outcome and prespecified baseline and treatment characteristics. Factors included in the model included presence of symptoms, number of brain metastases, PD-L1 status, type of systemic therapy, receipt of local therapy, presence of extracranial disease and location of extracranial disease. All factors were considered in the multivariate analysis. A competing risk analysis was performed to assess the cumulative incidence of the composite TTE. All statistical analyses were performed using R (version 4.2.3, R Foundation for Statistical Computing, Vienna, Austria) and some figures were created using GraphPad Prism, version 10. A two-sided p-value of <0.05 was considered statistically significant. The reported analyses, including OS, were exploratory in nature. Final data analysis was performed on 23 March 2023.

3 Results

3.1 Patient characteristics

One hundred and sixteen patients from seven Australian hospitals with NSCLC with brain metastases treated with first-line systemic therapy, diagnosed between December 2016 to January 2022, were included in this analysis (Table 1). The median age was 66 years (IQR 58-71). 65 (56%) were male and 101 (87%) had a European Cooperative Oncology Group Status (ECOG) of 0-1. The histology of the population included 103 (89%) with adenocarcinoma, 7 (6%) with squamous cell carcinoma and 6 (5%) with not-otherwise specified NSCLC. PD-L1 status was performed on 110 patients, 31(27%) had a PD-L1 status of <1%, 21 (18%) were PD-L1 1-49% and 61 (53%) were PD-L1 ≥50%. At the time of diagnosis, 64 patients (55%) were symptomatic of their brain metastases and 76 (66%) had multiple intracranial metastases. The sites and patterns of extra-thoracic metastatic disease were assessed at baseline, 54 (47%) had intracranial disease alone and 62 (53%) has ≥1 site of extracranial disease. Thirty-five (30%) had bone metastases, 23 (20%) had adrenal metastases, 18 (16%) had pleural metastases, 15 (13%) had liver metastases and 12 (10%) had other metastatic sites of disease (Supplementary Table 1).

10.3389/fonc.2024.1305720

TABLE 1 Baseline characteristics.

Characteristic	Overall N = 116 (%#)	Chemoimmunotherapy N=73 (%#)	Immunotherapy N=43 (%#)
Age*	66 (58-71)	65 (56 - 70)	70 (62-74)
Sex			
F	51 (44)	37 (51)	14 (33)
M	65 (56)	36 (49)	29 (67)
ECOG			
0	35 (30)	27 (37)	8 (19)
1	66 (57)	40 (55)	26 (60)
2	9 (8)	4 (5)	5 (12)
3	3 (3)	2 (3)	1 (2)
Not reported	3 (3)	0 (0)	3 (7)
Histology			
Adenocarcinoma	103 (89)	63 (87)	40 (93)
Squamous Cell	7 (6)	4 (5)	2 (5)
NOS	6 (5)	6 (8)	1 (2)
PD-L1 expression			
<1%	31 (27)	31 (43)	0 (0)
1-49%	21 (18)	20 (27)	1 (2)
≥50%	61 (53)	20 (27)	41 (95)
Not reported	3 (3)	2 (3)	1 (2)
Multiple vs. Single brain metastases at baseline			
Multiple	76 (66)	46 (63)	30 (70)
Single	35 (30)	24 (33)	11 (26)
Not reported	5 (4)	3 (4)	2 (5)
Symptomatic brain metastases			
No	50 (43)	35 (48)	15 (35)
Yes	64 (55)	37 (51)	27 (63)
Not reported	2 (2)	1 (1)	1 (2)
Site of extrathoracic metastases			
Intracranial disease alone	54 (47)	25 (34)	29 (67)
≥1 site of extracranial metastases	62 (53)	48 (66)	14 (33)

*Median and IQR. #Percentages are rounded to the whole number.

Eighty (69%) patients received upfront local therapy followed by systemic therapy. Forty (34%) received CNS radiotherapy and 40 (34%) had intracranial surgery prior to the commencement of systemic therapy. Thirty-six (31%) patients received systemic therapy alone (Figure 1A). Of the patients that underwent CNS radiotherapy prior to systemic therapy, 25 (25 of 40, 63%) underwent stereotactic radiosurgery (SRS), 15 (15 of 40, 36%) underwent whole brain radiotherapy (WBRT). Of the patients who had surgery, 37 (37 of 40, 93%) also received radiotherapy and 3 (3 of 40, 7%) had surgery alone. Post-operative radiotherapy (PORT) was administered to 36 patients, with 22 (22 of 36, 61%) receiving cavity SRS, 9 (9 of 36, 25%) received post-operative hypofractionated radiotherapy and 5 (5 of 36, 14%) receiving WBRT. One patient received pre-operative SRS (Figure 1B). The median time between diagnosis of brain metastases and commencement of systemic therapy, was 36.5 days, allowing for local therapies.

Seventy-three patients received combination chemoimmunotherapy (63%) as their first-line systemic therapy. Sixty-two patients (53%) received carboplatin, pemetrexed and pembrolizumab, 6 (5%) received carboplatin, paclitaxel and pembrolizumab and 5 (4%)

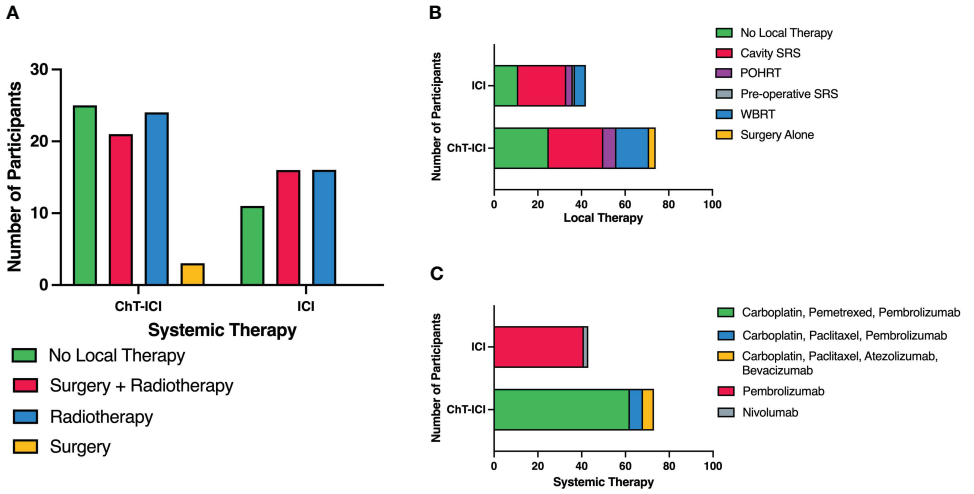

FIGURE 1
Summary of upfront systemic and local therapies. **(A)** Upfront Local Therapies by Systemic Therapy. **(B)** Upfront Local Therapies with Detailed Radiotherapy Modalities. **(C)** Types of Systemic Therapy. ChT, chemotherapy; ICI, Immune Checkpoint Inhibitor; SRS, Stereotactic radiosurgery; WBRT, whole brain radiotherapy; POHRT, Post-operative hypofractionated radiotherapy.

received carboplatin, paclitaxel, bevacizumab and atezolizumab. The remaining 43 (37%) patients were treated with anti-PD-1 monotherapy, 41 (34%) with pembrolizumab and 2 (1.7%) with nivolumab (Figure 1C). Two patients received concurrent chemoradiotherapy for stage III disease then progressed intracranially within 3-6 months of platinum-doublet chemotherapy, thus at clinician discretion were treated with anti-PD-1 monotherapy, despite one having an unknown PD-L1 status and one with PD-L1 with expression of 1-49%.

Thirty-two (28%) patients required salvage radiotherapy during or after progression on systemic therapy; 21 (21 of 32, 66%) of these were with treated with salvage SRS and 11 (11 of 32, 34%) with salvage WBRT (Supplementary Figure 1). Of these patients, 24 (24 of 32, 75%) had received upfront local therapy and 8 (8 of 32, 25%) did not receive upfront local therapy.

Whilst all patients were negative for EGFR, ALK and ROS1, 72 (62%) patients were also tested for KRAS and BRAF mutations with 25 (22%) patients undergoing further next generation sequencing for other mutations (Supplementary Table 2). Thirty-three patients (28%) had a KRAS mutation, of these 13 (13 of 33, 11%) were KRAS G12C. There were four patients had an ERBB2 amplification or insertion, three had a MET amplification/mutation, three with a PIK3CA mutation, two with a BRAF mutation, two with an NRASQ21R mutation.

3.2 Composite time-to-event outcome

The median follow-up for the study cohort was 28.6 months (IQR 20-37 months), the median TTE was 7.1 months (95% CI 5–9; Figure 2A). An event occurred in 68% of patients by 12 months (Supplementary Table 3). Extracranial progression of disease was the most common event to occur, followed by intracranial progression, need for stereotactic radiosurgery (SRS), death and need for whole brain radiotherapy (Figure 3).

There were no significant differences in TTE on univariate and multivariate analysis when patients were stratified according to systemic therapy, presence of brain metastasis symptoms, number of brain metastases, PD-L1 score, whether they received upfront local therapy or presence and number of other sites of metastatic disease (Table 2 and Supplementary Table 4).

The median TTE was similar for patients who received upfront local therapy (7 months, 95% CI 5-10) versus no upfront local therapy (7 months, 95% CI 4-11; p=0.53) (Supplementary Figure 2). The TTE was also similar for patients who received chemoimmunotherapy (7 months, 95% CI 5-9) versus immunotherapy alone (6 months, 95% CI 3-18; p=0.82) (Supplementary Figure 3). The median TTE for the different subgroups based on patient characteristics and therapy type is included in Supplementary Table 5.

3.3 Overall survival

The median OS was 17 months (95% CI 13 -27; Figure 2B). The landmark 12-month survival was 61%.

In univariate analysis, age, ECOG, presence of brain metastases symptoms, number of brain metastases, PD-L1 score, type of systemic therapy, upfront local therapy, site and number of extracranial metastases did not influence OS (Supplementary Table 6). However, when all factors were assessed in a multivariate analysis, patients who received chemoimmunotherapy had a longer OS (HR 0.35; 95% CI 0.14–0.86, p=0.01) and patients with PD-L1 score of ≥50% also had longer OS (HR 0.25; 95% CI 0.10–0.65, p<0.01) (Table 2).

Of note, patients who received upfront local therapy followed by systemic therapy had a numerically longer median OS (23 months; 95% CI 12–NA) compared to those who had systemic therapy alone (16 months; 95% CI 10–NA; p=0.13) (Supplementary Figure 4). The median OS was similar for patients who received chemoimmunotherapy (16 months; 95% CI 12–28) versus immunotherapy (17 months; 95% CI 6-44; p=0.95) (Supplementary Figure 5).

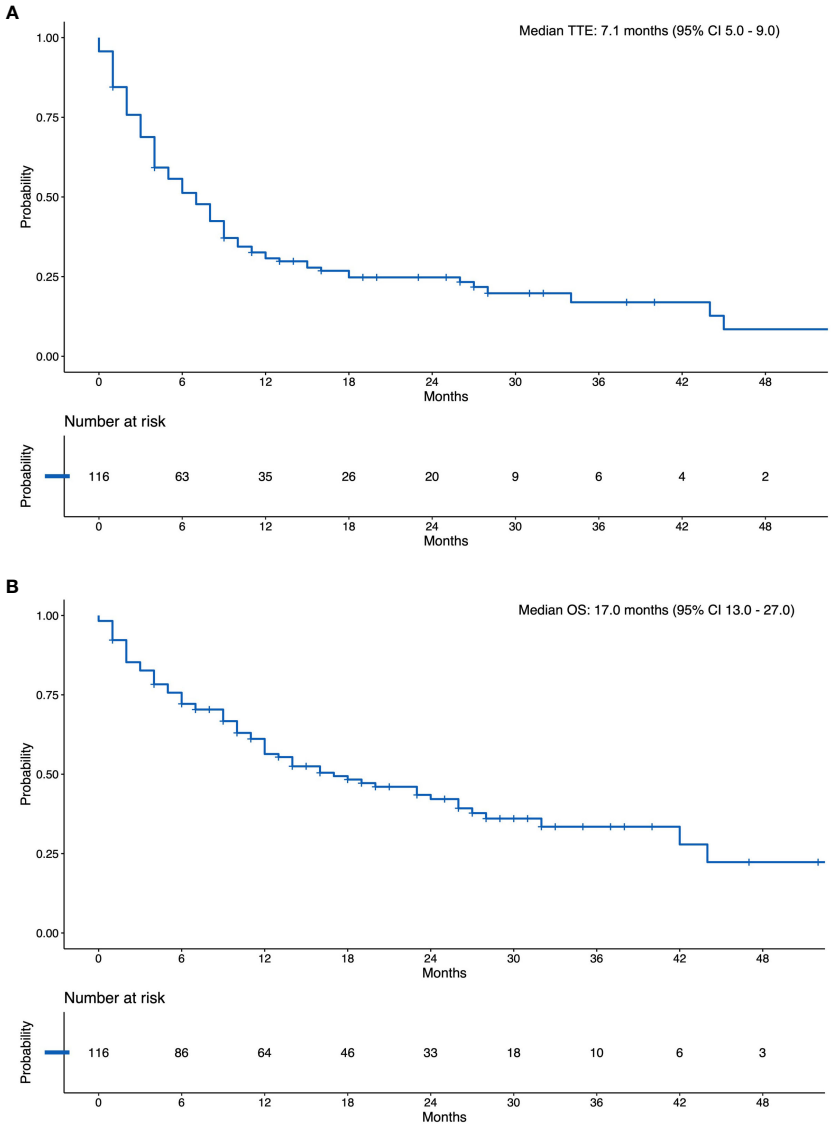

FIGURE 2
(A) Kaplan Meier Curve of the Composite Time-to-event Outcome. **(B)** Kaplan Meier Curve of Overall Survival. N, Number at Risk.

Patients with PD-L1≥ 50% (26 months, 95% CI 14– NA) had a longer median OS than those who had PD-L1 1-49% (11 months, 95% CI 9-NA) or PD-L1 <1% (12 months, 95% CI 6–23; p=0.05) (Supplementary Figure 6). Longer median OS was also noted in patients who were PD-L1≥50% treated with chemoimmunotherapy (median OS not reached; 95% CI 26–NA) versus those treated with immunotherapy alone (17 months; 95% CI 7–NA; p = 0.03) (Supplementary Figure 7). The median OS data for the different subgroups based on patient characteristics and therapy type is included in Supplementary Table 5.

3.4 Intracranial response rate

The iORR was 46.6%. The iORR was not evaluable in 28 patients (due to complete resection of intracranial disease or no available cranial imaging following commencement of systemic therapy). In the 88 patients with evaluable disease, 10 patients had CR (10 of 88, 11%), 31 had PR (31 of 88, 35%), 33 had stable disease (33 of 88, 38%) and 14 had PD (14 of 88, 16%). The median time to best response was 4.5 months (IQR 3-7 months). Of the 41 patients who had a response, 30 (30 of 41, 73%) had upfront local therapy (2 with surgery, 16 with radiotherapy and 12 with both upfront surgery and radiotherapy). The iORR was higher in patients who received chemoimmunotherapy (30 of 52, 58%) versus those who had immunotherapy alone (11 of 36, 31%, p=0.01). The iORR was similar in patients who received upfront local therapy (30 of 65, 46%) versus no upfront local therapy (11 of 23, 48% p=0.89).

Amongst the 36 patients who had systemic therapy only, there were 11 (11 of 36, 31%) patients with investigator-assessed iORR; 9 with PR (9 of 36, 25%) and 2 with CR (2 of 36, 8%) (Figure 4). Of the five patients who received bevacizumab in addition with chemoimmunotherapy, an iORR was noted in 3 patients, one of whom had upfront local therapy.

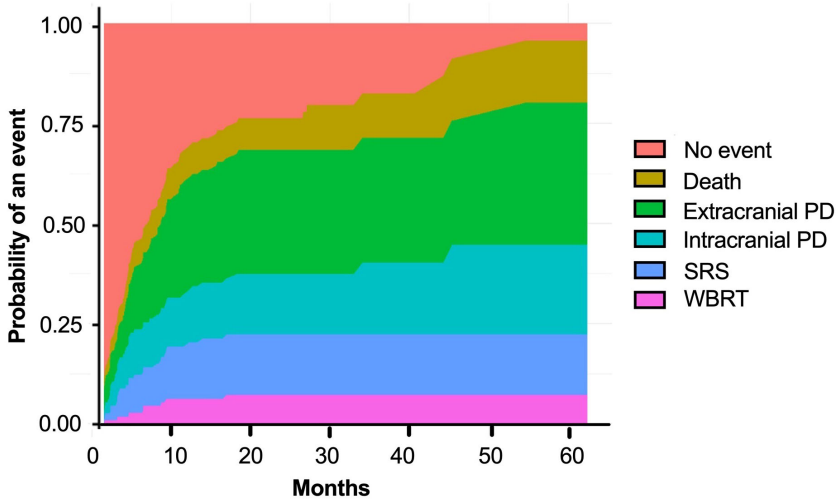

FIGURE 3
Cumulative risk of composite time-to-event outcome. PD, progressive disease; SRS, stereotactic radiosurgery; WBRT, whole brain radiotherapy.

On univariate analysis, patients who received chemoimmunotherapy had a higher iORR versus immunotherapy alone (OR 3.10, 95% CI 1.29 – 7.82; p=0.01). Other factors including upfront local therapy, PD-L1 status, number of intracranial metastases and symptoms of disease were not associated with higher iORR (Supplementary Table 7). Multivariate analysis confirmed chemoimmunotherapy was associated with improved iORR (HR 2.88, 95% CI 1.68 – 9.98, p=0.04) (Table 2).

3.5 Overall response rate

The ORR was 50%. In 13 patients, the extracranial response data was not evaluable. Five patients had CR (5 of 103, 5%) and 53 had PR (53 of 103, 51%). Concordance between extracranial and intracranial response was evaluated in 84 patients (Supplementary Table 8). A concordant extracranial and intracranial response was recorded in 70 (70 of 84, 83%) patients. In 14 (14 of 84, 17%) patients, a discordant response was recorded.

3.6 Patterns of management

Treatment varied across institutions with some institutions favoring upfront local therapy followed by systemic therapy, regardless of the presence or absence of symptoms, and some favoring systemic therapy alone for patients who were asymptomatic (Supplementary Figure 8).

Patients who were symptomatic were more likely to receive upfront local therapy versus asymptomatic patients (74% versus 25%, p<0.001). Similarly, patients with multiple brain metastases were also more likely to receive upfront local therapy versus patients with a single brain metastasis (73% versus 25%, p=0.03). PD-L1 status, ECOG and age did not influence whether a patient received local therapy (Supplementary Table 9). Patients who were over the age of 65 years were also more likely to receive immunotherapy over chemoimmunotherapy (70% versus 49%, p=0.03). Number of metastases and presence of symptoms did not impact systemic treatment choice (Supplementary Table 10).

4 Discussion

The data presented in this multi-institutional analysis provide valuable insights into the treatment patterns and outcomes of patients treated with first-line immunotherapy and chemoimmunotherapy for NSCLC and brain metastases. The median OS was 17 months whilst the median composite TTE was 7.1 months. In patients who received chemoimmunotherapy, an improved iORR was observed in the univariate and multivariate analysis (multivariate OR 2.88; p=0.04). Additionally, on multivariate analysis, receipt of chemoimmunotherapy (multivariate HR 0.35; p=0.01) and high PD-L1 (multivariate HR 0.25; p<0.01) were predictive of improved OS. This suggests that the combination of chemoimmunotherapy may be associated with enhanced intracranial activity and OS compared to immunotherapy alone. Despite differences in treatment sequencing across institutions, no significant difference in either outcome measure was observed based on receipt of upfront local therapy, symptoms at baseline, number of brain metastases.

The findings from our study support the results of recently prospective published studies assessing the activity of ICI's with chemotherapy in NSCLC with brain metastases (18, 19, 21). The results of the Phase II ATEZO-Brain trial by Nadal et al. assessed the use of chemotherapy combined with atezolizumab for patients with non-squamous NSCLC and untreated brain metastases demonstrated a similar iORR of 42.7% (18). The Phase II CAP-Brain study by Hou et al. also assessed the use of chemotherapy combined with camrelizumab for patients with non-squamous NSCLC and untreated brain metastases (19). This study also allowed inclusion of patients who were symptomatic of their brain disease and/or on steroids or mannitol. The iORR was 52.5% and the median OS was 21.0 months (95% CI 15.9 – NR). In our cohort, there was a 31% iORR in patients who received

TABLE 2 Multivariate analysis for TTE, OS and iORR.

Characteristic	TTE		OS		iORR	
	HR (95% CI)	P value	HR (95% CI)	P value	OR (95% CI)	P value
Presence of Symptoms						
No Symptoms	1.00	0.77	1.00	0.27	1.00	0.39
Symptoms	0.92 (0.51, 1.64)		0.69 (0.36, 1.32)		0.58 (0.17, 1.97)	
Number of Brain Metastases						
Multiple brain metastases	1.00	0.39	1.00	0.74	1.00	0.23
Single brain metastasis	0.71 (0.48, 1.31)		0.91 (0.52, 1.60)		1.90 (0.67, 5.72)	
PD-L1 expression						
PD-L1 <1%	1.00	0.08	1.00	**<0.01**	1.00	0.37
PD-L1 1-49%	0.71 (0.37, 1.35)		0.82 (0.40, 1.67)		2.77 (0.68, 12.50)	
PD-L1 ≥50%	0.44 (0.21, 0.89)		**0.25 (0.10, 0.65)**		1.65 (0.37, 7.82)	
Treatment Type						
Immunotherapy	1.00	0.30	1.00	**0.01**	1.00	**0.04**
Chemoimmunotherapy	0.70 (0.35, 1.40)		**0.35 (0.14, 0.86)**		**2.88 (1.68, 9.98)**	
Local Therapy						
No	1.00	0.74	1.00	0.64	1.00	0.24
Yes	0.95 (0.50, 1.79)		0.85 (0.44, 1.65)		2.15 (0.61, 8.37)	
Bone Metastases						
No	1.00	0.62	1.00	0.21	1.00	0.71
Yes	1.21 (0.57, 2.56)		1.80 (0.72, 4.54)		1.37 (0.27, 7.73)	
Adrenal Metastases						
No	1.00	0.10	1.00	0.49	1.00	0.32
Yes	0.51 (0.22, 1.15)		0.72 (0.28, 1.85)		2.26 (0.45, 12.8)	
Liver Metastases						
No	1.00	0.56	1.00	0.93	1.00	0.81
Yes	1.28 (0.56, 2.91)		0.96 (0.35, 2.60)		1.26 (0.19, 9.35)	
Pleural Metastases						
No	1.00	0.75	1.00	0.79	1.00	0.49
Yes	1.13 (0.52, 2.46)		1.14 (0.45, 2.88)		0.53 (0.08, 3.26)	
Extracranial Disease						
Brain only disease	1.00	0.93	1.00	0.40	1.00	0.88
Extracranial disease	0.96 (0.37, 2.49)		0.61 (0.19, 1.93)		0.86 (0.11, 6.32)	

TTE, Time to composite event; OS, Overall Survival; iORR, Intracranial objective response rate; HR, Hazard Ratio; OR, Odds Ratio; CI, Confidence interval.

systemic therapy alone without the need for upfront radiotherapy. The results of ATEZO-Brain, CAP-Brain (18, 19), and our study set a precedent for the use of chemoimmunotherapy prior to local therapy of radiotherapy or surgical management in select patient populations.

The median OS in our real-world population, although not directly comparable, was similar to trial populations of patients with pre-treated brain metastases treated with chemoimmunotherapy. In the CheckMate 9LA trial, patients treated with nivolumab plus ipilimumab and chemotherapy versus chemotherapy, the median OS (19.3 versus 6.8 months, HR 0.45, 95% CI 0.29–0.70), median intracranial PFS (13.5 versus 4.6 months, HR 0.36, 95% CI 0.22-0.60), iORR (39% versus 20%) and median time to development of new brain metastases (6.9 versus 5.3 months) were all improved (22). In pooled analyses of patients with brain metastases from the KEYNOTE -021, -189 and -407 trials of pembrolizumab plus

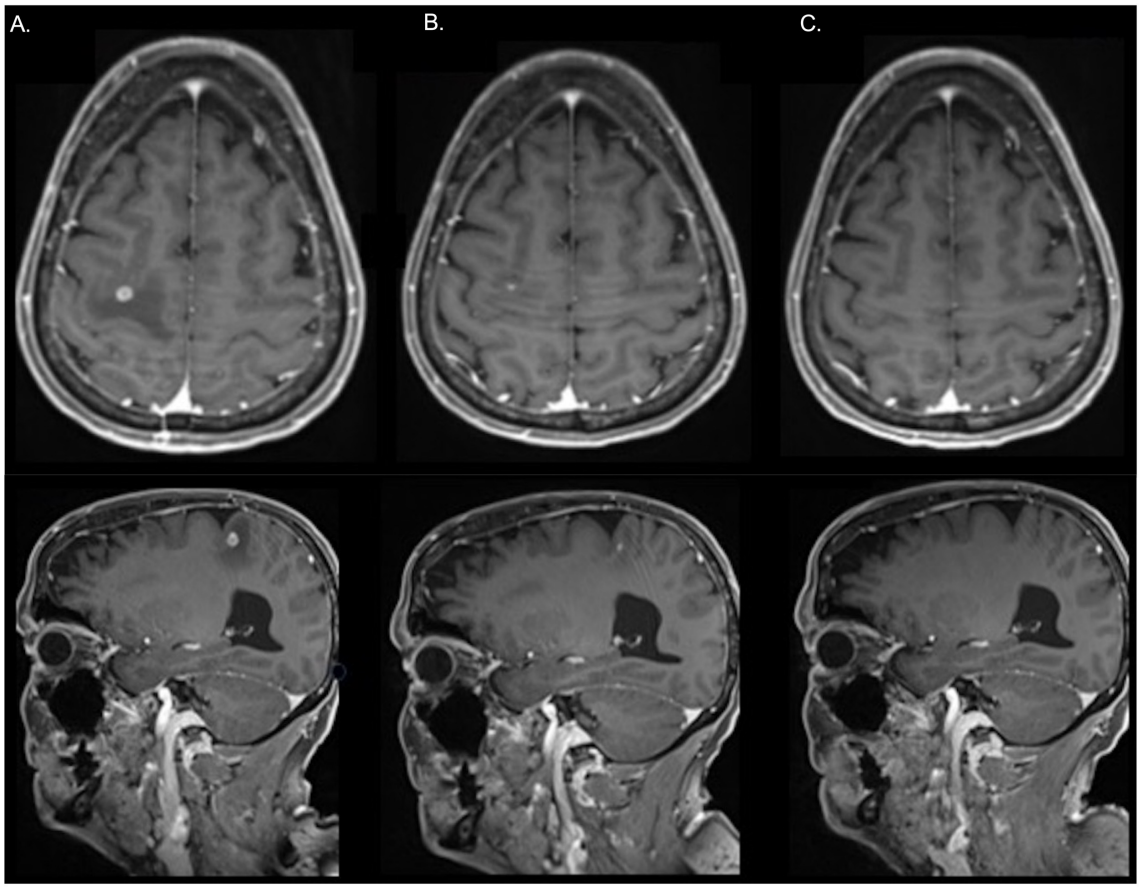

FIGURE 4
In a representative patient treated with carboplatin, pemetrexed and pembrolizumab without prior local therapy, a magnetic resonance imaging scan shows a solitary brain metastasis in the right parietal lobe at: **(A)** Pre-treatment **(B)** After 1 month of treatment **(C)** In complete response at 3 months following the commencement of systemic therapy.

chemotherapy also improved median OS versus chemotherapy (18.8 versus 7.6 months, HR 0.48, 95% CI 0.32-0.70) (17).

Immunotherapy alone has also been investigated as a potential approach for treating brain metastases in NSCLC. A trial of single-agent pembrolizumab in untreated brain metastases demonstrated an iORR of 29.7% in patients with PD-L1 ≥1% (23). In the CheckMate 227 study, nivolumab plus ipilimumab improved median OS (17.4 versus 13.7 months, HR 0.63, 95% CI 0.43 – 0.92) and decreased the rate of development of new brain metastases compared with chemotherapy (4% versus 20%) (24). This raises a hypothesis-generating question of whether anti-CTLA-4 has an intracranial priming effect. This hypothesis is best demonstrated in melanoma combination immunotherapy, which has a higher intracranial response rate compared with single-agent therapy (25). In contrast to studies containing nivolumab, the combination of pembrolizumab plus ipilimumab in the KEYNOTE-598 did not demonstrate any significant differences in survival between the two treatment groups in the subgroup of patients with brain metastases (26). However, this could represent differences in the baseline patient characteristics or the lower dose of ipilimumab (1mg/kg, 6 weekly, rather than 3mg/kg, 3 weekly, which was utilized in the melanoma study) and not lack of intracranial activity. In our study, although chemoimmunotherapy was not compared to chemotherapy alone, chemotherapy may fulfil the priming effect that has been achieved by anti-CTLA-4 in melanoma.

In our cohort, chemoimmunotherapy was associated with improved iORR and OS on multivariate analysis over the use of immunotherapy alone. Interestingly, a difference was not observed in univariate analysis for OS. However, this phenomenon can be observed with multivariate modelling upon inclusion of other covariates to better delineate the true source of influence on median OS. Notably, there was no significant difference between systemic therapies on the composite TTE. The cumulative risk of extracranial progression was the most common progression event to occur and comprises a significant proportion of the events in TTE. These results suggest chemoimmunotherapy and immunotherapy have similar efficacy in the control of extracranial disease. However, the combination of chemoimmunotherapy improved intracranial response and potentially led to increased OS.

Whilst our study did not demonstrate any benefit for OS or TTE from the receipt of upfront local therapy, there were no quality-of-life data or assessment of symptomatic control in our study where

additional benefits may have been noted. However, prior research has shown that radiotherapy can increase the efficacy of ICI's through the release of tumor-associated antigens and stimulation of the antitumor response (27–30). The secondary analysis of NSCLC patients in KEYNOTE-001 who received pembrolizumab demonstrated longer PFS and OS in those who had prior radiotherapy (29). Chemotherapy in addition to immunotherapy is also thought to enhance T-cell activation and cancer cell infiltration, thereby increasing the efficacy of ICIs (31). With the further addition of radiotherapy to amplify immunotherapy responses it is logical that a combination strategy of chemoimmunotherapy following radiotherapy may lead to further improved responses.

The difference in sequencing of local therapy and management across institutions also highlights the complexity of decision making for this population. For a select group of patients, it may be reasonable to commence systemic therapy without local treatment. Several prospective clinical trials are underway to explore the impact of different chemotherapy, immunotherapy, radiotherapy and novel combinations on survival outcomes and iORR (Supplementary Table 11). Some of these trials allow for untreated and symptomatic brain metastases to be enrolled on trial, and may provide further insights into the optimal treatment and sequencing for this population.

There are several important differences between patients included in the described clinical trials compared with our real-world population. Firstly, symptomatic patients are generally excluded from clinical trials whilst in our cohort 55% of patients were symptomatic at baseline. The proportion of patients who received baseline CNS imaging with MRI was also high (87.1%). In contrast, whilst many clinical trial participants have MRI imaging at baseline, this is generally not mandated by protocol, thereby potentially underestimating the number of patients who have brain metastases at baseline albeit with no symptoms. Secondly, the number of patients who had local therapy with surgery or radiotherapy immediately before starting systemic therapy was likely to be higher in real-world patients since a washout period of 4 weeks is usually mandated in clinical trials. In real-world patients, this may have conferred some synergistic or antagonistic effects, due to the immunosuppressive effects of surgery or the synergy between radiotherapy and immunotherapy. Thirdly, we observed 53% of patients in our cohort had a PD-L1 ≥50%, which is generally higher than the reported rates of PD-L1 ≥50% which is closer to 30% (32). Lastly, a significant majority of the study population had adenocarcinoma (89%) and only a small proportion of patients had squamous cell carcinoma (6%). It is known that patients with non-squamous NSCLC are more likely to develop brain metastases (33, 34). This is consistent with combined data from the landmark immunotherapy trials in NSCLC (17, 24, 26, 35, 36), which also reveal a higher percentage of non-squamous patients with brain metastases, comprising 70%-85%, in contrast to those with squamous cell lung cancer, who represent 15%-30% of the brain metastasis cases. The retrospective nature of our study likely contributed to a lower proportion of cases with squamous cell carcinoma, and the applicability of this study should be interpreted with caution when considering this group.

4.1 Limitations

This study provides a real-world insight into the outcomes for patients with NSCLC and brain metastases, however, there are some limitations to this methodology. The retrospective nature of this study is associated with unavoidable selection bias and although this was a multi-institutional study conducted at seven large cancer centers, the overall sample size is relatively small when compared to other real-world datasets. This limited sample size, along with the cohort's heterogeneity, may have influenced the identification of predictive factors associated with the composite TTE.

It is also important to note that data regarding steroid use was not available and thus the influence of steroid use on outcomes was unable to be assessed in this study. Steroid use is often reflective of the symptom burden and is used to reduce peritumoral edema (37). Additionally, the use of steroids and the impact on the efficacy of immunotherapy is controversial with some studies suggesting steroid use can dampen the immune response (38–40). Multiple prospective studies are underway, allowing the use of steroids (Supplementary Table 11) which may help to guide clinical practice for the use of concurrent steroids and immunotherapy in patients with brain metastases.

There are also inherent challenges in the interpretation of imaging responses retrospectively in patients with brain metastases. This includes patients lost to follow-up, the difference in scan frequency and scan type between centers. Other potential confounders include the use of anti-angiogenic agents such as bevacizumab in chemotherapy regimens and its effect on reducing contrast enhancement that has been demonstrated in the setting of primary brain cancers (41, 42). MRI is also considered to have a higher sensitivity for the detection of intracranial metastatic disease, given a small proportion of our cohort had CT imaging, there may be a proportion of patients whose response was over- or underestimated. Furthermore, the timing of scans amongst our cohort differed. Notably, the RECIST and RANO-BM response assessment methods also differ in the timing of recommended scans. The most appropriate intracranial response criteria to use in clinical trials is the subject of ongoing debate (43).

4.2 Conclusions

Findings from this study reveal that chemoimmunotherapy has promising intracranial activity and survival outcomes in the first-line setting. Individual treatment sequencing approaches across institutions reveal heterogeneity in the initial treatment paradigms for patients with brain metastases in the real-world setting. The results of future prospective studies are expected to answer questions about ideal response assessment criteria, optimal systemic therapy, and treatment sequencing to assist clinical decision making. Overall, the lack of survival benefit attributable to sequencing of surgery or radiotherapy before or after systemic therapy should give clinicians confidence that the outcomes may be similar when treating patients with NSCLC and brain metastases. However, prospective studies are required to answer this question definitively.

Data availability statement

The raw data is not available but requests can be directed to the corresponding author for consideration.

Ethics statement

The AUstralian Registry and biObank of thoracic cAncers (AURORA) has been approved by the PeterMacCallum Cancer Centre Human Research Ethics Committee and this study is in compliance with approved protocol number HREC/17/PMCC/42.

Author contributions

LB: Conceptualization, Data curation, Formal analysis, Investigation, Methodology, Project administration, Software, Visualization, Writing – original draft, Writing – review & editing. VK: Data curation, Investigation, Writing – review & editing. CB: Data curation, Formal analysis, Investigation, Software, Visualization, Writing – review & editing. MA: Data curation, Investigation, Project administration, Writing – review & editing. DJ: Data curation, Investigation, Writing – review & editing. JW: Data curation, Investigation, Writing – review & editing. LG: Data curation, Investigation, Writing – review & editing. SS: Data curation, Investigation, Writing – review & editing. WC: Data curation, Investigation, Writing – review & editing. SH: Data curation, Investigation, Writing – review & editing. AM: Data curation, Investigation, Writing – review & editing. LW: Data curation, Investigation, Writing – review & editing. MI: Data curation, Investigation, Writing – review & editing. JL: Data curation, Investigation, Writing – review & editing. NP: Data curation, Investigation, Writing – review & editing. SC: Data curation, Investigation, Writing – review & editing. MB: Investigation, Writing – review & editing, Data curation. AN: Data curation, Investigation, Writing – review & editing. IP: Data curation, Investigation, Writing – review & editing, Supervision. EH: Data curation, Investigation, Writing – review & editing. SK: Data curation, Investigation, Writing – review & editing. BK: Data curation, Investigation, Writing – review & editing, Conceptualization, Formal analysis, Methodology, Project administration, Supervision, Writing – original draft.

Funding

The author(s) declare that no financial support was received for the research, authorship, and/or publication of this article.

Conflict of interest

The authors declare that the research was conducted in the absence of any commercial or financial relationships that could be construed as a potential conflict of interest.

Publisher's note

Supplementary material

The Supplementary Material for this article can be found online at: https://www.frontiersin.org/articles/10.3389/fonc.2024.1305720/full#supplementary-material

References

1. Waqar SN, Samson PP, Robinson CG, Bradley J, Devarakonda S, Du L, et al. Non-small-cell lung cancer with brain metastasis at presentation. *Clin Lung Cancer* (2018) 19(4):e373–9. doi: 10.1016/j.cllc.2018.01.007

2. Sørensen JB, Hansen HH, Hansen M, Dombernowsky P. Brain metastases in adenocarcinoma of the lung: frequency, risk groups, and prognosis. *J Clin Oncol* (1988) 6(9):1474–80. doi: 10.1200/JCO.1988.6.9.1474

3. Ge M, Zhuang Y, Zhou X, Huang R, Liang X, Zhan Q. High probability and frequency of EGFR mutations in non-small cell lung cancer with brain metastases. *J Neurooncol* (2017) 135(2):413–8. doi: 10.1007/s11060-017-2590-x

4. Erickson AW, Brastianos PK, Das S. Assessment of effectiveness and safety of osimertinib for patients with intracranial metastatic disease: A systematic review and meta-analysis. *JAMA Netw Open* (2020) 3(3):e201617. doi: 10.1001/jamanetworkopen.2020.1617

5. Shaw AT, Bauer TM, de Marinis F, Felip E, Goto Y, Liu G, et al. First-line lorlatinib or crizotinib in advanced ALK-positive lung cancer. *New Engl J Med* (2020) 383(21):2018–29. doi: 10.1056/NEJMoa2027187

6. Hou X, Li M, Wu G, Feng W, Su J, Jiang H, et al. Gefitinib plus chemotherapy vs gefitinib alone in untreated EGFR-mutant non–small cell lung cancer in patients with brain metastases: the GAP BRAIN open-label, randomized, multicenter, phase 3 study. *JAMA Network Open* (2023) 6(2):e2255050. doi: 10.1001/jamanetworkopen.2022.55050

7. Hendriks LE, Kerr KM, Menis J, Mok TS, Nestle U, Passaro A, et al. Non-oncogene-addicted metastatic non-small-cell lung cancer: ESMO Clinical Practice Guideline for diagnosis, treatment and follow-up. *Ann Oncol* (2023) 34(4):358–76. doi: 10.1016/j.annonc.2022.12.013

8. Barlesi F, Gervais R, Lena H, Hureaux J, Berard H, Paillotin D, et al. Pemetrexed and cisplatin as first-line chemotherapy for advanced non-small-cell lung cancer (NSCLC) with asymptomatic inoperable brain metastases: a multicenter phase II trial (GFPC 07-01). *Ann Oncol* (2011) 22(11):2466–70. doi: 10.1093/annonc/mdr003

9. Bailon OK, Chouahnia K, Augier A, Bouillet T, Billot S, Coman I, et al. Upfront association of carboplatin plus pemetrexed in patients with brain metastases of lung adenocarcinoma. *Neuro Oncol* (2012) 14(4):491–5. doi: 10.1093/neuonc/nos004

10. Lee DH, Han JY, Kim HT, Yoon SJ, Pyo HR, Cho KH, et al. Primary chemotherapy for newly diagnosed nonsmall cell lung cancer patients with synchronous brain metastases compared with whole-brain radiotherapy administered first. *Cancer* (2008) 113(1):143–9. doi: 10.1002/cncr.23526

11. Langer CJ, Gadgeel SM, Borghaei H, Papadimitrakopoulou VA, Patnaik A, Powell SF, et al. Carboplatin and pemetrexed with or without pembrolizumab for

advanced, non-squamous non-small-cell lung cancer: a randomised, phase 2 cohort of the open-label KEYNOTE-021 study. *Lancet Oncol* (2016) 17(11):1497–508. doi: 10.1016/S1470-2045(16)30498-3

12. Gandhi L, Rodriguez-Abreu D, Gadgeel S, Esteban E, Felip E, Angelis De F, et al. Pembrolizumab plus chemotherapy in metastatic non-small-cell lung cancer. *N Engl J Med* (2018) 378(22):2078–92. doi: 10.1056/NEJMoa1801005

13. Novello S, Kowalski DM, Luft A, Gumus M, Vicente D, Mazieres J, et al. Pembrolizumab plus chemotherapy in squamous non-small-cell lung cancer: 5-year update of the phase III KEYNOTE-407 study. *J Clin Oncol* (2023) 2023:JCO2201990. doi: 10.1200/JCO.22.01990

14. Reck M, Rodríguez-Abreu D, Robinson AG, Hui R, Csőszi T, Fülöp A, et al. Five-year outcomes with pembrolizumab versus chemotherapy for metastatic non–small-cell lung cancer with PD-L1 tumor proportion score ≥ 50%. *J Clin Oncol* (2021) 39(21):2339–49. doi: 10.1200/JCO.21.00174

15. Reck M, Rodríguez-Abreu D, Robinson AG, Hui R, Csőszi T, Fülöp A, et al. Pembrolizumab versus chemotherapy for PD-L1–positive non–small-cell lung cancer. *New Engl J Med* (2016) 375(19):1823–33. doi: 10.1056/NEJMoa1606774

16. Mok TSK, Wu YL, Kudaba I, Kowalski DM, Cho BC, Turna HZ, et al. Pembrolizumab versus chemotherapy for previously untreated, PD-L1-expressing, locally advanced or metastatic non-small-cell lung cancer (KEYNOTE-042): a randomised, open-label, controlled, phase 3 trial. *Lancet* (2019) 393(10183):1819–30. doi: 10.1016/S0140-6736(18)32409-7

17. Powell SF, Rodríguez-Abreu D, Langer CJ, Tafreshi A, Paz-Ares L, Kopp HG, et al. Outcomes with pembrolizumab plus platinum-based chemotherapy for patients with NSCLC and stable brain metastases: pooled analysis of KEYNOTE-021, -189, and -407. *J Thorac Oncol* (2021) 16(11):1883–92. doi: 10.1016/j.jtho.2021.06.020

18. Nadal E, Rodríguez-Abreu D, Simó M, Massutí B, Juan O, Huidobro G, et al. Phase II trial of atezolizumab combined with carboplatin and pemetrexed for patients with advanced nonsquamous non–small-cell lung cancer with untreated brain metastases (Atezo-brain, GECP17/05). *J Clin Oncol* (2023) 41(28):JCO.22.02561. doi: 10.1200/JCO.22.02561

19. Hou X, Zhou C, Wu G, Lin W, Xie Z, Zhang H, et al. Efficacy, safety, and health-related quality of life with camrelizumab plus pemetrexed and carboplatin as first-line treatment for advanced nonsquamous NSCLC with brain metastases (CAP-BRAIN): A multicenter, open-label, single-arm, phase 2 study. *J Thorac Oncol* (2023) 18(6):769–79. doi: 10.1016/j.jtho.2023.01.083

20. Schwartz LH, Litière S, de Vries E, Ford R, Gwyther S, Mandrekar S, et al. RECIST 1.1-Update and clarification: From the RECIST committee. *Eur J Cancer* (2016) 62:132–7. doi: 10.1016/j.ejca.2016.03.081

21. Nigen B, Goronflot T, Herbreteau G, Mathiot L, Sagan C, Raimbourg J, et al. Impact of first-line immunotherapy on survival and intracranial outcomes in a cohort of non-small cell lung cancer patients with brain metastases at diagnosis. *Lung Cancer* (2023) 184:107321. doi: 10.1016/j.lungcan.2023.107321

22. Carbone D, Ciuleanu T, Cobo M, Schenker M, Zurawski B, Menezes J, et al. OA09.01 first-line nivolumab + Ipilimumab + Chemo in patients with advanced NSCLC and brain metastases: results from checkMate 9LA. *J Thorac Oncol* (2021) 16 (10). doi: 10.1016/j.jtho.2021.08.061

23. Goldberg SB, Schalper KA, Gettinger SN, Mahajan A, Herbst RS, Chiang AC, et al. Pembrolizumab for management of patients with NSCLC and brain metastases: long-term results and biomarker analysis from a non-randomised, open-label, phase 2 trial. *Lancet Oncol* (2020) 21(5):655–63. doi: 10.1016/S1470-2045(20)30111-X

24. Reck M, Ciuleanu TE, Lee JS, Schenker M, Zurawski B, Kim SW, et al. Systemic and intracranial outcomes with first-line nivolumab plus ipilimumab in patients with metastatic NSCLC and baseline brain metastases from checkMate 227 part 1. *J Thorac Oncol* (2023) 18(8):P1055–69. doi: 10.1016/j.jtho.2023.04.021

25. Long GV, Atkinson V, Lo S, Sandhu S, Guminski AD, Brown MP, et al. Combination nivolumab and ipilimumab or nivolumab alone in melanoma brain metastases: a multicentre randomised phase 2 study. *Lancet Oncol* (2018) 19(5):672–81. doi: 10.1016/S1470-2045(18)30139-6

26. Boyer M, Şendur MAN, Rodríguez-Abreu D, Park K, Lee DH, Çiçin I, et al. Pembrolizumab plus ipilimumab or placebo for metastatic non–small-cell lung cancer with PD-L1 tumor proportion score ≥ 50%: randomized, double-blind phase III KEYNOTE-598 study. *J Clin Oncol* (2021) 39(21):2327–38. doi: 10.1200/JCO.20.03579

27. Twyman-Saint Victor C, Rech AJ, Maity A, Rengan R, Pauken KE, Stelekati E, et al. Radiation and dual checkpoint blockade activate non-redundant immune mechanisms in cancer. *Nature* (2015) 520(7547):373–7. doi: 10.1038/nature14292

28. Deng L, Liang H, Burnette B, Weicheslbaum RR, Fu YX. Radiation and anti-PD-L1 antibody combinatorial therapy induces T cell-mediated depletion of myeloid-derived suppressor cells and tumor regression. *Oncoimmunology* (2014) 3:e28499. doi: 10.4161/onci.28499

29. Shaverdian N, Lisberg A, Bornazyan K, Veruttipong D, Goldman J, Formenti S, et al. Previous radiotherapy and the clinical activity and toxicity of pembrolizumab in the treatment of non-small-cell lung cancer: a secondary analysis of the KEYNOTE-001 phase 1 trial. *Lancet Oncol* (2017) 18(7):895–903. doi: 10.1016/S1470-2045(17)30380-7

30. Sharabi AB, Nirschl CJ, Kochel CM, Nirschl TR, Francica BJ, Velarde E, et al. Stereotactic radiation therapy augments antigen-specific PD-1–mediated antitumor immune responses *via* cross-presentation of tumor antigen. *Cancer Immunol Res* (2015) 3(4):345–55. doi: 10.1158/2326-6066.Cir-14-0196

31. Pfirschke C, Engblom C, Rickelt S, Cortez-Retamozo V, Garris C, Pucci F, et al. Immunogenic chemotherapy sensitizes tumors to checkpoint blockade therapy. *Immunity* (2016) 44(2):343–54. doi: 10.1016/j.immuni.2015.11.024

32. Aggarwal C, Abreu DR, Felip E, Carcereny E, Gottfried M, Wehler T, et al. Prevalence of PD-L1 expression in patients with non-small cell lung cancer screened for enrollment in KEYNOTE-001, -010, and -024. *Ann Oncol* (2016) 27:vi363. doi: 10.1093/annonc/mdw378.14

33. Wang S-y, Ye X, Ou W, Lin Y-b, Zhang B-b, Yang H, et al. Risk of cerebral metastases for postoperative locally advanced non-small-cell lung cancer. *Lung Cancer* (2009) 64(2):238–43. doi: 10.1016/j.lungcan.2008.08.012

34. Yokoi K, Kamiya N, Matsuguma H, Machida S, Hirose T, Mori K, et al. Detection of brain metastasis in potentially operable non-small cell lung cancer: A comparison of CT and MRI. *CHEST* (1999) 115(3):714–9. doi: 10.1378/chest.115.3.714

35. Li S, Zhang H, Liu T, Chen J, Dang J. The effect of asymptomatic and/or treated brain metastases on efficacy of immune checkpoint inhibitors in metastatic non–small cell lung cancer: a meta-analysis. *Front Oncol* (2021) 11. doi: 10.3389/fonc.2021.702924

36. Paz-Ares L, Ciuleanu T-E, Cobo M, Schenker M, Zurawski B, Menezes J, et al. First-line nivolumab plus ipilimumab combined with two cycles of chemotherapy in patients with non-small-cell lung cancer (CheckMate 9LA): an international, randomised, open-label, phase 3 trial. *Lancet Oncol* (2021) 22(2):198–211. doi: 10.1016/S1470-2045(20)30641-0

37. Vecht CJ, Hovestadt A, Verbiest HB, Vliet van JJ, van Putten WL. Dose-effect relationship of dexamethasone on Karnofsky performance in metastatic brain tumors: a randomized study of doses of 4, 8, and 16 mg per day. *Neurology* (1994) 44(4):675–80. doi: 10.1212/WNL.44.4.675

38. Skribek M, Rounis K, Afshar S, Grundberg O, Friesland S, Tsakonas G, et al. Effect of corticosteroids on the outcome of patients with advanced non–small cell lung cancer treated with immune-checkpoint inhibitors. *Eur J Cancer* (2021) 145:245–54. doi: 10.1016/j.ejca.2020.12.012

39. Diana VM, Karine T, Madhav KC, Victoria S, Helen Y, Cameron P, et al. Timing of steroid initiation and response rates to immune checkpoint inhibitors in metastatic cancer. *J ImmunoTher Cancer* (2021) 9(7):e002261. doi: 10.1136/jitc-2020-002261

40. Nelson BE, Greiner B, Hong A, Tipton S, Lee M, Dixon A, et al. Corticosteroid use and its impact on the efficacy of immunotherapy in multiple tumor types. *J Clin Oncol* (2021) 39(15_suppl):e14583. doi: 10.1200/JCO.2021.39.15_suppl.e14583

41. Pope WB, Lai A, Nghiemphu P, Mischel P, Cloughesy TF. MRI in patients with high-grade gliomas treated with bevacizumab and chemotherapy. *Neurology* (2006) 66 (8):1258–60. doi: 10.1212/01.wnl.0000208958.29600.87

42. Norden AD, Young GS, Setayesh K, Muzikansky A, Klufas R, Ross GL, et al. Bevacizumab for recurrent Malignant gliomas. *Efficacy toxic patterns recurrence* (2008) 70(10):779–87. doi: 10.1212/01.wnl.0000304121.57857.38

43. Wen PY, Bent Den Van MJ, Youssef G, Cloughesy TF, Ellingson BM, Weller M, et al. RANO 2.0: Proposal for an update to the Response Assessment in Neuro-Oncology (RANO) criteria for high- and low-grade gliomas in adults. *J Clin Oncol* (2023) 41(Suppl 16):2017–7. doi: 10.1200/JCO.2023.41.16_suppl.2017

frontiers | Frontiers in Immunology

TYPE Original Research
PUBLISHED 15 April 2024
DOI 10.3389/fimmu.2024.1373330

OPEN ACCESS

EDITED BY
Lin Zhou,
Sichuan University, China

REVIEWED BY
David Wasilewski,
Charité University Medicine Berlin, Germany
Rongrong Zhou,
Central South University, China

*CORRESPONDENCE
Feifei Teng
tengfeifei16@126.com

RECEIVED 19 January 2024
ACCEPTED 03 April 2024
PUBLISHED 15 April 2024

CITATION
Xu J, Wang P, Li Y, Shi X, Yin T, Yu J and Teng F (2024) Development and validation of an MRI-Based nomogram to predict the effectiveness of immunotherapy for brain metastasis in patients with non-small cell lung cancer.
Front. Immunol. 15:1373330.
doi: 10.3389/fimmu.2024.1373330

Development and validation of an MRI-Based nomogram to predict the effectiveness of immunotherapy for brain metastasis in patients with non-small cell lung cancer

Junhao Xu[1], Peiliang Wang[1,2], Yikun Li[1], Xiaonan Shi[1], Tianwen Yin[1,3], Jinming Yu[1] and Feifei Teng[1]*

[1]Department of Radiation Oncology, Shandong Cancer Hospital and Institute, Shandong First Medical University and Shandong Academy of Medical Sciences, Jinan, China, [2]Department of Radiation Oncology, Shandong Cancer Hospital and Institute, Cheeloo College of Medicine, Shandong University, Jinan, China, [3]Cancer Center, Union Hospital, Tongji Medical College, Huazhong University of Science and Technology, Wuhan, China

Introduction: The variability and unpredictability of immune checkpoint inhibitors (ICIs) in treating brain metastases (BMs) in patients with advanced non-small cell lung cancer (NSCLC) is the main concern. We assessed the utility of novel imaging biomarkers (radiomics) for discerning patients with NSCLC and BMs who would derive advantages from ICIs treatment.

Methods: Data clinical outcomes and pretreatment magnetic resonance images (MRI) were collected on patients with NSCLC with BMs treated with ICIs between June 2019 and June 2022 and divided into training and test sets. Metastatic brain lesions were contoured using ITK-SNAP software, and 3748 radiomic features capturing both intra- and peritumoral texture patterns were extracted. A clinical radiomic nomogram (CRN) was built to evaluate intracranial progression-free survival, progression-free survival, and overall survival. The prognostic value of the CRN was assessed by Kaplan–Meier survival analysis and log-rank tests.

Results: In the study, a total of 174 patients were included, and 122 and 52 were allocated to the training and validation sets correspondingly. The intratumoral radiomic signature, peritumoral radiomic signature, clinical signature, and CRN predicted intracranial objective response rate. Kaplan–Meier analyses showed a significantly longer intracranial progression-free survival in the low-CRN group than in the high-CRN group ($p < 0.001$). The CRN was also significantly associated with progression-free survival ($p < 0.001$) but not overall survival.

Discussion: Radiomics biomarkers from pretreatment MRI images were predictive of intracranial response. Pretreatment radiomics may allow the early prediction of benefits.

KEYWORDS

immunotherapy, brain metastasis, non-small cell lung cancer, radiomics, MRI

1 Introduction

Non-small cell lung cancer (NSCLC) is the predominant form of lung cancer, accounting for around 80-85% of all reported cases (1). Immune checkpoint inhibitors (ICIs) targeting programmed cell death-1 (PD-1), programmed cell death ligand-1 (PD-L1), and cytotoxic T-lymphocyte antigen-4 (CTLA-4) have shown promising results in advanced NSCLC and prolonged patient survival. ICIs have transformed the therapeutic prospect of metastatic NSCLC (2, 3).

Approximately 25% of patients with NSCLC are diagnosed with brain metastases (BMs) (4), and 20–40% of patients develop BMs throughout their whole life (5, 6). Patients with NSCLC and BMs have a high mortality rate (7). Although ICIs have resulted in improvements in advanced NSCLC treatment, their effectiveness in treating metastatic brain lesions remains controversial (8). Patients with baseline BMs benefited from pembrolizumab treatment in the KEYNOTE-189 study, whereas other studies, such as KEYNOTE-024, found no benefit (9, 10). Among the patients who had undergone therapy for brain metastases in the KEYNOTE-024 trial, the pembrolizumab group exhibited a longer median progression-free survival (PFS) in comparison to the chemotherapy group; however, no statistically significant difference in survival outcomes between the immunotherapy and chemotherapy groups. In a phase II trial involving 37 patients diagnosed with asymptomatic BMs in NSCLC, only a minority (29.7%) of individuals with PD-L1-positive NSCLC exhibited a favorable response in terms of BMs (11). Previous clinical trials have demonstrated that immunotherapy could potentially be beneficial for patients with NSCLC with BMs, and biomarkers to select patients who could benefit from ICIs are required. Although the potential biomarkers for immunotherapy, including PD-L1 expression levels, tumor-infiltrating lymphocytes (TILs), and tumor mutation burden (TMB), have been investigated, none of them have shown a significant association with the intracranial response or prognosis (11–13).

New opportunities have arisen with the recent advent of radiomics and quantitative imaging biomarkers. Different from conventional biopsy-based tests that only capture a portion of the tumor, imaging provides a complete perspective of the entire tumor burden, offering valuable insights into each cancerous lesion through a single non-invasive examination (14). Radiomics-based biomarkers have been successful in predicting patient survival, tumor microenvironment status, and the differentiation of malignant tumors (15–18). However, little research has investigated the correlation between radiomics and intracranial advancement in patients diagnosed with NSCLC and BMs undergoing immunotherapy. In this retrospective study, we employed contrast-enhanced magnetic resonance imaging (CE-MRI) to develop a radiomics nomogram that can predict the effectiveness of intracranial immunotherapy in patients with NSCLC with BMs.

2 Materials and methods

2.1 Patients

The study received approval from the medical ethics committee of the institutions, and the requirement for obtaining informed consent was exempted. We identified 340 advanced NSCLC patients with brain involvement who had received ICIs, including sintilimab, camrelizumab, tislelizumab, and pembrolizumab, between June 2019 and June 2022 at Shandong Cancer Hospital and Institution, and Cheeloo Hospital in Jinan, China. The inclusion criteria were (1) age ≥18 years; (2) Karnofsky Performance Status (KPS) ≥ 70; (3) baseline CE-MRI performed within 4 weeks before immunotherapy; and (4) BMs meeting the criteria for measurable disease according to Response Assessment in Neuro-Oncology Brain Metastases (RANO-BM) (≥ 0.5 cm) (19). Patients were excluded if they had: (1) prior treatment with any ICIs before being diagnosed with BMs; (2) low-quality MRI data due to motion artifacts or inadequate contrast injection; or (3) incomplete baseline data, or if there were no follow-up data available. The selected patients were separated into a training cohort from Shandong Cancer Hospital and Institution and an independent external validation cohort from Cheeloo Hospital. The recruitment process and exclusion criteria are shown in Figure 1A.

Baseline clinical characteristics, such as KPS score, age, gender, history of smoking, clinical stages, number and diameter of BMs, and blood indicators, were obtained from medical records, and imaging of baseline MRI were also downloaded. Two experienced neuroradiologists independently evaluated the quantifiable intracranial target lesions according to the RANO-BM guidelines and classified the intracranial response as good or poor, based on intracranial objective response rate (ORR) after 4 cycles of ICIs. If

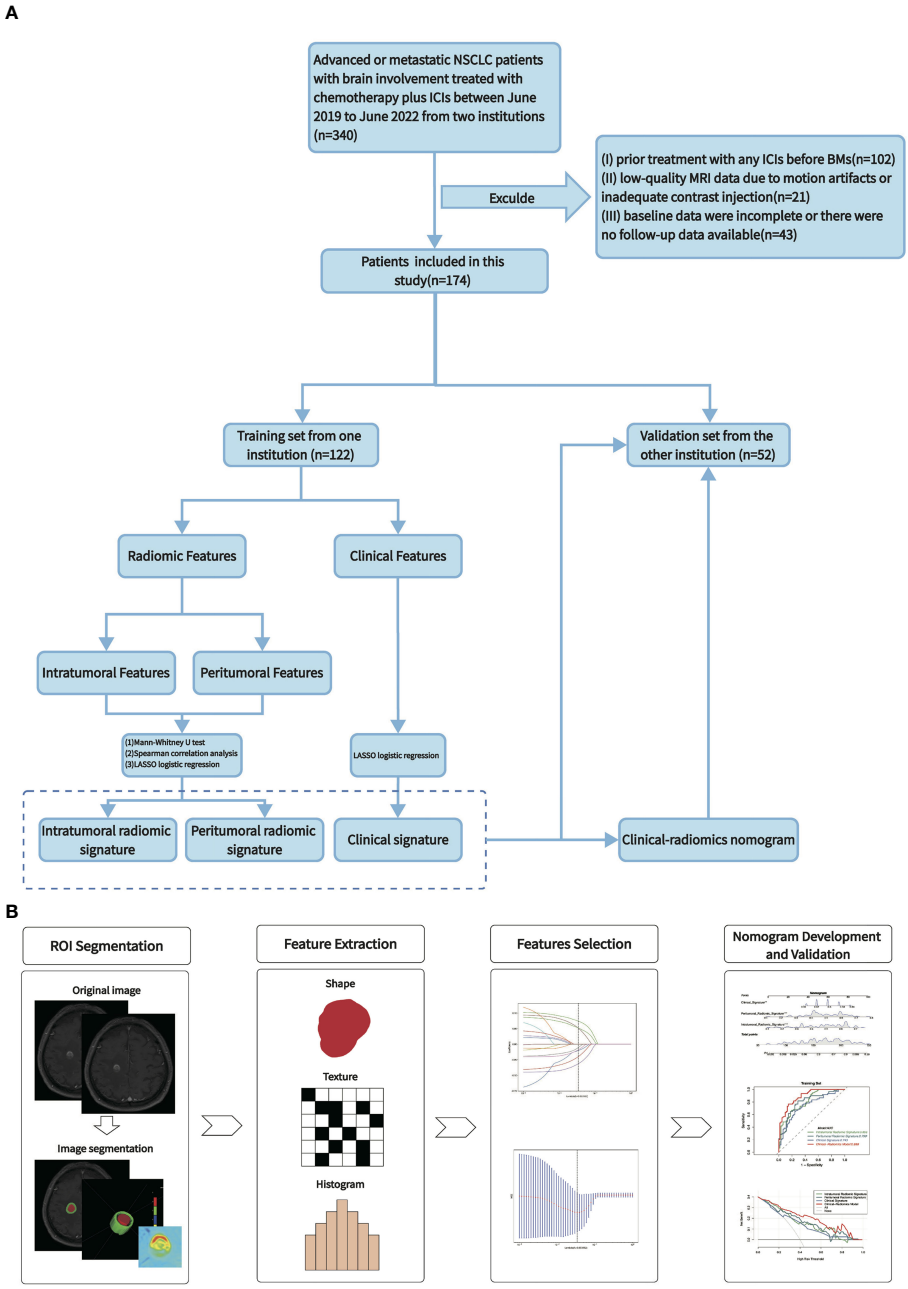

FIGURE 1
Study overview. **(A)** Workflow of the study. **(B)** Workflow of the radiomics analysis.

there was any conflict over the results of the assessment, another radiologist was invited to reach a final decision. Intracranial target lesions with any of the following were defined as having a good response: (1) intracranial complete response (iCR) or (2) intracranial partial response (iPR). The poor response was defined with any of the following: (1) intracranial progressive disease (iPD) or (2) stable disease (iSD). Continuous patient follow-up was performed throughout the study to ensure accurate ascertainment of survival outcomes. Intracranial progression-free survival (iPFS) pertains to the duration starting from the initiation of ICI treatment until the documented occurrence of brain progression or mortality due to any cause. Progression-free survival (PFS) is defined as the timeframe commencing from the first administration of ICI until the recorded manifestation of progression in any lesion or death resulting from any cause. Overall survival (OS) was determined by computing the period beginning with the initial application of ICI and ending at either demise or the most recent follow-up.

2.2 Magnetic resonance imaging acquisition

Patients from Shandong Cancer Hospital were scanned using an eight-channel phased-array surface coil on a 3.0T scanner system

from Siemens (Magnetom Verio, Siemens, Erlangen, Germany) according to the protocols: Repetition Time (TR)=270ms; Echo Time (TE)=2.48ms; Slice thickness=5mm, Field of View (FOV) = 194×230mm, Matrix Size = 320×216. Patients from Cheeloo Hospital were scanned using an eight-channel phased-array surface coil on a 3.0T scanner system from GE (GE Signa HDX, USA), according to the protocols: TR = 1400ms; TE = 9ms; Slice thickness = 6mm, FOV = 179×230mm, Matrix Size = 320×187. Prior to the MRI, gadodiamide (0.1 mmol/kg, Omniscan, GE Healthcare) was intravenously injected using a power injector with a speed of 2.5 mL/s. Subsequently, 20 mL saline solution was injected at the same rate to clear any remaining contrast agent. The scanning range in the supine position encompassed the scalp and lower neck.

The radiomics analysis workflow comprised image segmentation, feature extraction, feature selection, model development, and model validation (Figure 1B).

2.3 Image segmentation and radiomic feature extraction

Two experienced neuroradiologists, unaware of the patient's medical details, independently delineated the tumor region of interest (ROI) using ITK-SNAP (version 3.8.0, http://www.itksnap.org) on T1 contrast-enhanced MRI sequences (T1CE). The tumor area was delineated on the slice with the maximum tumor area, excluding peritumoral edema. The peritumor region was defined as the 5 mm area surrounding the tumor. Two ROIs were finally delineated for each metastatic brain lesion: (1) the intratumoral ROI, the whole metastatic brain lesion; and (2) the peritumoral ROI, extending 5 mm around the intratumoral region.

The radiomic features were obtained from the two ROIs utilizing Pyradiomics, an open-source Python package. Before feature extraction, MRI images are preprocessed, including image normalization, resampling, discretization, and filtering. Eight filters were used including Gaussian Laplacian, logarithm, wavelet, exponent, square, square root, ladder, and local binary mode.

2.4 Radiomic features selection and signatures constructed

The feature-selection process mentioned above was executed exclusively on a training set. After standardizing all radiomic features using z-score normalization, three steps were used to identify the optimal features of each ROI for predicting the intracranial response to immunotherapy. First, the Mann–Whitney U-test was performed to determine significant factors that distinguish patients in the good and poor response groups. Only the statistically significant features were retained for further analysis. Second, to eliminate redundant radiomic features, Spearman correlation analysis was performed, and features with a strong correlation coefficient (Spearman correlation coefficient > 0.9) were excluded. Finally, least absolute shrinkage and selection operator (LASSO) logistic regression with 5-fold cross-validation using the minimum criteria were performed. For predictive purposes, the intratumoral and peritumoral radiomic signatures were constructed using support vector machine (SVM) methods, by weighting the chosen characteristics from the two ROIs with their corresponding LASSO coefficients. Finally, two predictive models were constructed: the Intratumoral Radiomic Signature (IRS) and the Peritumoral Radiomic Signature (PRS).

2.5 Nomogram development and validation

The intracranial immunotherapy response was analyzed using LASSO logistic regression with 5-fold cross-validation and minimum criteria to identify clinically significant characteristics. Significant characteristics were weighted based on their respective LASSO coefficients and used SVM methods to construct Clinical Signature (CS). Subsequently, to offer a visually quantifiable tool for predictive purposes, a personalized clinical radiomics nomogram (CRN) was developed using a multivariable logistic regression algorithm in the training set, which effectively integrated intratumoral and peritumoral radiomics and clinical signatures. The prediction models were evaluated by analyzing the receiver-operating characteristic (ROC) curve and comparing them using the DeLong test on both the training and validation sets. The model performance was evaluated by calculating the average area under the curve (AUC) along with a 95% confidence interval (CI), sensitivity (SEN), specificity (SPE), accuracy (ACC), positive predictive value (PPV), and negative predictive value (NPV). To evaluate and compare the clinical efficacy of each model, decision-curve analysis (DCA) was employed. Additionally, the nomogram was assessed using the Hosmer-Lemeshow test, which quantified the correspondence between the predicted and observed probabilities in the CRN, followed by plotting a calibration curve. In order to evaluate the predictive prognostic significance of CRN, we calculated individual CRN scores for every participant and then classified them into high-risk (high CRN) and low-risk (low CRN) categories using the median CRN score as the threshold.

2.6 Statistical analysis

Chi-squared tests were utilized to assess the clinical characteristics between the training and validation cohorts in terms of categorical variables, while independent t-tests were employed for continuous variables. The statistical analyses were performed following established academic practices, utilizing R (version 4.2.0) and Python software (version 3.6.5). Statistically significant was defined as having two-sided p-values less than 0.05. To evaluate the differences in iPFS, PFS, and OS between the high-CRN and low-CRN cohorts, we performed Kaplan-Meier survival analysis along with log-rank tests.

3 Results

3.1 Patient clinical characteristics

After the implementation of the criteria for inclusion and exclusion, 174 cases were selected and stratified into two cohorts: (1) a training cohort (n = 122) from Shandong Cancer Hospital and Institution was used to construct the optimal prediction models, and (2) a validation cohort (n = 52) from Cheeloo Hospital was utilized to evaluate model performance and goodness-of-fit.

Of all the patients enrolled (n = 174), the median age was 59.0 years (range, 32–77 years) and 72.4% were male (126/174). Approximately 40% (70/174) of the patients had a KPS score ≥ 90, and 47.7% (83/174) were current or former smokers. Eighty-six patients (49.4%) achieved a good intracranial response, including 20 iCR and 66 iPR, whereas 88 patients (50.6%) achieved a poor intracranial response, including 42 iSD and 46 iPD. A total of 153 patients (87.9%) had adenocarcinoma; 38 (21.8%) had epidermal growth factor receptor (EGFR) mutations, and 52 (23%) developed liver metastases. Of the 174 patients, 52 (29.9%) received ICIs in combination with targeting therapy. Twenty-six patients (14.9%) received planned concurrent radiation therapy. Ninety-four patients (54.0%) had solitary BMs, and 80 patients (46.7%) had a maximum BM diameter < 1 cm. A comprehensive overview of the characteristics observed in both the training and validation groups is presented in Table 1. The clinical characteristics of the two cohorts were not significantly different (all $p > 0.05$).

Clinically significant features associated with poor intracranial response were liver metastases, EGFR mutations, and a KPS score ≤ 80. Conversely, a good intracranial response was associated with adenocarcinoma histopathology, concurrent brain radiotherapy, higher neutrophil counts, older age, and clinical stage N3 disease (Supplementary Figure S1). All the significantly selected clinical features were used for the clinical signature development.

3.2 Radiomic feature selection

A total of 1745 features were derived from each ROI. After conducting three steps to determine the optimal features for predicting the intracranial immunotherapy response, we ultimately identified 14 intratumoral and 17 peritumoral features that exhibited a significant potential association with the intracranial response. An overview of the LASSO feature selection process was provided in Supplementary Figures S2A, B, S3A, B. Based on the LASSO logistic regression model, the radiomic features that had a nonzero coefficient were shown in Supplementary Figures S2C, D, S3C, D, Supplementary Table 1.

3.3 Refinement and validation of signatures by constructing a nomogram

Based on the significant features associated with intracranial immunotherapy response in terms of intratumoral, peritumoral, and clinical factors, we used SVM to construct three predictive

TABLE 1 Characteristics of patients in the training and validation cohorts.

Characteristics	Training set (n = 122)	Validation set (n = 52)	P-value
Age, years*	60.00(52.00,65.00)	57.50(52.00,64.00)	0.607
Gender			0.669
Male	90 (73.8%)	36 (69.2%)	
Female	32 (26.2%)	16 (30.8%)	
KPS			0.227
≥90	45 (36.9%)	25 (48.1%)	
≤80	77 (63.1%)	27 (51.9%)	
Smoking history			0.920
Yes	59 (48.4%)	24 (46.2%)	
No	63 (51.6%)	28 (53.8%)	
Pathology			0.693
Squamous	16 (13.1%)	5 (9.62%)	
Adenocarcinoma	106 (86.9%)	47 (90.4%)	
EGFR			0.954
Negative or unknown	96 (78.7%)	40 (76.9%)	
Positive	26 (21.3%)	12 (23.1%)	
Clinical T stage			0.897
0,1,2	71 (58.2%)	29 (55.8%)	
3,4	51 (41.8%)	23 (44.2%)	
Clinical N stage			0.640
0,1,2	64 (52.5%)	30 (57.7%)	
3	58 (47.5%)	22 (42.3%)	
Liver involvement			1.000
No	94 (77.0%)	40 (76.9%)	
Yes	28 (23.0%)	12 (23.1%)	
Number of BMs			0.892
Solitary	65 (53.3%)	29 (55.8%)	
Multiple	57 (46.7%)	23 (44.2%)	
Max diameter of BMs			0.892
<1cm	57 (46.7%)	23 (44.2%)	
≥1cm	65 (53.3%)	29 (55.8%)	
LDH, U/L*	222.50 (188.75,307.75)	218.00 (176.50,263.75)	0.135
LYM,10^9/L*	1.39(1.04,1.73)	1.29(1.06,1.78)	0.986
NEUT,10^9/L*	4.31(2.94,5.53)	3.84(2.50,5.42)	0.273
NLR*	3.20(2.06,4.75)	3.01(1.97,4.08)	0.328
Combined targeting therapy			0.728

(Continued)

TABLE 1 Continued

Characteristics	Training set (n = 122)	Validation set (n = 52)	P-value
No	87 (71.3%)	35 (67.3%)	
Yes	35 (28.7%)	17 (32.7%)	
Concurrent brain radiotherapy			0.422
No	106 (86.9%)	42 (80.8%)	
Yes	16 (13.1%)	10 (19.2%)	
Intracranial response			0.691
Good (iCR+iPR)	62 (50.8%)	24 (46.2%)	
Poor (iSD+iPD)	60 (49.2%)	28 (53.8%)	

P-value of significant difference between training and validation cohorts. Abbreviations: KPS, Karnofsky Performance Status; EGFR, Epidermal Growth Factor Receptor; T, tumor; N, Node; BMs, brain metastasis; LDH, lactate dehydrogenase; NLR, Neutrophil to lymphocyte ratio; iCR, intracranial complete response; iPR, intracranial partial response; iSD, intracranial stable disease; iPD, intracranial progress disease. Data are numbers of patients, with percentages in parentheses. *Values refer to median (interquartile range).

signatures: IRS, PRS, and CS. We observed that patients with distinct intracranial responses exhibited statistically significant differences in all three signatures within the training and validation sets, confirming their discriminative capacity. A raincloud plot was used to visually represent the varying sample distributions (Figures 2A, B). Moreover, multivariate linear regression analysis conducted on the training set revealed that IRS, PRS, and CS were independent predictors of the intracranial response (all $p < 0.001$). Consequently, we developed a predictive CRN model in the training cohort by integrating these three signatures (Figure 3A).

The CRN accurately predicted the intracranial response to immunotherapy, with AUC values of 0.888 (95% CI: 0.834–0.944) and 0.833 (95% CI: 0.720–0.946), in the training and validation sets, respectively. The IRS, PRS, and CS AUC values were 0.809 (95% CI: 0.735–0.884), 0.799 (95% CI: 0.720–0.879), and 0.743 (95% CI: 0.655–0.831), respectively, in the training set, and 0.761 (95% CI: 0.630–0.892), 0.749 (95% CI: 0.616–0.883), and 0.770 (95% CI: 0.630–0.911), respectively, in the validation set. The corresponding ROCs are shown in Figures 3B, C.

According to the DeLong test (Supplementary Table 2), CRN showed the best predictive with SPE, ACC, and PPV among the four models in the training set (SPE: 85.48%, ACC: 81.15%, PPV: 83.64%). In the validation set, CRN showed moderate predictive performance compared with the other models (SEN: 78.57%, SPE: 79.17%, ACC: 78.85%, PPV: 81.48%, NPV: 76.00%). Detailed statistical results of different models assessing the efficacy of intracranial immunotherapy are presented in Table 2. DCA showed that the CRN is a reliable and valuable tool for predicting intracranial response to immunotherapy (Figures 3D, E). Furthermore, both in the training and validation sets, a calibration curve was constructed and a Hosmer-Lemeshow test showed that the CRN aligned well with the actual observations ($p > 0.05$; Figures 3F, G).

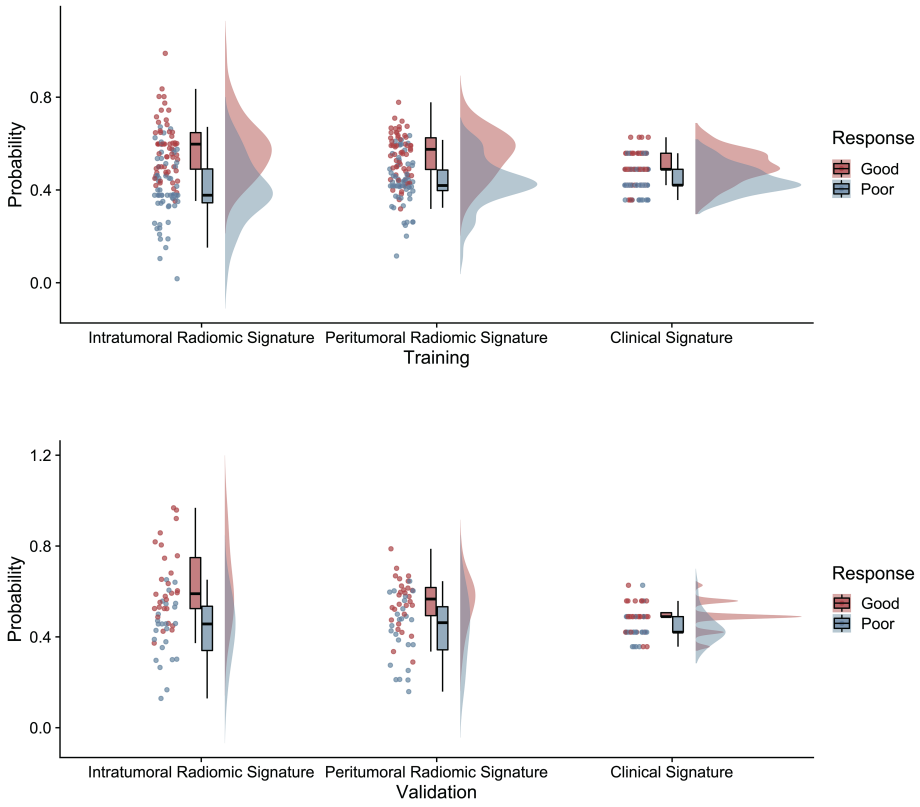

FIGURE 2
The raincloud plot visualizes the radiomics signature score, illustrating the spatial distribution and density of samples in both the training and validation sets of radiomics signatures.

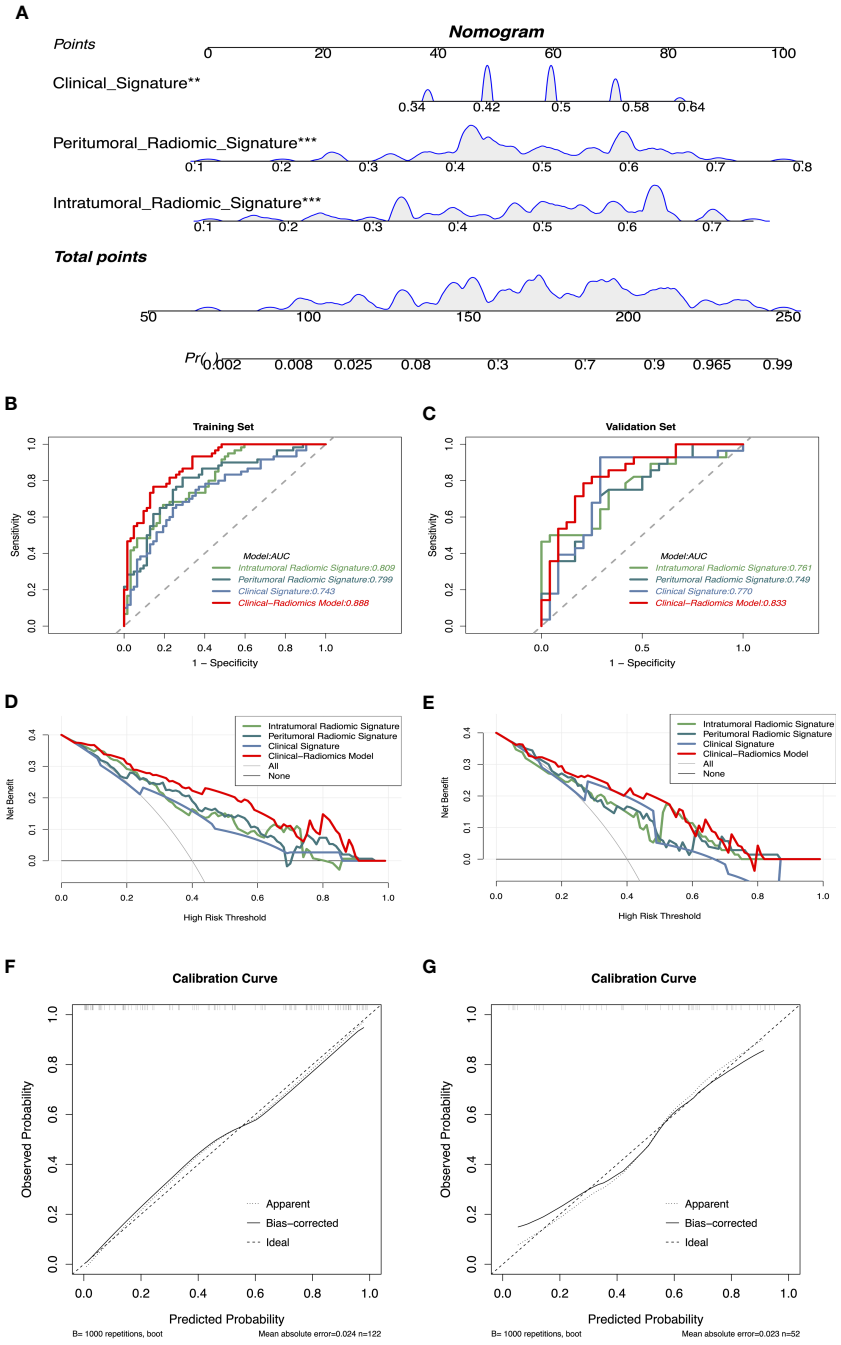

FIGURE 3
(A) CRN based on clinical and radiomics signatures, ** represents p < 0.01, *** represents p < 0.001. **(B, C)** Receiver operating characteristics curves demonstrate the accuracy in predicting the intracranial response of IRS, PRS, CS, and CRN in the training and validation sets. **(D, E)** Decision curve analysis demonstrates the clinical utility of different models for predicting the intracranial response in the training and validation sets. **(F, G)** Calibration curves of CRN for intracranial response prediction. CRN, Clinical-Radiomic nomogram; IRS, Intratumoral Radiomic Signature; PRS, Peritumoral Radiomic Signature; CS, Clinical Signature.

3.4 Outcomes

The median follow-up was 12.6 months. The median iPFS (miPFS) was 7.9 months (interquartile range [IQR]:3.7–14.0 months), the median PFS (mPFS) was 7.0 months (IQR: 3.2–13.5 months), and the median OS (mOS) was 12.6 months (IQR: 7.2–20.4 months).

The Kaplan–Meier analysis revealed that patients who had a low score based on CRN (low CRN) compared with those who had a high score (high CRN) had a higher miPFS (18.43 vs 8.63 months; $p < 0.001$; Figure 4A) and mPFS (13.37 vs 5.50 months; $p < 0.001$; Figure 4B). However, there was no significant difference in the mOS observed between the low and high CRN groups (30.73 vs. 26.60 months; $p = 0.53$; Figure 4C).

TABLE 2 Performance of models for predicting intracranial response in patients treated with ICIs.

Training set	AUC (95%CI)	SEN (%)	SPE (%)	ACC (%)	PPV (%)	NPV (%)
IRS	0.809(0.735-0.884)	66.67	80.65	73.77	76.92	71.43
PRS	0.799(0.720-0.879)	81.67	70.97	76.23	73.13	80.00
CS	0.743(0.655-0.831)	66.67	74.19	70.49	71.43	69.70
CRN	0.888(0.834-0.944)	76.67	85.48	81.15	83.64	79.10
Validation set	**AUC (95%CI)**	**SEN (%)**	**SPE (%)**	**ACC (%)**	**PPV (%)**	**NPV (%)**
IRS	0.761(0.630-0.892)	46.43	100.00	71.15	100.00	61.54
PRS	0.749(0.616-0.883)	67.86	75.00	71.15	76.00	66.67
CS	0.770(0.630-0.911)	92.86	70.83	82.69	78.79	89.47
CRN	0.833(0.720-0.946)	78.57	79.17	78.85	81.48	76.00

AUC, area under the receiver operating curve; CI, confidence interval; SEN, sensitivity; SPE: specificity; ACC, accuracy; PPV, positive predictive value; NPV, negative predictive value; IRS, intratumoral radiomic signature; PRS, peritumoral radiomic signature; CS, clinical signature; CRN, clinical-radiomics nomogram.

4 Discussion

In this study, we developed and validated a radiomic model called CRN, which utilizes T1CE images to evaluate the intracranial reaction to immunotherapy in NSCLC patients with BMs. Additionally, our model accurately detected individuals who are at an elevated risk of experiencing intracranial progression. Pretreatment radiomics could potentially forecast the intracranial reaction of NSCLC patients with BMs to early immunotherapy, offering the possibility of personalized treatment guidance for high-risk individuals.

Recently, ICIs have made noteworthy clinical advances in patients with NSCLC by overcoming immunosuppressive signals in the tumor microenvironment. However, the response of BMs to ICIs remains unclear. Data from the KEYNOTE-024, CheckMate 017, and 057 trials did not demonstrate any significant disparity in survival rates between patients with BMs who received ICI treatment and those who underwent chemotherapy (10, 20, 21). In contrast, the KEYNOTE-189 and OAK trials showed that patients with BMs treated with ICIs experienced extended OS than those who underwent chemotherapy (9, 22). In the past, the brain has been regarded as a privileged organ within the immune system because of the presence of the blood-brain barrier (BBB), which shields it from infiltration by immune cells (23). However, preclinical models have demonstrated that ICIs exert their effects by activating T cells capable of crossing the BBB (24). The potential mechanism underlying the intracranial response to ICIs may be attributed to the distinct microenvironment in BMs compared with that of primary tumors (25–27), and the prevailing immunosuppressive immune microenvironment in BMs (7, 28).

There is a requirement for the development of non-invasive biomarkers to accurately predict the intracranial response and prognosis to ICIs in patients with NSCLC. The level of PD-L1 expression is the only biomarker that has received approval for immunotherapy; however, its utility remains unclear (13, 29–33). TILs and TMB have also been explored as potential biomarkers for immunotherapy, but do not have a significant association with the intracranial response or prognosis (11–13). The inflammatory microenvironment of BMs varies considerably, with the presence of TILs ranging from complete absence to dense infiltration (34). Furthermore, the composition of TIL subtypes within this microenvironment varies, encompassing stimulated cytotoxic T cells, immune-suppressing T cells, and fatigued T cells (35). A previous study investigated TMB and T-cell richness in BMs (27).

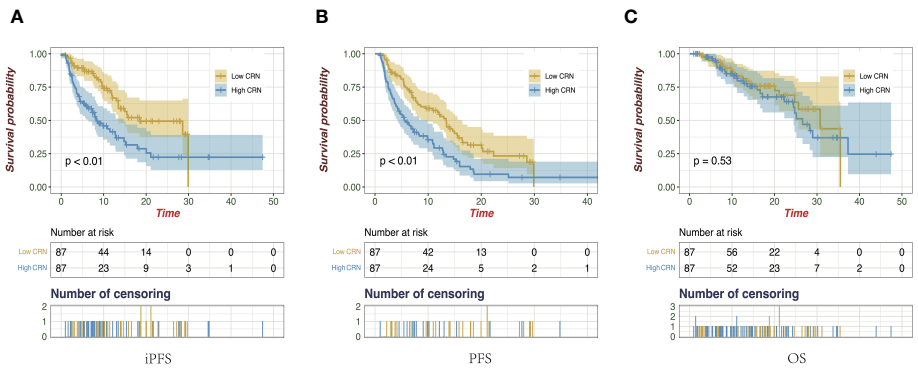

FIGURE 4
Kaplan-Meier survival curves of intracranial progression-free survival **(A)**, progression-free survival **(B)**, and overall survival **(C)** on the follow-up of all enrolled patients.

The results showed that the TMB was significantly increased in the BM samples compared to the primary NSCLC specimens. In contrast, the anticipated tumor neoantigen burden did not show any notable variation, while the richness of T-cell clones was significantly reduced in the BM samples compared to the primary samples. In summary, the search for new and robust biomarkers for predicting the intracranial response of BMs to ICIs remains challenging because of the inherent difficulty in obtaining BM biopsies and the significant heterogeneity and diversity of the immune landscape within the tumor microenvironment between BMs and the primary lesion.

Recently, several research studies have investigated the possible practicality of radiomic features extracted from images of malignant tumors and their correlation with immunotherapy response or outcome (15, 16, 36–39). Bhatia et al. (15) extracted radiomic features from MRI images and investigated the correlation between these features and OS in patients with melanoma BMs treated with ICIs. The findings indicate that radiomic features derived from MRI images are significantly correlated with patient OS, suggesting that radiomic features may serve as effective biomarkers for assessing treatment response and predicting patient prognosis. Li et al. (16) found that prognostic radiomic features from MRI were closely correlated with tumor-infiltrating macrophages and patient clinical outcomes in gliomas, which revealed a relationship between radiomic biomarkers and the tumor microenvironment. Sun et al. (40)discovered that imaging biomarkers may serve as a valuable tool for estimating the count of CD8 cells and for prognosticating the clinical responses of patients undergoing immunotherapy. However, a radiomic prediction model to evaluate the intracranial response to ICIs in patients with NSCLC BMs is still under development. In this study, the developed radiomic model could accurately predict the intracranial response and enhance clinical decision-making for ICI treatment in patients with NSCLC with BMs. Despite the observed correlation between radiomic biomarkers and patient survival, it appears that there are currently no systematic studies that thoroughly investigate the direct relationships between specific radiomic features and their biological implications further investigations are warranted to delve into the intrinsic relationship between radiomics and the BM microenvironment (41).

This study has some limitations. First, it was a retrospective study, and despite including data from two centers, the overall size of the sample was comparatively limited. To prevent fitting risks due to the small data volume, all features we selected using LASSO with 5-fold cross-validation via minimum criteria, which can reduce unnecessary model complexity and assist in variable selection when the number of samples is small size, thereby mitigating the risk of overfitting. Incorporating a subset of patient data from external institutions as an independent validation set also mitigated the risk of overfitting. Second, the analysis was limited to baseline radiomic features before treatment owing to the absence of enhanced MRI scans at a certain time point during treatment. Thirdly, the nomogram could not predict OS, because some patients had received other therapy post-immunotherapy progression which may influence the result of predicted OS. These limitations should be fully taken into account in future prospective research to build predictive models with generalizability and reliability. To validate these models, it is necessary to conduct extensive prospective research across multicenters.

5 Conclusion

In conclusion, we constructed a radiomic nomogram using MRI as a biomarker to predict the intracranial response to ICIs in patients with NSCLC with BMs. The nomogram was also predictive of iPFS and PFS. The nomogram offers personalized treatment guidance for high-risk individuals before they receive immunotherapy.

Data availability statement

The original contributions presented in the study are included in the article/Supplementary Material. Further inquiries can be directed to the corresponding author.

Ethics statement

The studies involving humans were approved by Shandong Cancer Hospital and Institution and Cheeloo Hospital Research Ethics Committee. The studies were conducted in accordance with the local legislation and institutional requirements. Written informed consent for participation was not required from the participants or the participants' legal guardians/next of kin in accordance with the national legislation and institutional requirements.

Author contributions

JX: Conceptualization, Data curation, Formal Analysis, Investigation, Methodology, Project administration, Resources, Software, Validation, Visualization, Writing – original draft, Writing – review & editing. PW: Conceptualization, Data curation, Methodology, Validation, Writing – review & editing. YL: Data curation, Writing – review & editing. XS: Data curation, Writing – review & editing. TY: Data curation, Writing – review & editing. JY: Conceptualization, Funding acquisition, Methodology, Project administration, Resources, Supervision, Writing – review & editing. FT: Conceptualization, Data curation, Formal Analysis, Funding acquisition, Investigation, Methodology, Project administration, Resources, Software, Supervision, Validation, Visualization, Writing – review & editing.

Funding

The author(s) declare financial support was received for the research, authorship, and/or publication of this article. This study

was supported by grants from the Academic Promotion Program of Shandong First Medical University (2019ZL002), the Research Unit of Radiation Oncology, Chinese Academy of Medical Sciences (2019RU071), the foundation of National Natural Science Foundation of China (81627901, 81972863 and 82030082), the foundation of Natural Science Foundation of Shandong (ZR201911040452), and the Youth Fund from Natural Science Foundation of Shandong Province (Grant number ZR2020QH244).

Conflict of interest

The authors declare that the research was conducted in the absence of any commercial or financial relationships that could be construed as a potential conflict of interest.

Publisher's note

Supplementary material

The Supplementary Material for this article can be found online at: https://www.frontiersin.org/articles/10.3389/fimmu.2024.1373330/full#supplementary-material

References

1. Siegel RL, Miller KD, Jemal A. Cancer statistics, 2020. *CA Cancer J Clin*. (2020) 70:7–30. doi: 10.3322/caac.21590

2. Grant MJ, Herbst RS, Goldberg SB. Selecting the optimal immunotherapy regimen in driver-negative metastatic NSCLC. *Nat Rev Clin Oncol*. (2021) 18:625–44. doi: 10.1038/s41571-021-00520-1

3. Wang M, Herbst RS, Boshoff C. Toward personalized treatment approaches for non-small-cell lung cancer. *Nat Med*. (2021) 27:1345–56. doi: 10.1038/s41591-021-01450-2

4. Cagney DN, Martin AM, Catalano PJ, Redig AJ, Lin NU, Lee EQ, et al. Incidence and prognosis of patients with brain metastases at diagnosis of systemic Malignancy: a population-based study. *Neuro Oncol*. (2017) 19:1511–21. doi: 10.1093/neuonc/nox077

5. Mujoomdar A, Austin JH, Malhotra R, Powell CA, Pearson GD, Shiau MC, et al. Clinical predictors of metastatic disease to the brain from non-small cell lung carcinoma: primary tumor size, cell type, and lymph node metastases. *Radiology*. (2007) 242:882–8. doi: 10.1148/radiol.2423051707

6. Barnholtz-Sloan JS, Sloan AE, Davis FG, Vigneau FD, Lai P, Sawaya RE. Incidence proportions of brain metastases in patients diagnosed (1973 to 2001) in the Metropolitan Detroit Cancer Surveillance System. *J Clin Oncol*. (2004) 22:2865–72. doi: 10.1200/JCO.2004.12.149

7. Kudo Y, Haymaker C, Zhang J, Reuben A, Duose DY, Fujimoto J, et al. Suppressed immune microenvironment and repertoire in brain metastases from patients with resected non-small-cell lung cancer. *Ann Oncol*. (2019) 30:1521–30. doi: 10.1093/annonc/mdz207

8. Ernani V, Stinchcombe TE. Management of brain metastases in non-small-cell lung cancer. *J Oncol Pract*. (2019) 15:563–70. doi: 10.1200/JOP.19.00357

9. Gandhi L, Rodríguez-Abreu D, Gadgeel S, Esteban E, Felip E, De Angelis F, et al. Pembrolizumab plus chemotherapy in metastatic non-small-cell lung cancer. *N Engl J Med*. (2018) 378:2078–92. doi: 10.1056/NEJMoa1801005

10. Reck M, Rodríguez-Abreu D, Robinson AG, Hui R, Csőszi T, Fülöp A, et al. Pembrolizumab versus chemotherapy for PD-L1-positive non-small-cell lung cancer. *N Engl J Med*. (2016) 375:1823–33. doi: 10.1056/NEJMoa1606774

11. Goldberg SB, Schalper KA, Gettinger SN, Mahajan A, Herbst RS, Chiang AC, et al. Pembrolizumab for management of patients with NSCLC and brain metastases: long-term results and biomarker analysis from a non-randomised, open-label, phase 2 trial. *Lancet Oncol*. (2020) 21:655–63. doi: 10.1016/S1470-2045(20)30111-X

12. Carbone DP, Reck M, Paz-Ares L, Creelan B, Horn L, Steins M, et al. First-line nivolumab in stage IV or recurrent non-small-cell lung cancer. *N Engl J Med*. (2017) 376:2415–26. doi: 10.1056/NEJMoa1613493

13. El Rassy E, Botticella A, Kattan J, Le Péchoux C, Besse B, Hendriks L. Non-small cell lung cancer brain metastases and the immune system: From brain metastases development to treatment. *Cancer Treat Rev*. (2018) 68:69–79. doi: 10.1016/j.ctrv.2018.05.015

14. Trebeschi S, Drago SG, Birkbak NJ, Kurilova I, Călin AM, Delli Pizzi A, et al. Predicting response to cancer immunotherapy using noninvasive radiomic biomarkers. *Ann Oncol*. (2019) 30:998–1004. doi: 10.1093/annonc/mdz108

15. Bhatia A, Birger M, Veeraraghavan H, Um H, Tixier F, McKenney AS, et al. MRI radiomic features are associated with survival in melanoma brain metastases treated with immune checkpoint inhibitors. *Neuro Oncol*. (2019) 21:1578–86. doi: 10.1093/neuonc/noz141

16. Li G, Li L, Li Y, Qian Z, Wu F, He Y, et al. An MRI radiomics approach to predict survival and tumour-infiltrating macrophages in gliomas. *Brain*. (2022) 145:1151–61. doi: 10.1093/brain/awab340

17. Zheng X, Yao Z, Huang Y, Yu Y, Wang Y, Liu Y, et al. Deep learning radiomics can predict axillary lymph node status in early-stage breast cancer. *Nat Commun*. (2020) 11:1236. doi: 10.1038/s41467-020-15027-z

18. Liu D, Chen J, Ge H, Hu X, Yang K, Liu Y, et al. Differentiation of Malignant brain tumor types using intratumoral and peritumoral radiomic features. *Front Oncol*. (2022) 12:848846. doi: 10.3389/fonc.2022.848846

19. Lin NU, Lee EQ, Aoyama H, Barani IJ, Barboriak DP, Baumert BG, et al. Response assessment criteria for brain metastases: proposal from the RANO group. *Lancet Oncol*. (2015) 16:e270–e8. doi: 10.1016/S1470-2045(15)70057-4

20. Borghaei H, Paz-Ares L, Horn L, Spigel DR, Steins M, Ready NE, et al. Nivolumab versus docetaxel in advanced nonsquamous non-small-cell lung cancer. *N Engl J Med*. (2015) 373:1627–39. doi: 10.1056/NEJMoa1507643

21. Brahmer J, Reckamp KL, Baas P, Crinò L, Eberhardt WE, Poddubskaya E, et al. Nivolumab versus docetaxel in advanced squamous-cell non-small-cell lung cancer. *N Engl J Med*. (2015) 373:123–35. doi: 10.1056/NEJMoa1504627

22. Fehrenbacher L, von Pawel J, Park K, Rittmeyer A, Gandara DR, Ponce Aix S, et al. Updated efficacy analysis including secondary population results for OAK: A randomized phase III study of atezolizumab versus docetaxel in patients with previously treated advanced non-small cell lung cancer. *J Thorac Oncol*. (2018) 13:1156–70. doi: 10.1016/j.jtho.2018.04.039

23. Louveau A, Smirnov I, Keyes TJ, Eccles JD, Rouhani SJ, Peske JD, et al. Structural and functional features of central nervous system lymphatic vessels. *Nature*. (2015) 523:337–41. doi: 10.1038/nature14432

24. Pardoll DM. The blockade of immune checkpoints in cancer immunotherapy. *Nat Rev Cancer*. (2012) 12:252–64. doi: 10.1038/nrc3239

25. Cacho-Díaz B, García-Botello DR, Wegman-Ostrosky T, Reyes-Soto G, Ortiz-Sánchez E, Herrera-Montalvo LA. Tumor microenvironment differences between primary tumor and brain metastases. *J Transl Med*. (2020) 18:1. doi: 10.1186/s12967-019-02189-8

26. Achrol AS, Rennert RC, Anders C, Soffietti R, Ahluwalia MS, Nayak L, et al. Brain metastases. *Nat Rev Dis Primers*. (2019) 5:5. doi: 10.1038/s41572-018-0055-y

27. Mansfield AS, Ren H, Sutor S, Sarangi V, Nair A, Davila J, et al. Contraction of T cell richness in lung cancer brain metastases. *Sci Rep*. (2018) 8:2171. doi: 10.1038/s41598-018-20622-8

28. Forrester JV, McMenamin PG, Dando SJ. CNS infection and immune privilege. *Nat Rev Neurosci*. (2018) 19:655–71. doi: 10.1038/s41583-018-0070-8

29. Teixido C, Vilarino N, Reyes R, Reguart N. PD-L1 expression testing in non-small cell lung cancer. *Ther Adv Med Oncol*. (2018) 10:1758835918763493. doi: 10.1177/1758835918763493

30. Schoenfeld AJ, Rizvi H, Bandlamudi C, Sauter JL, Travis WD, Rekhtman N, et al. Clinical and molecular correlates of PD-L1 expression in patients with lung adenocarcinomas. *Ann Oncol*. (2020) 31:599–608. doi: 10.1016/j.annonc.2020.01.065

31. Riethdorf S, O'Flaherty L, Hille C, Pantel K. Clinical applications of the CellSearch platform in cancer patients. *Adv Drug Delivery Rev*. (2018) 125:102–21. doi: 10.1016/j.addr.2018.01.011

32. Fumet JD, Truntzer C, Yarchoan M, Ghiringhelli F. Tumour mutational burden as a biomarker for immunotherapy: Current data and emerging concepts. *Eur J Cancer*. (2020) 131:40–50. doi: 10.1016/j.ejca.2020.02.038

33. Reuben A, Gittelman R, Gao J, Zhang J, Yusko EC, Wu CJ, et al. TCR repertoire intratumor heterogeneity in localized lung adenocarcinomas: an association with predicted neoantigen heterogeneity and postsurgical recurrence. *Cancer Discovery*. (2017) 7:1088–97. doi: 10.1158/2159-8290.CD-17-0256

34. Berghoff AS, Fuchs E, Ricken G, Mlecnik B, Bindea G, Spanberger T, et al. Density of tumor-infiltrating lymphocytes correlates with extent of brain edema and overall survival time in patients with brain metastases. *Oncoimmunology*. (2016) 5:e1057388. doi: 10.1080/2162402X.2015.1057388

35. Berghoff AS, Lassmann H, Preusser M, Höftberger R. Characterization of the inflammatory response to solid cancer metastases in the human brain. *Clin Exp Metastasis*. (2013) 30:69–81. doi: 10.1007/s10585-012-9510-4

36. Mu W, Tunali I, Gray JE, Qi J, Schabath MB, Gillies RJ. Radiomics of (18)F-FDG PET/CT images predicts clinical benefit of advanced NSCLC patients to checkpoint blockade immunotherapy. *Eur J Nucl Med Mol Imaging*. (2020) 47:1168–82. doi: 10.1007/s00259-019-04625-9

37. Khorrami M, Prasanna P, Gupta A, Patil P, Velu PD, Thawani R, et al. Changes in CT radiomic features associated with lymphocyte distribution predict overall survival and response to immunotherapy in non-small cell lung cancer. *Cancer Immunol Res*. (2020) 8:108–19. doi: 10.1158/2326-6066.CIR-19-0476

38. Ladwa R, Roberts KE, O'Leary C, Maggacis N, O'Byrne KJ, Miles K. Computed tomography texture analysis of response to second-line nivolumab in metastatic non-small cell lung cancer. *Lung Cancer Manag*. (2020) 9:Lmt38. doi: 10.2217/lmt-2020-0002

39. Liu C, Gong J, Yu H, Liu Q, Wang S, Wang J. A CT-based radiomics approach to predict nivolumab response in advanced non-small-cell lung cancer. *Front Oncol*. (2021) 11:544339. doi: 10.3389/fonc.2021.544339

40. Sun R, Limkin EJ, Vakalopoulou M, Dercle L, Champiat S, Han SR, et al. A radiomics approach to assess tumour-infiltrating CD8 cells and response to anti-PD-1 or anti-PD-L1 immunotherapy: an imaging biomarker, retrospective multicohort study. *Lancet Oncol*. (2018) 19:1180–91. doi: 10.1016/S1470-2045(18)30413-3

41. Bera K, Braman N, Gupta A, Velcheti V, Madabhushi A. Predicting cancer outcomes with radiomics and artificial intelligence in radiology. *Nat Rev Clin Oncol*. (2022) 19:132–46. doi: 10.1038/s41571-021-00560-7

frontiers | Frontiers in Oncology

TYPE Original Research
PUBLISHED 22 May 2024
DOI 10.3389/fonc.2024.1400792

OPEN ACCESS

EDITED BY
Lin Zhou,
Sichuan University, China

REVIEWED BY
Guoqing Zhang,
First Affiliated Hospital of Zhengzhou University, China
Alessia Pellerino,
University Hospital of the City of Health and Science of Turin, Italy

*CORRESPONDENCE
Yingqiu Song
syq18900917411@163.com
Tianlu Wang
wangtianlu@cancerhosp-ln-cmu.com

†These authors have contributed equally to this work

RECEIVED 14 March 2024
ACCEPTED 03 May 2024
PUBLISHED 22 May 2024

CITATION
Li J, Zhang X, Wang Y, Jin Y, Song Y and Wang T (2024) Clinicopathological characteristics and prognosis of synchronous brain metastases from non-small cell lung cancer compared with metachronous brain metastases.
Front. Oncol. 14:1400792.
doi: 10.3389/fonc.2024.1400792

Clinicopathological characteristics and prognosis of synchronous brain metastases from non-small cell lung cancer compared with metachronous brain metastases

Jing Li[1,2†], Xiaofang Zhang[2,3†], Ye Wang[1,2], Yi Jin[4], Yingqiu Song[5*] and Tianlu Wang[2,5,6,7*]

[1]School of Graduate, Dalian Medical University, Dalian, Liaoning, China, [2]Department of Radiotherapy, Cancer Hospital of China Medical University, Liaoning Cancer Hospital and Institute, Shenyang, Liaoning, China, [3]School of Graduate, China Medical University, Shengyang, Liaoning, China, [4]Department of Breast Surgery, Liaoning Cancer Hospital and Institute, Shenyang, Liaoning, China, [5]Department of Radiotherapy, Cancer Hospital of China Medical University, Shenyang, Liaoning, China, [6]Department of Radiotherapy, Cancer Hospital of Dalian University of Technology, Shenyang, Liaoning, China, [7]Faculty of Medicine, Dalian University of Technology, Shenyang, Liaoning, China

Purpose: Brain metastasis (BM) from non-small cell lung cancer (NSCLC) is a serious complication severely affecting patients' prognoses. We aimed to compare the clinicopathological features and prognosis of synchronous and metachronous BM from NSCLC.

Methods: Clinical data of 461 patients with brain metastases from NSCLC who visited the Cancer Hospital of China Medical University from 2005 to 2017 were retrospectively collected. We analyzed the pathophysiological characteristics of synchronous and metachronous BM from NSCLC and survival rates of the patients. Propensity score matching analysis was used to reduce bias between groups. In addition, we used the Kaplan-Meier method for survival analysis, log-rank test to compare survival rates, and Cox proportional hazards regression model for multivariate prognosis analysis.

Results: Among 461 patients with BM, the number of people who met the inclusion criteria was 400 cases, and after 1:2 propensity score matching,130 had synchronous BM and 260 had metachronous BM. The survival time was longer for metachronous BM in driver mutation-negative patients with squamous cell carcinoma than synchronous BM. Conversely, metachronous and synchronous BM with gene mutations and adenocarcinoma showed no differences in survival time. Multivariate analysis showed that metachronous BM was an independent prognostic factor for overall survival. Furthermore, the pathological type squamous cell carcinoma and Karnofsky Performance Status score <80 were independent risk factors affecting overall survival.

Conclusion: BM status is an independent factor influencing patient outcome. Moreover, synchronous and metachronous BM from NSCLC differ in gene mutation profile, pathological type, and disease progression and hence require different treatments.

KEYWORDS

lung cancer, synchronous, metachronous, brain metastasis, prognosis

Introduction

Over the last several decades, lung cancer has become one of the world's most common cancers and a major cause of death (1–3), with non-small cell lung cancer (NSCLC), representing over 80% of cases (1, 3, 4). The most common histologic subtypes of NSCLC are lung adenocarcinoma (LUAD), squamous cell carcinoma (LUSC), and large cell carcinoma (4). Central nervous system (CNS) metastasis is a common complication of NSCLC. Data from the National Cancer Institute show that the risk of CNS metastasis in patients with LUAD, LUSC, and large cell carcinoma is 11%, 6%, and 12%, respectively (5, 6).

The most common CNS metastasis in NSCLC is brain metastasis (BM). The occurrence of BM leads to a poor prognosis and severely impacts patients' quality of life and survival rates (6–8). The survival time of patients with NSCLC diagnosed with BM is significantly short, with an average of only 1–3 months if left untreated (6). However, in recent years, the development of different therapies, such as surgery, radiation therapy, medical interventions, and, particularly, targeted therapy, have led to better outcomes in patients with NSCLC-associated BM, improving their quality of life and prolonging their survival time.

EGFR-tyrosine kinase inhibitors (TKIs), one of the most recently introduced therapies, have demonstrated significant improvements in survival in *EGFR*-mutated advanced NSCLC (9–12), becoming the therapeutic choice for patients with advanced NSCLC and *EGFR*-sensitive mutations.

Unfortunately, due to the blood-brain barrier (BBB), most of the available drugs cannot effectively enter brain tissue, resulting in poor therapeutic efficacy. As a consequence, the 5-year survival rate of patients with BM remains low (13). BM is classified according to the time elapsed between its occurrence and lung cancer diagnosis. However, in various literatures, the criteria for distinguishing the timing of synchronous and metachronous brain metastases vary. In this paper, we consider that synchronous BM is detected within 2 months after the diagnosis of NSCLC, while metachronous BM is detected after 2 months following the NSCLC diagnosis (14, 15). The incidence rate of NSCLC-related BM is 10% (5, 16, 17) and increases with disease progression, reaching up to 40–50% in cases of advanced disease.

The factors influencing prognosis and treatment choices for NSCLC-associated BM remain unclear. In this study, we performed a retrospective analysis involving 400 patients with NSCLC, comparing the pathophysiological characteristics and survival rates between those with metachronous BM and those with synchronous BM. We aimed to determine the factors affecting NSCLC-related BM progression and explore whether patients can benefit from personalized treatment plans according to the time of BM onset.

Materials and methods

Study population

We collected data from a unicentral retrospective cohort of 461 patients with NSCLC-associated BM, who visited the Cancer Hospital of China Medical University between January 2005 and December 2017. The inclusion criteria encompassed (1) age ≥18 years; (2) a confirmed pathological diagnosis of NSCLC through tracheoscopy, lung puncture biopsy, metastasis biopsy, or surgical biopsy; (3) a pathological diagnosis of LUSC or LUAD; (4) NSCLC-induced BM confirmed by imaging and/or pathology, such as head-enhanced magnetic resonance imaging (MRI); (5) access to complete clinical data and follow-up information; (6) the absence of other malignancies. All enrolled patients who did not have an endpoint event (death) were followed up through outpatient visits, inpatient care, or telephone follow-up for at least 1 year.

Data collection

Various pathological variables in patients at the time of their BM diagnosis were documented, including age (< 65 vs. ≥ 65), gender (male vs. female), pathological type (LUSC vs. LUAD), general health status score assessed by the Karnofsky Performance Status (KPS < 80 vs. ≥ 80), synchronous BM occurrence (yes/no), number of intracranial metastases (single vs. multiple), number of extracranial organs affected (1–2 vs. > 2), radiotherapy (yes/no), surgery (yes/no), chemotherapy (yes/no), EGFR gene mutation(yes/no), and

PET-CT (yes/no). Overall survival is defined as the date from the date of BM diagnosis to the date of patient death or last follow-up visit.

Statistical methods

IBM SPSS 26.0 software was used to create patient groups with synchronous versus metachronous BM originating from lung cancer through a 1:2 propensity score matching (PSM) approach. This was done to reduce selection bias and account for potential confounding variables. Univariate and multivariate Cox proportional hazards regression analyses, for both the raw and the propensity score-matched dataset, were used to assess survival risk factors. Variables with p-values < 0.1 in the univariate analysis were included in the multivariate analysis. Results were expressed as hazard ratio (HR) and 95% confidence interval (CI). Additionally, a univariate Cox proportional risk regression analysis was used to assess the effect of gene mutation and pathological type on survival stratification in patients with synchronous versus metachronous BM. Kaplan–Meier analysis and a two-sided log-rank test were used to assess the effect of the type of lung cancer and the presence of driver mutations on survival outcomes. A chi-square test was performed using R 4.2.1 to analyze the baseline characteristics before and after PSM. A Cox proportional risk regression model was used for assessing prognostic correlations, survival curve plotting, and survival data analysis. All hypothesis tests were two-sided, and results were considered significant when p-values were less than 0.05.

Result

Patient characteristics

A total of 461 patients who were initially diagnosed with BM from NSCLC and admitted to the Cancer Hospital of China Medical University from March 2005 to December 2017 were included in this study. The selection process resulted in the exclusion of 61 patients for the following reasons: 19 patients due to an unclear diagnosis of pathological types, 11 patients with pathological types other than lung adenocarcinoma and squamous lung cancer, 23 patients due to missed visits, and 8 patients with incomplete clinical information. Ultimately, 400 patients were included in this study. Among them, 130 patients had synchronous BM and 270 patients had metachronous BM. On this basis, a 1:2 PSM was performed, resulting in 130 patients with synchronous metastases and 260 patients with metachronous metastases, achieving a balanced distribution between the groups (Figure 1).

Clinical features of the 400 patients are presented in Table 1. There was no significant stats discrepancy between the two groups of patients with synchronous versus metachronous brain metastases from lung cancer before PSM in terms of age at diagnosis of brain metastases [years], gender, KPS score, type of pathology, number of metastases, number of affected extracranial organs, brain surgery, brain radiotherapy, EGFR genetic mutations, and PET-CT (p > 0.05). There were between-group differences in whether chemotherapy was administered (p < 0.05), and further equalization of baseline characteristics was required. the distribution of baseline characteristics was well balanced between the two groups of patients with synchronous and metachronous brain metastases after PSM, and no statistically significant difference was observed between the two groups (p > 0.05).

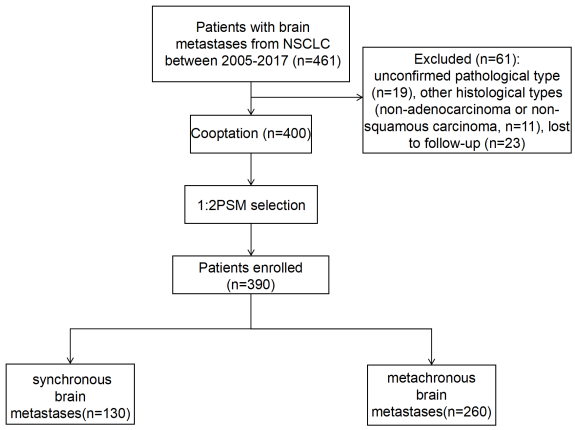

FIGURE 1
The flow chart for the selection of the study population. NSCLC, non-small cell lung cancer.

Impact of metachronous brain metastasis on overall survival rate

Univariate analyses were used to analyze the influence of different covariates on OS. In the univariate analysis conducted before PSM, synchronous BM (HR: 1.242 [95% CI: 1.003–1.539], p = 0.047), squamous carcinoma (HR: 1.522 [95% CI: 1.145–2.024], p = 0.004), and KPS score < 80 (HR: 1.264 [95% CI: 1.024–1.558, p = 0.029) were identified as risk factors affecting OS of BM in patients with NSCLC. On the other hand, female sex (HR: 0.725 [95% CI: 0.592– 0.889], p = 0.002) and EGFR gene positivity (HR: 0.656 [95% CI: 0.513–0.839], p < 0.001) were identified as significant protective factors associated with longer OS. Multifactor analysis was performed for elements with p-values less than 0.1 in the univariate analysis (Table 2), depicting synchronous BM (HR: 1.335 [95% CI: 1.076–1.657], p = 0.009), pathological type of squamous carcinoma (HR: 1.361 [95% CI: 1.018–1.820], p = 0.037), KPS score < 80 (HR: 1.392 [95% CI: 1.124–1.724], p = 0.002) as risk factors affecting OS of BM in patients with NSCLC.

The univariate and multivariate analysis results for 390 patients with NSCLC-associated BM after PSM were generally consistent with those before PSM. In the univariate analysis following PSM: a male sex, a pathological type of squamous carcinoma, KPS score < 80, and EGFR gene negativity were identified as risk factors for OS in patients with NSCLC exhibiting BM. On the other hand, metachronous BM (HR: 0.771 [95% CI: 0.622–0.957], p = 0.018) emerged as a protective factor for OS. The multifactor analysis was performed on factors with p-values less than 0.1 in the results after

TABLE 1 Baseline characteristics of patients with synchronous versus metachronous brain metastases before and after PSM.

Characteristic	Before PSM			After PSM		
	synchronous brain n=130	metachronous brain n=270	*p*	Synchronous brain n=130	metachronous brain n=260	*p*
Age						
<65	74 (18.5%)	157 (39.2%)	0.816	74 (19%)	150(38.5%)	0.885
>=65	56 (14%)	113 (28.2%)		56 (14.4%)	110 (28.2%)	
Gender						
Female	64 (16%)	132 (33%)	0.949	64 (16.4%)	127 (32.6%)	0.934
Male	66 (16.5%)	138 (34.5%)		66 (16.9%)	133 (34.1%)	
Pathological type						
Squamous carcinoma	19 (4.8%)	38 (9.5%)	0.885	19 (4.9%)	37 (9.5%)	0.919
Adenocarcinoma	111 (27.8%)	232 (58%)		111 (28.5%)	223 (57.2%)	
KPS						
<80	83 (20.8%)	171 (42.8%)	0.921	83 (21.3%)	166 (42.6%)	1.000
>=80	47 (11.8%)	99 (24.8%)		47 (12.1%)	94 (24.1%)	
No. of intracranial metastases						
Single shot	83 (20.8%)	175 (43.8%)	0.850	83 (21.3%)	168 (43.1%)	0.881
Multi-incidence	47 (11.8%)	95 (23.8%)		47 (12.1%)	92 (23.6%)	
Number of affected extra-cranial organs						
1-2	115 (28.7%)	223 (55.8%)	0.129	115 (29.5%)	214 (54.9%)	0.115
>2	15 (3.8%)	47 (11.8%)		15 (3.8%)	46 (11.8%)	
radiotherapy						
No	42 (10.5%)	65 (16.2%)	0.081	42 (10.8%)	62 (15.9%)	0.075
Yes	88 (22%)	205 (51.2%)		88 (22.6%)	198 (50.8%)	
Surgery						
NO	123 (30.8%)	256 (64%)	0.933	123 (31.5%)	247 (63.3%)	0.871
YES	7 (1.8%)	14 (3.5%)		7 (1.8%)	13 (3.3%)	
Chemotherapy						
NO	49 (12.2%)	132 (33%)	0.035	49 (12.6%)	124 (31.8%)	0.061
YES	81 (20.2%)	138 (34.5%)		81 (20.8%)	136 (34.9%)	
Genetic mutations						
NO	99 (24.8%)	210 (52.5%)	0.717	99 (19%)	202 (51.8%)	0.733
YES	31 (7.8%)	60 (15%)		31 (7.9%)	58 (14.9%)	
PET-CT						
NO	109 (27.3%)	238 (59.5%)	0.235	109 (27.9%)	229 (58.7%)	0.247
YES	21 (5.2%)	32 (8%)		21 (5.4%)	31 (7.9%)	

A total of 89 cases were positive for gene mutations after PSM. PSM, propensity score matching

univariate analysis (Table 3), identified metachronous BM (HR: 0.715 [95% CI: 0.575–0.889], $p = 0.002$) as an independent protective factor for OS; whereas the pathological type of squamous carcinoma and KPS score < 80 were identified as independent risk factors for OS in NSCLC-associated BM. Moreover, subgroup analyses according to patients' clinical characteristics confirmed that metachronous BM was associated with a significantly longer OS in all subgroups (Figure 2).

TABLE 2 Univariate and Multivariate analysis of the effect of NSCLC brain metastasis on OS (before PSM).

Characteristics	Total(N)	Univariate analysis		Multivariate analysis	
		Hazard ratio (95% CI)	*P* value	Hazard ratio (95% CI)	*P* value
Age of diagnosis of brain metastases	400		0.291		
<65	231	Reference			
≥65	169	1.116 (0.911 - 1.366)	0.289		
Gender	400		**0.002**		
Male	204	Reference		Reference	
Female	196	0.725 (0.592 - 0.889)	**0.002**	0.825 (0.666 - 1.023)	0.079
Brain metastases status	400		0.050		
metachronous	270	Reference		Reference	
synchronous	130	1.242 (1.003 - 1.539)	**0.047**	1.335 (1.076 - 1.657)	**0.009**
Pathological type	400		**0.006**		
Adenocarcinoma	343	Reference		Reference	
squamous carcinoma	57	1.522 (1.145 - 2.024)	**0.004**	1.361 (1.018 - 1.820)	**0.037**
KPS	400		**0.027**		
≥80	146	Reference		Reference	
<80	254	1.264 (1.024 - 1.558)	**0.029**	1.392 (1.124 - 1.724)	**0.002**
No. of intracranial metastases	400		0.782		
Multiple	142	Reference			
Single	258	1.030 (0.835 - 1.270)	0.783		
Number of affected extra-cranial organs	400		0.573		
1-2	338	Reference			
>2	62	1.084 (0.822 - 1.428)	0.569		
radiotherapy	400		0.807		
YES	293	Reference			
NO	107	0.972 (0.773 - 1.222)	0.807		
Surgery	400		0.332		
YES	21	Reference			
NO	379	1.244 (0.788 - 1.964)	0.348		
Chemotherapy	400		0.336		
NO	181	Reference			
YES	219	0.905 (0.740 - 1.108)	0.335		
Genetic mutations	400		**<0.001**		
NO	309	Reference		Reference	

(Continued)

TABLE 2 Continued

Characteristics	Total(N)	Univariate analysis		Multivariate analysis	
		Hazard ratio (95% CI)	*P* value	Hazard ratio (95% CI)	*P* value
YES	91	0.656 (0.513 - 0.839)	**<0.001**	0.914 (0.697 - 1.198)	0.514
PET-CT	400		0.093		
NO	347	Reference			
YES	53	0.779 (0.576 - 1.052)	0.103		

PSM, propensity score matching; NSCLC, non-small cell lung cancer; OS, overall survival.
Bold values means results were considered significant when p-values were less than 0.05.

The Kaplan–Meier curves of OS in patients with BM from lung cancer according to the results of multivariate analysis conducted before and after PSM, under each independent factor, showed that metachronous BM is associated with a significantly longer OS (Figure 3).

Pathology type and EGFR genes of synchronous and metachronous BM

To further evaluate the prognostic impact of synchronous versus metachronous BM on patients with NSCLC, we analyzed

TABLE 3 Univariate and Multivariate analysis of the effect of NSCLC brain metastasis on OS (after PSM).

Characteristics	Total(N)	Univariate analysis		Multivariate analysis	
		Hazard ratio (95% CI)	*P* value	Hazard (95% CI)	*P* value
Age of diagnosis of brain metastases	390		0.232		
<65	224	Reference			
≥65	166	1.134 (0.923 - 1.392)	0.231		
Gender	390		**0.002**		
Female	191	Reference		Reference	
Male	199	1.392 (1.133 - 1.711)	**0.002**	1.221 (0.983 -1.518)	0.072
brain metastases status	390		**0.020**		
synchronous	130	Reference		Reference	
metachronous	260	0.771 (0.622 - 0.957)	**0.018**	0.715 (0.575- 0.889)	**0.002**
Pathological type	390		**0.004**		
Adenocarcinoma	334	Reference		Reference	
squamous carcinoma	56	1.552 (1.164 - 2.069)	**0.003**	1.397 (1.041 -1.873)	**0.026**
KPS	390		**0.017**		
≥80	141	Reference		Reference	
<80	249	1.292 (1.044 - 1.598)	**0.019**	1.430 (1.151 -1.777)	**0.001**
No. of intracranial metastases	390		0.828		
Multiple	139	Reference			

(Continued)

TABLE 3 Continued

Characteristics	Total(N)	Univariate analysis		Multivariate analysis	
		Hazard ratio (95% CI)	*P* value	Hazard (95% CI)	*P* value
Single	251	1.024 (0.828 - 1.265)	0.828		
Number of extracranial organs affected	390		0.510		
1-2	329	Reference			
>2	61	1.099 (0.832 - 1.453)	0.505		
radiotherapy	390		0.769		
YES	286	Reference			
NO	104	0.966 (0.765 - 1.219)	0.770		
surgery	390		0.278		
NO	370	Reference			
YES	20	0.779 (0.488 - 1.244)	0.296		
Chemotherapy	390		0.543		
YES	217	Reference			
NO	173	1.066 (0.868 - 1.309)	0.542		
Genetic mutations	390		**<0.001**		
YES	89	Reference		Reference	
NO	301	1.532 (1.194 - 1.966)	**<0.001**	1.094 (0.831 - 1.441)	0.520
PET-CT	390		0.098		
YES	52	Reference			
NO	338	1.283 (0.947 - 1.739)	0.108		

PSM, propensity score matching; NSCLC, non-small cell lung cancer.
Bold values means results were considered significant when p-values were less than 0.05.

the relationship between the presence or absence of synchronous BM and the pathological type and EGFR driver genes. The impact on OS in patients with synchronous and metachronous BM showed no significant difference when considering the pathological type of adenocarcinoma (p = 0.075). However, patients with metachronous BM of squamous carcinoma had longer OS than those with synchronous BM (p = 0.01) (Table 4 and Figure 4A). In terms of EGFR genes, there was no difference in the effect of synchronous BM with positive EGFR genes versus metachronous BM on OS (p = 0.270). However, metachronous BM with negative EGFR genes had longer OS compared to those with synchronous BM (p = 0.044) (Table 4 and Figure 4B).

Distribution characteristics of patients with BM

The distribution characteristics of patients with BM are illustrated in Sankey plots. These plots visualize the relationship between BM status, pathological type, and EGFR gene mutation. The analysis indicates that the pathological type of synchronous BM and metachronous BM is mostly LUSC and most of the LUSC do not exhibit gene mutations (Figure 5).

Patients with adenocarcinoma with positive EGFR had longer OS at 1,2, and 3 years

According to the results of univariate analysis and multivariate analysis using the COX proportional hazards regression model, we incorporated pathological types and EGFR genes into the model. Subsequently, Nomogram plots of the 1-year, 2-year, and 3-year survival probabilities of lung cancer with BM were generated (Figure 6). The Nomogram plots enable the assignment of scores for each variable by drawing an upward vertical line along the score axis for each assigned variable. These scores are then accumulated to determine the prognostic score for each variable. According to the prognosis score of each patient, a vertical line along the

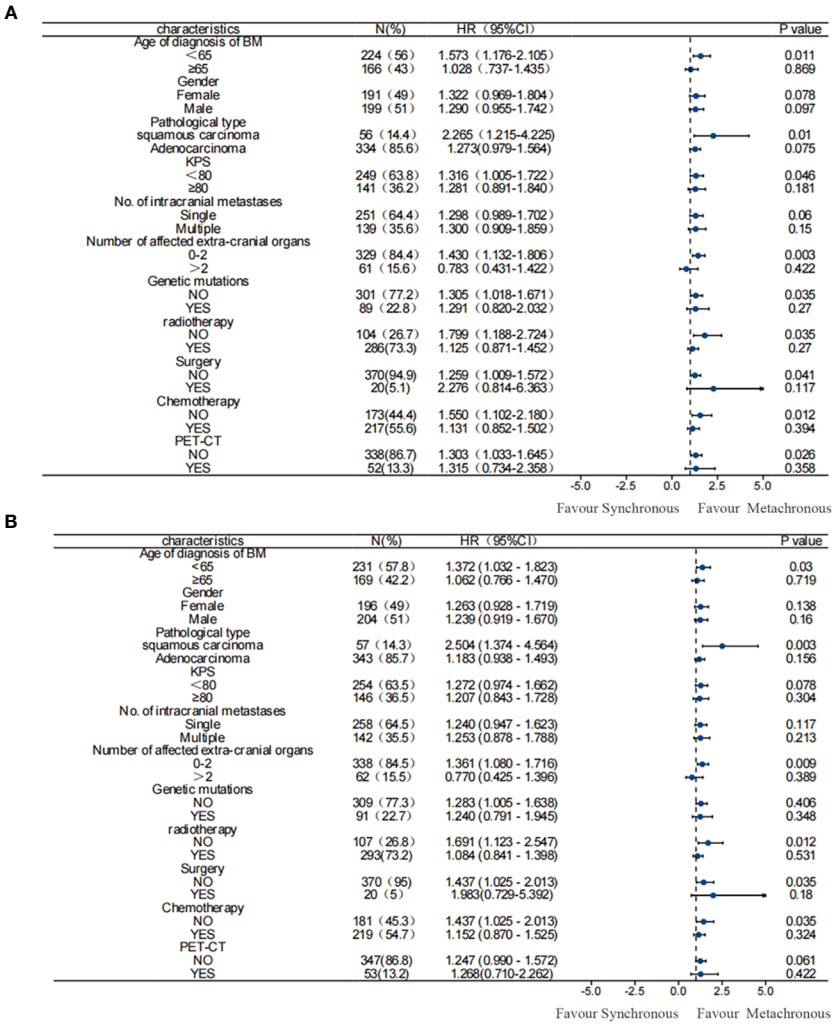

FIGURE 2
Subgroup analysis of OS among patients. **(A)** before PSM; **(B)** after PSM. Results before and after PSM suggested that metachronous BM was associated with significantly longer OS. PSM, propensity score matching; OS, overall survival.

probability axis is drawn downward, to obtain the corresponding 1-year, 2-year, and 3-year survival probability values.

The calibration of the nomogram was assessed through calibration plots. Nomogram predicted and actual 1-year, 2-year, and 3-year OS rates were plotted and compared to further validate the predictive performance of the nomogram (Figure 6).

The discriminative ability of the nomogram to predict 1-year, 2-year, and 3-year OS was assessed using the area under the curve (AUC) of the receiver operating characteristic curve (ROC). The C indices of 1-year, 2-year, and 3-year predicted survival were 0.660, 0.631, and 0.685, respectively. The AUC was between 0.5 and 1.0, indicating a decent level of discriminative ability for the nomogram, with 0.5 representing a random outcome (Figure 6).

Discussion

The fundamental reason for the difference in treatment between synchronous and metachronous BM in NSCLC is the timing of BM. Synchronous BM refers to the detection of BM within 2 months after diagnosis of NSCLC.At this time, targeted BM treatment should be carried out in addition to systemic treatment. Metachronous BM refers to BM detected 2 months after diagnosis of NSCLC.Active treatment should be given to the primary focus of the lung cancer first, and once BM occurs, treatment should be directed towards it.

Some previous studies have also shown that the prognosis of patients with synchronous BM is worse than that of patients with metachronous BM (18, 19). In other studies, there was no difference in median OS between patients with synchronous metastases and those with metachronous metastases. Nevertheless, the main limitation of these studies was the small number of patients included and unconvincing conclusions (20, 21). In addition, patients were treated mainly with radiotherapy and chemotherapy, in which there may be a time shift in analysis. In this study, we obtained data from 400 patients (including 130 patients with synchronous and 270 with metachronous BM). The results showed that metachronous BM was a protective factor for OS (p = 0.002).

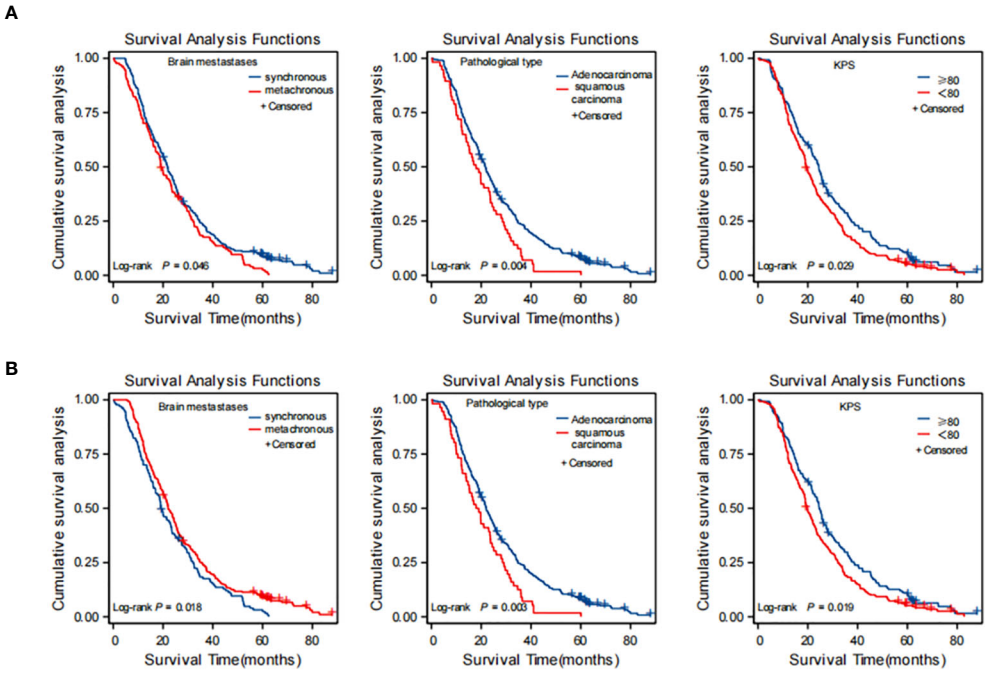

FIGURE 3
Kaplan-Meier curves for each independent factor affecting overall survival (OS) in NSCLC brain metastasis (BM) patients. **(A)** before PSM; **(B)** after PSM. **(A)** before PSM: synchronous brain metastases, squamous carcinoma, KPS score <80 were risk factors affecting OS of brain metastasis in NSCLC. **(B)** after PSM: metachronous brain metastases was an independent protective factor for OS; squamous carcinoma and KPS score <80 were independent risk factors for OS in brain metastases from NSCLC. PSM, propensity score matching; NSCLC, non-small cell lung cancer.

Considering the heterogeneity of pathological factors, we excluded large cell lung cancer and other subtypes of lung cancer. We only collected data from the two most common pathological types of NSCLC: LUAD and LUSC. Our results showed that the pathological type of NSCLC correlated with BM status. Furthermore, the pathological type was an independent prognostic factor affecting OS. Additionally, we found significant differences in prognosis between LUAD and LUSC: patients with LUAD exhibited significantly longer OS compared to those with LUSC, a pattern consistent with previous studies (22–24).

To address potential selection bias between driver mutation-negative and mutation-positive LUAD and LUSC cases, we performed a stratified analysis. Within the dataset of patients with BM from lung cancer, patients underwent mutation gene testing using next-generation sequencing (NGS) technology, and 89 patients were found to be positive for driver gene mutations, of

TABLE 4 Stratified analysis of pathological types and driver genes before and after PSM.

Characteristics	Variable	Before PSM		After PSM	
		Hazard ratio (95% CI)	*P* value	Hazard ratio (95% CI)	P value
Squamous carcinoma	synchronous brain metastases	REF		REF	
	metachronous brain metastases	2.504 (1.374-4.564)	0.003	2.271 (1.217-4.235)	**0.010**
Adenocarcinoma	synchronous brain metastases	REF		REF	
	metachronous brain metastases	1.183 (0.938-1.493)	0.156	1.237 (0.979-1.564)	0.075
EGFR Genetic mutations	synchronous brain metastases	REF		REF	
	Metachronous brain metastases	1.240 (0.791-1.945)	0.348	1.291 (0.820-2.032)	0.270
No EGFR genetic mutation	synchronous brain metastases	REF		REF	
	Metachronous brain metastases	1.283 (1.005-1.638)	**0.046**	1.291 (1.007-1.656)	**0.044**

PSM, propensity score matching; EGFR, epidermal growth factor receptor.
Bold values means results were considered significant when p-values were less than 0.05.

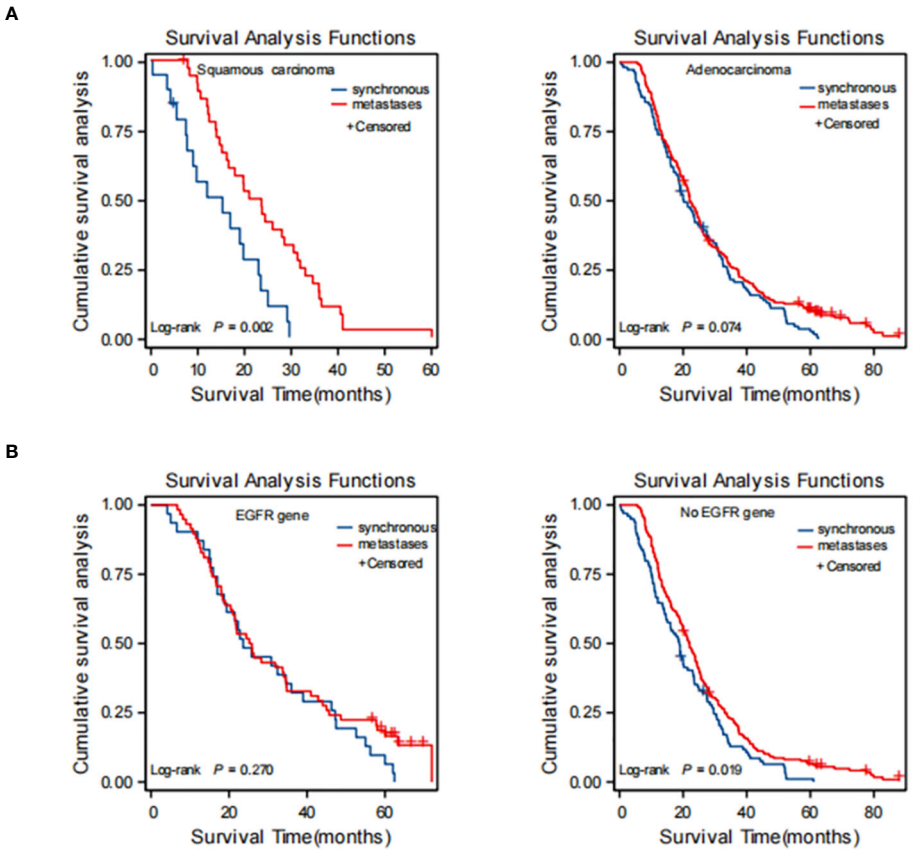

FIGURE 4
Kaplan-Meier curve of synchronous BM and metachronous BM based on the results of stratification analysis: type of patholog **(A)** and driver genes **(B)**. Type of pathologypatients with metachronous brain metastases with pathological type of squamous carcinoma had longer OS than synchronous brain metastases. Driver genes: patients with metachronous brain metastases with negative EGFR genes had longer OS than synchronous brain metastases. BM, brain metastasis; OS, overall survival; EGFR, epidermal growth factor receptor.

which 81 patients exhibited EGFR gene mutations. There were 31 simultaneous BM (all EGFR mutations) and 58 metachronous BM. Among these, 50 patients had EGFR mutations and the remaining 8 exhibited ALK mutations. Our results showed a difference in survival rates between metachronous and synchronous BM in EGFR mutation-negative patients with LUSC, whereas there was no difference in survival between metachronous and synchronous BM in EGFR mutation-positive patients with LUAD. Three generations of targeted drugs for EGFR mutations have emerged; FLAURA research shows that the prognosis of BM treated with third-generation targeted drugs is better and the progression rate is lower (25). Our findings also suggest that patients with BM exhibiting positive EGFR gene mutation experience better treatment outcomes when subjected to targeted therapy. On the

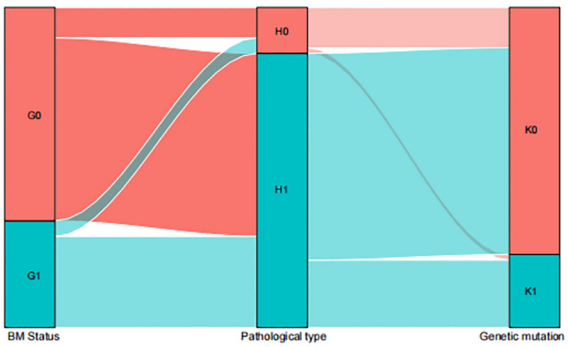

FIGURE 5
Sankey map among the influencing factors. G0=metachronous G1=synchronous; H0=LUAD H1=LUSC; K0=NO EGFR genetic mutations K1=EGFR genetic mutations.

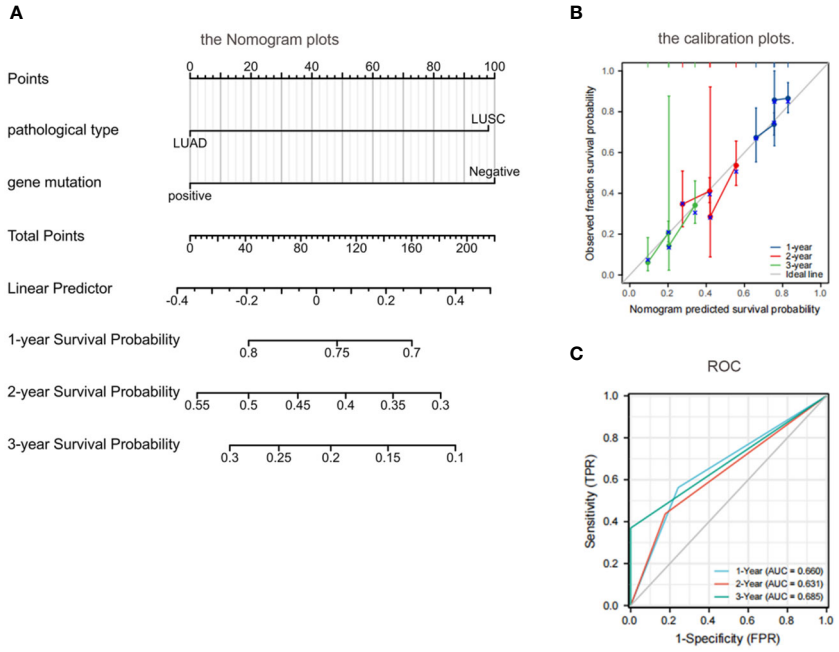

FIGURE 6
Prognostic modeling and ROC curves by nomogram. **(A)** Nomogram plots: patients with adenocarcinoma with a positive EGFR gene had higher OS at 1 year, 2 years, and 3 years than those with a negative squamous cell carcinoma with EGFR; **(B)** Calibration plots further validate the predictive performance of the nomogram; **(C)** ROC: the AUC was between 0.5 and 1.0, indicating a decent level of discriminative ability for the nomogram. OS, overall survival; EGFR, epidermal growth factor receptor; ROC, Receiver operating characteristic; AUC, area under the curve.

other hand, for patients with EGFR mutation-negative LUSC, treatment options are limited, and the disease progresses faster. Therefore, in the context of EGFR gene mutations, synchronous BM and metachronous BM necessitate different treatment approaches, with targeted therapy offering prolonged survival and good prognosis among patients with positive EGFR gene mutations (9–12).

Currently, driver mutation-negative patients have more treatment options, owing to the rise of immunotherapy. Immune checkpoint inhibitors (ICIs) have revolutionized the treatment of patients with advanced driver gene-negative NSCLC, increasing the 5-year survival rate from 5% (26) during the chemotherapy era to 13.4–23.2% (27). This may be related to programmed death-ligand 1 (PD-L1) expression, with ICIs providing more pronounced benefit to patients with PD-L1 expression (tumor proportion score ≥ 50%). Still, some patients with negative PD-L1 expression still have achieved good progression-free survival with first-line immunotherapy (28). However, due to the complexity of the immunotherapeutic mechanism and the uncertainty of predicting the efficacy of immunotherapy by PD-L1 expression status alone, further studies are needed to determine which patients are more likely to benefit from ICIs. However, patients with EGFR mutations have certainly limited benefit from first-line immunotherapy (29).

One of the limitations of our study is that we included data from cases recorded before the formal approval of immunotherapy, resulting in the absence of information regarding immunotherapy. In the future, we will be expanding the sample size will enable us to explore the efficacy of immunotherapy in driver mutation-negative patients and LUSC. Indeed, disease progression differs among patients with different types of lung cancer-related BM. Consequently, tailoring individualized treatment plans based on patient characteristics is of paramount importance.

Data availability statement

The original contributions presented in the study are included in the article/supplementary material. Further inquiries can be directed to the corresponding authors.

Ethics statement

The studies involving humans were approved by Medical Ethics Committee of Liaoning Cancer Hospital and the number is 2020X0102. The studies were conducted in accordance with the local legislation and institutional requirements. The participants provided their written informed consent to participate in this study.

Author contributions

JL: Writing – review & editing, Writing – original draft. XZ: Writing – review & editing. YW: Writing – review & editing. YJ: Writing – review & editing, Funding acquisition. YS: Writing – review & editing, Funding acquisition. TW: Writing – review & editing.

Funding

The author(s) declare financial support was received for the research, authorship, and/or publication of this article. This work is supported by the Fundamental Research Funds for the Central Universities [LD2023032, LD2023011, LD202221],Ministry of Science and Technology of the People's Republic of China [G2023127016L].

Acknowledgments

We are very grateful to the participants who participated in the study because they spend precious time participating in the study.

Conflict of interest

The authors declare that the research was conducted in the absence of any commercial or financial relationships that could be construed as a potential conflict of interest.

Publisher's note

References

1. Naresh G, Malik PS, Khurana S, Pushpam D, Sharma V, Yadav M, et al. Assessment of brain metastasis at diagnosis in non-small-cell lung cancer: A prospective observational study from North India. *JCO Glob Oncol*. (2021) 7:593–601. doi: 10.1200/GO.20.00629

2. Bray F, Ferlay J, Soerjomataram I, Siegel RL, Torre LA, Jemal A. Global cancer statistics 2018: GLOBOCAN estimates of incidence and mortality worldwide for 36 cancers in 185 countries. *CA Cancer J Clin*. (2018) 68:394–424. doi: 10.3322/caac.21492

3. De Carlo E, Bertoli E, Del Conte A, Stanzione B, Berto E, Revelant A, et al. Brain metastases management in oncogene-addicted non-small cell lung cancer in the targeted therapies era. *Int J Mol Sci*. (2022) 23(12):6477. doi: 10.3390/ijms23126477

4. Jiang K, Parker M, Materi J, Azad TD, Kamson DO, Kleinberg L, et al. Epidemiology and survival outcomes of synchronous and metachronous brain metastases: a retrospective population-based study. *Neurosurg Focus*. (2023) 55:E3. doi: 10.3171/2023.5.FOCUS23212

5. Goncalves PH, Peterson SL, Vigneau FD, Shore RD, Quarshie WO, Islam K, et al. Risk of brain metastases in patients with nonmetastatic lung cancer: Analysis of the Metropolitan Detroit Surveillance, Epidemiology, and End Results (SEER) data. *Cancer*. (2016) 122:1921–7. doi: 10.1002/cncr.30000

6. Wang B, Guo H, Xu H, Yu H, Chen Y, Zhao G. Research progress and challenges in the treatment of central nervous system metastasis of non-small cell lung cancer. *Cells*. (2021) 10(10):2620. doi: 10.3390/cells10102620

7. Zhang F, Zheng W, Ying L, Wu J, Wu S, Ma S, et al. A nomogram to predict brain metastases of resected non-small cell lung cancer patients. *Ann Surg Oncol*. (2016) 23:3033–9. doi: 10.1245/s10434-016-5206-3

8. Berger A, Mullen R, Bernstein K, Alzate JD, Silverman JS, Sulman EP, et al. Extended survival in patients with non-small-cell lung cancer-associated brain metastases in the modern era. *Neurosurgery*. (2023) 93:50–9. doi: 10.1227/neu.0000000000002372

9. Maemondo M, Inoue A, Kobayashi K, Sugawara S, Oizumi S, Isobe H, et al. Gefitinib or chemotherapy for non-small-cell lung cancer with mutated EGFR. *N Engl J Med*. (2010) 362:2380–8. doi: 10.1056/NEJMoa0909530

10. Mok TS, Wu Y-L, Ahn M-J, Garassino MC, Kim HR, Ramalingam SS, et al. Osimertinib or platinum–pemetrexed in EGFR T790M–positive lung cancer. *New Engl J Med*. (2017) 376:629–40. doi: 10.1056/NEJMoa1612674

11. Soria JC, Ohe Y, Vansteenkiste J, Reungwetwattana T, Chewaskulyong B, Lee KH, et al. Osimertinib in untreated EGFR-mutated advanced non-small-cell lung cancer. *N Engl J Med*. (2018) 378:113–25. doi: 10.1056/NEJMoa1713137

12. Zhang S, Liu J, Yang C, Li S, Cheng Y. [Research progress of immunotherapy for brain metastases in patients with drive gene negative NSCLC]. *Zhongguo Fei Ai Za Zhi*. (2018) 21:610–4. doi: 10.3779/j.issn.1009-3419.2018.08.06

13. Li H, Harrison EB, Li H, Hirabayashi K, Chen J, Li QX, et al. Targeting brain lesions of non-small cell lung cancer by enhancing CCL2-mediated CAR-T cell migration. *Nat Commun*. (2022) 13:2154. doi: 10.1038/s41467-022-29647-0

14. Wang W, Liu H, Li G. What's the difference between lung adenocarcinoma and lung squamous cell carcinoma? Evidence from a retrospective analysis in a cohort of Chinese patients. *Front Endocrinol (Lausanne)*. (2022) 13:947443. doi: 10.3389/fendo.2022.947443

15. Flannery TW, Suntharalingam M, Kwok Y, Koffman BH, Amin PP, Chin LS, et al. Gamma knife stereotactic radiosurgery for synchronous versus metachronous solitary brain metastases from non-small cell lung cancer. *Lung Cancer*. (2003) 42:327–33. doi: 10.1016/S0169-5002(03)00357-X

16. Proescholdt MA, Schödel P, Doenitz C, Pukrop T, Höhne J, Schmidt NO, et al. The management of brain metastases-systematic review of neurosurgical aspects. *Cancers (Basel)*. (2021) 13(7):1616. doi: 10.3390/cancers13071616

17. Hubbs JL, Boyd JA, Hollis D, Chino JP, Saynak M, Kelsey CR. Factors associated with the development of brain metastases: analysis of 975 patients with early stage nonsmall cell lung cancer. *Cancer*. (2010) 116:5038–46. doi: 10.1002/cncr.25254

18. Ashworth AB, Senan S, Palma DA, Riquet M, Ahn YC, Ricardi U, et al. An individual patient data metaanalysis of outcomes and prognostic factors after treatment of oligometastatic non-small-cell lung cancer. *Clin Lung Cancer*. (2014) 15:346–55. doi: 10.1016/j.cllc.2014.04.003

19. Chen K, Zhang F, Fan Y, Cheng G. Lung-molGPA index predicts survival outcomes of non-small-cell lung cancer patients with synchronous or metachronous brain metastases. *Onco Targets Ther*. (2020) 13:8837–44. doi: 10.2147/OTT.S255478

20. Fleckenstein J, Petroff A, Schäfers HJ, Wehler T, Schöpe J, Rübe C. Long-term outcomes in radically treated synchronous vs. metachronous oligometastatic non-small-cell lung cancer. *BMC Cancer*. (2016) 16:348. doi: 10.1186/s12885-016-2379-x

21. Shibahara I, Kanamori M, Watanabe T, Utsunomiya A, Suzuki H, Saito R, et al. Clinical features of precocious, synchronous, and metachronous brain metastases and the role of tumor resection. *World Neurosurg*. (2018) 113:e1–9. doi: 10.1016/j.wneu.2017.10.145

22. Kawase A, Yoshida J, Ishii G, Nakao M, Aokage K, Hishida T, et al. Differences between squamous cell carcinoma and adenocarcinoma of the lung: are adenocarcinoma and squamous cell carcinoma prognostically equal? *Jpn J Clin Oncol*. (2012) 42:189–95. doi: 10.1093/jjco/hyr188

23. Nakamura H, Sakai H, Kimura H, Miyazawa T, Marushima H, Saji H. Difference in postsurgical prognostic factors between lung adenocarcinoma and squamous cell carcinoma. *Ann Thorac Cardiovasc Surg*. (2017) 23:291–7. doi: 10.5761/atcs.oa.17-00020

24. Meng F, Zhang L, Ren Y, Ma Q. The genomic alterations of lung adenocarcinoma and lung squamous cell carcinoma can explain the differences of their overall survival rates. *J Cell Physiol*. (2019) 234:10918–25. doi: 10.1002/jcp.27917

25. Ouyang W, Yu J, Zhou Y, Xu Y, Li J, Gong J, et al. Metachronous Brain Metastasis in patients with EGFR-mutant NSCLC indicates a worse prognosis. *J Cancer*. (2020) 11:7283–90. doi: 10.7150/jca.46462

26. Siegel RL, Miller KD, Jemal A. Cancer statistics, 2019. *CA Cancer J Clin*. (2019) 69:7–34. doi: 10.3322/caac.21551

27. Garon EB, Hellmann MD, Rizvi NA, Carcereny E, Leighl NB, Ahn MJ, et al. Five-year overall survival for patients with advanced non–;small-cell lung cancer treated with pembrolizumab: results from the phase I KEYNOTE-001 study. *J Clin Oncol*. (2019) 37:2518–27. doi: 10.1200/JCO.19.00934

28. Dantoing E, Piton N, Salaün M, Thiberville L, Guisier F. Anti-PD1/PD-L1 immunotherapy for non-small cell lung cancer with actionable oncogenic driver mutations. *Int J Mol Sci*. (2021) 22(12):6288. doi: 10.3390/ijms22126288

29. Liu L, Li F, Zhao J, Zhuo X, Lai J, Wang J, et al. The real-world therapeutic analysis of first-line immunotherapy in Chinese patients with drive gene positive for advanced non-small cell lung cancer. *J Cancer*. (2023) 14:952–65. doi: 10.7150/jca.77199

frontiers | Frontiers in Immunology

TYPE Original Research
PUBLISHED 27 August 2024
DOI 10.3389/fimmu.2024.1399613

OPEN ACCESS

EDITED BY
Lin Zhou,
Sichuan University, China

REVIEWED BY
Hongqing Zhuang,
Peking University Third Hospital, China
Xiaoyan Li,
Capital Medical University, China
Assaf Moore,
Rabin Medical Center, Israel

*CORRESPONDENCE
Anhui Shi
anhuidoctor@163.com

†These authors have contributed equally to this work

RECEIVED 12 March 2024
ACCEPTED 07 August 2024
PUBLISHED 27 August 2024

CITATION
Zhang J, Yu J, Yang D, Jiang L, Dong X, Liu Z, Yu R, Yu H and Shi A (2024) Bevacizumab reduces cerebral radiation necrosis due to stereotactic radiotherapy in non-small cell lung cancer patients with brain metastases: an inverse probability of treatment weighting analysis. *Front. Immunol.* 15:1399613. doi: 10.3389/fimmu.2024.1399613

Bevacizumab reduces cerebral radiation necrosis due to stereotactic radiotherapy in non-small cell lung cancer patients with brain metastases: an inverse probability of treatment weighting analysis

Jingwei Zhang[1†], Jiayi Yu[2†], Dan Yang[2], Leilei Jiang[2], Xin Dong[2], Zhiyan Liu[2], Rong Yu[2], Huiming Yu[2] and Anhui Shi[2*]

[1]School of Basic Medical Sciences, Capital Medical University, Beijing, China, [2]Key Laboratory of Carcinogenesis and Translational Research (Ministry of Education/Beijing), Department of Radiation Oncology, Peking University Cancer Hospital and Institute, Beijing, China

Background: Cerebral radiation necrosis (RN), a severe complication of stereotactic radiotherapy (SRT), has been shown to significantly decrease patient survival time and quality of life. The purpose of this study was to analyze whether bevacizumab can prevent or reduce the occurrence of SRT-induced cerebral RN in non-small cell lung cancer (NSCLC) patients with brain metastases.

Materials and methods: We retrospectively reviewed the clinical records of NSCLC patients with brain metastases from March 2013 to June 2023 who were treated with SRT. Patients were divided into two groups: those in the bevacizumab group received SRT with four cycles of bevacizumab, and patients in the control group received SRT only. Inverse probability of treatment weighting (IPTW) was performed based on a multinomial propensity score model to balance the baseline characteristics. The chi-square test was used. A Cox model was used to evaluate overall survival (OS).

Results: A total of 80 patients were enrolled, namely, 28 patients in the bevacizumab group and 52 patients in the control group. The possibility of developing cerebral RN and/or symptomatic edema (RN/SE) was significantly decreased in patients treated with bevacizumab compared to those who did not receive bevacizumab before IPTW (p=0.036) and after IPTW (p=0.015) according to chi-square analysis. The IPTW-adjusted median OS was 47.7 months (95% CI

27.4-80.8) for patients in the bevacizumab group and 44.1 months (95% CI 36.7-68.0) (p=0.364) for patients in the control group.

Conclusion: The application of bevacizumab concurrent with SRT may prevent or reduce the occurrence of cerebral RN in NSCLC patients with brain metastases.

KEYWORDS

bevacizumab, radiation, radionecrosis, stereotactic, NSCLC, brain metastases

1 Introduction

Lung cancer is most often detected in stage IV when it has metastasized via blood and lymphatic vessels (1). Approximately 40% of non-small cell lung cancer (NSCLC) patients develop brain metastases, with appreciable morbidity and mortality (2). The efficacy of chemotherapy for brain metastasis is mostly poor (3); thus, treating brain metastases in patients with NSCLC is challenging, and a multidisciplinary approach is needed to control intracranial disease effectively.

With advancements in the treatment paradigm of stereotactic radiotherapy (SRT), this technique has become the usual clinical treatment of choice for cerebral metastases (4). Although SRT is an effective and noninvasive strategy for treating cerebral metastases (5), cerebral radiation necrosis (RN) is a common complication in patients after SRT with an occurrence of 5% to 25% and should be given more attention (6–9).

The mechanisms of cerebral RN are still under investigation. One commonly accepted mechanism involves the vascular system. Vascular endothelial growth factor (VEGF), usually considered an angiogenic factor plays an important role in abnormal neovascularization, which promotes tumor progression. An abnormal and disordered vessel structure with high capillary permeability leads to the development of brain edema, which ultimately deteriorates into cerebral RN (10, 11).

According to existing mechanisms, many clinical treatments have been used including bevacizumab treatment. Recent studies have focused mainly on the efficacy and safety of bevacizumab treatment for brain necrosis and have confirmed that bevacizumab remains the most thoroughly characterized and most widely used angiogenesis inhibitor across a range of advanced cancers with poor prognosis (12). In addition, the incidence of cerebral RN is irreversible; thus, treatment with bevacizumab can relieve patients' cerebral RN symptoms and improve their quality of life but not cure cerebral RN (11). There is little research on the use of bevacizumab as a precautionary measure to reduce the toxicity of irradiation in patients with NSCLC to minimize the occurrence of RN. Thus, we designed this study to compare the outcomes of NSCLC patients with brain metastases treated with SRT concurrent with 1 cycle of bevacizumab and followed by 3 continuous cycles of bevacizumab with the outcomes of those treated with SRT only. To our knowledge, this is the first study to explore whether bevacizumab can prevent the occurrence of SRT-induced cerebral RN. This study shed a light on the prevention of cerebral RN which may provide patients with an improvement of quality of life with fewer adverse reaction.

2 Materials and methods

2.1 Eligibility criteria

We retrospectively reviewed the clinical records of NSCLC patients with brain metastases from March 2013 to June 2023 treated with SRT. This retrospective study was approved by the Institutional Review Board (IRB) of Peking University Cancer Hospital & Institute. Informed consent was exempted by the IRB due to the retrospective nature of this research. All methods were performed in accordance with relevant guidelines and regulations. Patient records were anonymized and deidentified before analysis of the data.

The inclusion criteria for the study were defined as follows: (1) histologically or cytologically confirmed NSCLC; (2) age 18 years or older; (3) Karnofsky Performance Status (KPS) score of ≥70; (4) 10 or fewer cerebral metastases confirmed by computed tomography (CT) or magnetic resonance imaging (MRI); and (5) SRT administered for cerebral metastases.

Eighty patients were divided into two groups according to the application of bevacizumab: 28 patients in the bevacizumab group received SRT and four cycles of bevacizumab, and 52 patients in the control group received SRT only.

2.2 SRT technique

In all patients, SRT was delivered using the volumetric-modulated arc radiotherapy (VMAT) technique. All treatment plans were designed with the Eclipse treatment planning system based on a 6-MV photon beam from a Varian linear accelerator (True Beam or Edge). All patients underwent a simulated computed

tomography scan, fusion into thin layers, contrast-enhanced T1-weighted MRI. The gross tumor volume (GTV) was determined based on T1-weighted axial-enhanced MRI, occasionally guided by positron emission tomography, and was expanded with an additional 2-mm margin to determine the planning target volume (PTV). Most patients were administered a short-term prophylactic course of dexamethasone after SRT. Based on the specific size and location of the tumor, the PTV was prescribed at a dose of 18-24 Gy in 1 fraction, 27-30 Gy in 3 fractions or 30 Gy in 5 fractions. Organs at risk comprised the brain tissue and brainstem. The maximum dose to the brainstem was less than or equal to 10 Gy, conditionally suggesting that limiting the volume to 12 Gy was less than or equal to10 cm^3 of a single segmentation of brain tissue. A representative example is given in Figure 1.

The organs at risk comprised the brain stem, eyes, hippocampus, lens and optic nerve. The brain stem delineates the entire brain stem within the scanning range and increases it by 3mm to form the PRV. The maximum brain stem dose did not exceed 31Gy. As for eyes, the mean eyes dose did not exceed 20Gy and the maximum eyes dose did not exceed 35Gy. The maximum dose to optic nerve and optic chiasma was less than 22.5Gy for both sides. The volume of the lens is exposed to a dose less than 6Gy.

2.3 Bevacizumab treatment

A total of 4 cycles of bevacizumab were administered: the first cycle involved a dosage of 7.5 mg/kg bevacizumab administered once every 3 weeks, with the first dose on the same day as the first SRT fraction; following SRT, 3 additional cycles of bevacizumab were administered. The time of administration was more than 90 min for the first treatment and more than 60 min for each subsequent treatment. Patients were monitored by electrocardiogram throughout the administration process to closely observe their reactions to the medication.

2.4 Diagnosis of RN

Pathological examination is a highly reliable diagnostic method for distinguishing local tumor recurrence from cerebral RN. However, it is difficult to carry out in clinical practice (13, 14) for several reasons. First, there are many important functional areas or cranial base structures around intracranial tumors that are hard to resect surgically or biopsy stereotactically. In addition, few patients consent to biopsy after SRT. Moreover, the results of pathological examination can only reflect local lesions rather than showing overall pathological changes. Finally, conducting surgical resection or stereotactic biopsy contradict the goals of SRT, which are to increase survival time and improve patient quality of life.

The presumption of a symptomatic RN was based on the occurrence of adverse events of at least CTCAE v5.0 grade 2 (Common Terminology Criteria for Adverse Events). The suspicion of RN was based on typical MRI morphological findings on contrast-enhanced (CE) T1 sequences, which included the appearance of a spreading wavefront, spread to the contralateral hemisphere and/or multiple foci with discrete contrast enhancement only, and/or dynamic 18F-FET PET findings showing increasing time activity curves specifically in cases of RN (15). A stereotactic, usually PET-guided, biopsy was performed in specific cases to eliminate the possibility of tumor progression and to ascertain the suspicion of RN. The identification of necrotic tissue, absence of viable tumor tissue, and low proliferation indices (Ki-67) labeling index within the range of 1%) provided strong evidence supporting the diagnosis of RN. The structural and molecular imaging results and histological findings were examined by relevant experts and presented and dissected during multidisciplinary treatment (MDT) team meetings. A representative example is given in Figure 1. Patients who did not exhibit typical signs of either RN or tumor progression but continued to experience high levels of symptoms, such as severe headache, drowsiness, and paresis, for more than 6 weeks after SRT due to persistent symptomatic edema (SE) despite steroid treatment (as evidenced by T2-weighted follow-up MRI results) were categorized as SE patients. All patients with an SE diagnosis had to exhibit clinical stabilization/improvement over time to exclude tumor progression. The diagnosis of SE was also resolved by an MDT team. Patients with imaging-diagnosed edema or pathologically diagnosed cerebral RN (RN/SE) were included in the study.

In addition, dose diffusion magnetic resonance imaging (DWI) as an auxiliary method was used to differentiate RN from tumor recurrence, which present similar characteristics in standard MR images (16). DWI is able to acquire a signal for the movement of water protons in cellular spaces of the body, which can describe normal and histopathological characteristics. The apparent diffusion coefficient (ADC) value, including qualitative methods that are either restricted or facilitated and quantitative methods, is a sensitive method for detecting cerebral RN (17). Low levels on DWI and high ADC values suggest metastasis and RN, whereas high levels on DWI and low ADC values suggest tumor recurrence.

2.5 Outcomes

Patients' cerebral edema index (EI), brain necrosis incidence rate, and difference in overall survival (OS) time were observed, and the toxicity and side effects of bevacizumab were evaluated with further exploration of their mechanism. Local control (LC) rate was defined as the time after SRT treatment until local failure.

2.6 Statistical methods

IBM SPSS 20.0 software and R were used to analyze the data. Measurement data are described as the mean ± standard deviation or the median (quartile) and were analyzed with a rank-based nonparametric method. Enumeration data are described as the frequency, relative frequency, and constituent ratio and were tested with the chi-square test and Fisher's precision probability test. We used propensity score matching to select and pair the exposed group with controls according to their basic conditions and symptoms before treatment. Multifactorial

10.3389/fimmu.2024.1399613

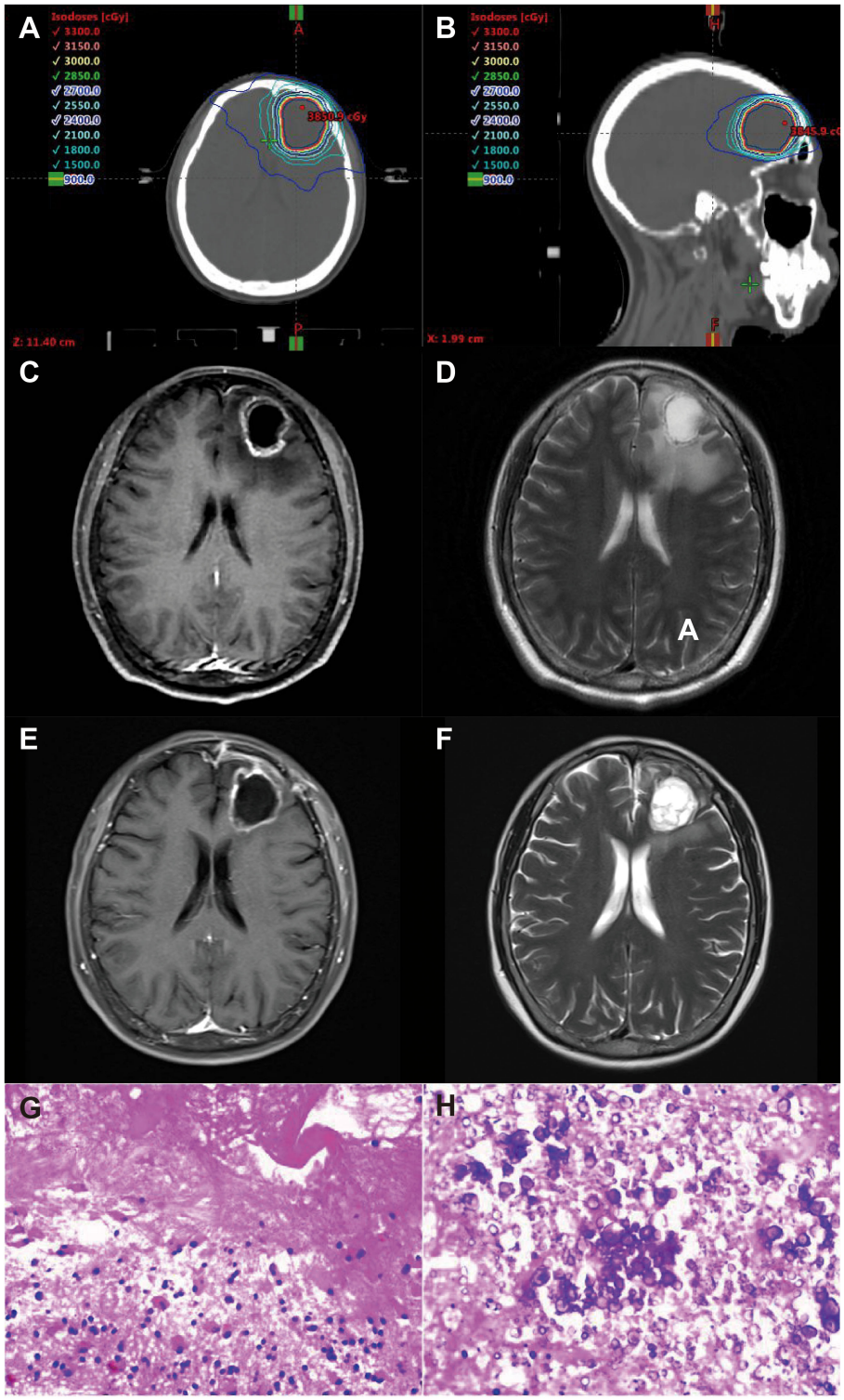

FIGURE 1
61 year old, female patient with non-small cell lung cancer treated with SRT without bevacizumab. Representative axial **(A)** and sagittal **(B)** plane of a VMAT plan of SRT treatment [PTV, 30 Gy isodose line (yellow)]. Representative axial planes in CE-T1 and T2 MRI sequences before SRT **(C, D)** and two months after surgical resection **(E, F)** with symptomatic radiation necrosis resulting in dizziness and headache. **(G, H)** representative pathological staining images diagnosis of radiation necrosis.

logistic regression analysis and generalized linear models were used for clinical data analysis to control for potential confounding factors. The curves for OS were plotted using the Kaplan–Meier method. The log-rank method and Cox proportional hazard model were used to conduct single-factor and multivariate analyses. Bonferroni correction was used for multiple comparisons.

To minimize the effects of potential confounding factors between the two treatment groups to ensure the reliability and rigor for different clinical outcomes, inverse probability of treatment weighting (IPTW) based on a multinomial propensity score model was used. We used a logistic regression model to estimate the multinomial propensity including the following potential confounders: sex, age, smoking status, tumor lymph node metastasis (TNM) stage and mutation type. To assess the covariate balance in the IPTW sample, standardized mean differences in covariate values were applied. The covariables were sex classified as male or female; age classified as ≥60 or age <60 years old; smoking status classified as yes or no; TNM stage classified as stage III or stage IV; and EGFR mutation classified as yes or no. Both IPTW-adjusted and unadjusted Kaplan–Meier estimates of OS rates are presented. For sensitivity analyses, doubly robust IPTW analysis using the Cox model was performed to adjust for potential residual confounding. Significance was set to p=0.05.

3 Results

3.1 Patient demographics

We identified 109 lesions in 80 NSCLC patients with a pathological diagnosis of brain metastasis whose characteristics are shown in Table 1. There were 46 men and 34 women with a median age of 66 years (range, 27-85 years). Epidermal growth factor receptor (EGFR) mutation was observed in 37 (46.25%) patients, which was close to half of the patients; 1 (1.25%) patient had a KRAS mutation, 1 (1.25%) patient had a BRAF mutation,

TABLE 1 Patient demographics and baseline clinical characteristics of patients.

	Unweighted, number(%)				Weighted, mean(%)			
Characteristic	Overall (n=80)	Bevacizumab-used(n=28)	Bevacizumab-unused(n=52)	P	Bevacizumab-used	Bevacizumab-unused	P	test SMD
Age				0.453			0.906	0.030
Median(range)	66(27-85)	65.5(40-85)	66(27-85)					
≥60	23(28.8%)	10(35.7%)	13(25.0%)		72.2	70.9		
<60	57(71.2%)	18(64.3%)	39(75.0%)		27.8	29.1		
Sex				0.029			0.924	0.025
Female	34(42.5%)	17(60.7%)	17(32.7%)		43.5	42.3		
male	46(57.5%)	11(39.3%)	35(67.3%)		56.5	57.7		
Smoking				1.000			0.735	0.091
Yes	30(37.5%)	10(35.7%)	20(38.5%)		41.8	37.3		
No	50(62.5%)	18(64.3%)	32(61.5%)		58.2	62.7		
TNM stage				1.000			0.728	0.096
I	9(11.3%)	3(10.7%)	6(11.5%)					
II	11(13.8%)	3(10.7%)	8(15.4%)					
III	21(23.3%)	3(10.7%)	18(34.6%)		19.7	16.0		
IV	39(48.8%)	19(67.9%)	20(38.5%)		80.3	84.0		
Gene mutation				0.009			0.979	0.007
EGFR	37(46.3%)	19(67.9%)	18(34.6%)		45.3	45.0		
ALK	7(8.8%)	1(3.6%)	6(11.5%)					
BRAF	1(1.3%)	0(0.0%)	1(1.9%)					
KRAS	1(1.3%)	0(0.0%)	1(1.9%)					
Non-non-oncogenic driver	4(5.0%)	3(10.7%)	1(1.9%)					
NA	29(36.3%)	5(17.9%)	24(46.2%)		54.7	55.0		

7 (8.75%) patients had an ALK mutation, 4 (5.00%) patients had nononcogenic driver mutations, and 29 (36.25%) patients had no genetic mutation.

Twenty-nine patients had received first-line treatment, and 10 had received second-line chemotherapy. The most commonly used chemotherapeutic agents were carboplatin (n=31), pemetrexed (n=23), etoposide (n=11), and albumin-bound paclitaxel (n=10). Twenty-eight patients were treated with 1 cycle of bevacizumab concurrent with SRT and 3 continuous cycles of bevacizumab after SRT, and 52 patients who were not administered bevacizumab after SRT were included as the control group. The median tumor size is 2.5cm (0.8-14.6 cm). Over all, the median gross tumor volumes (GTV) is 5.6 cm^3 (0.2-38.5 cm^3) and the median planning target volumes (PTV) is 14.2 cm^3 (1.0-85.1 cm^3). The median prescribed does and fraction (BED) is 56Gy (42.9-84.6Gy).

3.2 Correlation of RN/SE with the application of bevacizumab before and after IPTW

Bevacizumab was relatively well tolerated by those who received it during and after SRT, and these patients have, to date, exhibited a lower incidence of cerebral RN up to now. Only 1 patient administered bevacizumab as a precautionary measure had biopsy-proven cerebral RN, while 8 patients had symptomatic edema (SE), and 3 patients had pathologically diagnosed cerebral RN. The incidence of RN was significantly decreased in patients treated with bevacizumab compared to those who did not receive this treatment (p=0.036).

The propensity score model consisted of sex, age, smoking status, tumor lymph node metastasis (TNM) stage and EGFR mutation type. After applying IPTW adjustment, the baseline characteristics were found to be balanced between the bevacizumab and control groups, as shown in Table 1. After IPTW, it was found that patients treated with bevacizumab after SRT were significantly less likely (p=0.015) to develop RN/SE.

3.3 Survival analyses

The survival data for NSCLC patients who did or did not receive bevacizumab during and after SRT were analyzed. In our study, OS was defined as the time from the date of diagnosis until the date of death from any cause. The median follow-up of the entire cohort was 60.6 months [95% CI 45.1-76.1]. The median OS in patients with NSCLC receiving bevacizumab during and after SRT was 52.0 (95% CI 46.7-57.3) months compared with 44.1 (95% CI 16.5-71.7) months in patients not receiving bevacizumab (p=0.473; Figure 2A). The 1- and 3-year OS rates were 92.6% and 61.2%, respectively, in the group of NSCLC patients receiving bevacizumab and 84.3% and 49.8%, respectively, in the group not receiving bevacizumab (Figure 2A).

Patients with gene mutations had a significantly higher median OS of 87.7 (95% CI 48.9-125.5) months compared with a median OS of 21.4 (95% CI 15.3-27.5) months for patients without gene mutations (p<0.001). Among gene mutation patients, the median OS of 87.7 months (95% CI 49.9-125.5) in the bevacizumab group was higher than the median OS of 52.0 months (95% CI 44.2-59.8) in the control group, but the difference was not significant (p=0.333).

3.4 IPTW analysis of survival outcomes

The IPTW-adjusted median OS was 47.7 months (95% CI 27.4-80.8) for patients who received bevacizumab during and after SRT and 44.1 months (95% CI 36.7-68.0) (p=0.364) for patients who received SRT only. As shown in Figure 2, the comparison of bevacizumab group or control group shown no clear OS benefit.

3.5 Prognostic model

The influencing factors for RN/SE analyzed with the Cox regression model are presented in Table 2.

Bevacizumab treatment was not considerably associated with prolonged OS (HR, 0.159; 95% CI: 0.020-1.232; p=0.078) but was still a protective factor. Gene mutation (HR, 0.183; 95% CI: 0.086-0.387; p<0.001) and sex (HR, 0.457; 95% CI: 0.221-0.945; p=0.035) were protective factors that were significantly related to prolonged OS. Tumor lymph node metastasis (TNM) stage (HR, 1.629; 95% CI: 1.117-2.376; p=0.011) was a risk factor for prolonged OS.

3.6 Response

The median follow-up time was 43.2 months (range, 3.1-127.3 months) for the entire cohort. Overall, 28 patients and 43 lesions in the bevacizumab group and 52 patients and 66 lesions in control group were evaluated for best response. The partial response (PR), stable disease (SD) and progressive disease (PD) rate were 32.5%, 55.0% and 12.5%, respectively. At the end of follow-up, 1 patient in bevacizumab group and 11 patients in control group have experienced RN. The disease control rate is 87.5%. The local control rate for the patients in bevacizumab group and control group at 1 year was 88.9% and 84.3%, respectively.

3.7 Treatment-related toxicities

The use Bevacizumab was well tolerated in this study. The acute toxicities (defined as toxicity occurring between the start of treatment and up to 3 months after the completion of treatment and assessed according to the National Cancer Institute Common Terminology Criteria for Adverse Events version 5.0) were summarized in Table 3 and there was no late toxicity (more than 3 months after the completion of treatment and assessed according to the observed at the National Cancer Institute Common Terminology Criteria for Adverse Events version 5.0) end of

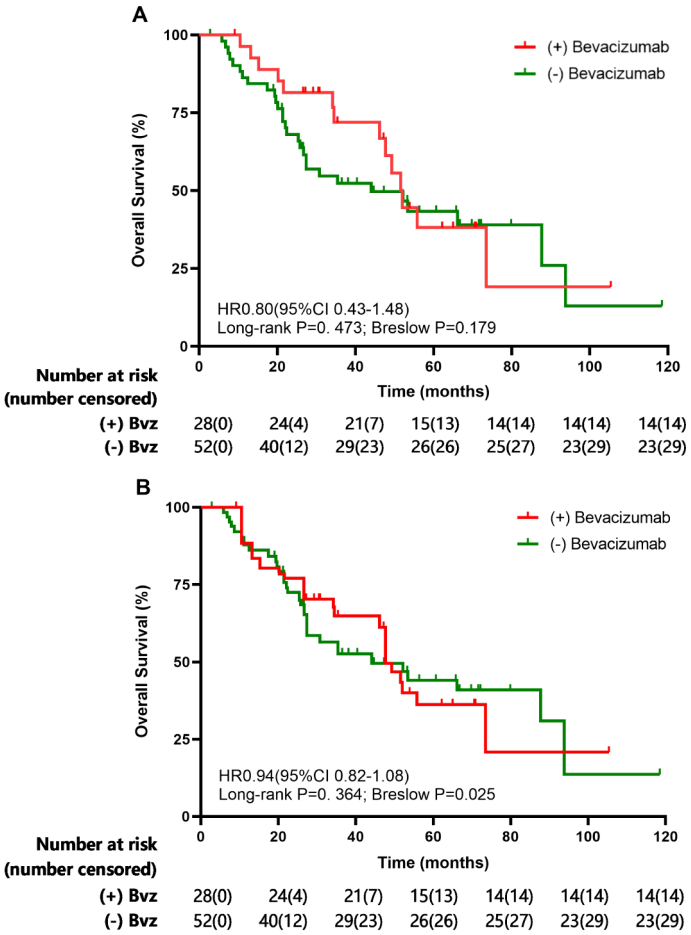

FIGURE 2
Overall survival (OS) evaluated the Kaplan-Meier method before **(A)** and after **(B)** inverse-probability of treatment weighting analysis for overall cohorts.

follow-up. 40 patients (50.0%) experienced grade 1-2 toxicities and only 4 patients (2.5%) experienced grade 3 toxicities. Overall, Leukopenia (32.5%) was most commonly seen in this cohort. Hypertension (22.5%), Headache (20.0%) and Neutropenia (20.0%) were commonly seen.

4 Discussion

The commonly use of SRT in the treatment of brain metastases in NSCLC patients proved to be a usual and effective option (18). However, 5% to 25% patients after SRT will experience cerebral RN which is one of the main limiting toxicities and severely influences patient survival time and quality of life. Bevacizumab now is the most thoroughly characterized and most widely used angiogenesis inhibitor across a range of advanced cancers with poor prognosis. There are many studies focusing on the efficacy and safety of bevacizumab to manage SRT-induced cerebral RN while there is little research focusing on preventing the occurrence of cerebral RN. The purpose of this study was to explore whether bevacizumab can prevent the occurrence of SRT-induced cerebral RN in patients with NSCLC.

We note several important findings in this study. First, bevacizumab can decrease the toxicity of irradiation and prevent the development of cerebral RN in NSCLC patients with brain metastases. Second, a clear OS benefit could not be demonstrated between bevacizumab group and control group. Third, the use of bevacizumab as a precautionary measure is safe in clinical application.

Cerebral RN, a severe complication of SRT, has severe symptoms like headache, epilepsy, cognitive disorder and so on which severely decrease patient quality of life. Previous studies have reported the frequency of RN after radiotherapy. For instance, an RN incidence rate of 10% to 15% in patients who were diagnosed with malignant gliomas and had survived for more than one year after irradiation has been reported (19). A W Lee et al. reported that the incidence of temporal lobe necrosis in patients with nasopharyngeal carcinoma after 9 months to 16 years of radiotherapy ranged from 1.6% to 22.0% (20). Given the widespread use and assessment of SRT, it is now clear that 2% to 5% of SRT patients will develop symptomatic focal cerebral necrosis, which is lower than the incidence rates noted above but remains a limitation of this treatment (21, 22). In our research, the total probability of biopsy-proven cerebral RN was 5% (4 of 80), while the incidence of SE was 10% (8 of 80).

TABLE 2 Multivariate analyses of prognostic factors related to OS before propensity score matching.

Variables	RE/SE-free survival univariate	Hazard ratio	95%-CI
BEV treatment	P=0.078	0.159	0.020-1.232
Sex	P=0.035	0.457	0.221-0.945
Age	P=0.544	0.816	0.422-1.575
Smoking	P=0.794	1.101	0.534-2.273
TNM	P=0.011	1.629	1.117-2.376
Mutation	P<0.001	0.183	0.086-0.387

At present, most clinical studies are based on bevacizumab treatment of refractory brain edema and cerebral RN after SRT (23–26). To our knowledge, this is the first study confirming that bevacizumab concurrent with SRT may prevent or reduce the occurrence of cerebral RN in NSCLC patients with brain metastases. Patients' quality of life and overall survival are both important. Though our result didn't show clear benefit of prolonging OS, improving NSCLC patients' quality of life was also essential.

The safety of bevacizumab is equally important to its efficacy. In our study, patients experienced few adverse reactions. Puyuan Xing et al. (27) confirmed that a first-line regimen containing bevacizumab in terms of safety assessment showed acceptable adverse reactions and better effectiveness than a non-bevacizumab regimen in patients with NSCLC. Ning Tang et al. (28) also reported that compared to chemotherapy alone, the combination of chemotherapy and bevacizumab as first-line and maintenance treatment resulted in improved curative rates and tolerable adverse events in patients with advanced NSCLC. In our study, decreased RN occurrence and manageable adverse events improved patients' quality of life confirming the efficacy and safety of bevacizumab.

Overall, among all the investigations using bevacizumab as an effective treatment measure for cerebral RN, this study provides a new angle from treatment to prevention. Nevertheless, this study certainly had limitations. First, it was geographically limited to one hospital. Patients from other health care environments may produce different outcomes or confirm our study. Second, the median OS of bevacizumab group and control group was 52.0 months and 44.1 months respectively which is much longer than commonly considered mean median OS of NSCLC patients with brain metastases. The median OS of patients in our study was defined as the time from the date of diagnosis until the date of death from any cause. Thus, the median OS in our study is much longer. Finally, the limited number and the unbalanced proportion of patients assessed may influence our results. To minimize the effects of potential confounding factors between the two treatment groups, inverse probability of treatment weighting (IPTW) based on a multinomial propensity score model was used to perfectly balance essential factors including, sex, age, smoking status, tumor lymph node metastasis (TNM) stage and mutation type.

Despite the limited number of patients assessed and the preliminary nature of the observations presented here, this study initially confirmed the efficacy of bevacizumab to prevent the occurrence of cerebral RN in patients with NSCLC, which may inform the clinical use of SRT for intracranial tumors. In the future, prospective studies and more clinical data are needed to confirm the

TABLE 3 Treatment-related acute toxicities.

	Bevacizumab group (n=28)				Control group (n=52)			
	Grade 1 No. (%)	Grade 2 No. (%)	Grade 3 No. (%)	Grade 4-5 No. (%)	Grade 1 No. (%)	Grade 2 No. (%)	Grade 3 No. (%)	Grade 4-5 No. (%)
Leukopenia	12(15.0)	7(8.8)	2(2.5)	0(0.0)	4(5.0)	1(1.3)	0(0.0)	0(0.0)
Neutropenia	8(10.0)	2(2.5)	1(1.3)	0(0.0)	2(2.5)	2(2.5)	1(1.3)	0(0.0)
Thrombocytopenia	2(2.5)	1(1.3)	0(0.0)	0(0.0)	3(3,8)	1(1.3)	0(0.0)	0(0.0)
Anemia	6(7.5)	3(3.8)	0(0.0)	0(0.0)	2(2.5)	0(0.0)	0(0.0)	0(0.0)
Elevated AST	0(0.0)	0(0.0)	0(0.0)	0(0.0)	0(0.0)	0(0.0)	0(0.0)	0(0.0)
Elevated ALT	4(5.0)	0(0.0)	0(0.0)	0(0.0)	0(0.0)	0(0.0)	0(0.0)	0(0.0)
Headache	8(10.0)	2(2.5)	0(0.0)	0(0.0)	4(5.0)	2(2.5)	0(0.0)	0(0.0)
Fatigue	3(3.8)	0(0.0)	0(0.0)	0(0.0)	3(3.8)	0(0.0)	0(0.0)	0(0.0)
Nausea	2(2.5)	0(0.0)	0(0.0)	0(0.0)	3(3.8)	0(0.0)	0(0.0)	0(0.0)
Hypertension	10(12.5)	4(5.0)	0(0.0)	0(0.0)	3(3.8)	1(1.3)	0(0.0)	0(0.0)
Proteinuria	4(5.0)	1(1.3)	0(0.0)	0(0.0)	0(0.0)	0(0.0)	0(0.0)	0(0.0)
Gastrointestinal perforation	0(0.0)	0(0.0)	0(0.0)	0(0.0)	0(0.0)	0(0.0)	0(0.0)	0(0.0)
Thromboembolism	0(0.0)	0(0.0)	0(0.0)	0(0.0)	0(0.0)	0(0.0)	0(0.0)	0(0.0)

ALT, alanine aminotransferase; AST, aspartate aminotransferase.

effectiveness of bevacizumab as a precautionary measure and establish a complete system for the application of bevacizumab to prevent the occurrence of cerebral RN.

Data availability statement

The original contributions presented in the study are included in the article/supplementary material. Further inquiries can be directed to the corresponding author.

Ethics statement

The studies involving humans were approved by Ethic committee of Beijing cancer hospital. The studies were conducted in accordance with the local legislation and institutional requirements. Written informed consent for participation was not required from the participants or the participants' legal guardians/next of kin in accordance with the national legislation and institutional requirements. Written informed consent was obtained from the individual(s) for the publication of any potentially identifiable images or data included in this article.

Author contributions

JZ: Writing – review & editing, Writing – original draft. JY: Writing – review & editing, Validation, Supervision, Project administration, Funding acquisition, Conceptualization. DY: Writing – review & editing, Resources. LJ: Writing – review & editing, Resources. XD: Writing – review & editing, Resources. ZL: Writing – review & editing. RY: Writing – review & editing, Resources. HY: Writing – review & editing, Resources. AS: Writing – review & editing, Visualization, Validation, Supervision, Software, Resources, Project administration, Methodology, Investigation, Funding acquisition, Formal analysis, Data curation, Conceptualization.

Funding

The author(s) declare financial support was received for the research, authorship, and/or publication of this article. Funding was provided by the Chinese Society of Clinical Oncology–Linghang Cancer Research (grant number Y-2019AZMS-0519), the Wu Jieping Medical Foundation (grant number 320.6750.2022–03–48), the Clinical Research Fund For Distinguished Young Scholars of Peking University Cancer Hospital (grant number QNJJ2022014), and Beijing-Tianjin-Hebei Basic Research Cooperation Special Project (grant number 22JCZXJC00180).

Conflict of interest

The authors declare that the research was conducted in the absence of any commercial or financial relationships that could be construed as a potential conflict of interest.

The reviewer XL declared a shared parent affiliation with the author JZ to the handling editor at the time of the review.

Publisher's note

References

1. Popper HH. Progression and metastasis of lung cancer. *Cancer Metastasis Rev.* (2016) 35:75–91. doi: 10.1007/s10555-016-9618-0

2. Buriolla S, Pelizzari G, Corvaja C, Alberti M, Targato G, Bortolot M, et al. Immunotherapy in NSCLC patients with brain metastases. *Int J Mol Sci.* (2022) 23:7068. doi: 10.3390/ijms23137068

3. Ernani V, Stinchcombe TE. Management of brain metastases in non-small-cell lung cancer. *J Oncol Pract.* (2019) 15:563–70. doi: 10.1200/JOP.19.00357

4. Patel TR, Knisely JP, Chiang VL. Management of brain metastases: surgery, radiation, or both? *Hematol Oncol Clin North Am.* (2012) 26:933–47. doi: 10.1016/j.hoc.2012.04.008

5. Chen WC, Baal UH, Baal JD, Pai JS, Boreta L, Braunstein SE, et al. Efficacy and safety of stereotactic radiosurgery for brainstem metastases: A systematic review and meta-analysis. *JAMA Oncol.* (2021) 7:1033–40. doi: 10.1001/jamaoncol.2021.1262

6. Du Four S, Hong A, Chan M, Charakidis M, Duerinck J, Wilgenhof S, et al. Symptomatic histologically proven necrosis of brain following stereotactic radiation and ipilimumab in six lesions in four melanoma patients. *Case Rep Oncol Med.* (2014) 2014:417913. doi: 10.1155/2014/417913

7. Rogers LR. Neurologic complications of radiation. *Continuum (Minneap Minn).* (2012) 18:343–54. doi: 10.1212/01.CON.0000413662.35174.a8

8. Lacy J, Saadati H, Yu JB. Complications of brain tumors and their treatment. *Hematol Oncol Clin North Am.* (2012) 26:779–96. doi: 10.1016/j.hoc.2012.04.007

9. Lee D, Riestenberg RA, Haskell-Mendoza A, Bloch O. Brain metastasis recurrence versus radiation necrosis: evaluation and treatment. *Neurosurg Clin N Am.* (2020) 31:575–87. doi: 10.1016/j.nec.2020.06.007

10. Zhuang H, Shi S, Yuan Z, Chang JY. Bevacizumab treatment for radiation brain necrosis: mechanism, efficacy and issues. *Mol Cancer.* (2019) 18:21. doi: 10.1186/s12943-019-0950-1

11. Boothe D, Young R, Yamada Y, Prager A, Chan T, Beal K. Bevacizumab as a treatment for radiation necrosis of brain metastases post stereotactic radiosurgery. *Neuro Oncol.* (2013) 15:1257–63. doi: 10.1093/neuonc/not085

12. Garcia J, Hurwitz HI, Sandler AB, Miles D, Coleman RL, Deurloo R, et al. Bevacizumab (Avastin®) in cancer treatment: A review of 15 years of clinical experience and future outlook. *Cancer Treat Rev.* (2020) 86:102017. doi: 10.1016/j.ctrv.2020.102017

13. Zhuang H, Yuan X, Zheng Y, Li X, Chang JY, Wang J, et al. A study on the evaluation method and recent clinical efficacy of bevacizumab on the treatment of radiation cerebral necrosis. *Sci Rep.* (2016) 6:24364. doi: 10.1038/srep24364

14. Kickingereder P, Dorn F, Blau T, Schmidt M, Kocher M, Galldiks N, et al. Differentiation of local tumor recurrence from radiation-induced changes after stereotactic radiosurgery for treatment of brain metastasis: case report and review of the literature. *Radiat Oncol.* (2013) 8:52. doi: 10.1186/1748-717X-8-52

15. Fleischmann DF, Jenn J, Corradini S, Ruf V, Herms J, Forbrig R, et al. Bevacizumab reduces toxicity of reirradiation in recurrent high-grade glioma. *Radiother Oncol*. (2019) 138:99–105. doi: 10.1016/j.radonc.2019.06.009

16. Bobek-Billewicz B, Stasik-Pres G, Majchrzak H, Zarudzki L. Differentiation between brain tumor recurrence and radiation injury using perfusion, diffusion-weighted imaging and MR spectroscopy. *Folia Neuropathol*. (2010) 48:81–92.

17. Roushdy MMM, Elsherif MMR, Kayed EMS, Farghaly S, Sayed AR. Does diffusion magnetic resonance imaging (DWI) has role in irradiated laryngeal carcinoma? *Indian J Otolaryngol Head Neck Surg*. (2022) 74:6339–46. doi: 10.1007/s12070-021-03071-0

18. de Azevedo Rosas F, Favareto SL, de Castro DG. Local ablative therapy of brain metastasis from non-small cell lung cancer: benefits and limitations. *J Thorac Dis*. (2021) 13:3289–94. doi: 10.21037/jtd-19-3321

19. Ruben JD, Dally M, Bailey M, Smith R, McLean CA, Fedele P. Cerebral radiation necrosis: incidence, outcomes, and risk factors with emphasis on radiation parameters and chemotherapy. *Int J Radiat Oncol Biol Phys*. (2006) 65:499–508. doi: 10.1016/j.ijrobp.2005.12.002

20. Lee AW, Ng SH, Ho JH, Tse VK, Poon YF, Tse CC, et al. Clinical diagnosis of late temporal lobe necrosis following radiation therapy for nasopharyngeal carcinoma. *Cancer*. (1988) 61:1535–42. doi: 10.1002/(ISSN)1097-0142

21. Swinson BM, Friedman WA. Linear accelerator stereotactic radiosurgery for metastatic brain tumors: 17 years of experience at the University of Florida. *Neurosurgery*. (2008) 62:1018–31; discussion 1031-2. doi: 10.1227/01.neu.0000325863.91584.09

22. Giglio P, Gilbert MR. Neurologic complications of cancer and its treatment. *Curr Oncol Rep*. (2010) 12:50–9. doi: 10.1007/s11912-009-0071-x

23. Zhuang H, Zhuang H, Shi S, Wang Y. Ultra-low-dose bevacizumab for cerebral radiation necrosis: A prospective phase II clinical study. *Onco Targets Ther*. (2019) 12:8447–53. doi: 10.2147/OTT.S223258

24. Wang Y, Pan L, Sheng X, Mao Y, Yao Y, Wang E, et al. Reversal of cerebral radiation necrosis with bevacizumab treatment in 17 Chinese patients. *Eur J Med Res*. (2012) 17:25. doi: 10.1186/2047-783X-17-25

25. Levin VA, Bidaut L, Hou P, Kumar AJ, Wefel JS, Bekele BN, et al. Randomized double-blind placebo-controlled trial of bevacizumab therapy for radiation necrosis of the central nervous system. *Int J Radiat Oncol Biol Phys*. (2011) 79:1487–95. doi: 10.1016/j.ijrobp.2009.12.061

26. Delishaj D, Ursino S, Pasqualetti F, Cristaudo A, Cosottini M, Fabrini MG, et al. Bevacizumab for the treatment of radiation-induced cerebral necrosis: A systematic review of the literature. *J Clin Med Res*. (2017) 9:273–80. doi: 10.14740/jocmr2936e

27. Yang X, Ren H, Fu J. Treatment of radiation-induced brain necrosis. *Oxid Med Cell Longev*. (2021) 2021:4793517. doi: 10.1155/2021/4793517

28. Xing P, Mu Y, Wang Y, Hao X, Zhu Y, Hu X, et al. Real world study of regimen containing bevacizumab as first-line therapy in Chinese patients with advanced non-small cell lung cancer. *Thorac Cancer*. (2018) 9:805–13. doi: 10.1111/1759-7714.12650

frontiers | Frontiers in Oncology

TYPE Original Research
PUBLISHED 03 September 2024
DOI 10.3389/fonc.2024.1433505

OPEN ACCESS

EDITED BY
Jianxin Xue,
Sichuan University, China

REVIEWED BY
Weimin Gao,
Barrow Neurological Institute (BNI), United States
Shih-Ying Wu,
Wake Forest Baptist Medical Center, United States

*CORRESPONDENCE
Tianlu Wang
wangtianlu@cancerhosp-ln-cmu.com

†These authors have contributed equally to this work

RECEIVED 16 May 2024
ACCEPTED 19 August 2024
PUBLISHED 03 September 2024

CITATION
Zhou C, Zhang X, Yan X, Xie H, Tan H, Song Y, Li M, Jin Y and Wang T (2024) Impact of lung adenocarcinoma subtypes on survival and timing of brain metastases.
Front. Oncol. 14:1433505.
doi: 10.3389/fonc.2024.1433505

Impact of lung adenocarcinoma subtypes on survival and timing of brain metastases

Chuyan Zhou[1,2†], Xiaofang Zhang[1,2†], Xingyu Yan[2†], Haitao Xie[1], Hao Tan[1], Yingqiu Song[1], Mo Li[1], Yi Jin[1] and Tianlu Wang[1,3*]

[1]Department of Radiotherapy, Cancer Hospital of China Medical University, Liaoning Cancer Hospital & Institute, Cancer Hospital of Dalian University of Technology, Shenyang, Liaoning, China, [2]School of Graduate, China Medical University, Shenyang, China, [3]Faculty of Medicine, Dalian University of Technology, Dalian, China

Purpose: Lung cancer is a devastating disease, with brain metastasis being one of the most common distant metastases of lung adenocarcinoma. This study aimed to investigate the prognostic characteristics of individuals with brain metastases originating from invasive lung adenocarcinoma of distinct pathological subtypes, providing a reference for the management of these patients.

Methods: Clinical data from 156 patients with lung adenocarcinoma-derived brain metastases were collected, including age, sex, smoking status, Karnofsky Performance Status scores, pathological subtype, lymph node metastasis, tumor site, treatment mode, T stage, and N stage. Patients were classified into two groups (highly differentiated and poorly differentiated) based on their pathological subtypes. Propensity score matching was used to control for confounding factors. The prognostic value of pathological subtypes was assessed using Kaplan-Meier analysis and Cox proportional hazards regression modeling.

Results: Kaplan-Meier analysis indicated that patients in the moderately to highly differentiated group had better prognoses. Multivariate analysis revealed that being in the poorly differentiated group was a risk factor for poorer prognosis. Thoracic tumor radiation therapy, chemotherapy, and surgery positively influenced the time interval between lung cancer diagnosis and brain metastasis.

Conclusions: The pathological subtypes of lung adenocarcinoma-derived brain metastases are associated with patient prognosis. Patients in the poorly differentiated group have worse prognoses compared to those in the moderately to highly differentiated group. Therefore, patients in the poorly differentiated group may require more frequent follow-ups and aggressive treatment.

KEYWORDS

invasive lung adenocarcinoma, brain metastasis, pathological subtype, prognosis, survival

1 Introduction

Lung cancer is a worldwide population health concern with a mortality rate higher than that of breast, prostate, and colorectal cancers combined (1). In China, lung cancer has the highest incidence and mortality rate among all cancer types (2, 3). Approximately 85% of lung cancer diagnoses are non-small-cell lung carcinomas (NSCLC) (4). Between 10% and 20% of patients with NSCLC develop brain metastases at presentation, and up to 50% of patients will develop brain metastases during the course of the disease (5, 6). Patients with brain metastases have a poor prognosis and a shortened median survival (7). With the continued development of molecular targeted therapies and immunotherapies, patients with lung cancer are living longer and, therefore, are at greater risk for brain metastases. Although the deleterious effects of brain metastases from lung cancer are widely understood, patients with brain metastases are less sensitive to drug therapy, and surgical interventions are limited. The median survival of patients with brain metastases is typically 4–9 months (8). Brain metastasis significantly impacts patient quality of life and has become a serious global social health problem (9–11).

Lung adenocarcinoma has a greater risk of brain metastasis among patients with NSCLC, according to a long-term follow-up in the US SEER database (12). However, the number of studies on prognostic factors for brain metastases in lung adenocarcinoma is limited. Cell type, primary tumor size, and lymph node stage have been associated with the probability of lung adenocarcinoma brain metastasis (13). Pathological subtypes of lung adenocarcinoma play a considerable role in cancer progression. Invasive non-mucinous adenocarcinomas are divided into five types: lepidic, acinar, papillary, micropapillary, and solid (14). Each pathological subtype has unique histological features that impact patient survival and treatment. Numerous studies have found that micropapillary and solid types are associated with a poorer prognosis, whereas the lepidic growth type is associated with a better prognosis (15–17). Therefore, lung adenocarcinomas with micropapillary and solid components are considered high-risk and require more thorough treatments. In contrast, the other subtypes are categorized as low risk.

Considering that NSCLC comprises numerous types that may be affected by various confounding factors, we selected lung adenocarcinoma, which is prone to brain metastases, as the study subject to reduce interference and improve the accuracy of the study. Moreover, to date, the impact of different pathologic subtypes on the prognosis of patients with brain metastases from aggressive lung adenocarcinoma has not been reported. Therefore, we retrospectively analyzed the relationship between pathologic subtypes of lung adenocarcinoma and survival after brain metastasis. In addition, we evaluated the relationship between pathologic subtypes and the time interval between lung cancer diagnosis and brain metastasis (brain metastasis interval). We evaluated 156 patients with brain metastases from invasive lung adenocarcinoma admitted to our hospital to provide a theoretical basis for future treatment approaches.

2 Methods

2.1 Study subjects

The clinical data of 156 patients with brain metastases from invasive lung adenocarcinoma were assessed. The patients were treated at the Liaoning Provincial Tumor Hospital (2008–2017). The inclusion criteria were as follows: (1) a clear diagnosis of lung adenocarcinoma and the existence of subtype classification according to clinicopathology or cytology; (2) brain metastasis confirmed by magnetic resonance imaging; and (3) age ≥18 years. The exclusion criteria were as follows: (1) no clear pathological diagnosis or secondary lung cancer; (2) primary tumor at other sites; and (3) incomplete clinical data.

2.2 Data collection

The relevant patient information was collected, including pathological type, sex, age, smoking status, Karnofsky Performance Status (KPS) score, lymph node metastasis, tumor site, treatment modality, T stage (size and extent of the primary tumor), and N stage (number of affected lymph nodes).

2.3 Grouping method

Lung cancer is divided into three grades: grade 1 indicates high differentiation, with predominantly lepidic growth type and a high-grade pattern (solid, micropapillary, or complex glandular) not exceeding 20%; grade 2 indicates moderate differentiation, with acinar or papillary predominance and a high-grade pattern not exceeding 20%; and grade 3 indicates poor differentiation, where the high-grade pattern is ≥20%. Patients were divided into two groups: a moderate- to high-differentiation group and a poor-differentiation group, according to their pathological subtypes.

2.4 Follow-up

The date of the patient's death or last follow-up was used as the cutoff date.

2.5 Statistical methods

After propensity score matching (PSM), the patients from the poor-differentiation group (n = 59) and moderate- to high-differentiation group (n = 59) were matched using a 1:1 ratio. The parameters of patient clinicopathological characteristics and the distinct pathological subtypes were compared using the chi-squared test. Multivariate Cox regression analysis was used to determine the prognostic risk factors. The Kaplan–Meier method was applied to the survival curves to calculate the survival rates (0:

moderate- to high-differentiation group; 1: poor-differentiation group), and the difference in survival was compared using the log-rank test. Differences were considered statistically significant when $P < 0.05$. All statistical analyses were performed using the IBM Statistical Package for the Social Sciences (SPSS) version 25.0.

3 Results

3.1 Patient characteristics

Hundred fifty-six patients who met the inclusion criteria were recruited for this analysis. Of those patients, 89 (57.1%) had moderately to highly differentiated invasive lung adenocarcinoma, and the remaining 67 (42.9%) had poorly differentiated invasive lung adenocarcinoma. More than half (66.7%) of the individuals were younger than 60 years, 79 (50.6%) were female, and the majority (76.2%) underwent chest chemotherapy. In the poor-differentiation group, patients were more likely to be male ($P < 0.05$). Lymph node involvement (N2–3; $P < 0.05$) was more severe in the moderate- to high-differentiation group than in the poor-differentiation group (Table 1).

TABLE 1 Baseline characteristics of patients with brain metastases.

Characteristic	0 (high and middle differentiation groups)	1 (low differentiation group)	p
n	89	67	
Age(year), n (%)			0.689
<60	61 (39.1%)	43 (27.6%)	
≥60	28 (17.9%)	24 (15.4%)	
Gender, n (%)			0.038
male	37 (23.7%)	40 (25.6%)	
female	52 (33.3%)	27 (17.3%)	
Whether smoke, n (%)			0.844
no	57 (36.5%)	41 (26.3%)	
yes	32 (20.5%)	26 (16.7%)	
KPS score, n (%)			0.380
≥90	43 (27.6%)	38 (24.4%)	
<90	46 (29.5%)	29 (18.6%)	
Lymph node metastasis, n (%)			0.641
no	24 (15.4%)	15 (9.6%)	
yes	65 (41.7%)	52 (33.3%)	
Whether brain metastases have occurred at the time of diagnosis, n (%)			0.487
no	68 (43.6%)	47 (30.1%)	
yes	21 (13.5%)	20 (12.8%)	
Tumor location, n (%)			0.842
central	15 (9.6%)	13 (8.3%)	
peripheral	74 (47.4%)	54 (34.6%)	
T stage, n (%)			0.294
0~2	64 (41%)	42 (26.9%)	
3~4	25 (16%)	25 (16%)	
N stage, n (%)			0.045
0~1	39 (25%)	18 (11.5%)	
2~3	50 (32.1%)	49 (31.4%)	
TNM stage, n (%)			0.547
1~3	48 (30.8%)	32 (20.5%)	
4	41 (26.3%)	35 (22.4%)	
Radiotherapy, n (%)			0.897
no	71 (45.5%)	52 (33.3%)	
yes	18 (11.5%)	15 (9.6%)	
Chemotherapy, n (%)			0.882
no	22 (14.1%)	15 (9.6%)	
yes	67 (42.9%)	52 (33.3%)	
Surgery, n (%)			0.064
no	36 (23.1%)	38 (24.4%)	
yes	53 (34%)	29 (18.6%)	

3.2 Survival analysis of overall survival and the brain metastasis interval before PSM

Case subtype was linked to brain metastasis survival in univariate analyses (hazard ratio [HR]: 1.421; 95% confidence interval [CI]: 1.020–1.981; $P = 0.038$) but not to the brain metastasis interval (HR: 1.190; 95% CI: 0.853–1.660; $P = 0.305$). The KPS, primary tumor site, T stage, thoracic tumor stage, thoracic tumor chemotherapy, thoracic tumor radiation therapy, and thoracic tumor surgical therapy were related to the brain metastasis interval ($P < 0.05$). Patients in the poor-differentiation group had a lower survival rate after brain metastasis (HR: 1.421; 95% CI: 1.020-1.981; $P = 0.038$) than those in the moderate- to high-differentiation group. As shown by the multivariate analysis, a peripheral primary tumor site (HR: 0.516; 95% CI: 0.331–0.802; $P = 0.003$), chemotherapy (HR: 0.415; 95% CI: 0.276–0.624; $P <$

0.001), and surgical treatment for thoracic tumors (HR: 0.266; 95% CI: 0.151–0.469; P < 0.001) were positive prognostic factors for the brain metastasis interval (Tables 2, 3).

3.3 Survival analysis of overall survival and the brain metastasis interval after PSM

The basic principle of PSM is to replace multiple covariates with a single score that equalizes the covariate distribution between the treatment and control groups. Before PSM, the moderate- to high-differentiation group included 89 patients, and the poor-differentiation group included 67 patients. After PSM, 59 clinically homogeneous patients were included in each group. In the moderate- to high-differentiation and poor-differentiation groups, the risk factors (age, sex, smoking status, the KPS score, lymph node metastasis, whether brain metastasis occurred at the time of diagnosis, location of the tumor in the thorax, T stage, N stage, tumor stage, chemotherapy, radiotherapy, and surgical treatment) influencing patient survival and the brain metastasis interval were balanced. Kaplan–Meier curves showed that patients with brain metastases in the moderate- to high-differentiation group had a longer overall survival (OS; P < 0.05) with a median OS (mOS) of 25.00 months (95% CI: 19.55–30.45 months) compared with an mOS of 14.67 months in the poor-differentiation group (95% CI: 11.80–17.53 months) (Figure 1).

In the univariate analysis, the pathological subtype was related to brain metastasis survival (HR: 1.546, 95% CI: 1.061–2.254; P = 0.023) but not to the brain metastasis interval (HR: 1.112; 95% CI: 0.762–1.621; P = 0.583). KPS, thoracic tumor staging, thoracic tumor chemotherapy, thoracic tumor radiation therapy, and thoracic tumor surgical treatment were related to the brain metastasis interval (P < 0.05). The survival of patients with brain metastases was lower in the poor-differentiation group (HR: 1.546; 95% CI: 1.061–2.254; P = 0.023) than in the moderate- to high-differentiation group in the multivariate analysis. Thoracic tumor radiation therapy (HR: 0.492; 95% CI: 0.282–0.858; P = 0.012), chemotherapy for thoracic tumors (HR: 0.399; 95% CI: 0.252–0.632; P < 0.001), and surgical treatment for thoracic tumors (HR: 0.198; 95% CI: 0.102–0.387; P < 0.001) were positive prognostic factors for the brain metastasis interval (Tables 4, 5).

4 Discussion

We evaluated the relationship between pathological subtype, patient survival after brain metastasis, and the interval between lung cancer diagnosis and brain metastases. This study revealed a longer mOS and OS in the moderate- to high-differentiation group. Furthermore, the pathological subtype of lung adenocarcinoma (P = 0.023) was revealed as an independent factor impacting survival time. Independent factors affecting the brain metastasis interval included radiation therapy for thoracic tumors (P = 0.012), chemotherapy for thoracic tumors (P < 0.001), and surgical treatment for thoracic tumors (P < 0.001).

In studies focusing on the interval between diagnosis and brain metastasis, the lung adenocarcinoma pathological subtype did not influence the brain metastasis interval; however, treatments

TABLE 2 Univariate and multivariate Cox regression analyses before propensity score matching to examine the overall survival.

Characteristics	Total(N)	Univariate analysis		Multivariate analysis	
		Hazard ratio (95% CI)	P value	Hazard ratio (95% CI)	P value
pathological subtype	156	1.421 (1.020-1.981)	**0.038**	1.421 (1.020-1.981)	**0.038**
age	156	1.002 (0.709-1.415)	0.993		
gender	156	0.790 (0.568-1.098)	0.161		
Whether smoke	156	1.175 (0.836-1.652)	0.353		
KPS score	156	1.206 (0.870-1.673)	0.260		
Lymph node metastasis	156	1.153 (0.786-1.690)	0.466		
Whether brain metastases have occurred at the time of diagnosis	156	0.765 (0.526-1.112)	0.161		
Tumor location	156	0.825 (0.541-1.256)	0.369		
T stage	156	0.933 (0.656-1.327)	0.701		
N stage	156	1.173 (0.834-1.649)	0.359		
TNM stage	156	0.852 (0.614-1.181)	0.336		
Thoracic tumor radiation	156	0.961 (0.643-1.438)	0.848		
Thoracic tumor chemotherapy	156	1.103 (0.756-1.609)	0.610		
Thoracic tumor surgery	156	0.991 (0.714-1.376)	0.957		

Bold values represent a valuable result.

10.3389/fonc.2024.1433505

TABLE 3 Univariate and multivariate Cox regression analyses before propensity score matching to examine the brain metastasis interval.

Characteristics	Total(N)	Univariate analysis		Multivariate analysis	
		Hazard ratio (95% CI)	P value	Hazard ratio (95% CI)	P value
pathological subtype	156	1.190 (0.853-1.660)	0.305		
age	156	1.149 (0.811-1.628)	0.434		
gender	156	0.923 (0.665-1.281)	0.631		
Whether smoke	156	0.946 (0.675-1.326)	0.748		
KPS score	156	1.680 (1.204-2.345)	**0.002**	1.226 (0.859-1.751)	0.261
Lymph node metastasis	156	1.158 (0.790-1.698)	0.452		
Whether brain metastases have occurred at the time of diagnosis	156	1997565716.821 (0.000-Inf)	0.994		
Tumor location	156	0.601 (0.393-0.919)	**0.019**	0.516 (0.331-0.802)	**0.003**
T stage	156	1.468 (1.025-2.102)	**0.036**	0.958 (0.656-1.400)	0.826
N stage	156	1.186 (0.843-1.670)	0.327		
TNM stage	156	2.952 (2.079-4.191)	**<0.001**	1.239 (0.730-2.105)	0.427
Thoracic tumor radiation	156	0.509 (0.337-0.768)	**0.001**	0.651 (0.416-1.019)	0.060
Thoracic tumor chemotherapy	156	0.439 (0.297-0.647)	**<0.001**	0.415 (0.276-0.624)	**<0.001**
Thoracic tumor surgery	156	0.212 (0.145-0.308)	**<0.001**	0.266 (0.151-0.469)	**<0.001**

Bold values represent a valuable result.

targeting thoracic tumors (surgical treatment, chemotherapy, and radiation) tended to delay the development of brain metastases. Similarly, some studies have found that patients with lung adenocarcinoma who did not receive complementary treatments were more prone to develop brain metastasis after a definitive diagnosis of lung cancer (18, 19). However, most studies evaluating the time interval between diagnosis and brain metastasis did not group patients by pathological subtypes (no comparative data have

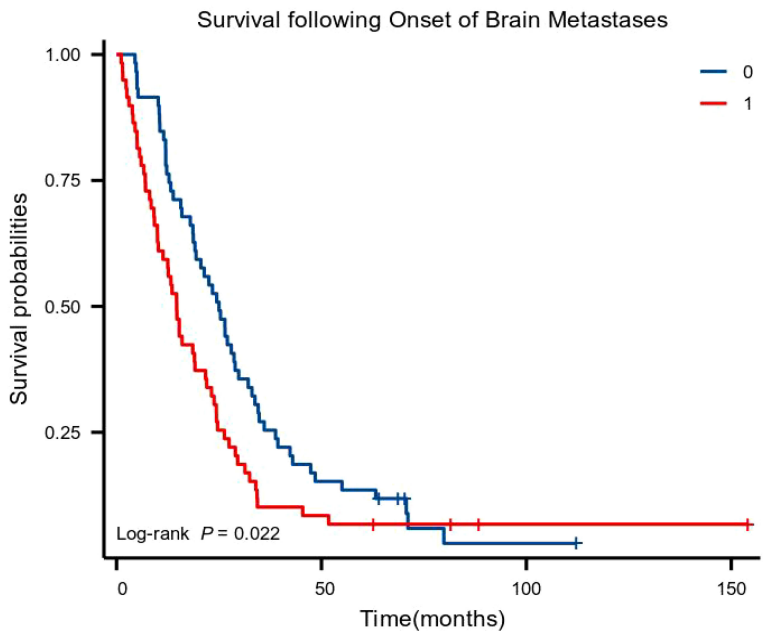

FIGURE 1
Kaplan–Meier curves for overall survival (0: moderate- to high-differentiation group; 1: poor-differentiation group).

TABLE 4 Univariate and multivariate Cox regression analyses after propensity score matching to examine overall survival.

Characteristics	Total(N)	Univariate analysis		Multivariate analysis	
		Hazard ratio (95% CI)	P value	Hazard ratio (95% CI)	P value
pathological subtype	118	1.546 (1.061-2.254)	**0.023**	1.546 (1.061-2.254)	**0.023**
age	118	1.035 (0.701-1.528)	0.863		
gender	118	1.074 (0.734-1.572)	0.712		
Whether smoke	118	1.020 (0.698-1.491)	0.917		
KPS score	118	1.234 (0.848-1.797)	0.273		
Lymph node metastasis	118	0.986 (0.647-1.502)	0.946		
Whether brain metastases have occurred at the time of diagnosis	118	0.757 (0.490-1.170)	0.211		
Tumor location	118	0.753 (0.436-1.302)	0.310		
T stage	118	0.983 (0.660-1.466)	0.934		
N stage	118	1.124 (0.765-1.652)	0.551		
TNM stage	118	0.855 (0.587-1.244)	0.413		
Thoracic tumor radiation	118	0.839 (0.516-1.364)	0.478		
Thoracic tumor chemotherapy	118	0.971 (0.635-1.487)	0.894		
Thoracic tumor surgery	118	1.014 (0.697-1.474)	0.944		

Bold values represent a valuable result.

TABLE 5 Univariate and multivariate Cox regression analyses after propensity score matching to examine the brain metastasis interval.

Characteristics	Total(N)	Univariate analysis		Multivariate analysis	
		Hazard ratio (95% CI)	P value	Hazard ratio (95% CI)	P value
pathological subtype	118	1.112 (0.762-1.621)	0.583		
age	118	1.105 (0.746-1.637)	0.618		
gender	118	0.896 (0.610-1.314)	0.574		
Whether smoke	118	0.939 (0.641-1.376)	0.746		
KPS score	118	2.039 (1.384-3.003)	**<0.001**	1.373 (0.911-2.069)	0.130
Lymph node metastasis	118	1.000 (0.655-1.527)	1.000		
Whether brain metastases have occurred at the time of diagnosis	118	2350794642.420 (0.000-Inf)	0.995		
Tumor location	118	0.744 (0.430-1.289)	0.292		
T stage	118	1.413 (0.942-2.120)	0.095	1.031 (0.674-1.578)	0.889
N stage	118	1.131 (0.769-1.662)	0.532		
TNM stage	118	2.715 (1.822-4.046)	**<0.001**	0.852 (0.460-1.579)	0.611
Thoracic tumor radiation	118	0.443 (0.263-0.747)	**0.002**	0.492 (0.282-0.858)	**0.012**
Thoracic tumor chemotherapy	118	0.420 (0.270-0.652)	**<0.001**	0.399 (0.252-0.632)	**<0.001**
Thoracic tumor surgery	118	0.207 (0.134-0.321)	**<0.001**	0.198 (0.102-0.387)	**<0.001**

Bold values represent a valuable result.

been found at this time). Yang et al. (20) observed that shorter brain metastasis time intervals adversely affect the survival of patients undergoing surgery. Hence, our understanding of the relationship between brain metastasis time intervals and pathological subtypes needs to be improved to ensure timely treatment.

Various histological subtypes of lung adenocarcinoma show diverse clinical features, and the risk of recurrence and prognosis also differ. Yaldız et al. (21) found that solid and micropapillary histological subtypes were poor prognostic factors in invasive lung adenocarcinomas undergoing surgical treatment. Additionally, Russell et al. (22) found that micropapillary adenocarcinomas had a lower survival rate than papillary- and vesicular-dominant adenocarcinomas. Several studies exploring the relationship between pathological subtypes and brain metastasis found that patients with micropapillary and solid types are prone to brain metastases with lower survival (23–25). Consistent with previous studies, this study found a significant correlation between pathological subtypes and the progression and prognosis of brain metastases in invasive lung adenocarcinoma. Therefore, patients with a pathology suggestive of solid and micropapillary types should be closely followed up with postoperative examinations to observe tumor metastasis, and these should be treated aggressively.

The pathological subtypes also offer insights into the clinical treatment options. The response of distinct lung adenocarcinoma subtypes to targeted therapy and immunotherapy requires further investigation. For patients with invasive adenocarcinoma, there are a number of conventional targets for mutation detection related to the specific histological growth pattern of adenocarcinomas. The epidermal growth factor receptor (EGFR) gene is the most well-studied molecular target in lung cancer and is a biomarker for predicting the effectiveness of targeted therapies (26). Various studies have reported that EGFR mutations have the highest incidence rate in micropapillary tumors, followed by alveolar and solid tumor types (27–29). Studying the relationship between pathological subtype and gene mutation status provides important information to assist patients in their therapeutic choices. The expression of programmed death-ligand 1 (PD-L1) in invasive lung adenocarcinomas also varies greatly according to the histological type. PD-L1-positive tumors are more common in alveolar and solid adenocarcinomas than in other adenocarcinoma subtypes (30). This pathological classification can have a meaningful impact when screening patients for lung adenocarcinomas who are more suitable for immunotherapy, both for postoperative adjuvant chemotherapy and for treatment after recurrence. The patient's pathological subtype may assist in selecting the most appropriate treatment regimen.

Each histological subtype of invasive lung adenocarcinoma is associated with a distinct prognosis, and the underlying mechanisms have been somewhat elucidated. One study found that, at the single-cell level, the tumor microenvironment in solid-type invasive lung adenocarcinoma was more hypoxic and acidic than that in other histological subtypes. This leads to fewer T cells, an increase in immunosuppressive myeloid cells, and a higher incidence of tumor metastasis (31). In addition, when typing lung adenocarcinomas according to different DNA methylation levels, the hypermethylated subtypes tend to be micropapillary-predominant cases. This demonstrates that patients with brain metastases from invasive pulmonary adenocarcinomas of the solid and micropapillary types have a worse prognosis, adding to the credibility of our study (32). Patients with early-stage cancer have a higher risk of metastasis if their tumors contain a highly aggressive component, requiring more stringent adjuvant therapy and close follow-up.

This study has some limitations. It was a single-center retrospective study; therefore, selection bias and confounding factors are unavoidable. Furthermore, follow-ups were not continued to obtain patient survival data. Moreover, in our cohort, the proportion of patients with gene mutations was not analyzed.

In conclusion, the findings indicate that pathological subtype is an independent risk factor affecting prognosis. Additionally, patients with poorly differentiated pathological subtypes had a lower survival rate. This provides important information for clinicians to judge patient prognosis without the need for other auxiliary techniques, as well as a reliable experimental basis for guiding the time window of treatment for this type of patient. Future prospective randomized cohort studies with large sample sizes need to be conducted for more detailed analyses. In addition, further research should consider the proportion of patients with gene mutations to draw relevant conclusions. In the near future, we expect to be able to analyze the progression of lung adenocarcinoma in terms of tumor recurrence, lymph node metastasis, and hematopoietic metastasis according to pathological subtypes, thereby leading to more accurate diagnosis and treatment.

Data availability statement

The raw data supporting the conclusions of this article will be made available by the authors, without undue reservation.

Ethics statement

The studies involving humans were approved by Medical Ethics Committee of Liaoning Cancer Hospital and the number is 2020X0102. The studies were conducted in accordance with the local legislation and institutional requirements. The participants provided their written informed consent to participate in this study.

Author contributions

CZ: Writing – original draft. XZ: Writing – original draft. XY: Writing – original draft. HX: Writing – review & editing. HT: Writing – review & editing. YS: Writing – review & editing. ML: Writing – review & editing. YJ: Writing – review & editing. TW: Writing – original draft, Writing – review & editing.

Funding

The author(s) declare financial support was received for the research, authorship, and/or publication of this article. This work is supported by the Fundamental Research Funds for the Central Universities [LD2023032, LD2023011, LD202221], Ministry of Science and Technology of the People's Republic of China [G2023127016L].

Acknowledgments

We are very grateful to the participants who participated in the study because they spend precious time participating in the study.

Conflict of interest

The authors declare that the research was conducted in the absence of any commercial or financial relationships that could be construed as a potential conflict of interest.

Publisher's note

References

1. Siegel RL, Miller KD, Wagle NS, Jemal A. Cancer statistics, 2023. *CA: Cancer J Clin*. (2023) 73:17–48. doi: 10.3322/caac.21763

2. Chen P, Liu Y, Wen Y, Zhou C. Non-small cell lung cancer in China. *Cancer Commun (London England)*. (2022) 42:937–70. doi: 10.1002/cac2.12359

3. Lu S, Yu Y, Yang Y. Retrospect and prospect for lung cancer in China: clinical advances of immune checkpoint inhibitors. *oncologist*. (2019) 24:S21–s30. doi: 10.1634/theoncologist.2019-IO-S1-s02

4. de Castro J, Tagliaferri P, de Lima VCC, Ng S, Thomas M, Arunachalam A, et al. Systemic therapy treatment patterns in patients with advanced non-small cell lung cancer (NSCLC): PIvOTAL study. *Eur J Cancer Care*. (2017) 26:e12734. doi: 10.1111/ecc.12734

5. Page S, Milner-Watts C, Perna M, Janzic U, Vidal N, Kaudeer N, et al. Systemic treatment of brain metastases in non-small cell lung cancer. *Eur J Cancer (Oxford England: 1990)*. (2020) 132:187–98. doi: 10.1016/j.ejca.2020.03.006

6. Duma N, Santana-Davila R, Molina JR. Non-small cell lung cancer: epidemiology, screening, diagnosis, and treatment. *Mayo Clinic Proc*. (2019) 94:1623–40. doi: 10.1016/j.mayocp.2019.01.013

7. Farris JC, Hughes RT, Razavian NB, Pearce JB, Snavely AC, Chan MD, et al. Brain metastasis incidence and patterns of presentation after definitive treatment of locally advanced non-small cell lung cancer: A potential argument for brain magnetic resonance imaging surveillance. *Adv Radiat Oncol*. (2023) 8:101058. doi: 10.1016/j.adro.2022.101058

8. Peters S, Bexelius C, Munk V, Leighl N. The impact of brain metastasis on quality of life, resource utilization and survival in patients with non-small-cell lung cancer. *Cancer Treat Rev*. (2016) 45:139–62. doi: 10.1016/j.ctrv.2016.03.009

9. Gupta S, Singh S, Chophy A, Nair S, Ahuja R, Kusum K, et al. Analysis of prognostic factors in patients with brain metastases affecting survival. *J Egyptian Natl Cancer Institute*. (2022) 34:45. doi: 10.1186/s43046-022-00146-z

10. Zhu H, Zhou L, Guo Y, Yang G, Dong Q, Zhang Z, et al. Factors for incidence risk and prognosis in non-small-cell lung cancer patients with synchronous brain metastasis: a population-based study. *Future Oncol (London England)*. (2021) 17:2461–73. doi: 10.2217/fon-2021-0103

11. Han X, Li H. Research progress in the treatment of brain metastases from non-small cell lung cancer. *Zhongguo Fei Ai Za Zhi Chin J Lung Cancer*. (2020) 23:1087–94. doi: 10.3779/j.issn.1009-3419.2020.102.39

12. Jena A, Taneja S, Talwar V, Sharma JB. Magnetic resonance (MR) patterns of brain metastasis in lung cancer patients: correlation of imaging findings with symptom. *J Thorac Oncol: Off Publ Int Assoc Study Lung Cancer*. (2008) 3:140–4. doi: 10.1097/JTO.0b013e318161d775

13. Won YW, Joo J, Yun T, Lee GK, Han JY, Kim HT, et al. A nomogram to predict brain metastasis as the first relapse in curatively resected non-small cell lung cancer patients. *Lung Cancer (Amsterdam Netherlands)*. (2015) 88:201–7. doi: 10.1016/j.lungcan.2015.02.006

14. Nicholson AG, Tsao MS, Beasley MB, Borczuk AC, Brambilla E, Cooper WA, et al. The 2021 WHO classification of lung tumors: impact of advances since 2015. *J Thorac Oncol*. (2022) 17:362–87. doi: 10.1016/j.jtho.2021.11.003

15. Chang C, Sun X, Zhao W, Wang R, Qian X, Lei B, et al. Minor components of micropapillary and solid subtypes in lung invasive adenocarcinoma (≤ 3 cm): PET/CT findings and correlations with lymph node metastasis. *La Radiol Med*. (2020) 125:257–64. doi: 10.1007/s11547-019-01112-x

16. Xu L, Zhou H, Wang G, Huang Z, Xiong R, Sun X, et al. The prognostic influence of histological subtypes of micropapillary tumors on patients with lung adenocarcinoma ≤ 2 cm. *Front Oncol*. (2022) 12:954317. doi: 10.3389/fonc.2022.954317

17. Takeno N, Tarumi S, Abe M, Suzuki Y, Kinoshita I, Kato T. Lung adenocarcinoma with micropapillary and solid patterns: Recurrence rate and trends. *Thorac Cancer*. (2023) 14:2987–92. doi: 10.1111/1759-7714.15087

18. Ilhan-Mutlu A, Osswald M, Liao Y, Gömmel M, Reck M, Miles D, et al. Bevacizumab prevents brain metastases formation in lung adenocarcinoma. *Mol Cancer Ther*. (2016) 15:702–10. doi: 10.1158/1535-7163.Mct-15-0582

19. Chamberlain MC, Baik CS, Gadi VK, Bhatia S, Chow LQ. Systemic therapy of brain metastases: non-small cell lung cancer, breast cancer, and melanoma. *Neuro-oncology*. (2017) 19:i1–i24. doi: 10.1093/neuonc/now197

20. Yang Z, Chen H, Jin T, Sun L, Li L, Zhang S, et al. The impact of time interval on prognosis in patients with non-small cell lung cancer brain metastases after metastases surgery. *World Neurosurg*. (2023) 180:e171–82. doi: 10.1016/j.wneu.2023.09.021

21. Yaldız D, Örs Kaya Ş, Ceylan KC, Acar A, Aydoğdu Z, Gürsoy S, et al. Prognostic effects of predominant histologic subtypes in resected pulmonary adenocarcinomas. *Balkan Med J*. (2019) 36:347–53. doi: 10.4274/balkanmedj.galenos.2019.2019.1.130

22. Russell PA, Wainer Z, Wright GM, Daniels M, Conron M, Williams RA. Does lung adenocarcinoma subtype predict patient survival?: A clinicopathologic study based on the new International Association for the Study of Lung Cancer/American Thoracic Society/European Respiratory Society international multidisciplinary lung adenocarcinoma classification. *J Thorac Oncol*. (2011) 6:1496–504. doi: 10.1097/JTO.0b013e318221f701

23. Lengel HB, Mastrogiacomo B, Connolly JG, Tan KS, Liu Y, Fick CN, et al. Genomic mapping of metastatic organotropism in lung adenocarcinoma. *Cancer Cell*. (2023) 41:970–985.e973. doi: 10.1016/j.ccell.2023.03.018

24. Arrieta O, Salas AA, Cardona AF, Díaz-García D, Lara-Mejía L, Escamilla I, et al. Risk of development of brain metastases according to the IASLC/ATS/ERS lung adenocarcinoma classification in locally advanced and metastatic disease. *Lung Cancer (Amsterdam Netherlands)*. (2021) 155:183–90. doi: 10.1016/j.lungcan.2021.01.023

25. Casteillo F, Guy JB, Dal-Col P, Karpathiou G, Pommier B, Bayle-Bleuez S, et al. Pathologic subtypes of lung adenocarcinoma brain metastasis is a strong predictor of survival after resection. *Am J Surg Pathol*. (2018) 42:1701–7. doi: 10.1097/pas.0000000000001161

26. Araghi M, Mannani R, Heidarnejad maleki A, Hamidi A, Rostami S, Safa SH, et al. Recent advances in non-small cell lung cancer targeted therapy; an update review. *Cancer Cell Int*. (2023) 23:162. doi: 10.1186/s12935-023-02990-y

27. Chen Z, Liu X, Zhao J, Yang H, Teng X. Correlation of EGFR mutation and histological subtype according to the IASLC/ATS/ERS classification of lung adenocarcinoma. *Int J Clin Exp Pathol*. (2014) 7(11):8039–45.

28. Kim HJ, Choi EY, Jin HJ, Shin KC. Relationship between EGFR mutations and clinicopathological features of lung adenocarcinomas diagnosed via small biopsies. *Anticancer Res*. (2014) 34:3189–95.

29. Song Z, Zhu H, Guo Z, Wu W, Sun W, Zhang Y. Correlation of EGFR mutation and predominant histologic subtype according to the new lung adenocarcinoma classification in Chinese patients. *Med Oncol (Northwood London England)*. (2013) 30:645. doi: 10.1007/s12032-013-0645-1

30. Miyazawa T, Marushima H, Saji H, Kojima K, Hoshikawa M, Takagi M, et al. PD-L1 expression in non-small-cell lung cancer including various adenocarcinoma subtypes. *Ann Thorac Cardiovasc Surgery: Off J Assoc Thorac Cardiovasc Surgeons Asia*. (2019) 25:1–9. doi: 10.5761/atcs.oa.18-00163

31. Li D, Yu H, Hu J, Li S, Yan Y, Li S, et al. Comparative profiling of single-cell transcriptome reveals heterogeneity of tumor microenvironment between solid and acinar lung adenocarcinoma. *J Trans Med*. (2022) 20:423. doi: 10.1186/s12967-022-03620-3

32. Ito Y, Usui G, Seki M, Fukuyo M, Matsusaka K, Hoshii T, et al. Association of frequent hypermethylation with high grade histological subtype in lung adenocarcinoma. *Cancer Sci*. (2023) 114(7):3003–13. doi: 10.1111/cas.15817

frontiers | Frontiers in Oncology

TYPE Systematic Review
PUBLISHED 21 October 2024
DOI 10.3389/fonc.2024.1448336

OPEN ACCESS

EDITED BY
Lin Zhou,
Sichuan University, China

REVIEWED BY
Mohamed Rahouma,
NewYork-Presbyterian, United States
Song Xu,
Tianjin Medical University General Hospital, China

*CORRESPONDENCE
Shihao Zhang
15607972002@163.com

RECEIVED 13 June 2024
ACCEPTED 02 October 2024
PUBLISHED 21 October 2024

CITATION
Chen Z, Fu X, Zhu L, Wen X and Zhang S (2024) The benefit and risk of addition of chemotherapy to EGFR tyrosine kinase inhibitors for EGFR-positive non-small cell lung cancer patients with brain metastases: a meta-analysis based on randomized controlled trials.
Front. Oncol. 14:1448336.
doi: 10.3389/fonc.2024.1448336

The benefit and risk of addition of chemotherapy to EGFR tyrosine kinase inhibitors for EGFR-positive non-small cell lung cancer patients with brain metastases: a meta-analysis based on randomized controlled trials

Zhigang Chen[1], Xiang Fu[1], Lingping Zhu[1], Xiurong Wen[2] and Shihao Zhang[2*]

[1]Department of Oncology, Shangrao People's Hospital, Shangrao, China, [2]Department of Respiratory and Critical Care Medicine, Ganzhou People's Hospital, Ganzhou, China

Background: Combining epidermal growth factor receptor (EGFR) tyrosine kinase inhibitors (TKIs) with chemotherapy (ETC) offers more advantages for patients with EGFR-positive non-small cell lung cancer (NSCLC) than using EGFR TKIs alone (ET). However, whether this conclusion applies to patients with brain metastases (BM) remains controversial. This meta-analysis was performed to evaluate the benefits and risks of the two groups.

Methods: Six databases were systematically searched for relevant literatures comparing ETC versus ET in treating EGFR-positive NSCLC patients with BM. The primary outcome assessed was overall survival (OS), while secondary outcomes included progression-free survival (PFS), and central nervous system (CNS)-PFS, responses, progression status and safety.

Results: Seven studies based on five randomized clinical trials with 550 patients were included. The ETC group exhibited better OS (hazard ratio [HR]: 0.64 [0.48, 0.87]), PFS (HR: 0.42 [0.34, 0.52]), and CNS-PFS (HR: 0.42 [0.31, 0.57]). The benefits in survival for OS, PFS, and CNS-PFS were validated in nearly all subgroups. Meanwhile, the overall objective response rate (ORR) (risk ratio [RR]: 1.25 [1.02, 1.52]) and CNS-ORR (RR: 1.19 [0.93, 1.51]) also tended to favor the ETC group. However, the addition of chemotherapy also brought about more grade 3-5/serious adverse events (AEs). The top five grade 3-5 AEs in the ETC group were alanine aminotransferase increase (11.25%), neutropenia (7.5%), nausea (7.5%), anorexia (5%), and diarrhea (5%).

Conclusions: ETC appears to be better than ET in treating EGFR-positive NSCLC patients with BM, with better OS, PFS, CNS-PFS, and responses. However, its poorer safety profile also needs to be taken into consideration.

Systematic review registration: https://www.crd.york.ac.uk/PROSPERO/, identifier CRD42024551073.

KEYWORDS

EGFR, tyrosine kinase inhibitors, chemotherapy, non-small cell lung cancer, brain metastases, meta-analysis

Introduction

Lung cancer is the foremost cause of both incidence and mortality among malignant tumors globally, with non-small cell lung cancer (NSCLC) making up about 90% of cases (1). Epidermal growth factor receptor (EGFR) mutations are the most common type among NSCLC cases, occurring in approximately 15% of Western NSCLC patients and 30-40% of Asian patients (2). For advanced EGFR-positive NSCLC, EGFR tyrosine kinase inhibitors (TKIs) significantly extend progression-free survival (PFS) and overall survival (OS) compared to traditional chemotherapy, while reducing the occurrence of adverse events (AEs) (3). The combination of chemotherapy with EGFR-TKIs (ETC) further improves patient outcomes (4). However, there remains clinical debate regarding whether this conclusion applies to EGFR-positive NSCLC patients with brain metastases (BM).

The National Comprehensive Cancer Network (NCCN) and the European Society for Medical Oncology (ESMO) guidelines recommended both EGFR-TKI alone (ET) and ETC as first-line treatments for EGFR-positive NSCLC patients with BM (5, 6). Studies by Lou et al. and Hou et al. had demonstrated that ETC significantly improves patients' OS and PFS (7, 8). Janne et al. also reported that ETC significantly enhances patients' central nervous system (CNS) PFS (9). However, study by Miyauchi et al. indicated that ETC did not improve the OS of EGFR-positive NSCLC patients with BM and significantly increases the occurrence of AEs (10).

Addressing the clinical controversy outlined above, this meta-analysis compared the efficacy and safety of ETC and ET treatments in EGFR-positive NSCLC patients with BM.

Abbreviations: AEs, Adverse effects; BM, Brain metastases; CI, Confidence interval; CNS, Central Nervous System; CR, Complete response; CT, Cohort study; ECOG, Eastern Cooperative Oncology Group; EGFR, Epidermal growth factor receptor; ET, EGFR tyrosine kinase inhibitors alone; ETC, EGFR tyrosine kinase inhibitors in combination of chemotherapy; ESMO, European Society for Medical Oncology; GRADE, Grading of Recommendations, Assessment, Development, and Evaluation; HR, Hazard ratio; LC, Lung cancer; M/F, male/female; NCCN, National Comprehensive Cancer Network; NCI-CTCAE, National Cancer Institute Common Terminology Criteria for Adverse; NSCLC, Non-small cell lung cancer; ORR, Objective response rate; OS, Overall survival; OSR, Overall survival rate; P, Probability; PFS, Progression-free survival; PICOS, Participants, Intervention, Control, Outcome and Study design; PRISMA, Preferred Reporting Items for Systematic Reviews and Meta-Analysis; RCT, randomized controlled trial; RR, Risk ratio; TKIs, Tyrosine kinase inhibitors; TRAEs, Treatment-related adverse effects.

Materials and methods

Selection criteria

Inclusion criteria: (1) Population: EGFR-positive NSCLC patients with BM; (2) Intervention and comparison: ETC versus ET; (3) Outcomes: survival, responses, progression status, and safety; (4) Study design: Randomized clinical trial (RCT).

Exclusion criteria: (1) Case reports, reviews, or meta-analyses; (2) Animal studies; (3) Studies with inaccessible full-text or from which useful data cannot be extracted.

Search strategy

A computerized search was conducted in PubMed, Scopus, EMBASE, ScienceDirect, Cochrane Library, and Web of Science, covering studies published up to August 27, 2024, that compared ETC and ET in treating EGFR-positive NSCLC patients with BM. The English search terms used were: "EGFR," "Chemotherapy," "Lung cancer," and "Randomized" (Supplementary Table S1).

Data extraction

After independently screening the literature and extracting data, two researchers conducted a cross-check. The extracted data included baseline characteristics of studies (study design, number of patients, etc.), survival outcomes (OS, PFS, CNS-PFS, etc.), responses (ORR, DCR, etc.), progression status (total progression, CNS progression, etc.), and safety indicators (Total AEs, grade 3-5 AEs, etc. AEs were graded according to the National Cancer

Institute Common Terminology Criteria for Adverse Events [NCI-CTCAE], version 4.0/5.0) (11, 12). In instances of discrepancies, a third researcher was consulted to make a decision.

Outcome assessments

The survival rates of PFS, OS, and CNS-PFS were analyzed at 6 to 60 months. Subgroup analyses of PFS, OS, and CNS-PFS were also conducted according to age, sex, ECOG PS, EGFR mutation type, extracranial metastases, and EGFR TKIs.

Quality assessment

The five-point Jadad scale was used to assess the quality of RCTs, which evaluates randomization, blinding, and patient accountability. Studies with scores of 3 points or higher were considered to be of high quality (13).

The Grades of Recommendations Assessment, Development, and Evaluation (GRADE) system was employed to evaluate the evidence categories of the results, considering five aspects: imprecision, risk of bias, indirectness, inconsistency, and publication bias. The evidence was divided into four categories: very low, low, moderate, and high (14).

Statistical analysis

The effect measures used included the risk ratio (RR) for binary data and the hazard ratio (HR) for survival data. All effect sizes were presented with 95% confidence intervals (CI). Prior to combining the effect sizes, a test for heterogeneity should be conducted. Heterogeneity among included studies will be assessed using the default Chi-square test. If the p-value is less than 0.1 and the I^2 statistic is more than 50%, indicating significant heterogeneity. A fixed-effect model will be applied for data analysis if heterogeneity is non-significant. Otherwise, a random-effects model will be used. Funnel plots, Egger's test, and Begg's test were conducted to assess publication bias (15–17). REVMAN 5.3 and STATA 12.0 were used for data analysis. This study was conducted following the PRISMA guidelines and registered in PROSPERO (ID: CRD42024551073) (Supplementary Table S2).

Results

Search results

Seven studies based on 5 RCTs were included (274 patients were in the ETC group, while 276 were in the ET group) (Figure 1) (7–10, 18–20). Table 1 detailed the baseline characteristics of 5 RCTs. Four RCTs (7, 8, 10, 19, 20) were conducted in Asia and another one (9, 18) was global multicenter study. According to the quality assessment, all studies were of medium to high quality (Supplementary Table S3, Supplementary Figure S1). The quality of evidence for all results, as per the GRADE system, ranged from medium to high (Supplementary Table S4).

Survival

The OS was better in the ETC group (HR: 0.64 [0.48, 0.87]) (Figure 2). The overall survival rate (OSR) also tended to favor the ETC group at 12 to 60 months (Figure 3).

The PFS was better in the ETC group (HR: 0.42 [0.34, 0.52]) (Figure 4). The progression-free survival rate (PFSR) also tended to favor the ETC group at 6 to 30 months (Figure 5).

The CNS-PFS was better in the ETC group (HR: 0.42 [0.31, 0.57]) (Figure 4). The central nervous system progression-free survival rate (CNS-PFSR) also tended to favor the ETC group at 6 to 30 months (Supplementary Figure S2).

Subgroup analysis of survival

The survival advantages of OS, PFS, and CNS-PFS in the ETC group were confirmed in almost all subgroups according to age, sex, ECOG PS, EGFR mutation type, extracranial metastases, and EGFR TKIs. ECOG PS = 0, EGFR mutation - Ex19del, and a large intracranial tumor size < 20mm might be favorable factors for the ETC group (Table 2, Supplementary Figures S3–S5).

Responses

In the analysis of overall responses, the overall response rate (ORR) (RR: 1.25 [1.02, 1.52]) and partial response (PR) (RR: 1.25 [1.02, 1.52]) were higher in the ETC group. The disease control rate (DCR) was similar between the two groups. The stable disease (SD) (RR: 0.49 [0.26, 0.90]) was higher in the ET group (Supplementary Figure S6).

In the analysis of CNS responses, the CNS-ORR (RR: 1.19 [0.93, 1.51]) and CNS-CR (RR: 1.31 [1.02, 1.70]) were higher in the ETC group. The CNS-DCR, CNS-PR, and CNS-SD were similar between the two groups (Supplementary Figure S7).

Progression status

At the cutoff time of the studies, the total progression (RR: 0.85 [0.72, 1.01]) and CNS progression (RR: 0.72 [0.58, 0.90]) tended to favor the ETC group. The addition of chemotherapy was particularly effective in controlling newly developed intracranial lesions (RR: 0.63 [0.45, 0.87]) (Figure 6).

Safety

The rates of grade 3-5 AEs (RR: 2.10 [1.59, 2.77]), serious AEs (RR: 1.69 [1.10, 2.59]), discontinuation due to AEs (RR: 7.73 [3.57, 16.77]), and grade 3-5 treatment-related AEs (TRAEs) (RR: 3.65 [2.17, 6.15]) were higher in the ETC group. The total AEs, fatal AEs, dose interruption due to AEs, total TRAEs, serious TRAEs, and fatal TRAEs tended to favor the ET group without statistical differences (Table 3, Supplementary Figure S8).

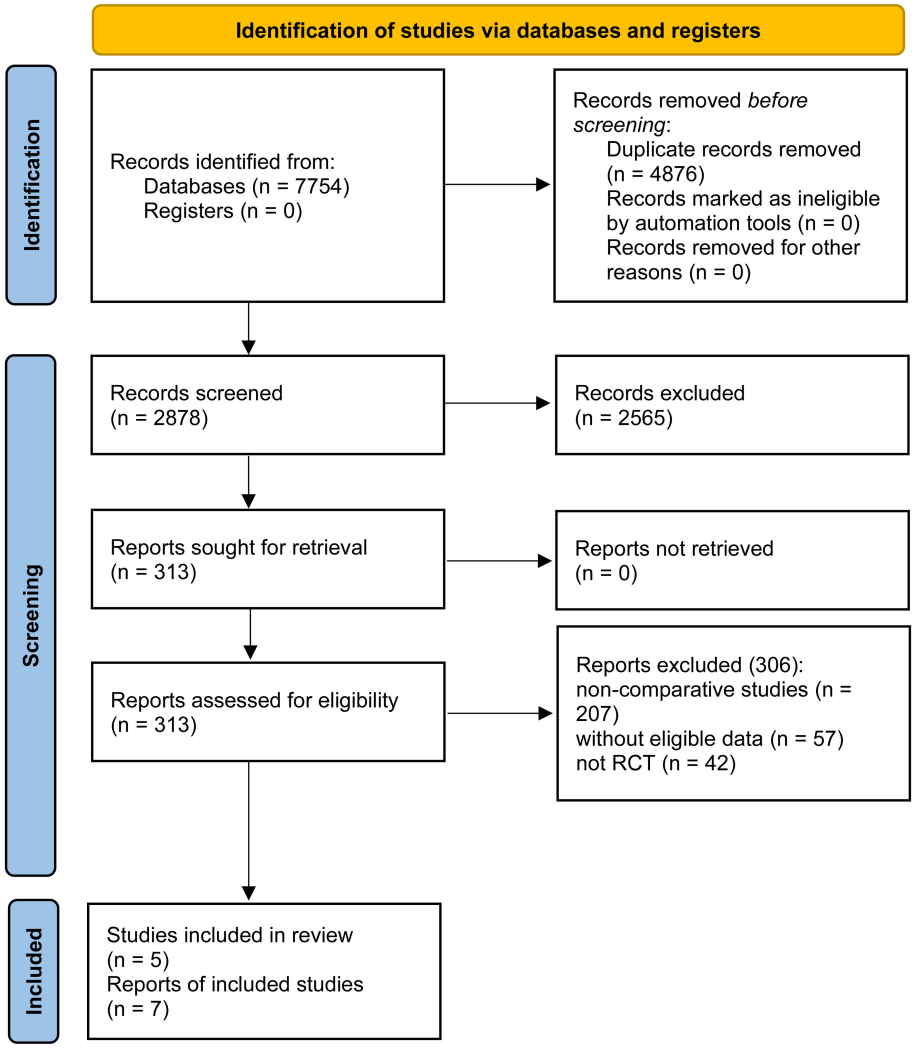

FIGURE 1
Flow chart.

In the analysis of any grade AEs, more cases of anorexia, alanine aminotransferase increase, neutropenia, alkaline phosphatase increase, nausea, fatigue, vomiting, blood creatinine increase, thrombocytopenia, and constipation were found in the ETC group (Table 4, Supplementary Figure S9).

In the analysis of grade 3-5 AEs, most AEs tended to favor the ET group without statistical differences. The top 5 grade 3-5 AEs in the ETC group were alanine aminotransferase increase (11.25%), neutropenia (7.5%), nausea (7.5%), anorexia (5%), and diarrhea (5%) (Supplementary Table S5, Supplementary Figure S10).

Sensitivity analysis

Sensitivity analyses of OS and PFS were performed, demonstrating that excluding any single study had no impact on the credibility of the results (Supplementary Figure S11).

Publication bias

Funnel plots of survival, OSR, CNS responses, and safety summary were constructed. It was observed that studies were evenly distributed on both sides of the funnel plot, with almost all falling within its confines. This suggested minimal publication bias in this study (Figure 7). Egger's and Begg's tests based on OS and PFS also showed no significant publication bias (Supplementary Figure S11).

Discussion

In recent years, for advanced NSCLC patients with EGFR mutations, EGFR-TKI has become the standard first-line treatment, replacing chemotherapy. The antitumor mechanisms of EGFR-TKI and chemotherapy differ, and relevant preclinical and clinical studies have confirmed the potential of combination therapy (21, 22). Numerous studies have demonstrated that

TABLE 1 Baseline characteristics of the included studies.

Study	Phase	Country	Groups	Patients	Sex (M/F)	Age (Mean, year)	Histologic type (Adeno/ Others)	EGFR TKI	Outcomes assessed	Follow up (months)
NCT04035486(FLAURA2, 2020.06-2021.12)										
Janne 2024 (9), Planchard 2023 (18)	III	Global multicenter	ETC	118	36/82	60	118/0	Osimertinib	Survival, Responses, Progression Status,AEs	22
			ET	104	38/66	61	104/0			24
NCT01951469(GAP BRAIN, 2016.01-2021.08)										
Hou 2023 (8)	III	China	ETC	80	36/44	55	76/4	Gefitinib	Survival, Responses, Progression Status,AEs	21
			ET	81	38/43	56	77/4			21
UMIN000006340(NEJ009, 2011.10-2015.09)										
Miyauchi 2022 (10), Hosomi 2020 (19)	III	Japan	ETC	38	–	64	38/0	Gefitinib	Survival	84
			ET	50	–	65	50/0			84
NCT02148380(2011.04-2015.12)										
Lou 2022 (7)	II	China	ETC	8	–	–	8/0	Gefitinib	Survival	–
			ET	7	–	–	7/0			–
CTRI/2016/08/007149(2016.08-2018.08)										
Noronha 2020 (20)	III	India	ETC	30	–	54	30/0	Gefitinib	Survival	17
			ET	34	–	56	34/0			17

EGFR, Epidermal growth factor receptor; ET, EGFR tyrosine kinase inhibitors alone; ETC, EGFR tyrosine kinase inhibitors in combination of chemotherapy; M/F, Male/Female; TKIs, Tyrosine kinase inhibitors.

combination therapy can achieve better OS and PFS for advanced EGFR-positive NSCLC (23, 24). The survival advantage of combination therapy has also been confirmed by numerous meta-analyses, not only compared to chemotherapy, but also compared to EGFR-TKI monotherapy (Supplementary Table S6). However, whether this conclusion applies to patients with BM remains controversial in clinical practice. This meta-analysis, for the first time, compared the ETC and ET treatments in EGFR-positive NSCLC patients with BM based on RCTs. The results showed that the ETC group exhibited better survival, which was confirmed across almost all subgroups. Additionally, the overall objective response rate (ORR) and CNS-ORR tended to favor the ETC group. However, the addition of chemotherapy also led to more grade 3-5/serious AEs.

The greatest advantage of ETC over the ET group lies in its superior survival outcomes (OS, PFS, and CNS-PFS). This conclusion was supported by evidence from studies by Lou et al. and Hou et al. (7, 8). Preclinical studies had found that the ETC exerted a synergistic inhibitory effect on EGFR-sensitive cells (25, 26), as confirmed in trials such as CALGB30406, FASTACT-2, and NEJ005/TCOG0902 (27–29). NEJ005 also indicated a significant advantage in OS for EGFR-TKI combined with chemotherapy compared to sequential treatment, although the difference in PFS between patients was not significant (29). The enhanced efficacy of ETC might be related to the reduction of

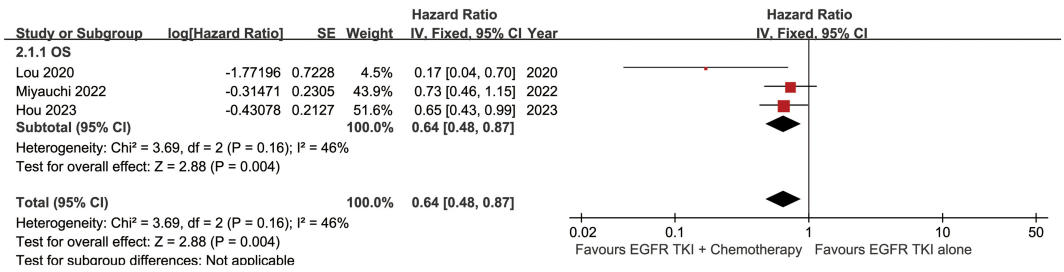

FIGURE 2
Forest plots of overall survival associated with ETC versus ET.

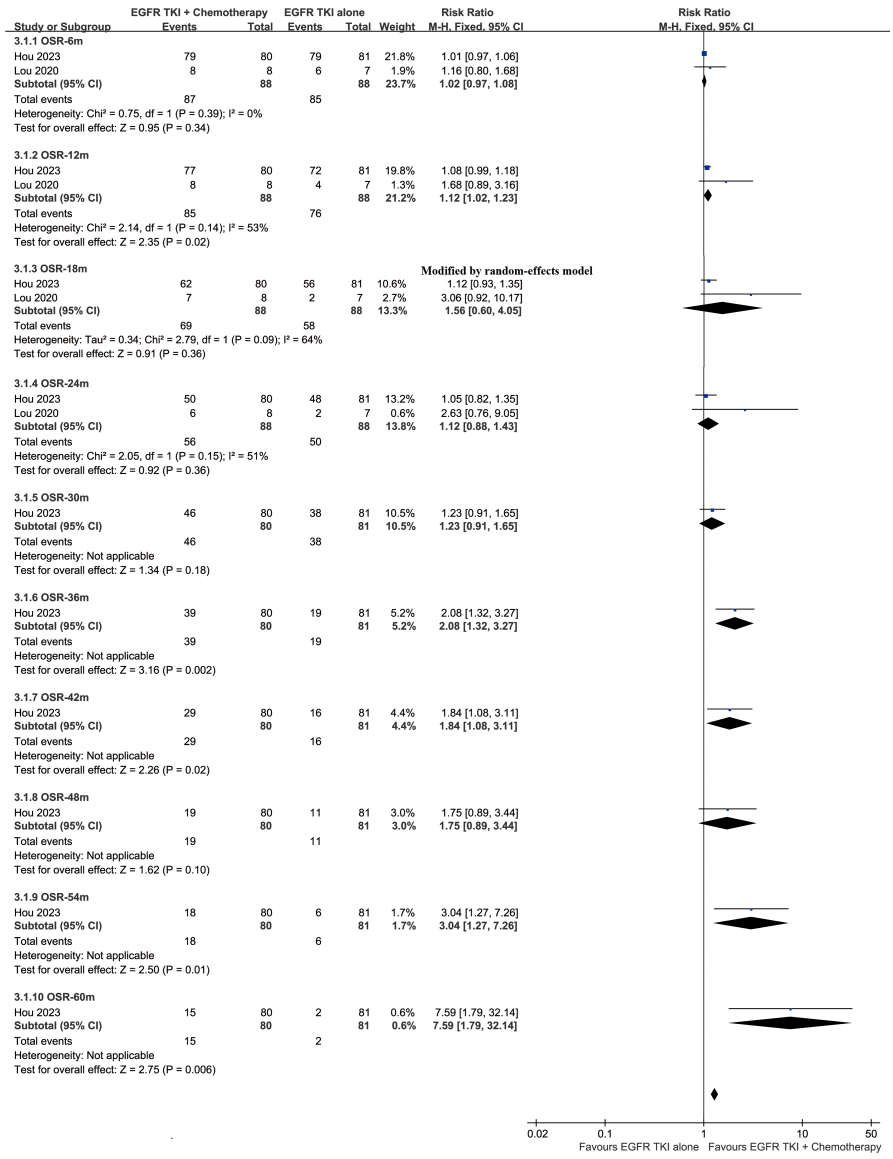

FIGURE 3
Forest plots of OSR at 6-60 months associated with ETC versus ET.

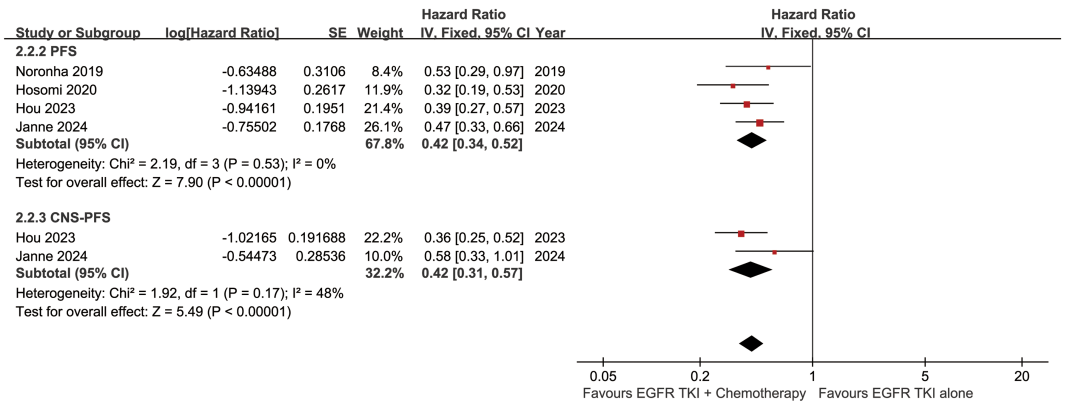

FIGURE 4
Forest plots of progression-free survival, and CNS-progression-free survival associated with ETC versus ET.

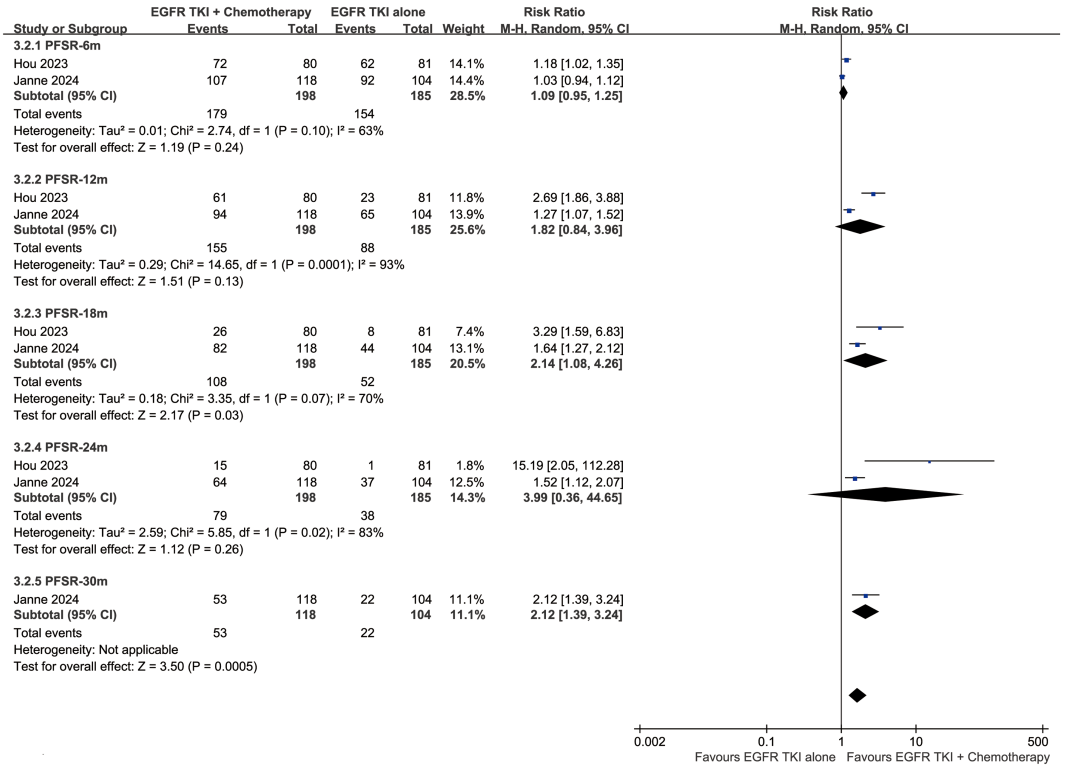

FIGURE 5
Forest plots of PFSR at 3-30 months associated with ETC versus ET.

TABLE 2 Subgroup analysis of overall survival, progression-free survival, and CNS-progression-free survival.

Subgroups	Overall survival		Progression-free survival		CNS-Progression-free survival	
	HR (95% CI)	*P*	HR (95% CI)	*P*	HR (95% CI)	*P*
All patients	0.64 [0.48, 0.87]	0.004	0.42 [0.34, 0.52]	<0.00001	0.42 [0.31, 0.57]	<0.00001
Age						
< 65 years	0.64 [0.40, 1.02]	0.06	0.40 [0.26, 0.62]	<0.0001	0.40 [0.26, 0.61]	<0.0001
> 65 years	1.05 [0.40, 2.75]	0.92	0.42 [0.15, 1.19]	0.1	0.21 [0.06, 0.74]	0.01
Sex						
Female	0.64 [0.35, 1.17]	0.15	0.33 [0.18, 0.60]	0.0003	0.28 [0.16, 0.49]	<0.0001
Male	0.60 [0.34, 1.07]	0.08	0.45 [0.26, 0.78]	0.004	0.43 [0.25, 0.73]	0.002
Smoking status						
Smoker	0.77 [0.35, 1.69]	0.51	0.43 [0.20, 0.92]	0.03	0.49 [0.24, 1.00]	0.05
Non-smoker	0.56 [0.34, 0.94]	0.03	0.36 [0.22, 0.58]	<0.0001	0.28 [0.18, 0.45]	<0.00001
ECOG PS						
0	0.36 [0.13, 0.99]	0.05	0.31 [0.13, 0.73]	0.008	0.20 [0.09, 0.46]	0.0001
1	0.78 [0.49, 1.24]	0.29	0.42 [0.27, 0.66]	0.0001	0.43 [0.28, 0.66]	0.0001
Large intracranial tumor size						
< 20mm	0.53 [0.32, 0.88]	0.01	0.32 [0.18, 0.57]	0.0001	0.31 [0.19, 0.51]	<0.00001
> 20mm	0.97 [0.46, 2.04]	0.94	0.43 [0.24, 0.77]	0.005	0.44 [0.23, 0.86]	0.02

(Continued)

TABLE 2 Continued

Subgroups	Overall survival		Progression-free survival		CNS-Progression-free survival	
	HR (95% CI)	*P*	HR (95% CI)	*P*	HR (95% CI)	*P*
EGFR mutation						
Ex19del	0.40 [0.22, 0.73]	0.003	0.39 [0.24, 0.63]	0.0001	0.29 [0.17, 0.50]	<0.0001
L858R	0.83 [0.45, 1.54]	0.55	0.34 [0.15, 0.77]	0.009	0.34 [0.19, 0.62]	0.0004
Extracranial metastases						
Yes	0.54 [0.33, 0.88]	0.01	0.47 [0.33, 0.66]	<0.0001	0.35 [0.22, 0.55]	<0.00001
No	0.76 [0.31, 1.88]	0.55	0.39 [0.30, 0.52]	<0.00001	0.30 [0.14, 0.65]	0.002
EGFR TKIs						
Osimertinib	–	–	–	–	0.58 [0.33, 1.01]	0.06
Gefitinib	–	–	–	–	0.36 [0.25, 0.52]	<0.00001

CI, Confidence interval; CNS, Central Nervous System; ECOG, Eastern Cooperative Oncology Group; EGFR, Epidermal growth factor receptor; HR, Hazard ratio; P, Probability; TKIs, Tyrosine kinase inhibitors.

EGFR T790M mutation, which could promote resistance to EGFR TKIs (30). Another reason was the better drug response observed in the ETC group. Our study indicated that the ETC group exhibits superior ORR and CNS-ORR. The survival advantages of OS, PFS, and CNS-PFS in the ETC group were confirmed across almost all subgroups, particularly in patients with ECOG performance status = 0, EGFR mutation - Ex19del, and large intracranial tumor size < 20mm. In conclusion, due to its superior systemic and intracranial efficacy, we believed that combination therapy should be considered as the preferred treatment for EGFR-positive NSCLC patients with BM.

The main concern among clinical physicians regarding the ETC regimen is the potential for chemotherapy to induce more severe AEs (31, 32). Our study indicated that the rates of grade 3-5 AEs, serious AEs, discontinuation due to AEs, and grade 3-5 TRAEs were higher in the ETC group. The top 5 grade 3-5 AEs in the ETC group were alanine aminotransferase increase (11.25%), neutropenia (7.5%), nausea (7.5%), anorexia (5%), and diarrhea (5%). Studies by Janne et al. and Hou et al. had also found a significant increase in AEs occurrence in the ETC group, primarily concentrated in any grade AEs (8, 9). Although most grade 3-5 AEs tended to favor the ET group, they did not reach statistical significance. Therefore, we believe that the combined use of EGFR TKIs and chemotherapy, while potentially increasing the occurrence of AEs, remains within an acceptable range in terms of incidence and severity.

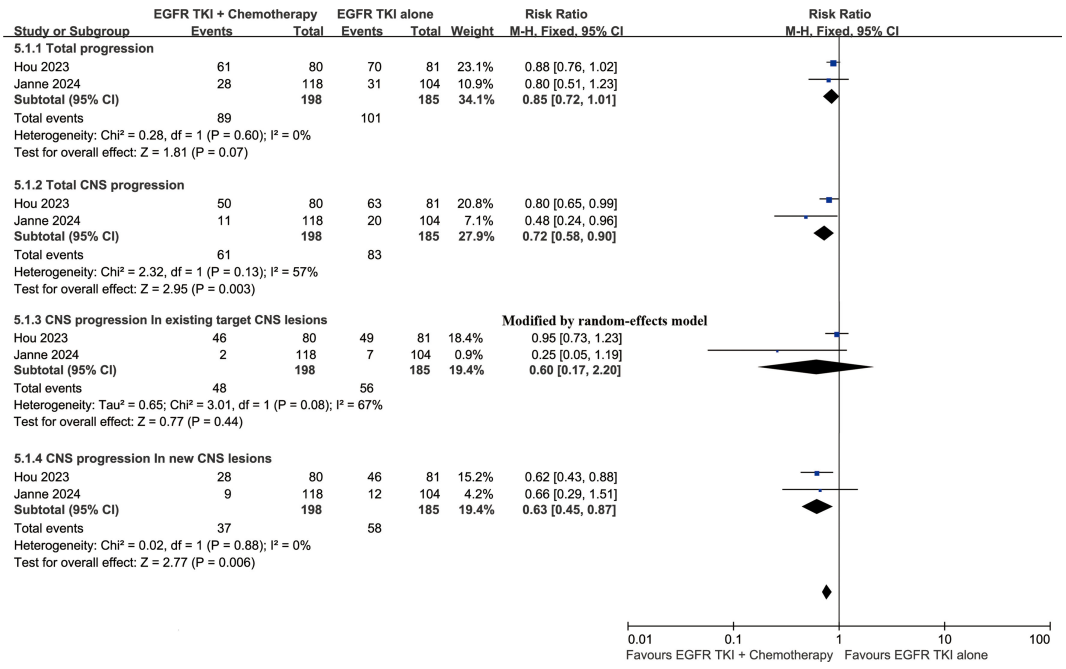

FIGURE 6
Forest plots of progression status associated with ETC versus ET.

TABLE 3 Summary of adverse events.

Adverse events	ETC		ET		Risk ratio [95% CI]	P
	Event/total	%	Event/total	%		
Total adverse events	196/198	98.99%	177/185	95.68%	1.04 [0.96, 1.12]	0.39
Grade 3-5 adverse events	107/198	54.04%	47/185	25.41%	2.10 [1.59, 2.77]	<0.00001
Serious adverse events	44/118	37.29%	23/104	22.12%	1.69 [1.10, 2.59]	0.02
Fatal adverse events	7/118	5.93%	3/104	2.88%	2.06 [0.55, 7.75]	0.29
Discontinuation due to adverse events	56/198	28.28%	6/185	3.24%	7.73 [3.57, 16.77]	<0.00001
Dose interruption due to adverse events	10/80	12.50%	7/81	8.64%	1.45 [0.58, 3.61]	0.43
Treatment-related adverse events	112/118	94.92%	92/104	88.46%	1.07 [0.99, 1.16]	0.09
Grade 3-5 treatment-related adverse events	58/118	49.15%	14/104	13.46%	3.65 [2.17, 6.15]	<0.00001
Serious treatment-related adverse events	20/118	16.95%	9/104	8.65%	1.96 [0.93, 4.11]	0.08
Fatal treatment-related adverse events	3/198	1.52%	0/185	0.00%	3.75 [0.42, 33.49]	0.24

CI, Confidence interval; ET, EGFR tyrosine kinase inhibitors alone; ETC, EGFR tyrosine kinase inhibitors in combination of chemotherapy; P, Probability.

TABLE 4 Any grade adverse events.

Adverse events	ETC		ET		Risk ratio [95% CI]	P
	Event/total	%	Event/total	%		
Anorexia	58/80	72.50%	15/81	18.52%	3.92 [2.43, 6.30]	<0.00001
Alanine aminotransferase increase	56/80	70.00%	42/81	51.85%	1.35 [1.05, 1.74]	0.02
Leukopenia	50/80	62.50%	6/81	7.41%	8.44 [3.84, 18.56]	<0.00001
Neutropenia	49/80	61.25%	6/81	7.41%	8.27 [3.75, 18.21]	<0.00001
Aspartate aminotransferase increase	46/80	57.50%	41/81	50.62%	1.14 [0.85, 1.51]	0.38
Anemia	45/80	56.25%	25/81	30.86%	1.82 [1.25, 2.66]	0.002
Alkaline phosphatase increase	45/80	56.25%	31/81	38.27%	1.47 [1.05, 2.06]	0.03
Rash	45/80	56.25%	45/81	55.56%	1.01 [0.77, 1.33]	0.93
Nausea	40/80	50.00%	3/81	3.70%	13.50 [4.35, 41.87]	<0.00001
Fatigue	37/80	46.25%	20/81	24.69%	1.87 [1.20, 2.93]	0.006
Vomiting	32/80	40.00%	1/81	1.23%	32.40 [4.54, 231.46]	0.0005
Hypoalbuminemia	30/80	37.50%	21/81	25.93%	1.45 [0.91, 2.30]	0.12
Pruritus	26/80	32.50%	29/81	35.80%	0.91 [0.59, 1.40]	0.66
Blood creatinine increase	22/80	27.50%	6/81	7.41%	3.71 [1.59, 8.67]	0.002
Diarrhea	20/80	25.00%	26/81	32.10%	0.78 [0.48, 1.28]	0.32
Thrombocytopenia	19/80	23.75%	2/81	2.47%	9.62 [2.32, 39.95]	0.002
Hypocalcemia	19/80	23.75%	13/81	16.05%	1.48 [0.78, 2.79]	0.23
Constipation	18/80	22.50%	4/81	4.94%	4.56 [1.61, 12.87]	0.004
Hypokalemia	11/80	13.75%	16/81	19.75%	0.70 [0.34, 1.41]	0.31
Hyponatremia	9/80	11.25%	13/81	16.05%	0.70 [0.32, 1.55]	0.38
Blood bilirubin increase	7/80	8.75%	11/81	13.58%	0.64 [0.26, 1.58]	0.34
Paronychia	6/80	7.50%	9/81	11.11%	0.68 [0.25, 1.81]	0.43

(Continued)

TABLE 4 Continued

Adverse events	ETC		ET		Risk ratio [95% CI]	P
	Event/total	%	Event/total	%		
Hypercalcemia	5/80	6.25%	1/81	1.23%	5.06 [0.60, 42.37]	0.13
Hyperkalemia	3/80	3.75%	1/81	1.23%	3.04 [0.32, 28.59]	0.33

CI, Confidence interval; ET, EGFR tyrosine kinase inhibitors alone; ETC, EGFR tyrosine kinase inhibitors in combination of chemotherapy; P, Probability.

Limitations of this meta-analysis include: 1. The inclusion criteria were limited to English-published studies, potentially reducing the comprehensiveness of the analysis. 2. Some survival data were collected from subgroup analyses of large-scale RCTs, where differences in baseline characteristics among patients might affect the reliability of the data. 3. The number of studies included in some result analyses was small, compromising the clinical guidance value of the final results. 4. The majority of studies included in the analysis were conducted in Asia, potentially limiting the applicability of the data analysis conclusions to patients in other regions. 5. The included studies used different evaluation criteria to assess AEs, which would increase the heterogeneity of AEs analysis.

Conclusion

ETC appears to outperform ET in treating EGFR-positive NSCLC patients with BM, showing improvements in OS, PFS, CNS-PFS, and responses. The survival advantages of OS, PFS, and CNS-PFS in the ETC group were observed across nearly all subgroups, particularly in those with ECOG performance status = 0, EGFR mutation - Ex19del, and large intracranial tumor size < 20mm. However, the poorer safety profile of ETC should also be considered. Given the aforementioned limitations, it is essential to conduct additional high-quality randomized controlled trials to validate these conclusions.

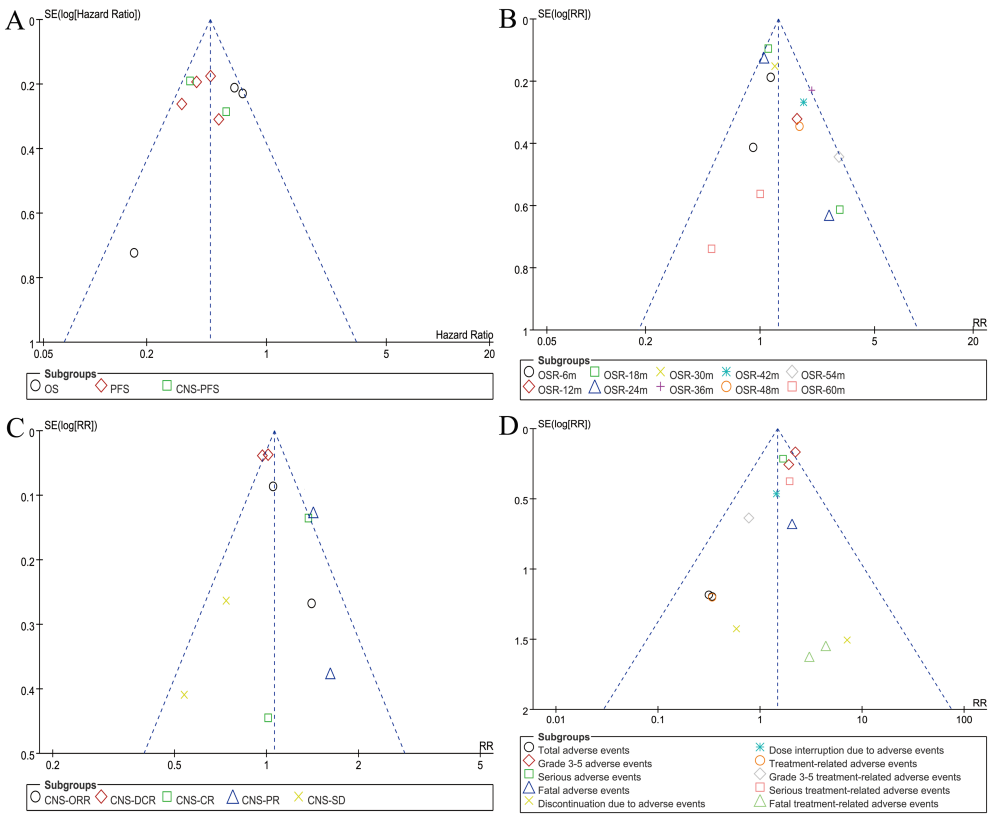

FIGURE 7
Funnel plots of overall survival **(A)**, overall survival rate **(B)**, CNS responses **(C)**, and safety summary **(D)**.

Data availability statement

The original contributions presented in the study are included in the article/Supplementary Material. Further inquiries can be directed to the corresponding author.

Author contributions

ZC: Conceptualization, Data curation, Formal analysis, Investigation, Methodology, Project administration, Resources, Software, Supervision, Validation, Visualization, Writing – original draft, Writing – review & editing. XF: Conceptualization, Data curation, Formal Analysis, Writing – original draft. LZ: Conceptualization, Data curation, Formal analysis, Writing – original draft. XW: Conceptualization, Data curation, Formal analysis, Writing – original draft. SZ: Conceptualization, Data curation, Formal analysis, Investigation, Methodology, Project administration, Resources, Software, Supervision, Validation, Visualization, Writing – original draft, Writing – review & editing.

Funding

The author(s) declare that no financial support was received for the research, authorship, and/or publication of this article.

Acknowledgments

The authors thank professor Wenxiong Zhang, MD (Department of Thoracic Surgery, The second affiliated hospital of Nanchang University) for his data collection and statistical advice.

Conflict of interest

The authors declare that the research was conducted in the absence of any commercial or financial relationships that could be construed as a potential conflict of interest.

Publisher's note

Supplementary material

The Supplementary Material for this article can be found online at: https://www.frontiersin.org/articles/10.3389/fonc.2024.1448336/full#supplementary-material

SUPPLEMENTARY FIGURE 1
Cochrane Risk Assessment.

SUPPLEMENTARY FIGURE 2
Forest plots of CNS-PFSR at 3-30 months associated with ETC versus ET.

SUPPLEMENTARY FIGURE 3
Forest plots of subgroup analysis of overall survival associated with ETC versus ET.

SUPPLEMENTARY FIGURE 4
Forest plots of subgroup analysis of progression-free survival associated with ETC versus ET.

SUPPLEMENTARY FIGURE 5
Forest plots of subgroup analysis of CNS-progression-free survival associated with ETC versus ET.

SUPPLEMENTARY FIGURE 6
Forest plots of overall responses associated with ETC versus ET.

SUPPLEMENTARY FIGURE 7
Forest plots of CNS responses associated with ETC versus ET.

SUPPLEMENTARY FIGURE 8
Forest plots of safety summary associated with ETC versus ET.

SUPPLEMENTARY FIGURE 9
Forest plots of any grade adverse events associated with ETC versus ET.

SUPPLEMENTARY FIGURE 10
Forest plots of grade 3-5 adverse events associated with ETC versus ET.

SUPPLEMENTARY FIGURE 11
Sensitivity analysis of overall survival **(A)** and progression-free survival **(B)**.

SUPPLEMENTARY FIGURE 12
Egger's and Begg's tests based on OS **(A)** and PFS **(B)**.

References

1. Siegel RL, Giaquinto AN, Jemal A. Cancer statistics, 2024. *CA Cancer J Clin.* (2024) 74:12–49. doi: 10.3322/caac.21820

2. Ma J, Song YD, Bai XM. Global, regional, and national burden and trends of early-onset tracheal, bronchus, and lung cancer from 1990 to 2019. *Thorac Cancer.* (2024) 15:601–13. doi: 10.1111/1759-7714.15227

3. Kanagalingam S, Ul Haq Z, Victory N Srinivasan, Khan AI, Mashat GD, Hazique M, et al. Comparing gefitinib and traditional chemotherapy for better survival in patients with non-small cell lung cancer: A systematic review. *Cureus.* (2023) 15: e33691. doi: 10.7759/cureus.33691

4. Zhu CM, Lian XY, Zhang HY, Bai L, Yun WJ, Zhao RH, et al. EGFR tyrosine kinase inhibitors alone or in combination with chemotherapy for non-small-cell lung cancer with EGFR mutations: A meta-analysis of randomized controlled trials. *J Cancer Res Ther.* (2021) 17:664–70. doi: 10.4103/jcrt.JCRT_195_20

5. Riely GJ, Wood DE, Ettinger DS, Aisner DL, Akerley W, Bauman JR, et al. Non-small cell lung cancer, version 4.2024. *J Natl Compr Canc Netw.* (2024) 22:249–74. doi: 10.6004/jnccn.2204.0023

6. Hendriks LE, Kerr KM, Menis J, Mok TS, Nestle U, Passaro A, et al. Oncogene-addicted metastatic non-small-cell lung cancer: ESMO Clinical Practice Guideline for

diagnosis, treatment and follow-up. *Ann Oncol*. (2023) 34:339–57. doi: 10.1016/j.annonc.2022.12.009

7. Lou Y, Xu J, Zhang Y, Lu J, Chu T, Zhang X, et al. Chemotherapy plus EGFR-TKI as first-line treatment provides better survival for advanced EGFR-positive lung adenocarcinoma patients: updated data and exploratory *in vitro* study. *Target Oncol*. (2020) 15:175–84. doi: 10.1007/s11523-020-00708-y

8. Hou X, Li M, Wu G, Feng W, Su J, Jiang H, et al. Gefitinib plus chemotherapy vs gefitinib alone in untreated EGFR-mutant non-small cell lung cancer in patients with brain metastases: the GAP BRAIN open-label, randomized, multicenter, phase 3 study. *JAMA Netw Open*. (2023) 6:e2255050. doi: 10.1001/jamanetworkopen.2022.55050

9. Jänne PA, Planchard D, Kobayashi K, Cheng Y, Lee CK, Valdiviezo N, et al. CNS efficacy of osimertinib with or without chemotherapy in epidermal growth factor receptor-mutated advanced non-small-cell lung cancer. *J Clin Oncol*. (2024) 42:808–20. doi: 10.1200/JCO.23.02219

10. Miyauchi E, Morita S, Nakamura A, Hosomi Y, Watanabe K, Ikeda S, et al. Updated analysis of NEJ009: gefitinib-alone versus gefitinib plus chemotherapy for non-small-cell lung cancer with mutated EGFR. *J Clin Oncol*. (2022) 40:3587–92. doi: 10.1200/JCO.21.02911

11. Chen AP, Setser A, Anadkat MJ, Cotliar J, Olsen EA, Garden BC, et al. Grading dermatologic adverse events of cancer treatments: the Common Terminology Criteria for Adverse Events Version 4.0. *J Am Acad Dermatol*. (2012) 67:1025–39. doi: 10.1016/j.jaad.2012.02.010

12. National Institutes of Health. Common Terminology Criteria for Adverse Events (CTCAE) Version 5.0 (2017). U.S. DEPARTMENT OF HEALTH AND HUMAN SERVICES. Available online at: https://ctep.cancer.gov/protocoldevelopment/electronic_applications/docs/CTCAE_v5_Quick_Reference_8.5x11.pdf (Accessed August 27, 2024).

13. Jadad AR, Moore RA, Carroll D, Jenkinson C, Reynolds DJ, Gavaghan DJ, et al. Assessing the quality of reports of randomized clinical trials: is blinding necessary? *Control Clin Trials*. (1996) 17:1–12. doi: 10.1016/0197-2456(95)00134-4

14. Guyatt GH, Oxman AD, Schünemann HJ, Tugwell P, Knottnerus A. GRADE guidelines: a new series of articles in the Journal of Clinical Epidemiology. *J Clin Epidemiol*. (2011) 64:380–2. doi: 10.1016/j.jclinepi.2010.09.011

15. Sterne JA, Sutton AJ, Ioannidis JP, Terrin N, Jones DR, Lau J, et al. Recommendations for examining and interpreting funnel plot asymmetry in meta-analyses of randomised controlled trials. *BMJ*. (2011) 343:d4002. doi: 10.1136/bmj.d4002

16. Langhorne P. Bias in meta-analysis detected by a simple, graphical test. Prospectively identified trials could be used for comparison with meta-analyses. *BMJ*. (1998) 316:471.

17. Begg CB, Mazumdar M. Operating characteristics of a rank correlation test for publication bias. *Biometrics*. (1994) 50:1088–101. doi: 10.2307/2533446

18. Planchard D, Jänne PA, Cheng Y, Yang JC, Yanagitani N, Kim SW, et al. Osimertinib with or without chemotherapy in EGFR-mutated advanced NSCLC. *N Engl J Med*. (2023) 389:1935–48. doi: 10.1056/NEJMoa2306434

19. Hosomi Y, Morita S, Sugawara S, Kato T, Fukuhara T, Gemma A, et al. Gefitinib alone versus gefitinib plus chemotherapy for non-small-cell lung cancer with mutated epidermal growth factor receptor: NEJ009 study. *J Clin Oncol*. (2020) 38:115–23. doi: 10.1200/JCO.19.01488

20. Noronha V, Patil VM, Joshi A, Menon N, Chougule A, Mahajan A, et al. Gefitinib versus gefitinib plus pemetrexed and carboplatin chemotherapy in EGFR-mutated lung cancer. *J Clin Oncol*. (2020) 38:124–36. doi: 10.1200/JCO.19.01154

21. Halmos B, Rai P, Min J, Hu X, Chirovsky D, Shamoun M, et al. Real-world outcomes on platinum-containing chemotherapy for EGFR-mutated advanced nonsquamous NSCLC with prior exposure to EGFR tyrosine kinase inhibitors. *Front Oncol*. (2024) 14:1285280. doi: 10.3389/fonc.2024.1285280

22. Zhang Q, Wang R, Xu L. Clinical advances in EGFR-TKI combination therapy for EGFR-mutated NSCLC: a narrative review. *Transl Cancer Res*. (2023) 12:3764–78. doi: 10.21037/tcr

23. Cui X, Li X, Lv C, Yan S, Wang J, Wu N. Efficacy and safety of adjuvant EGFR TKI alone and in combination with chemotherapy for resected EGFR mutation-positive non-small cell lung cancer: A Bayesian network meta-analysis. *Crit Rev Oncol Hematol*. (2023) 186:104010. doi: 10.1016/j.critrevonc.2023.104010

24. Xue J, Li B, Wang Y, Huang Z, Liu X, Guo C, et al. Efficacy and safety of epidermal growth factor receptor (EGFR)-tyrosine kinase inhibitor combination therapy as first-line treatment for patients with advanced EGFR-mutated, non-small cell lung cancer: A systematic review and bayesian network meta-analysis. *Cancers (Basel)*. (2022) 14:4894. doi: 10.3390/cancers14194894

25. Okabe T, Okamoto I, Tsukioka S, Uchida J, Iwasa T, Yoshida T, et al. Synergistic antitumor effect of S-1 and the epidermal growth factor receptor inhibitor gefitinib in non-small cell lung cancer cell lines: role of gefitinib-induced down-regulation of thymidylate synthase. *Mol Cancer Ther*. (2008) 7:599–606. doi: 10.1158/1535-7163.MCT-07-0567

26. La Monica S, Madeddu D, Tiseo M, Vivo V, Galetti M, Cretella D, et al. Combination of gefitinib and pemetrexed prevents the acquisition of TKI resistance in NSCLC cell lines carrying EGFR-activating mutation. *J Thorac Oncol*. (2016) 11:1051–63. doi: 10.1016/j.jtho.2016.03.006

27. Wang S, Gao A, Liu J, Sun Y. First-line therapy for advanced non-small cell lung cancer with activating EGFR mutation: is combined EGFR-TKIs and chemotherapy a better choice? *Cancer Chemother Pharmacol*. (2018) 81:443–53. doi: 10.1007/s00280-017-3516-1

28. Mok T, Ladrera G, Srimuninnimit V, Sriuranpong V, Yu CJ, Thongprasert S, et al. Tumor marker analyses from the phase III, placebo-controlled, FASTACT-2 study of intercalated erlotinib with gemcitabine/platinum in the first-line treatment of advanced non-small-cell lung cancer. *Lung Cancer*. (2016) 98:1–8. doi: 10.1016/j.lungcan.2016.04.023

29. Sugawara S, Oizumi S, Minato K, Harada T, Inoue A, Fujita Y, et al. Randomized phase II study of concurrent versus sequential alternating gefitinib and chemotherapy in previously untreated non-small cell lung cancer with sensitive EGFR mutations: NEJ005/TCOG0902. *Ann Oncol*. (2015) 26:888–94. doi: 10.1093/annonc/mdv063

30. Menzel M, Kirchner M, Kluck K, Ball M, Beck S, Allgäuer M, et al. Genomic heterogeneity at baseline is associated with T790M resistance mutations in EGFR-mutated lung cancer treated with the first-/second-generation tyrosine kinase inhibitors. *J Pathol Clin Res*. (2024) 10:e354. doi: 10.1002/cjp2.354

31. Gendarme S, Zebachi S, Corre R, Greillier L, Justeau G, Bylicki O, et al. Predictors of three-month mortality and severe chemotherapy-related adverse events in patients aged 70 years and older with metastatic non-small-cell lung cancer: A secondary analysis of ESOGIA-GFPC-GECP 08-02 study. *J Geriatr Oncol*. (2023) 101506. doi: 10.1016/j.jgo.2023.101506

32. Herbach E, O'Rorke MA, Carnahan RM, McDowell BD, Allen B, Grumbach I, et al. Cardiac adverse events associated with chemo-radiation versus chemotherapy for resectable stage III non-small-cell lung cancer: A surveillance, epidemiology and end results-medicare study. *J Am Heart Assoc*. (2022) 11:e027288. doi: 10.1161/JAHA.122.027288

frontiers | Frontiers in Oncology

TYPE Review
PUBLISHED 29 October 2024
DOI 10.3389/fonc.2024.1411432

OPEN ACCESS

EDITED BY
Jianxin Xue,
Sichuan University, China

REVIEWED BY
Timothy F. Burns,
University of Pittsburgh, United States
Hongru Li,
Fujian Medical University, China

*CORRESPONDENCE
Parth J. Sampat
sampatp@upstate.edu

†These authors have contributed equally to this work and share first authorship

RECEIVED 02 April 2024
ACCEPTED 04 October 2024
PUBLISHED 29 October 2024

CITATION
Sampat PJ, Cortese A, Goodman A, Ghelani GH, Mix MD, Graziano S and Basnet A (2024) Treatment of brain metastases from non-small cell lung cancer: preclinical, clinical, and translational research.
Front. Oncol. 14:1411432.
doi: 10.3389/fonc.2024.1411432

Treatment of brain metastases from non-small cell lung cancer: preclinical, clinical, and translational research

Parth J. Sampat[1*†], Alyssa Cortese[1†], Alexandra Goodman[1†], Ghanshyam H. Ghelani[1], Michael D. Mix[2], Stephen Graziano[1] and Alina Basnet[1]

[1]Division of Hematology and Medical Oncology, Department of Medicine, SUNY Upstate Medical University, Syracuse, NY, United States, [2]Department of Radiation Oncology, SUNY Upstate Medical University, Syracuse, NY, United States

Lung cancer is the second most common type of cancer and is the leading cause of cancer-related deaths in the United States. Approximately 10-40% of patients with solid tumors develop brain metastases, with non-small cell lung cancer accounting for approximately 50% of all cases of patients with brain metastases. Many management options are available which can include surgery, radiation, and systemic therapy. A variety of factors go into the selection of management of brain metastases. In this review, we will focus on the treatment strategies and optimizing the management of brain metastases in patients with non-small cell lung cancer.

KEYWORDS

brain metastases, non-small cell lung cancer, non-small cell adenocarcinoma, lung cancer, squamous cell lung cancer

Introduction

Lung cancer is the second most common type of cancer and is the leading cause of cancer-related deaths in the United States (1). Although the most recent World Health Organization (WHO) classification does not classify non-small cell lung cancer separately (2), historically, lung cancers can be divided into small cell lung cancer (SCLC), and non-small cell lung cancer (NSCLC). NSCLC accounts for approximately 81% of all lung cancers, and SCLC accounts for approximately 14% of all cases (1).

In this review, we will focus on treatment strategies and optimizing the management of brain metastases (BM) in patients with NSCLC.

Clinical diagnosis of brain metastasis

Early detection of BM is crucial in the management of NSCLC, hence the National Comprehensive Cancer Network (NCCN) guidelines recommend brain magnetic resonance imaging (MRI) with contrast with all clinical stage II disease or greater to identify BM in patients with symptoms, or occult BM (3). A contrast-enhanced Computed tomography (CT) brain is recommended for individuals with a contraindication to MRI (3). Contrast-enhanced MRI with T1-weighted images and T2-weighted fluid-attenuation inversion recovery (FLAIR) is most commonly used to identify BM, which provides information on size and morphological characteristics (4). Metastases typically appear iso- or hypointense on T1-weighted images, and variable in intensity on T2-weighted imaging (5). Presence of edema is identified using FLAIR sequencing and metastasis enhance on postcontrast imaging (5). The sensitivity of detecting BM with CT imaging is lower than MRI (5). An example of a patient with a BM in NSCLC is in Figure 1.

Pattern of metastases

Metastases can manifest as solitary, multiple, or as leptomeningeal disease. Intracranial metastases typically exhibit enhancement post-contrast as they lack a blood-brain barrier (5). The enhancing patterns may present as either ring-enhancing lesions or solid nodules (6). In differential diagnoses, ring-enhancing lesions on MRI necessitate consideration of various pathologies such as gliomas, metastatic lesions, abscesses, multiple sclerosis lesions, and other less common etiologies (7). T2-hypointensity trends might help differentiate between different pathologies, for instance, a hypointense arc on T2 and heterogenous center is more indicative of a tumor, whereas multiple enhancing lesions are more suggestive of metastases (7). Nodular enhancing lesions can be attributed to various etiologies including hematogenous spread of infections or metastatic disease (5). Discriminating single ring-enhancing metastatic lesions from glioblastoma remains a challenge, as they often appear similar on standard MRI imaging (5). Integration of advanced imaging techniques and the incorporation of artificial intelligence can aid in the detection and classification of these tumors (4). Furthermore, assessing the total extracranial disease burden in such patients is imperative, for which imaging techniques such as positron emission tomography (PET/CT) or CT are employed.

General principles of management of BM

A range of considerations influence the choice of treatment for BM in NSCLC, including factors such as BM size, number, location, associated symptoms, the presence or absence of actionable mutation, and the preferences of both patient and physician. Local therapies, such as surgery, and stereotactic radiosurgery (SRS) are typically recommended for symptomatic brain metastases, and in cases where patients have a limited number of BM.

According to guidelines from American Society of Clinical Oncology (ASCO)/American Society for Radiation Oncology (ASTRO), it is recommended that all patients with symptomatic BM should be offered local therapy. Specifically, surgery is preferred in patients with large or solitary tumors causing significant mass effect (8). Local therapies can be considered in patients who have a limited number of BM. There is no consensus on what accounts for limited brain metastasis, however, most studies define limited as less than 4 BM (9–13). In patients with multiple brain metastases, surgery is considered only when required for acute or impending symptomatology. The utilization of SRS has broadened in clinical practice to encompass patients with up to 10 metastases (14). However, despite this expansion, there is a lack of randomized data supporting its use in this context. The optimal selection criteria for patients with more than 4 BM remains contentious and is currently under investigation in ongoing research efforts.

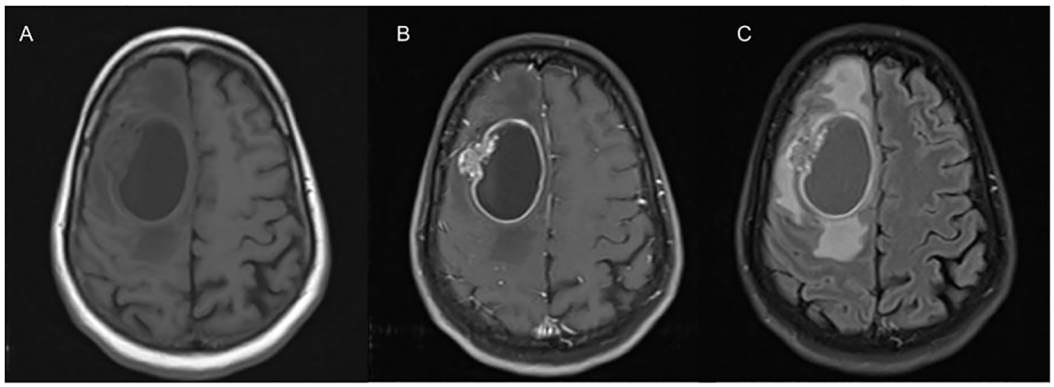

FIGURE 1
This is an axial view of T1 **(A)** revealing an ovoid-shaped hypodensity representing a cystic lesion in the right frontal lobe with perilesional edema with mass effect on contralateral hemisphere and posteriorly. On T1 post contrast imaging **(B)**, there is hyperintensity representing enhancement in the margins with heterogenous hyperintensity on the lateral wall appearing to invade brain parenchyma. FLAIR imaging **(C)** showing significant perilesional edema causing effacement of the sulci.

Treatment sequencing and individualized treatment approaches with shared decision-making

All patients with symptomatic brain metastases should be offered local therapy with surgery or radiation therapy in addition to systemic steroids to minimize swelling or vasogenic edema that may be present. Refer to sections covering their role for detailed discussion.

With the significant growth in treatment options and shifting landscape for patients with advanced NSCLC, it becomes increasingly important to have an open discussion with the patient regarding their current clinical and molecular status, findings, and how it influences their treatment options. At this time, more people are living with and surviving from lung cancer than ever before. Shared decision-making with the patient has become pivotal and the oncologist needs to guide patients to determine the best individualized treatment plan based on treatment side effects, functional status, goals of care, and patient expectations regarding quality of life. A multi-disciplinary approach and discussion between neurosurgery, medical oncology, radiation oncology, and neuro-oncology, along with the patient preferences is important to develop an individualized treatment plan.

Surgery for BM and management of post-surgical cavities

Multiple advances in the field of neurosurgery have led to improvements in surgical techniques. Preoperative Functional MRIs along with high-resolution MRIs can identify high-risk structures and facilitate safer surgical planning (15). Minimally invasive craniotomy and keyhole approaches for tumor resection can achieve preservation of normal brain parenchyma without affecting the extent of tumor resection. Neuronavigation, which was first introduced in 1986 (16), has become an important tool in identifying the location of tumors and nearby structures. The use of intraoperative ultrasound, intraoperative mapping, and endoscope has also improved surgical techniques, making neurosurgery safer (15).

The role of surgery in patients with single BM in addition to WBRT was established in 1990 by Patchell et al. (17), as resection improved survival relative to WBRT alone. However, surgery alone was deemed suboptimal following a second randomized control trial by Patchell et al. (18), in which patients were assigned to either receive postoperative WBRT or observation. WBRT reduced rates of recurrence at both original sites (10% vs. 46%) or elsewhere in the brain (14% vs. 37%), however, no difference in overall survival was noted. Over time, there has been increasing use of adjuvant Stereotactic radiosurgery (SRS) to the surgical cavity as an alternative to WBRT in patients who have a single or limited number of BM (11, 19–23).

Mahajan et al. (24) recruited patients from a single center, who had complete resection of 1-3 BM with a maximum diameter of 4 cm. Patients were randomly assigned in a 1:1 ratio to either receive SRS within 30 days of surgery or observation. 12-month freedom from local recurrence was 43% in the observation group and 72% in the SRS group. Kocher et al. (12) in their study of adjuvant WBRT after radiosurgery or surgical resection of 1-3 cerebral metastases showed a reduced 2-year relapse rate at the initial site (27% vs 59%) or elsewhere (23% vs 42%), without significant difference in overall survival. These studies recapitulate the results of the original Patchell data, emphasizing the need for adjuvant radiotherapy to optimize control while underscoring the appropriateness of SRS as opposed to WBRT as an attractive strategy. Concern surrounding the neurocognitive effects (25–27) of WBRT fueled further interest in an approach that would spare unnecessary brain irradiation.

In the NCCTG N107C/CEC.3 randomized controlled phase 3 trial, 194 adult patients with one resected BM from 48 centers in the USA and Canada were randomly assigned to either postoperative SRS vs. WBRT (28). A battery of neuro-psychiatric tests were performed prospectively on the study population to evaluate a potential difference between the two radiotherapy approaches. The findings demonstrate that the cognitive deterioration-free survival was longer in patients assigned to the SRS group vs. the WBRT group (3.7 months vs. 3 months). Median overall survival (OS) was 12.2 months in the SRS group vs. 11.6 months in the WBRT group. These data serve to cement the notion that WBRT can be avoided without compromising survival and offer one of the best descriptions of neurocognitive comparisons of SRS and WBRT to date.

Adjuvant SRS has traditionally been delivered in a single fraction. However, the use of fractionated SRS (fSRS) has increased over time (for both resected and *in situ* lesions) with the thought that it may reduce the risk of radiation necrosis (RN) while maintaining local control (29), especially in larger targets. No prospective comparative data are available, but a recent cooperative group trial (Alliance A071801 - Clinical trial ID: NCT04114981) (30) randomized surgical cavity to single vs multi-fraction SRS will likely be instructive on the matter.

As described above, local failure rates at the surgical cavity approach are around 60% without the use of adjuvant radiotherapy (12), and the traditional approach utilizes RT following surgery. However, an alternative paradigm has emerged which offers SRS before surgical resection. A retrospective multi-institutional analysis suggested that preoperative SRS may reduce the risk of leptomeningeal recurrence, among other treatment-related conveniences (31). NRG Oncology is leading a randomized trial comparing pre- and post-operative SRS with a primary endpoint evaluating local tumor progression, adverse radiation effect, and nodular leptomeningeal recurrence. (NRG BN012, Clinical trial ID: NCT05438212) (32).

Role of radiation in the management of unresected BM

The decision between surgical resection and stereotactic radiation (SRS) for patients with a single BM, is individualized, as there is no clear evidence demonstrating the superiority of one approach over the other. Treatment choices should be made on a

case-by-case basis, considering the patient's specific medical condition and preferences (33). Most data available is inclusive of trials that enroll all patients with BM and not just NSCLC.

SRS has long been used in patients who have a limited number of BM. There were several trials conducted to evaluate its utility alongside WBRT, or vice versa. In the randomized phase III RTOG 9508 trial, 333 patients with one to three BM were assigned to receive WBRT alone or WBRT with an SRS boost (13). This study demonstrated a survival benefit with the use of a boost in those with a single metastasis (median survival 6.5 versus 4.9 months, p = 0.0393) (13). There did not appear to be a benefit to the use of a boost with 2-3 lesions, and despite these results, routine use of radiosurgical boost following WBRT did not persist in routine practice.

Other studies asked the inverse question of whether routine use of WBRT had a benefit in addition to SRS for limited BM. In a phase III trial, JRSOG 99-1 (34), which randomly assigned 132 patients, with 4 or fewer BM to receive SRS with or without WBRT, the median survival was 7.5 months in the WBRT plus SRS group and 8 months in the SRS group alone (p = 0.42). However, the 12-month brain tumor recurrence rate was 46.8% for the SRS plus WBRT group versus 76.4% for the SRS alone group (p = <0.001). In the EORTC 22952-26001 study with a similar design (though local therapy could be either SRS or surgery) (12), 199 patients received SRS, out of which 100 patients were assigned to the observation group and 99 patients were assigned to the WBRT group. Overall survival was similar in both groups, however, WBRT reduced the 2-year relapse rate at the initial sites (19% vs 31%; p=0.04), and at new sites (33% vs 48%; p=0.023). Finally, Brown et al. (11) published the results of the N0574 trial in 2016, which randomized 213 patients with 1-3 BM to WBRT or observation following SRS. Consistent with prior results, WBRT improved distant brain control without improving overall survival. Less cognitive decline was seen at 3 and 12 months in the observation arm.

Taken together, these trials suggest that despite the improved intracranial control rates, WBRT can be omitted in those with a limited number of BM without compromising survival. This is largely due to the option of radiosurgical salvage of distant brain failures. This has been a welcome conclusion in the neuro-oncology world, given the above.

As WBRT remains an important treatment in those who aren't good candidates for management with SRS alone, there has been significant interest in reducing the neurocognitive impacts. RTOG 0614, investigated the use of memantine, an NMDA receptor agonist, as a possible mitigator (35). In this randomized, double-blind, placebo-controlled trial, patients in the experimental arm had a significantly longer time to cognitive decline (hazard ratio 0.78 (CI 0.62 - 0.99; p=0.01), though the primary endpoint of the trial (delayed recall at 24 weeks) just missed statistical significance (53.8% versus 64.9%; p= 0.059) (35). Memantine is now routinely recommended alongside WBRT for 6 months based on these data.

Though it is incompletely understood, a key component of the neurocognitive toxicity and memory deficit may be a result of injury to hippocampal neural stem cells, marked by increased apoptosis and reduced neurogenesis (36). Efforts to protect the hippocampus aim to partially spare this effect. Intensity-modulated radiotherapy can be used to preferentially avoid the hippocampal stem cell compartment during WBRT (HA-WBRT) to this aim. A single-arm phase 2 trial of HA-WBRT using prespecified comparison with a historical control group without hippocampal avoidance (37). HA-WBRT was then tested in a phase III trial (NRG CC001), randomizing against patients receiving traditional WBRT. 518 patients were randomized and stratified by RPA class, and prior receipt of SRS/surgery or not (38). The primary endpoint was time to cognitive failure, and both arms received a dose of 30 Gy in 10 fractions. The trial was positive, with less deterioration in executive function (at 4 months) and learning/memory (at 6 months) in the HA-WBRT arm. Patient reported outcomes also favored the novel approach, and there was no difference in survival or intracranial progression.

These improvements in the delivery of WBRT have been incorporated into routine practice, though controversy remains regarding optimal scenarios for its use in up-front settings, compared with SRS. As noted earlier, the majority of trials enroll between one to four BM, but a well-defined upper limit that is appropriate for SRS remains elusive. A landmark publication from the Japanese detailed their prospective observational study data on the management of up to 10 BM in 1194 patients (14). All were managed with SRS, and those with a single lesion had better OS, but when grouped in 2-4 vs 5-10, there was no apparent difference. A more recent multi-institutional report of over 2000 patients similarly suggested no difference in survival between 2-4 BM and 5-15 BM cohorts - though the latter composed only 10% of the patients (39). It has now become common practice to offer SRS for properly selected patients with up to 10 (or more) lesions. Selection criteria should include age, performance status, size/location of tumors, systemic disease control, and availability of effective systemic therapy. There are clinical trials ongoing in space hoping to better define who benefits best from which approach, including most notably CCTG. CE.7 trial (Clinical trial ID: NCT03550391) (40), comparing HA-WBRT with SRS for patients with 5 or more lesions.

Systemic therapies for brain metastases

The role of systemic therapy in treating NSCLC with brain metastasis is not well-defined due to limited trials focused solely on brain metastasis control. Most studies exclude patients with brain metastases. Systemic therapies include chemotherapy, immunotherapy, and targeted therapy. Per NCCN guidelines, systemic therapy alone may be considered for select patients with small, asymptomatic brain metastases, using agents with good CNS penetration (3). It's reasonable to delay radiation therapy, though the impact on neurologic deficits or survival isn't well-documented. Close MRI surveillance is recommended with the option to initiate radiation if needed while on systemic therapy along with radiation oncologist.

Targeted therapies and their efficacy in brain metastases

Patients with driver mutations such as epidermal growth factor receptor (EGFR) mutation or Anaplastic lymphoma kinase (ALK) translocations with asymptomatic limited metastases may now be considered for systemic therapy as an early intervention.

Ongoing research is currently addressing the controversy surrounding our understanding of microenvironmental mechanisms within the brain and the potential breakdown of the blood-brain barrier (BBB) to improve the effectiveness of systemic therapies for the treatment of BMs (41). Current evidence suggests that EGFR tyrosine kinase inhibitor (TKI) therapy appears to be more effective than chemotherapy in controlling metastatic disease in the brain along with extracranial (EC) disease (41). Iuchi et al. (42), demonstrated that Gefitinib and Erlotinib, first-generation EGFR TKIs, have shown significant intracranial activity. A second-generation EGFR TKI, Afatinib has also demonstrated significant intracranial efficacy (43). The third-generation EGFR TKIs, AZD 3759, and Osimertinib have shown promising evidence of BBB penetration (44, 45). Additionally Osimertinib has the potential to exhibit sustained tumor regression and greater distribution into mouse brain tissue compared to Gefitinib, Rociletinib, or Afatinib (45). The FLAURA trial demonstrated that osimertinib had superior efficacy compared to standard EGFR-TKIs as first-line therapy for EGFR-positive (Exon 19 deletion or Exon 21 L858R mutation) NSCLC, for which 19% of patients, treated with Osimertinib, had intracranial (IC) metastases when enrolled (46). Patients who exhibit T790M-positive NSCLC have shown greater efficacy with osimertinib compared to Platinum/Pemetrexed, which includes CNS metastasis in a second-line setting (45). The FLAURA 2 trial demonstrated that among patients with brain metastases at baseline, the median progression-free survival was 24.9 months in patients who received Osimertinib with Pemetrexed plus Platinum-based chemotherapy versus 13.8 months in patients who received Osimertinib alone (47). Osimertinib is currently the preferred EGFR tyrosine kinase inhibitor for treating tumors with specific EGFR mutations, including the T790M mutation, NSCLC. Osimertinib CNS activity was evaluated using pooled data from two phase II studies including the AURA extension and AURA2. In this study, the primary outcome was the CNS objective response rate (ORR) assessed by a blinded independent central neuroradiology review (BICR). The confirmed CNS ORR was 54%. The median CNS duration of response was not reached within 1-15 months. At the 9-month mark, it was estimated that 75% of patients (with a 95% confidence interval of 53-88) remained in response (48). Other regimens that can be considered are pulsatile Erlotinib, Afatinib, daily Erlotinib, and Gefitinib. A *post hoc* analysis of the LUX-lung 3 as well as LUX-lung 6 demonstrated an increased progression-free survival (PFS) benefit (p= 0.0297) in patients with asymptomatic brain metastases treated with Afatinib at 8.2 months vs. standard chemotherapy at 5.4 months. From each group, roughly 33% of the patients had prior whole-brain radiation (43).

The incidence of BMs in Anaplastic lymphoma kinase (ALK) rearrangement NSCLC continues to be a problem. Targeted ALK rearrangement TKIs include Crizotinib, Ceritinib, Alectinib, Loratinib, and Brigatinib (41). The drugs developed after Crizotinib like Ceritinib, Alectinib, Brigatinib, and Lorlatinib induced a significant CNS response in those pretreated with Crizotinib (41). Phase 3 clinical trials looking at Brigatinib and Lorlatinib efficacy over Crizotinib, included 29% and 26% of patients, in the treatment arm, with IC metastases, respectively (49, 50).

There is also evidence that amivantamab is an EGFR-MET bispecific antibody. In the MARIPOSA study, a phase 3, randomized study evaluating the efficacy and safety of Amivantamab and lazertinib combination compared to osimertinib, showed that in a subgroup analysis for progression free survival in patients with BM, median PFS was 18.3 months (95% CI 16.6 - 23.7) for amivantamab-lazertinib group when compared to osimertinib, which was 13 months (95% CI 12.2 - 16.4) with hazard ratio of 0.69 (95% CI, 0.53 - 0.92) (51). In a single-arm phase 2 study, amivantamab and lazertinib with EGFR mutations, showed intracranial objective response rate of 40% for patients with BM and 23% for patients with leptomeningeal disease. In the MARIPOSA-2 study, in patients with EGFR mutated patients, amivantamab-lazertinib-chemotherapy, and amivanatmab-chemotherapy group had median intracranial PFS duration of 12.8 months and 12.5 months, when compared to chemotherapy alone, which was 8.3 months (52).

Identifying other clinically important mutations in NSCLC such as ROS1, MET, BRAF, NTRK and so on is important in identifying the most appropriate therapy for the patients. Table 1 presents a summary of common targetable mutations in NSCLC and their CNS efficacy in NSCLC. The efficacy of oral TKI against RET rearragements is high. The efficacy of selpercatinib is mentioned in Table 1. Pralsetinib, another highly selective RET inhibitor, has shown efficacy with its ability to penetrate the blood brain barrier and have anti-tumoral effect. Pre-clinical studies has demonstrated activity in intracranial tumor models (53). The phase 1/2 ARROW study (54) demonstrated efficacy of pralsetinib in patients with NSCLC and brain metastases. A shrinkage of intracranial metastases was seen in all 9 patients with measurable brain metastases. 5 of 9 patients had an intracranial response and 3 had complete responses. Kaplan-Meier estimate of probability of ongoing intracranial response at 6 months was 80% and 53% at 12 months (54). Larotrectinib, a NTRK inhibitor, has also shown rapid and durable responses in patients with brain metastases, where the objective response rate has been 75% amongst use in all tumors (55). Entrectinib is also effective in intracranial disease in patients with NTRK mutation with objective response rates close to 60% with durable responses (12-month event free duration of response rate of 91%) (56). Repotrectinib has shown intracranial activity in ROS1 fusion-positive NSCLC (57). Of the patients with measurable metastases at baseline, intracranial response occurred in 8 of 9 (89%) who had not previously received a ROS1 TKI and in 5 of 13 (38%) who had previously received one ROS1 TKI and not received chemotherapy (57). There is not much data of efficacy of BRAF inhibitors in intracranial disease with NSCLC, however, there are some case reports which have shown benefit to vemurafenib for intracranial disease in NSCLC (58).

The combination of RT and TKIs is promising and aims to optimize the effect of SRS, WBRT, or stereotactic radiotherapy (SRT). A retrospective study demonstrated that patients with exon 21

TABLE 1 Select targeted drugs with CNS efficacy with select studies demonstrating efficacy.

Drug	Targeted mutation	Type of study	Number of patients	Response	CNS PFS
Osimertinib	EGFR	Pooled analysis of 2 phase 2 studies (Goss et al.) (48)	50 with measurable CNS BM	ORR = 54% (95% CI 39 to 68)	Not reached (NR) at 11 months
		CNS response analysis of patients in FLAURA trial (Vansteenkiste et al.) (147)	61 patients analyzed in osimertinib arm	ORR=57%(95% CI, 44-70)	NR
Adagrasib	KRAS G12C	Phase 2 clinical trial (Janne et al.) (148)	42 patients out of 116 had BM (33 patients with radiologically evaluable BM)	ORR = 33% (95% CI 18-51.8)	5.4 months (95% CI 3.3 - 11.6)
Capmatinib	MET Exon 14 skipping mutation	Phase 2 clinical trial (Wolf et al.) (149)	14 of 97 with MET exon 14 skipping mutation (13 with evaluable BM)	7 of 13 patients with intracranial response and 4 patients with complete response	NA
Tepotinib	MET Exon 14 skipping mutation	Phase 2 clinical trial: *ad hoc* retrospective analysis to evaluate intracranial activity (Le et al.) (150)	23 of 152 patients with BM. 15 with evaluable BM and 7 measurable target lesions for response evaluation	Intracranial disease control in 13 patients. 5 of 7 measurable disease had partial response	NA
Selpercaptinib	RET fusion	Phase 1/2 clinical trial (Subbiah et al.) (151)	80 of 531 patients with BM. 22 patients with measurable BM.	ORR = 82% (95% CI 60-95). 23% patients with CR, 59% patients with PR. Intracranial disease control = 100%.	13.7 months (11.9 - not estimable)
Brigatinib	ALK rearrangement	Phase 3 clinical trial (Camidge et al.) (49)	90 of 275 patients with BM. 39 with measurable BM. 18 in the Brigatinib arm.	Overall ORR = 83% (95% CI, 59 - 96)	NA
		Phase 2 clinical trial (Kim et al.) (152)	153 of 222 patients with BM. 44 with measurable BM.	ORR = 42% (11 of 26 patients) in arm A (90 mg dose) and 67% (12 of 18 patients) in arm B (180 mg dose)	15.6 months (95% CI, 7.3 to 15.7) in arm A and 12.8 months (11.0 to not reached) in arm B
Lorlatinib	ALK rearrangement	Phase 3 clinical trial: *post hoc* analysis of intracranial efficacy (Solomon et al.) (50)	38 of 149 patients in the lorlatinib arm had BM.	ORR = 66%; Complete CNS response = 23/38 (61%);	NA
Alectinib	ALK rearrangement	Phase 3 clinical trial (Peters et.al.) (153)	64 of 152 patients in alectinib arm with BM. 21 patients with measurable disease.	CNS response= 17/21 patients. 8 patients with CR. Median duration of intracranial response = 17.3 months (95% CI, 14.8 to not estimable).	NA
		Pooled analysis from data from 2 phase 2 trials (Gandhi et al.) (154)	Measurable BM in 50 patients with RECIST criteria and 43 by RANO-HGG criteria.	CNS objective response =64% (95% CI, 49.2 - 77.1)(RECIST) and 53.5% (95% CI, 37.7-68.8) (RANO-HGG)	10.8 months with RESICT and 11.1 months with RANO-HGG
Ceritinib	ALK rearrangement	Phase 1 trial (Kim et al.) (155)	94 of 246 patients with BM. 36 with measurable BM based on RECIST 1.1.	Intracranial disease control rate=62·5% (5/8; 95% CI 24·5–91·5) in ALKi-naïve patients and 60·7% (17/28; 95% CI 40·6–78·5) in ALKi-pretreated patients. Duration of response= 8·2 months (95% CI 5·6–NE) in ALKi-naïve and 11.1 months (95% CI 2·8–NE) in ALKi-pretreated patients	NA
Entrectinib	ROS1 mutation	Updated analysis of 3 phase 1 or 2 trials. (Dziadziuszko et al.) (156)	46 patients with BM, and 24 patients with measurable BM.	Intracranial ORR in all patients with baseline CNS = 52.2% (n = 24; 95% CI, 37.0 to 67.1). intracranial ORR for patients with measurable disease was 79.2% (n = 19, 95% CI, 57.9 to 92.9	8.3 months (6.4 to 15.7) in all (measurable and unmeasurable). 12 months (6.2 - 19.3) in patients with measurable disease.

NA, not available.

mutation treated with WBRT and TKI had significantly higher OS and PFS than TKI alone (59). Another possible option being investigated is the combination of immunotherapy and RT, with some recent retrospective studies looking at the SRS before and concurrently with checkpoint inhibitors (41). Pseudo-progression is known to occur in these combined modalities and should be considered when evaluating response to treatment. Further investigation in this area, through clinical trials, would assist in the timing, dosing of treatments, and appropriate imaging modalities.

Antibody-drug conjugates (ADCs) have become other targeted options that can be considered in certain patients with BM. In patients who have human epidermal growth factor receptor 2 - mutant (HER2 mutant) metastatic NSCLC, the use of trastuzumab deruxtecan has shown efficacy and safety in management of BM. In a pooled analysis from DESTINY-Lung01 (60) and DESTINY-Lung02 (61) study showed that patients with baseline BM showed intracranial efficacy with some complete responses (62). Patritumab deruxtecan is a humanized monoclonal antibody to HER3 attached to a topoisomerase inhibitor payload (63). In the phase 2 HERTHENA-Lung01 trial (63), patritumab deruxtecan was evaluated in EGFR-mutated NSCLC previously treated with EGFR TKI and platinum-based chemotherapy. In analysis of 30 patients with BM without prior radiation therapy, the CNS objective response rate was 33.3% (95% CI, 17.3 - 52.8) with 9 complete responses and one partial response. Median duration of intracranial response was 8.4 months.

It is crucial to consider that metastatic disease in the brain has the potential to exhibit genomic alterations distinct from those observed at the primary tumor site (64–66).This would imply that targeted therapies that may be effective outside the brain can fail to impact BM lesions (41). In cases where no actionable mutations were initially detected at the primary site, performing a biopsy of the brain metastasis lesion or identifying mutations through circulating or liquid genetic sequencing may uncover new actionable mutations that can be leveraged to explore additional treatment options (41). Further evaluation and clinical trials are needed to better understand and determine the best treatment options for patients with NSCLC BMs without mutation.

Chemotherapy regimens and response rates

The approach of initially treating asymptomatic brain metastases with systemic therapy instead of radiation therapy aims to control both systemic disease and brain metastases simultaneously. However, it has been historically challenging to treat brain metastases with chemotherapy due to the limitations posed by the blood-brain barrier, which restricts the passage of many drugs into the brain. This limitation has led to the exploration of targeted therapies and other treatments with better central nervous system penetration for managing brain metastases in patients with metastatic lung cancer (67). A randomized pilot trial randomized 48 patients to either chemotherapy (Gemcitabine and Vinorelbine) followed by WBRT vs WBRT followed by chemotherapy (68). The study showed there was no significant difference in response rate or survival between groups. Franciosi et al. (69) in a prospective study of previously untreated patients with NSCLC treated with cisplatin and etoposide showed a complete response (CR) in 7% and CR or partial response (PR) in 30% of patients. The median survival was found to be 32 weeks. Another study looked at the use of a standard of care regimen for NSCLC, paclitaxel-cisplatin with the addition of either vinorelbine or gemcitabine, as front-line therapy in 26 chemotherapy-naive patients (70) which found that there was an intracranial response rate in 38% of the patients.

Immunotherapies and their applications in BM

Immunotherapy drugs are classes of drugs that bind to programmed cell death-1 (PD-1) or programmed death ligand 1 (PD-L1). Although data is limited, both can be considered for systemic treatment in individuals with NSCLC and asymptomatic BM.

Hellmann et al. (71) evaluated the efficacy of Nivolumab and Ipilimumab as a frontline treatment for advanced NSCLC in the CheckMate 227 study. This trial showed that irrespective of the PD-L1 expression, the dual immunotherapy (IO) was superior with a median OS of 17.1 months (95% CI, 15.2 to 19.9) compared to 13.9 months with chemotherapy. Among the participants in the trial, 81 patients (10.2%) had CNS metastasis, and those receiving dual immunotherapy had a favorable median OS of 16.8 months with HR of 0.68 (0.41-1.11).

In a non-randomized, open-label, phase 2 trial conducted by Goldberg et al. (72), the role of Pembrolizumab was evaluated in patients with NSCLC who had untreated brain metastases and PD-L1 expression. The trial found that 6 out of 18 patients enrolled (33%) showed a positive response to Pembrolizumab treatment. This suggests a potential benefit of Pembrolizumab in this specific patient population. The CNS effect of Pembrolizumab in the phase 3 KEYNOTE-024 trial for patients with PD-L1 ≥50% was favorable (73). There were 18 participants (11.7%) with brain metastasis and the PFS rate HR was 0.55 with a CI of 0.20-1.56.

Gauvain et al. (74) in their retrospective multicenter study on patients with NSCLC and BM treated with Nivolumab, the primary endpoint of intracerebral objective response rate according to the RECIST criteria found only modest benefit with a 9% objective response rate in those who had pretreated BM vs. 11% in active BM.

The OAK trial compared atezolizumab to docetaxel in previously treated NSCLC which showed that in patients with CNS metastases, the median overall survival was 20.1 months in atezolizumab arm, when compared to 11.9 months in docetaxel arm with a hazard ratio of 0.54 (95% CI, 0.31-0.94), favoring the atezolizumab arm (75). The use of Durvalumab consolidation after chemoradiotherapy in stage III NSCLC has been associated with lower incidence of development of brain metastasis with a rate of 5.5% in the Durvalumab arm versus 11% in placebo arm (76). The EMPOWER-Lung study showed the efficacy of cemiplimab in patients with PD-L1 of at least 50% (77). Data from *post-hoc* analysis at a median follow up of 33 months among patients with

clinically stable BM at randomization, cemiplimab prolonged median OS (NR vs 20.7 months) and median PFS (12.5 months vs 5.3 months) when compared to chemotherapy (78).

A meta-analysis performed by Chu et al. (79), 3160 participants with NSCLC and BM showed that patients treated with immunotherapy were associated with a longer PFS and a longer OS when compared to immunotherapy-naive patients. No obvious difference in PFS and OS was noted among different types of immune checkpoint inhibitors. The combination of immune check point inhibitors and anti-angiogenic agents has shown good anti-tumoral activity and tolerable safety profile and may have synergistic anti-tumor effect in NSCLC BM (80). It has been noted that antiangiogenic drugs may increase infiltration of T cells in BM after inhibiting VEGF (81). In a *post hoc* analysis of the IMpower 150 trial, lower rate of new BMs were noted in atezolizumab plus bevacizumab plus chemotherapy group when compared to atezolizumab plus chemotherapy group, giving a suggestion that combination of immunotherapy with VEGF inhibitors may have the potential of delaying occurrence of BM (82).

Combination with radiotherapy and immunotherapy may cause synergy through the release of danger associated molecular patterns (DAMPs) and cytokines (83). There are several retrospective studies that have highlighted the benefit of immunotherapy and radiotherapy (83). The phase I/II trial (NCT02696993) is currently recruiting to assess the side effects and efficacy of Nivolumab with SRS or WBRT with or without Ipilimumab. Safety data from phase I portion of concurrent nivolumab and ipilimumab with SRS has been reported and has been reported safe and has encouraging durable intracranial response (84).

Impact of BM and treatment on neurocognitive function and rehabilitation strategies

Neurocognitive Function (NCF) impairment is noted to be extremely common in those with brain tumors, with one study finding 90% of its participants having some form of NCF deficits at baseline including fine motor control, executive function, and memory (85). The neurocognitive decline observed in individuals with NSCLC and BM appears to have a multifactorial pathology. Contributing factors include tumor invasion into the brain, medications used for symptomatic management (such as steroids), systemic chemotherapy, and WBRT (86).

The strategies for reducing the effects of WBRT are discussed in the section above.

Leptomeningeal metastases

Leptomeningeal metastases, also known as leptomeningeal carcinomatosis, is an uncommon but grave complication of advanced lung cancer. Leptomeningeal metastases occur in 3-5% with NSCLC (87). Common symptoms of leptomeningeal metastasis include headaches, visual disturbances, cranial nerve deficits, seizures, and cauda equina syndrome among others (88). The gold standard for diagnosis of leptomeningeal disease is through cerebrospinal fluid (CSF) cytology, however, repeated lumbar punctures might be required for increasing sensitivity of CSF cytology (87). False negatives may still exist despite repeated examinations (89), and thus many times a clinical diagnosis needs to be made based on clinical and imaging findings. If CSF cytology remains negative for malignant cells, analysis of CSF protein is informative and is usually higher in patients with leptomeningeal disease (88). MRI is instrumental in diagnosing leptomeningeal carcinomatosis, necessitating comprehensive imaging of the entire neural axis, encompassing both the brain and spine (90). Leptomeningeal enhancement, which may present as either diffuse or focal enhancement due to tumor nodules can be noted on MRI imaging (90). Furthermore, there is growing evidence that use of cell-free DNA (cfDNA) from CSF could improve sensitivity and accuracy for diagnosing leptomeningeal metastases (91–94). These tests are currently only available at limited number of tertiary cancer centers, and as per the Americal Society of Clinical Oncology/ Society for Neuro-Oncology consensus review, these techniques require validation and regulatory certifications before they can routinely be incorporated in clinical practice (95). NCCN guidelines (Central Nervous System Cancers, version 1.2023) stratify patients with leptomeningeal metastases into “good risk” [Karnofsky performance status (KPS) > 60, no major neurological deficits, minimal systemic disease, and reasonable treatment options] and “poor risk” [KPS <60, multiple neurological deficits, extensive systemic disease with few treatment options, bulky CNS disease and encephalopathy] (96). For patients with poor risk disease, palliative or best supportive care is considered, with consideration given to involved field radiation therapy (IFRT) for palliation of symptoms. In patients with good risk disease, systemic therapy, intra-CSF therapy or radiation therapy can be considered (96). When radiation is considered, IFRT in the form of Whole brain radiation therapy (WBRT) and/or focal spine RT is used (97). When treating patients with systemic treatment, systemic therapies with good CNS penetration should be selected. In patients with targetable mutations such as EGFR mutation, treatment with targeted therapies such as Osimertinib and ‘pulsatile’ high dose Erlotinib have shown responses in CNS disease and leptomeningeal metastases (98–100). In a single-arm phase 1/2 clinical trial involving patients with EGFR-mutant NSCLC and leptomeningeal metastases who had previously failed tyrosine kinase inhibitors, the administration of intrathecal (IT) Pemetrexed with dexamethasone demonstrated a noteworthy clinical response rate of 84.6%. Additionally, the trial reported a median overall survival rate of 9 months among participants (101). These findings suggest that such a treatment approach could be a viable consideration for patients with similar characteristics. Other chemotherapeutic drugs used for intrathecal chemotherapy in patients without targetable mutations and with good performance status include IT Methotrexate, Cytarabine, and Thiotepa (102).

Follow-up and surveillance strategies for brain metastases

Imaging modalities for surveillance

The gold standard for brain tumor imaging is MRI due to its excellent tumor delineation and high tissue anatomy resolution. However, it's sensitive to movement, not suitable for patients with certain implants, and can be problematic for claustrophobic individuals. CT with and without contrast is an alternative for these cases, but it has a lower resolution and may not be ideal for those with renal issues. Specialized tests like MR spectroscopy (metabolite assessment) and MR perfusion (cerebral blood flow measurement) can help distinguish true progression from pseudoprogression, guide response monitoring, or assist in biopsy target selection. However, they may have limitations when tumors are near bone, vessels, or air spaces.

Monitoring treatment response and disease progression

In the setting of surgical resection of a brain tumor it is recommended to obtain imaging, preferably with MRI with contrast, 48-72 hours post-surgery to avoid surgery-related enhancement which can frequently mimic a residual tumor. Imaging post-surgery has been found to help guide subsequent treatment (103). The recommendations thereafter are to obtain a Brain MRI every 2-3 months for 1-2 years and then every 4-6 months indefinitely if there are no further changes or concerns (104, 105).

If there are any changes in the patient's signs or symptoms, repeating imaging is appropriate to assess their condition.

The Response Assessment in Neuro-Oncology Brain Metastases (RANO-BM) group, is an international, multidisciplinary effort to develop progression and response criteria for brain metastases, which is commonly used to assess response in clinical trials and practice (106). The best overall CNS response is defined as complete response (disappearance of all CNS target lesions sustained for 4 weeks with no use of steroids), partial response (30% decrease in the sum of longest diameter of lesion), progressive disease (20% or more increase in the sum of longest diameter of lesion, or unequivocal presence of new lesion), or stable disease (Neither sufficient shrinkage or increase to qualify for progressive disease or partial response) (106).

Management of recurrent or progressive brain metastases and radiation necrosis

Recurrent or progressive brain metastases are metastases that recur in either the original site or non-original site after initial therapy. When dealing with recurrent or progressive brain metastases, it's advisable to involve a multidisciplinary team to create an individualized treatment plan. This approach is recommended because there is currently insufficient data to definitively compare the overall benefits of one therapy over another, leading to a lack of definitive treatment recommendations. An individualized plan takes into account the unique characteristics and needs of each patient to provide the best possible care. These factors are similar to those mentioned above when discussing WBRT vs SRS. Many of these clinical factors may have changed since the initial decision regarding the management of the BM.

Depending on the scenario and the nature of the recurrence, options include re-irradiation (if local failure), either WBRT or SRS, surgical excision, or systemic therapy. Limited number of distant brain progressive lesions are typically managed with continued SRS, unless acutely symptomatic. Repeat WBRT is generally avoided given increased risk of toxicity, unless other options are infeasible, and the patient remains reasonably well controlled, systemically. Progression within a treated lesion can be more challenging, given the differential of radiation necrosis (RN), which is another important complication of radiation therapy. The exact incidence of RN is not known, but ranges between 0 to 30% (107). Differentiating between RN and tumor progression is important but can be challenging to delineate (107). Pathological assessment of tissue is the gold standard for diagnosis, however, is not always feasible due to the potential complications from surgery required to obtain tissue (108). On conventional MRI, RN usually appears as a ring-enhancing lesion on T1-weighted imaging, with surrounding T2/FLAIR signal, which represents vasogenic edema, which is non-specific and may also be seen in setting of tumor recurrence (108). Perfusion weighted MRI can help distinguish between recurrence of tumors from RN (109). It is theorized that as viable tumor has intact vasculature which leads to higher perfusion and increased relative cerebral blood volume (rCBV), which is not the case in RN, in which case the rCBV will be low (108, 109). Other imaging techniques such as magnetic resonance spectroscopy (MRS) and fluorodexoyglucose (FDG) and amino acid positron-emission tomography (PET) can be considered to differentiate between RN and tumor progression, however the Response Assessment in Neuro-Oncology Brain Metastasis group suggests that at this time current literature is 'insufficiently robust' to recommend any one particular modality routinely (107). In symptomatic patients with RN, the initial treatment is usually with a glucocorticoid, favorably dexamethasone, which provides symptomatic relief by improvement in cerebral edema. In patients who do not achieve symptomatic relief, non-surgical options include bevacizumab and laser interstitial thermal therapy (LITT) (110, 111). Two small randomized trials and retrospective case series have indicated bevacizumab may be useful in certain cases. In a double-blinded clinical trial, 14 patients with RN were randomly assigned to receive bevacizumab (7.5 mg/kg every 3 weeks for 4 doses) or saline-placebo which noted that all patients who received bevacizumab had improvement in neurological symptoms or imaging findings (112). Another open-label trial compared bevacizumab (5 mg/kg every 2 weeks for 4 doses) with glucocorticoids in patients with nasopharyngeal carcinomas with 112 patients showed that there was increased rates of radiological response (65.5 versus 31.5%) and clinical improvement (62.1 versus 42.6%) at 60 days (113). LITT is also a potential option for patients with RN which is effective in

local control and symptom management (110, 114). Finally surgical resection of the necrotic tissue may sometimes be required, which can achieve palliative benefit and reduce mass effect.

The available evidence in management of recurrent BM is predominantly class III, comprising case series, concerning retreatment of brain metastasis with WBRT, SRS, or surgery. Notably, three distinct case series have investigated the use of WBRT for recurrent BM following WBRT as the initial treatment. The average re-irradiation dose of 20 to 25 Gy was delivered in multiple fractions, with a post-re-radiation median survival ranging from 4 to 5 months (115–117). Conversely, treatment with SRS subsequent to WBRT as an initial intervention yielded median survival from 4.5 to 19 months across different case series (118–120). When SRS was administered following SRS as the initial treatment, the median survival extended to 22.4 months, with 72% of patients achieving complete response, while the remaining 27% exhibited partial response or stable disease (121). Furthermore, the outcomes associated with surgery after SRS as the primary treatment demonstrated a median survival of 11 months, with a time to relapse within the brain of 5 months (122). These retrospective data contain significant bias, however, as those selected for one modality or another carry with them confounding variables that contribute to outcome. One factor that has emerged to potentially aid in decision making between WBRT and SRS is brain metastasis velocity (BMV). BMV is defined as the ratio of new lesions developing over time, and increasing value is associated with worse outcome (123). There is an ongoing trial evaluating SRS vs WRBT in patients with high BMV (NRG BN009, clinical trial ID: NCT04588246) (124).

Multidisciplinary approaches and care in brain metastases

Integrating supportive care services for comprehensive patient management

Supportive care services such as palliative care and integrative medicine have shown to be extremely valuable to patients with cancer as well as their loved ones by helping in areas such as quality of life, depression, anxiety, health care utilization, and even survival thus improving their overall experience (125). In 2009 a randomized controlled trial, involving 312 patients with advanced cancer (35% with lung cancer) provided a psychoeducation intervention consisting of four weekly educational sessions and monthly follow-up sessions. It showed an improvement in quality of life and a reduction in depressed mood (126). The following year a single institution randomized controlled trial evaluated early referrals to palliative care with standard oncology care versus standard oncology care alone. There were 151 patients with newly diagnosed metastatic non-small cell lung cancer. It was found that there were fewer depressive symptoms in the palliative care group (6% vs. 38%, respectively; p = .01). Also, although fewer patients in the early palliative care group received aggressive end-of-life care compared with the standard care group, the median survival was longer among patients receiving palliative care (11.6 vs. 8.9 months; p = .02) (127). Certain symptoms can serve as indicators to healthcare providers that a patient with advanced illness is approaching the end of life. These symptoms may include fatigue and increased confusion, along with headaches, blurry vision, swallowing or speaking difficulties, focal weakness, or seizures. These symptoms can lead to reduced oral intake, malnutrition, dehydration, and aspiration, which can cause dyspnea or pneumonia. Initial treatment with steroids can help alleviate many of these symptoms. For further management, oral medications may be used to prevent seizures and manage anxiety. When patients can no longer take pills, they can switch to liquid lorazepam. Nausea can be addressed with medications like disintegrating ondansetron, metoclopramide, prochlorperazine, and lorazepam. Open communication with caregivers is crucial to prepare them for expected symptoms and provide information on available resources, including hospice care (128).

Prognostic factors and treatment decision-making in brain metastases

Predictive factors for treatment response and survival outcomes

The overall survival of patients diagnosed with BMs remains poor but has improved over the last couple of decades (129). The prognosis may depend on a multitude of different factors such as age, performance status, time from diagnosis, disease activity, as well as the disease location and extension into the intra or extracranial space (41).

The Radiation Therapy Oncology Group (RTOG) developed a prognostication tool, recursive partitioning analysis (RPA) based on Karnofsky performance status (KPS), primary tumor status, presence of extracranial disease, and age which divides patients into three classes (130). However, this scale does not take into account the pathological and molecular features of the tumor into account while determining prognostication. More recently, a diagnosis specific graded prognostic assessment (GPA) is being used to determine prognostication based on types of cancers, histology and molecular factors such as EGFR, ALK and PD-L1 status (131). An online calculator is available.

More recently, with the ongoing development of advanced targeted therapies, we must identify predictive and prognostic factors to help guide treatment. This information has the potential to not only aid in preventing BMs but may also provide further insight into specific treatment options, which may better act upon and treat the disease that has spread to the brain.

In NSCLC, several predictive and prognostic biomarkers have emerged, and testing should be performed on all locally advanced to stage IV NSCLC patients (132). Predictive biomarkers to be tested for, as per the NCCN guidelines (3), are listed in Table 2.

The risk of acquiring BMs in the setting of particular biomarkers continues to be evaluated. Li et al. (133) performed a meta-analysis of 22 studies, incorporating 8,152 patients, to evaluate the correlation between EGFR status with the incidence of BMs in NSCLC and

TABLE 2 Predictive Biomarkers.

	Predictive
Molecular Biomarkers (somatic genomic alterations)	ALK rearrangements
	BRAF p.V600E point mutations
	EGFR mutations
	ERBB2(HER2)*
	KRAS† mutations
	METex14‡ skipping mutations
	NTRK1/2/3§ gene fusions
	RET¶ rearrangements
	ROS proto-oncogene 1
Immune Biomarkers	PD-L1

*ERBB2(HER2) = v-erb-b2 avian erythroblastic leukemia viral oncogene homolog 2 (human epidermal growth factor receptor 2).
†KRAS = Kirsten Rat Sarcoma virus.
‡METex14 = mesenchymal-epithelial transition factor exon 14.
§NTK1/2/3 = neurotrophic tyrosine receptor kinase 1/2/3.
¶RET = rearranged during transfection.

concluded that EGFR mutations are associated with a significantly higher incidence of BMs. This increased incidence is attributed to the downstream effects of EGFR on activated MET through the mitogen-activated protein kinases (MAPK) pathway and the STAT3 pathway which increases the expression of IL6 (133). Similarly, harboring an ALK mutation results in the production of a fusion protein which ultimately activates a signal transduction cascade, cell proliferation, inhibition of apoptosis, and eventually the stimulation of tumor growth; therefore patients with ALK-positive NSCLC are at higher risk of developing BMs (134). In fact, a study looking at the comparison of ALK-positive versus EGFR-positive patients showed that ALK-positive tumors exhibited greater metastatic ability, particularly when it came to brain metastases (135).

The presence of KRAS mutations is a poor prognostic marker of survival for patients with NSCLC, compared to those who do not harbor the KRAS mutations, independent of therapy, and have shown to have increased rates of BM development (136, 137). ROS1-positive NSCLC has lower rates of brain mets compared to EGFR/ALK mutations (138). Another study demonstrated that there was no statistically significant difference in BM development based on ROS1, ALK, EGFR, KRAS, or BRAF mutation status (139). Although the discovery of these biomarkers has led to nuanced targeted agents, the impact of these alterations (EGFR, ALK, KRAS, ROS1, RET and others) on BM development and the explanation behind this association still need to be fully elucidated (137).

Identifying patients with driver-oncogene mutations continues to drive treatment options as next-generation ALK inhibitors and TKIs have been associated with significant intracranial response rates and are effective in BMs (140). Specifically, third-generation EGFR-TKI osimertinib proved to have an intracranial response rate of over 80% while ALK inhibitors including Alectinib, Lorlatinib, and Brigatinib had an intracranial response rate of over 65% (140).

Similarly, the oncology community wanted to know the implications of immune biomarkers and their impact on the development of BM. Lee et al. (141) investigated the association of PD-L1 expression and BM in NSCLC patients and found that tumors exhibiting positive PD-L1 expression had a higher frequency and risk of developing BM. Unfortunately, BM has shown variable response rates to anti-PD-L1 therapies, possibly due to PD-L1 discordance between primary and BM (142). Additional studies are needed to better understand the mechanism behind this.

Clinical trials and emerging treatments for brain metastases

Overview of ongoing clinical trials in brain metastases

Clinical trials play an important role in the treatment of metastatic diseases and allow physicians to find new ways to improve quality of life and prolong survival. The US Food and Drug Administration (FDA) has made recommendations to include patients with brain metastases in cancer clinical trials (143). It is recommended to include patients with BM in a separate subgroup within the trial. Patients with stable or treated BM should be included in clinical trials unless there is a strong rationale to exclude them. Patients with active BM or leptomeningeal disease should not be automatically exluded from trials and should be included in clinical trials if there is a strong likelihood of CNS activity of any drug being investigated, unless known CNS toxicities exist or there is an immediate need of CNS specific treatment (143). In early clinical development for drugs with potential to increase risk of bleeding, patients with hemorrhagic BM or receiving anticoagulation should be excluded. Also with drugs with a potential to lower seizure threshold, patients should be carefully assessed and exclusion of these patients till safety data is available may be important (143). Currently, ongoing trials are looking into combined targeted therapies to enhance the efficacy of RT treatments to BMs. Other studies focus on understanding current targeted therapies and their ability to pervade the BBB to reach CNS tumors.

One important aspect to recognize is that NSCLC BMs may result in a common lineage and continue to evolve to acquire genomic alterations not found at the primary site (144). For instance, gene mutations were evaluated across BMs in breast, lung, and melanoma for which a new PIK3CA gene mutation has been identified, suggesting that PIK3CA may play a role in the metastatic process in the brain which could improve targeted treatment modalities (144). The ongoing challenge remains to be the difficulty of drug permeation across the BBB and the study of the pharmacokinetics of drugs in IC metastasis.

Investigational therapies and their mechanisms

There are hundreds of clinical trials currently recruiting patients to look more closely into the mechanism of metastatic brain disease in NSCLC and how it can be effectively treated to impact PFS and

OS. Recently a variety of treatments such as chemotherapy, EGFR TKIs, Temozolomide, Nitroglycerin, Endostar, Enzastaurin, and Veliparib have been added to RT to determine impact on newly diagnosed BMs (145). A portion of these studies have already been completed and some have required further investigation.

To provide a few examples, the oncology community has expressed interest in exploring the combination of icotinib, a first-generation EGFR TKI, with WBRT for the treatment of EGFR-mutated NSCLC that has spread to the brain (146). There has also been continued interest in the proven efficacy of other EGFR TKIs, such as Osimertinib and Almonertinib, in combination with RT treatments such as WBRT and SRS. Also under investigation are other treatments proven to help in other primary brain tumors, such as Temozolomide, in combination with RT for NSCLC BMs (145).

Promising results and potential future treatments

Due to the recent and rapid development of targeted therapies in NSCLC and BMs this has been a focus for clinical trials. However, there are still a significant number of patients who are negative for both the EGFR/ALK mutations (145), and therefore future clinical trials would benefit from optimizing therapy options for patients with non-targetable NSCLC BMs.

Given the specificity of the biology of BMs, novel clinical trials that specifically target the microenvironment have been and continue to be evaluated. Combining specific treatment modalities and where to sequence them will prove to be immensely important as current trials navigate between the best combinations of chemo/immunotherapy, targeted therapy, surgery, and/or radiation treatment options.

Author contributions

PS: Writing – original draft, Writing – review & editing. AC: Writing – original draft, Writing – review & editing. AG: Writing – original draft, Writing – review & editing. GG: Writing – review & editing, Writing – original draft. MM: Writing – review & editing, Writing – original draft. SG: Writing – review & editing, Writing – original draft. AB: Writing – review & editing, Writing – original draft.

Funding

The author(s) declare that no financial support was received for the research, authorship, and/or publication of this article.

Conflict of interest

The authors declare that the research was conducted in the absence of any commercial or financial relationships that could be construed as a potential conflict of interest.

Publisher's note

References

1. Cancer facts & figures(2023). Available online at: https://www.cancer.org/research/cancer-facts-statistics/all-cancer-facts-figures/2023-cancer-facts-figures.html. (accessed September 29, 2023).

2. Nicholson AG, Tsao MS, Beasley MB, Borczuk AC, Brambilla E, Cooper WA, et al. The 2021 WHO classification of lung tumors: impact of advances since 2015. *J Thorac Oncol*. (2022) 17:362–87. doi: 10.1016/j.jtho.2021.11.003

3. Network NCC. Non-small cell lung cancer (Version 3.2023). Available online at: https://www.nccn.org/professionals/physician_gls/pdf/nscl.pdf. (accessed September 29, 2023).

4. Tong E, McCullagh KL, Iv M. Advanced imaging of brain metastases: from augmenting visualization and improving diagnosis to evaluating treatment response. *Front Neurol*. (2020) 11:270. doi: 10.3389/fneur.2020.00270

5. WB POPE. Brain metastases: neuroimaging. *Handb Clin Neurol*. (2018) 149:89–112. doi: 10.1016/B978-0-12-811161-1.00007-4

6. Barajas RF, Cha S. Metastasis in adult brain tumors. *Neuroimaging Clin N Am*. (2016) 26:601–20. doi: 10.1016/j.nic.2016.06.008

7. Schwartz KM, Erickson BJ, Lucchinetti C. Pattern of T2 hypointensity associated with ring-enhancing brain lesions can help to differentiate pathology. *Neuroradiology*. (2006) 48:143–9. doi: 10.1007/s00234-005-0024-5

8. Vogelbaum MA, Brown PD, Messersmith H, Brastianos PK, Burri S, Cahill D, et al. Treatment for brain metastases: ASCO-SNO-ASTRO guideline. *JCO*. (2022) 40:492–516. doi: 10.1200/JCO.21.02314

9. Churilla TM, Ballman KV, Brown PD, Twohy EL, Jaeckle K, Farace E, et al. Stereotactic radiosurgery with or without whole-brain radiation therapy for limited brain metastases: A secondary analysis of the north central cancer treatment group N0574 (Alliance) randomized controlled trial. *Int J Radiat Oncol Biol Phys*. (2017) 99:1173–8. doi: 10.1016/j.ijrobp.2017.07.045

10. Aoyama H, Tago M, Shirato H, Investigators JROSG 99 1 (JROSG 99 1). Stereotactic radiosurgery with or without whole-brain radiotherapy for brain metastases: secondary analysis of the JROSG 99-1 randomized clinical trial. *JAMA Oncol*. (2015) 1:457–64. doi: 10.1001/jamaoncol.2015.1145

11. Brown PD, Jaeckle K, Ballman KV, Farace E, Cerhan JH, Anderson SK, et al. Effect of radiosurgery alone vs radiosurgery with whole brain radiation therapy on cognitive function in patients with 1 to 3 brain metastases: A randomized clinical trial. *JAMA*. (2016) 316:401–9. doi: 10.1001/jama.2016.9839

12. Kocher M, Soffietti R, Abacioglu U, Villà S, Fauchon F, Baumert BG, et al. Adjuvant whole-brain radiotherapy versus observation after radiosurgery or surgical resection of one to three cerebral metastases: results of the EORTC 22952-26001 study. *JCO*. (2011) 29:134–41. doi: 10.1200/JCO.2010.30.1655

13. Andrews DW, Scott CB, Sperduto PW, Flanders AE, Gaspar LE, Schell MC, et al. Whole brain radiation therapy with or without stereotactic radiosurgery boost for patients with one to three brain metastases: phase III results of the RTOG 9508 randomised trial. *Lancet*. (2004) 363:1665–72. doi: 10.1016/S0140-6736(04)16250-8

14. Yamamoto M, Serizawa T, Shuto T, Akabane A, Higuchi Y, Kawagishi J, et al. Stereotactic radiosurgery for patients with multiple brain metastases (JLGK0901): a multi-institutional prospective observational study. *Lancet Oncol*. (2014) 15:387–95. doi: 10.1016/S1470-2045(14)70061-0

15. Ng PR, Choi BD, Aghi MK, Nahed BV. Surgical advances in the management of brain metastases. *Neuro Oncol Adv*. (2021) 3:v4–15. doi: 10.1093/noajnl/vdab130

16. Roberts DW, Strohbehn JW, Hatch JF, Murray W, Kettenberger H. A frameless stereotaxic integration of computerized tomographic imaging and the operating microscope. *J Neurosurg*. (1986) 65:545–9. doi: 10.3171/jns.1986.65.4.0545

17. Patchell RA, Tibbs PA, Walsh JW, Dempsey RJ, Maruyama Y, Kryscio RJ, et al. A randomized trial of surgery in the treatment of single metastases to the brain. *N Engl J Med*. (1990) 322:494–500. doi: 10.1056/NEJM199002223220802

18. Patchell RA, Tibbs PA, Regine WF, Dempsey RJ, Mohiuddin M, Kryscio RJ, et al. Postoperative radiotherapy in the treatment of single metastases to the brainA randomized trial. *JAMA*. (1998) 280:1485–9. doi: 10.1001/jama.280.17.1485

19. Lamba N, Muskens IS, DiRisio AC, Meijer L, Briceno V, Edrees H, et al. Stereotactic radiosurgery versus whole-brain radiotherapy after intracranial metastasis resection: a systematic review and meta-analysis. *Radiat Oncol*. (2017) 12:106. doi: 10.1186/s13014-017-0840-x

20. Akanda ZZ, Hong W, Nahavandi S, Haghighi N, Phillips C, Kok DL. Post-operative stereotactic radiosurgery following excision of brain metastases: A systematic review and meta-analysis. *Radiother Oncol*. (2020) 142:27–35. doi: 10.1016/j.radonc.2019.08.024

21. Mathieu D, Kondziolka D, Flickinger JC, Fortin D, Kenny B, Michaud K, et al. Tumor bed radiosurgery after resection of cerebral metastases. *Neurosurgery*. (2008) 62:817–4. doi: 10.1227/01.neu.0000316899.55501.8b

22. Do L, Pezner R, Radany E, Liu A, Staud C, Badie B. Resection followed by stereotactic radiosurgery to resection cavity for intracranial metastases. *Int J Radiat Oncol Biol Phys*. (2009) 73:486–91. doi: 10.1016/j.ijrobp.2008.04.070

23. Karlovits BJ, Quigley MR, Karlovits SM, Miller L, Johnson M, Gayou O, et al. Stereotactic radiosurgery boost to the resection bed for oligometastatic brain disease: challenging the tradition of adjuvant whole-brain radiotherapy. *Neurosurg Focus*. (2009) 27:E7. doi: 10.3171/2009.9.FOCUS09191

24. Mahajan A, Ahmed S, McAleer MF, Weinberg JS, Li J, Brown P, et al. Post-operative stereotactic radiosurgery versus observation for completely resected brain metastases: a single-centre, randomised, controlled, phase 3 trial. *Lancet Oncol*. (2017) 18:1040–8. doi: 10.1016/S1470-2045(17)30414-X

25. DeAngelis LM, Delattre JY, Posner JB. Radiation-induced dementia in patients cured of brain metastases. *Neurology*. (1989) 39:789–9. doi: 10.1212/WNL.39.6.789

26. Li J, Bentzen SM, Li J, Renschler M, Mehta MP. Relationship between neurocognitive function and quality of life after whole-brain radiotherapy in patients with brain metastasis. *Int J Radiat Oncol Biol Phys*. (2008) 71:64–70. doi: 10.1016/j.ijrobp.2007.09.059

27. Chang EL, Wefel JS, Hess KR, Allen PK, Lang FF, Kornguth DG, et al. Neurocognition in patients with brain metastases treated with radiosurgery or radiosurgery plus whole-brain irradiation: a randomised controlled trial. *Lancet Oncol*. (2009) 10:1037–44. doi: 10.1016/S1470-2045(09)70263-3

28. Brown PD, Ballman KV, Cerhan JH, Anderson SK, Carrero XW, Whitton AC, et al. Postoperative stereotactic radiosurgery compared with whole brain radiotherapy for resected metastatic brain disease (NCCTG N107C/CEC·3): a multicentre, randomised, controlled, phase 3 trial. *Lancet Oncol*. (2017) 18:1049–60. doi: 10.1016/S1470-2045(17)30441-2

29. Lehrer EJ, Peterson JL, Zaorsky NG, Brown PD, Sahgal A, Chiang VL, et al. Single versus multifraction stereotactic radiosurgery for large brain metastases: an international meta-analysis of 24 trials. *Int J Radiat Oncol Biol Phys*. (2019) 103:618–30. doi: 10.1016/j.ijrobp.2018.10.038

30. Alliance for Clinical Trials in Oncology. *Phase III Trial of Post-Surgical Single Fraction Stereotactic Radiosurgery (SRS) Compared With Fractionated SRS for Resected Metastatic Brain Disease*. clinicaltrials.gov (2023). Available at: https://clinicaltrials.gov/study/NCT04114981.

31. Prabhu RS, Dhakal R, Vaslow ZK, Dan T, Mishra MV, Murphy ES, et al. Preoperative radiosurgery for resected brain metastases: the PROPS-BM multicenter cohort study. *Int J Radiat Oncol Biol Phys*. (2021) 111:764–72. doi: 10.1016/j.ijrobp.2021.05.124

32. NRG Oncology. *A Randomized Phase III Trial of Pre-Operative Compared to Post-Operative Stereotactic Radiosurgery in Patients With Resectable Brain Metastases*. clinicaltrials.gov (2024). Available at: https://clinicaltrials.gov/study/NCT05438212.

33. Fuentes R, Osorio D, Hernandez JE, Simancas-Racines D, Martinez-Zapata MJ, Cosp XB. Surgery versus stereotactic radiotherapy for people with single or solitary brain metastasis. *Cochrane Database Syst Rev*. (2018) 8:CD012086. doi: 10.1002/14651858.CD012086.pub2

34. Aoyama H, Shirato H, Tago M, Nakagawa K, Toyoda T, Hatano K, et al. Stereotactic radiosurgery plus whole-brain radiation therapy vs stereotactic radiosurgery alone for treatment of brain metastasesA randomized controlled trial. *JAMA*. (2006) 295:2483–91. doi: 10.1001/jama.295.21.2483

35. Brown PD, Pugh S, Laack NN, Wefel JS, Khuntia D, Meyers C, et al. Memantine for the prevention of cognitive dysfunction in patients receiving whole-brain radiotherapy: a randomized, double-blind, placebo-controlled trial. *Neuro-Oncol*. (2013) 15:1429–37. doi: 10.1093/neuonc/not114

36. Monje ML, Mizumatsu S, Fike JR, Palmer TD. Irradiation induces neural precursor-cell dysfunction. *Nat Med*. (2002) 8:955–62. doi: 10.1038/nm749

37. Gondi V, Pugh SL, Tome WA, Caine C, Corn B, Kanner A, et al. Preservation of memory with conformal avoidance of the hippocampal neural stem-cell compartment during whole-brain radiotherapy for brain metastases (RTOG 0933): a phase II multi-institutional trial. *J Clin Oncol Off J Am Soc Clin Oncol*. (2014) 32:3810–6. doi: 10.1200/JCO.2014.57.2909

38. Brown PD, Gondi V, Pugh S, Tome WA, Wefel JS, Armstrong TS, et al. Hippocampal avoidance during whole-brain radiotherapy plus memantine for patients with brain metastases: phase III trial NRG oncology CC001. *J Clin Oncol*. (2020) 38:1019–29. doi: 10.1200/JCO.19.02767

39. Hughes RT, Masters AH, McTyre ER, Farris MK, Chung C, Page BR, et al. Initial SRS for patients with 5 to 15 brain metastases: results of a multi-institutional experience. *Int J Radiat Oncol Biol Phys*. (2019) 104:1091–8. doi: 10.1016/j.ijrobp.2019.03.052

40. Canadian Cancer Trials Group. *A Phase III Trial of Stereotactic Radiosurgery Compared With Hippocampal-Avoidant Whole Brain Radiotherapy (HA-WBRT) Plus Memantine for 5 or More Brain Metastases*. clinicaltrials.gov (2024). Available at: https://clinicaltrials.gov/study/NCT03550391.

41. Preusser M, Winkler F, Valiente M, Manegold C, Moyal E, Widhalm G, et al. Recent advances in the biology and treatment of brain metastases of non-small cell lung cancer: summary of a multidisciplinary roundtable discussion. *ESMO Open*. (2018) 3:e000262. doi: 10.1136/esmoopen-2017-000262

42. Iuchi T, Shingyoji M, Sakaida T, Hatano K, Nagano O, Itakura M, et al. Phase II trial of gefitinib alone without radiation therapy for Japanese patients with brain metastases from EGFR-mutant lung adenocarcinoma. *Lung Cancer Amst Neth*. (2013) 82:282–7. doi: 10.1016/j.lungcan.2013.08.016

43. Schuler M, Wu YL, Hirsh V, O'Byrne K, Yamamoto N, Mok T, et al. First-line afatinib versus chemotherapy in patients with non-small cell lung cancer and common epidermal growth factor receptor gene mutations and brain metastases. *J Thorac Oncol Off Publ Int Assoc Study Lung Cancer*. (2016) 11:380–90. doi: 10.1016/j.jtho.2015.11.014

44. Kim DW, Yang JCH, Chen K, Cheng Z, Yin L, Martin PD, et al. AZD3759, an EGFR inhibitor with blood brain barrier (BBB) penetration for the treatment of non-small cell lung cancer (NSCLC) with brain metastasis (BM): Preclinical evidence and clinical cases. *J Clin Oncol*. (2015) 33:8016–6. doi: 10.1200/jco.2015.33.15_suppl.8016

45. Ballard P, Yates JWT, Yang Z, Kim DW, Yang JCH, Cantarini M, et al. Preclinical comparison of osimertinib with other EGFR-TKIs in EGFR-mutant NSCLC brain metastases models, and early evidence of clinical brain metastases activity. *Clin Cancer Res Off J Am Assoc Cancer Res*. (2016) 22:5130–40. doi: 10.1158/1078-0432.CCR-16-0399

46. Soria JC, Ohe Y, Vansteenkiste J, Reungwetwattana T, Chewaskulyong B, Lee KH, et al. Osimertinib in untreated EGFR-mutated advanced non–small-cell lung cancer. *N Engl J Med*. (2018) 378:113–25. doi: 10.1056/NEJMoa1713137

47. Planchard D, Jänne PA, Cheng Y, Yang JCH, Yanagitani N, Kim SW, et al. Osimertinib with or without chemotherapy in EGFR-mutated advanced NSCLC. *N Engl J Med*. (2023) 389:1935–48. doi: 10.1056/NEJMoa2306434

48. Goss G, Tsai CM, Shepherd FA, Ahn MJ, Bazhenova L, Crinò L, et al. CNS response to osimertinib in patients with T790M-positive advanced NSCLC: pooled data from two phase II trials. *Ann Oncol Off J Eur Soc Med Oncol*. (2018) 29:687–93. doi: 10.1093/annonc/mdx820

49. Camidge DR, Kim HR, Ahn MJ, Yang JCH, Han JY, Lee JS, et al. Brigatinib versus crizotinib in ALK-positive non–small-cell lung cancer. *N Engl J Med*. (2018) 379:2027–39. doi: 10.1056/NEJMoa1810171

50. Solomon BJ, Bauer TM, Ou SHI, Liu G, Hayashi H, Bearz A, et al. *Post hoc* analysis of lorlatinib intracranial efficacy and safety in patients with ALK-positive advanced non–small-cell lung cancer from the phase III CROWN study. *JCO*. (2022) 40:3593–602. doi: 10.1200/JCO.21.02278

51. Cho BC, Lu S, Felip E, Spira AI, Girard N, Lee JS, et al. Amivantamab plus lazertinib in previously untreated EGFR-mutated advanced NSCLC. *N Engl J Med*. (2024). doi: 10.1056/NEJMoa2403614

52. Passaro A, Wang J, Wang Y, Lee SH, Melosky B, Shih JY, et al. Amivantamab plus chemotherapy with and without lazertinib in EGFR-mutant advanced NSCLC after disease progression on osimertinib: primary results from the phase III MARIPOSA-2 study☆. *Ann Oncol*. (2024) 35:77–90. doi: 10.1016/j.annonc.2023.10.117

53. Evans E, Hu W, Cao F, Hoeflich K, Dorsch M. P2.03-44 BLU-667 demonstrates robust activity in RET fusion-driven intracranial tumor models. *J Thorac Oncol*. (2019) 14:S701. doi: 10.1016/j.jtho.2019.08.1491

54. Gainor JF, Curigliano G, Kim DW, Lee DH, Besse B, Baik CS, et al. Pralsetinib for RET fusion-positive non-small-cell lung cancer (ARROW): a multi-cohort, open-label, phase 1/2 study. *Lancet Oncol*. (2021) 22:959–69. doi: 10.1016/S1470-2045(21)00247-3

55. Drilon A, Tan DSW, Lassen UN, Leyvraz S, Liu Y, Patel JD, et al. Efficacy and safety of larotrectinib in patients with tropomyosin receptor kinase fusion–positive lung cancers. *JCO Precis Oncol*. (2022) 6):e2100418. doi: 10.1200/PO.21.00418

56. Cho BC, Chiu CH, Massarelli E, Buchschacher GL, Goto K, Overbeck TR, et al. Updated efficacy and safety of entrectinib in NTRK fusion-positive non-small cell lung cancer. *Lung Cancer*. (2024) 188. doi: 10.1016/j.lungcan.2023.107442

57. Drilon A, Camidge DR, Lin JJ, Kim SW, Solomon BJ, Dziadziuszko R, et al. Repotrectinib in ROS1 fusion–positive non–small-cell lung cancer. *N Engl J Med*. (2024) 390:118–31. doi: 10.1056/NEJMoa2302299

58. Robinson SD, O'Shaughnessy JA, Lance Cowey C, Konduri K. BRAF V600E-mutated lung adenocarcinoma with metastases to the brain responding to treatment with vemurafenib. *Lung Cancer*. (2014) 85:326–30. doi: 10.1016/j.lungcan.2014.05.009

59. Zhu Q, Sun Y, Cui Y, Ye K, Yang C, Yang D, et al. Clinical outcome of tyrosine kinase inhibitors alone or combined with radiotherapy for brain metastases from epidermal growth factor receptor (EGFR) mutant non small cell lung cancer (NSCLC). *Oncotarget*. (2017) 8:13304–11. doi: 10.18632/oncotarget.14515

60. Li BT, Smit EF, Goto Y, Nakagawa K, Udagawa H, Mazières J, et al. Trastuzumab deruxtecan in HER2-mutant non–small-cell lung cancer. *N Engl J Med*. (2022) 386:241–51. doi: 10.1056/NEJMoa2112431

61. Goto K, Goto Y, Kubo T, Ninomiya K, Kim SW, Planchard D, et al. Trastuzumab deruxtecan in patients with HER2-mutant metastatic non–small-cell lung cancer: primary results from the randomized, phase II DESTINY-lung02 trial. *J Clin Oncol*. (2023) 41:4852–63. doi: 10.1200/JCO.23.01361

62. Li BT, Planchard D, Goto K, Smit EF, De Langen J, Goto Y, et al. 1321MO Trastuzumab deruxtecan (T-DXd) in patients (pts) with HER2 (ERBB2)-mutant (HER2m) metastatic non–small cell lung cancer (NSCLC) with and without brain metastases (BMs): Pooled analyses from DESTINY-Lung01 and DESTINY-Lung02. *Ann Oncol*. (2023) 34:S762–3. doi: 10.1016/j.annonc.2023.09.2354

63. Yu HA, Goto Y, Hayashi H, Felip E, Chih-Hsin Yang J, Reck M, et al. HERTHENA-lung01, a phase II trial of patritumab deruxtecan (HER3-DXd) in epidermal growth factor receptor–mutated non–small-cell lung cancer after epidermal growth factor receptor tyrosine kinase inhibitor therapy and platinum-based chemotherapy. *J Clin Oncol*. (2023) 41:5363–75. doi: 10.1200/JCO.23.01476

64. Brastianos PK, Carter SL, Santagata S, Cahill DP, Taylor-Weiner A, Jones RT, et al. Genomic characterization of brain metastases reveals branched evolution and potential therapeutic targets. *Cancer Discovery*. (2015) 5:1164–77. doi: 10.1158/2159-8290.CD-15-0369

65. Shih DJH, Nayyar N, Bihun I, Dagogo-Jack I, Gill CM, Aquilanti E, et al. Genomic characterization of human brain metastases identifies drivers of metastatic lung adenocarcinoma. *Nat Genet*. (2020) 52:371–7. doi: 10.1038/s41588-020-0592-7

66. Watkins TBK, Lim EL, Petkovic M, Elizalde S, Birkbak NJ, Wilson GA, et al. Pervasive chromosomal instability and karyotype order in tumour evolution. *Nature*. (2020) 587:126–32. doi: 10.1038/s41586-020-2698-6

67. Sun YW, Xu J, Zhou J, Liu WJ. Targeted drugs for systemic therapy of lung cancer with brain metastases. *Oncotarget*. (2017) 9:5459–72. doi: 10.18632/oncotarget.23616

68. Lee DH, Han JY, Kim HT, Yoon SJ, Pyo HR, Cho KH, et al. Primary chemotherapy for newly diagnosed nonsmall cell lung cancer patients with synchronous brain metastases compared with whole-brain radiotherapy administered first: result of a randomized pilot study. *Cancer*. (2008) 113:143–9. doi: 10.1002/cncr.v113:1

69. Franciosi V, Cocconi G, Michiara M, Costanzo FD, Fosser V, Tonato M, et al. Front-line chemotherapy with cisplatin and etoposide for patients with brain metastases from breast carcinoma, nonsmall cell lung carcinoma, or Malignant melanoma. *Cancer*. (1999) 85:1599–605. doi: 10.1002/(SICI)1097-0142(19990401)85:7<1599::AID-CNCR23>3.0.CO;2-#

70. Cortes J, Rodriguez J, Aramendia JM, Salgado E, Gurpide A, Garcia-Foncillas J, et al. Front-LinePaclitaxel/cisplatin-based chemotherapy in brain metastases from non-smaii-celi lung cancer. *Oncology*. (2003) 64(1):28–35. doi: 10.1159/000066520

71. Hellmann MD, Paz-Ares L, Caro RB, Zurawski B, Kim SW, Costa EC, et al. Nivolumab plus ipilimumab in advanced non–small-cell lung cancer. *N Engl J Med*. (2019) 381:2020–31. doi: 10.1056/NEJMoa1910231

72. Goldberg SB, Gettinger SN, Mahajan A, Chiang AC, Herbst RS, Sznol M, et al. A Phase II trial of pembrolizumab for patients with melanoma or non-small cell lung cancer and untreated brain metastases. *Lancet Oncol*. (2016) 17:976–83. doi: 10.1016/S1470-2045(16)30053-5

73. Reck M, Rodríguez-Abreu D, Robinson AG, Hui R, Csőszi T, Fülöp A, et al. Pembrolizumab versus chemotherapy for PD-L1–positive non–small-cell lung cancer. *N Engl J Med*. (2016) 375:1823–33. doi: 10.1056/NEJMoa1606774

74. Gauvain C, Vauleon E, Chouaid C, Rhun EL, Jabot L, Scherpereel A, et al. Intracerebral efficacy and tolerance of nivolumab in non–small-cell lung cancer patients with brain metastases. *Lung Cancer*. (2018) 116:62–6. doi: 10.1016/j.lungcan.2017.12.008

75. Rittmeyer A, Barlesi F, Waterkamp D, Park K, Ciardiello F, von Pawel J, et al. Atezolizumab versus docetaxel in patients with previously treated non-small-cell lung cancer (OAK): a phase 3, open-label, multicentre randomised controlled trial. *Lancet*. (2017) 389:255–65. doi: 10.1016/S0140-6736(16)32517-X

76. Antonia SJ, Villegas A, Daniel D, Vicente D, Murakami S, Hui R, et al. Durvalumab after chemoradiotherapy in stage III non–small-cell lung cancer. *N Engl J Med*. (2017) 377:1919–29. doi: 10.1056/NEJMoa1709937

77. Sezer A, Kilickap S, Gümüş M, Bondarenko I, Özgüroğlu M, Gogishvili M, et al. Cemiplimab monotherapy for first-line treatment of advanced non-small-cell lung cancer with PD-L1 of at least 50%: a multicentre, open-label, global, phase 3, randomised, controlled trial. *Lancet*. (2021) 397:592–604. doi: 10.1016/S0140-6736(21)00228-2

78. Kilickap S, Özgüroğlu M, Sezer A, Gumus M, Bondarenko I, Gogishvili M, et al. 10MO EMPOWER-Lung 1: Cemiplimab (CEMI) monotherapy as first-line (1L) treatment of patients (pts) with brain metastases from advanced non-small cell lung cancer (aNSCLC) with programmed cell death-ligand 1 (PD-L1) ≥50% — 3-year update. *J Thorac Oncol*. (2023) 18:S42–3. doi: 10.1016/S1556-0864(23)00264-2

79. Chu X, Niu L, Xiao G, Peng H, Deng F, Liu Z, et al. The long-term and short-term efficacy of immunotherapy in non-small cell lung cancer patients with brain metastases: A systematic review and meta-analysis. *Front Immunol*. (2022) 13:875488/full. doi: 10.3389/fimmu.2022.875488/full

80. Fang L, Zhao W, Ye B, Chen D. Combination of immune checkpoint inhibitors and anti-angiogenic agents in brain metastases from non-small cell lung cancer. *Front Oncol*. (2021) 11:670313/full. doi: 10.3389/fonc.2021.670313/full

81. Yan X, Qu F, Zhou Y. Progress of immune checkpoint inhibitors therapy for non-small cell lung cancer with brain metastases. *Lung Cancer*. (2023) 184:107322. doi: 10.1016/j.lungcan.2023.107322

82. Cappuzzo F, Reck M, Socinski MA, Mok TSK, Jotte RM, Finley GG, et al. IMpower150: Exploratory analysis of brain metastases development. *J Clin Oncol*. (2020) 38:9587–7. doi: 10.1200/JCO.2020.38.15_suppl.9587

83. Rios-Hoyo A, Arriola E. Immunotherapy and brain metastasis in lung cancer: connecting bench side science to the clinic. *Front Immunol*. (2023) 14:1221097/full. doi: 10.3389/fimmu.2023.1221097/full

84. Li J, Wang Y, Tang C, Welsh JW, Guha- Thakurta N, Carter BW, et al. Concurrent nivolumab and ipilimumab with brain stereotactic radiosurgery for brain metastases from non-small cell lung cancer: A phase I trial. *J Clin Oncol*. (2020) 38:2531–1. doi: 10.1200/JCO.2020.38.15_suppl.2531

85. Meyers CA, Smith JA, Bezjak A, Mehta MP, Liebmann J, Illidge T, et al. Neurocognitive function and progression in patients with brain metastases treated with whole-brain radiation and motexafin gadolinium: results of a randomized phase III trial. *J Clin Oncol Off J Am Soc Clin Oncol*. (2004) 22:157–65. doi: 10.1200/JCO.2004.05.128

86. Dye N, Gondi V, Mehta M. Strategies for preservation of memory function in patients with brain metastases. *Chin Clin Oncol*. (2015) 4:24. doi: 10.3978/j.issn.2304-3865.2015.05.05

87. Cheng H, Perez-Soler R. Leptomeningeal metastases in non-small-cell lung cancer. *Lancet Oncol*. (2018) 19:e43–55. doi: 10.1016/S1470-2045(17)30689-7

88. Nayar G, Ejikeme T, Chongsathidkiet P, Elsamadicy AA, Blackwell KL, Clarke JM, et al. Leptomeningeal disease: current diagnostic and therapeutic strategies. *Oncotarget*. (2017) 8:73312. doi: 10.18632/oncotarget.20272

89. Weston CL, Glantz MJ, Connor JR. Detection of cancer cells in the cerebrospinal fluid: current methods and future directions. *Fluids Barriers CNS*. (2011) 8:14. doi: 10.1186/2045-8118-8-14

90. Gleissner B, Chamberlain MC. Neoplastic meningitis. *Lancet Neurol*. (2006) 5:443–52. doi: 10.1016/S1474-4422(06)70443-4

91. Azad TD, Nanjo S, Jin MC, Chabon JJ, Kurtz DM, Chaudhuri AA, et al. Quantification of cerebrospinal fluid tumor DNA in lung cancer patients with suspected leptomeningeal carcinomatosis. *NPJ Precis Oncol*. (2024) 8:1–10. doi: 10.1038/s41698-024-00582-1

92. Wu X, Xing P, Shi M, Guo W, Zhao F, Zhu H, et al. Cerebrospinal fluid cell-free DNA-based detection of high level of genomic instability is associated with poor prognosis in NSCLC patients with leptomeningeal metastases. *Front Oncol*. (2022) 12:664420/full. doi: 10.3389/fonc.2022.664420/full

93. White MD, Klein RH, Shaw B, Kim A, Subramanian M, Mora JL, et al. Detection of leptomeningeal disease using cell-free DNA from cerebrospinal fluid. *JAMA Netw Open*. (2021) 4:e2120040. doi: 10.1001/jamanetworkopen.2021.20040

94. Di WY, Chen YN, Cai Y, Geng Q, Tan YL, Li CH, et al. The diagnostic significance of cerebrospinal fluid cytology and circulating tumor DNA in meningeal carcinomatosis. *Front Neurol*. (2023) 14:1076310. doi: 10.3389/fneur.2023.1076310

95. Wilcox JA, Chukwueke UN, Ahn MJ, Aizer AA, Bale TA, Brandsma D, et al. Leptomeningeal metastases from solid tumors: A Society for Neuro-Oncology and American Society of Clinical Oncology consensus review on clinical management and future directions. *Neuro-Oncol*. (2024) 26(10):noae103. doi: 10.1093/neuonc/noae103

96. *NCCN Guidelines Version 1.2023 Central Nervous System Cancers*. National Comprehensive Cancer Network. Available at: https://www.nccn.org/guidelines/guidelines-detail?category=1&id=1425.

97. Barbour AB, Kotecha R, Lazarev S, Palmer JD, Robinson T, Yerramilli D, et al. Radiation therapy in the management of leptomeningeal disease from solid tumors. *Adv Radiat Oncol*. (2024) 9. https://www.advancesradonc.org/article/S2452-1094(23)00205-1/fulltext.

98. Yang JCH, Kim SW, Kim DW, Lee JS, Cho BC, Ahn JS, et al. Osimertinib in patients with epidermal growth factor receptor mutation–positive non–small-cell lung cancer and leptomeningeal metastases: the BLOOM study. *J Clin Oncol*. (2020) 38:538–47. doi: 10.1200/JCO.19.00457

99. Nanjo S, Hata A, Okuda C, Kaji R, Okada H, Tamura D, et al. Standard-dose osimertinib for refractory leptomeningeal metastases in T790M-positive EGFR-mutant non-small cell lung cancer. *Br J Cancer*. (2018) 118:32–7. doi: 10.1038/bjc.2017.394

100. Grommes C, Oxnard GR, Kris MG, Miller VA, Pao W, Holodny AI, et al. Pulsatile" high-dose weekly erlotinib for CNS metastases from EGFR mutant non-small cell lung cancer. *Neuro Oncol*. (2011) 13:1364–9. doi: 10.1093/neuonc/nor121

101. Fan C, Zhao Q, Li L, Shen W, Du Y, Teng C, et al. Efficacy and safety of intrathecal pemetrexed combined with dexamethasone for treating tyrosine kinase inhibitor-failed leptomeningeal metastases from EGFR-mutant NSCLC—a prospective, open-label, single-arm phase 1/2 clinical trial (Unique identifier: ChiCTR1800016615). *J Thorac Oncol*. (2021) 16:1359–68. doi: 10.1016/j.jtho.2021.04.018

102. Wang Y, Yang X, Li NJ, Xue JX. Leptomeningeal metastases in non-small cell lung cancer: Diagnosis and treatment. *Lung Cancer*. (2022) 174:1–13. doi: 10.1016/j.lungcan.2022.09.013

103. Kiesel B, Thomé CM, Weiss T, Jakola AS, Darlix A, Pellerino A, et al. Perioperative imaging in patients treated with resection of brain metastases: a survey by the European Association of Neuro-Oncology (EANO) Youngsters committee. *BMC Cancer*. (2020) 20:410. doi: 10.1186/s12885-020-06897-z

104. Derks SHAE, van der Veldt AAM, Smits M. Brain metastases: the role of clinical imaging. *Br J Radiol*. (2022) 95:20210944. doi: 10.1259/bjr.20210944

105. Bachmann N, Leiser D, Ermis E, Vulcu S, Schucht P, Raabe A, et al. Impact of regular magnetic resonance imaging follow-up after stereotactic radiotherapy to the surgical cavity in patients with one to three brain metastases. *Radiat Oncol*. (2019) 14:45. doi: 10.1186/s13014-019-1252-x

106. Lin NU, Lee EQ, Aoyama H, Barani IJ, Barboriak DP, Baumert BG, et al. Response assessment criteria for brain metastases: proposal from the RANO group. *Lancet Oncol*. (2015) 16:e270–8. doi: 10.1016/S1470-2045(15)70057-4

107. Aizer AA, Lamba N, Ahluwalia MS, Aldape K, Boire A, Brastianos PK, et al. Brain metastases: A Society for Neuro-Oncology (SNO) consensus review on current management and future directions. *Neuro Oncol*. (2022) 24:1613–46. doi: 10.1093/neuonc/noac118

108. Mayo ZS, Billena C, Suh JH, Lo SS, Chao ST. The dilemma of radiation necrosis from diagnosis to treatment in the management of brain metastases. *Neuro-Oncol*. (2024) 26:S56–65. doi: 10.1093/neuonc/noad188

109. Mitsuya K, Nakasu Y, Horiguchi S, Harada H, Nishimura T, Bando E, et al. Perfusion weighted magnetic resonance imaging to distinguish the recurrence of metastatic brain tumors from radiation necrosis after stereotactic radiosurgery. *J Neurooncol*. (2010) 99:81–8. doi: 10.1007/s11060-009-0106-z

110. Palmisciano P, Haider AS, Nwagwu CD, Wahood W, Aoun SG, Abdullah KG, et al. Bevacizumab vs laser interstitial thermal therapy in cerebral radiation necrosis from brain metastases: a systematic review and meta-analysis. *J Neurooncol*. (2021) 154:13–23. doi: 10.1007/s11060-021-03802-x

111. Vellayappan B, Lim-Fat MJ, Kotecha R, Salles AD, Fariselli L, Levivier M, et al. A systematic review informing the management of symptomatic brain radiation necrosis after stereotactic radiosurgery and international stereotactic radiosurgery society recommendations. *Int J Radiat Oncol Biol Phys*. (2024) 118:14–28. doi: 10.1016/j.ijrobp.2023.07.015

112. Levin VA, Bidaut L, Hou P, Kumar AJ, Wefel JS, Bekele BN, et al. Randomized double-blind placebo-controlled trial of bevacizumab therapy for radiation necrosis of the central nervous system. *Int J Radiat Oncol Biol Phys*. (2011) 79:1487–95. doi: 10.1016/j.ijrobp.2009.12.061

113. Xu Y, Rong X, Hu W, Huang X, Li Y, Zheng D, et al. Bevacizumab monotherapy reduces radiation-induced brain necrosis in nasopharyngeal carcinoma patients: A randomized controlled trial. *Int J Radiat Oncol Biol Phys*. (2018) 101:1087–95. doi: 10.1016/j.ijrobp.2018.04.068

114. Chan M, Tatter S, Chiang V, Fecci P, Strowd R, Prabhu S, et al. Efficacy of laser interstitial thermal therapy for biopsy-proven radiation necrosis in radiographically recurrent brain metastases. *Neuro Oncol Adv*. (2023) 5:vdad031. doi: 10.1093/noajnl/vdad031

115. Cooper JS, Steinfeld AD, Lerch IA. Cerebral metastases: value of reirradiation in selected patients. *Radiology*. (1990) 174:883–5. doi: 10.1148/radiology.174.3.2305074

116. Sadikov E, Bezjak A, Yi QL, Wells W, Dawson L, Millar BA, et al. Value of whole brain re-irradiation for brain metastases–single centre experience. *Clin Oncol R Coll Radiol G B*. (2007) 19:532–8. doi: 10.1016/j.clon.2007.06.001

117. Wong WW, Schild SE, Sawyer TE, Shaw EG. Analysis of outcome in patients reirradiated for brain metastases. *Int J Radiat Oncol Biol Phys*. (1996) 34:585–90. doi: 10.1016/0360-3016(95)02156-6

118. Sheehan J, Kondziolka D, Flickinger J, Lunsford LD. Radiosurgery for patients with recurrent small cell lung carcinoma metastatic to the brain: outcomes and prognostic factors. *J Neurosurg*. (2005) 102 Suppl:247–54. doi: 10.3171/jns.2005.102.s_supplement.0247

119. Hoffman R, Sneed PK, McDermott MW, Chang S, Lamborn KR, Park E, et al. Radiosurgery for brain metastases from primary lung carcinoma. *Cancer J Sudbury Mass*. (2001) 7(2):121–31.

120. Combs SE, Schulz-Ertner D, Thilmann C, Edler L, Debus J. Treatment of cerebral metastases from breast cancer with stereotactic radiosurgery. *Strahlenther Onkol Organ Dtsch Rontgengesellschaft Al*. (2004) 180:590–6. doi: 10.1007/s00066-004-1299-x

121. Shuto T, Fujino H, Inomori S, Nagano H. Repeated gamma knife radiosurgery for multiple metastatic brain tumours. *Acta Neurochir (Wien)*. (2004) 146:989–93; discussion 993. doi: 10.1007/s00701-004-0306-4

122. Vecil GG, Suki D, Maldaun MVC, Lang FF, Sawaya R. Resection of brain metastases previously treated with stereotactic radiosurgery. *J Neurosurg*. (2005) 102:209–15. doi: 10.3171/jns.2005.102.2.0209

123. McTyre ER, Soike MH, Farris M, Ayala-Peacock DN, Hepel JT, Page BR, et al. Multi-institutional validation of brain metastasis velocity, a recently defined predictor of outcomes following stereotactic radiosurgery. *Radiother Oncol J Eur Soc Ther Radiol Oncol*. (2020) 142:168–74. doi: 10.1016/j.radonc.2019.08.011

124. NRG Oncology. *Phase III Trial of Salvage Stereotactic Radiosurgery (SRS) or SRS + Hippocampal-Avoidant Whole Brain Radiotherapy (HA-WBRT) for First or Second Distant Brain Relapse After Upfront SRS With Brain Metastasis Velocity </= 4 Brain Metastases/Year*. clinicaltrials.gov (2024). Available at: https://clinicaltrials.gov/study/NCT04588246.

125. Balboni TA, Hui KKP, Kamal AH. Supportive care in lung cancer: improving value in the era of modern therapies. *Am Soc Clin Oncol Educ Book*. (2018) 38:716–25. doi: 10.1200/EDBK_201369

126. Bakitas M, Lyons KD, Hegel MT, Balan S, Brokaw FC, Seville J, et al. Effects of a palliative care intervention on clinical outcomes in patients with advanced cancer: the project ENABLE II randomized controlled trial. *JAMA*. (2009) 302(7):741–9. doi: 10.1001/jama.2009.1198

127. Temel JS, Greer JA, Muzikansky A, Gallagher ER, Admane S, Jackson VA, et al. Early palliative care for patients with metastatic non–small-cell lung cancer. *N Engl J Med*. (2010) 363:733–42. doi: 10.1056/NEJMoa1000678

128. Sharma A, Mrugala MM. Supportive care for patients with brain metastases from lung cancer. *J Thorac Dis*. (2021) 13:3258–68. doi: 10.21037/jtd-2019-rbmlc-11

129. Fuchs J, Früh M, Papachristofilou A, Bubendorf L, Häuptle P, Jost L, et al. Resection of isolated brain metastases in non-small cell lung cancer (NSCLC) patients - evaluation of outcome and prognostic factors: A retrospective multicenter study. *PloS One*. (2021) 16:e0253601. doi: 10.1371/journal.pone.0253601

130. Gaspar LE, Scott C, Murray K, Curran W. Validation of the RTOG recursive partitioning analysis (RPA) classification for brain metastases. *Int J Radiat Oncol Biol Phys*. (2000) 47:1001–6. doi: 10.1016/S0360-3016(00)00547-2

131. Sperduto PW, Mesko S, Li J, Cagney D, Aizer A, Lin NU, et al. Survival in patients with brain metastases: summary report on the updated diagnosis-specific graded prognostic assessment and definition of the eligibility quotient. *J Clin Oncol*. (2020) 38:3773–84. doi: 10.1200/JCO.20.01255

132. Kerr KM, Bubendorf L, Edelman MJ, Marchetti A, Mok T, Novello S, et al. Second ESMO consensus conference on lung cancer: pathology and molecular biomarkers for non-small-cell lung cancer. *Ann Oncol Off J Eur Soc Med Oncol*. (2014) 25:1681–90. doi: 10.1093/annonc/mdu145

133. Li B, Sun SZ, Yang M, Shi JL, Xu W, Wang XF, et al. The correlation between EGFR mutation status and the risk of brain metastasis in patients with lung adenocarcinoma. *J Neurooncol*. (2015) 124:79–85. doi: 10.1007/s11060-015-1776-3

134. Griesinger F, Roeper J, Pöttgen C, Willborn KC, Eberhardt WEE. Brain metastases in ALK-positive NSCLC – time to adjust current treatment algorithms. *Oncotarget*. (2018) 9:35181–94. doi: 10.18632/oncotarget.26073

135. Kang Y, Jin Y, Li Q, Yuan X. Advances in lung cancer driver genes associated with brain metastasis. *Front Oncol*. (2021) 10:606300. doi: 10.3389/fonc.2020.606300

136. Slebos RJ, Kibbelaar RE, Dalesio O, Kooistra A, Stam J, Meijer CJ, et al. K-ras oncogene activation as a prognostic marker in adenocarcinoma of the lung. *N Engl J Med*. (1990) 323:561–5. doi: 10.1056/NEJM199008303230902

137. Gillespie CS, Mustafa MA, Richardson GE, Alam AM, Lee KS, Hughes DM, et al. Genomic alterations and the incidence of brain metastases in advanced and metastatic NSCLC: A systematic review and meta-analysis. *J Thorac Oncol Off Publ Int Assoc Study Lung Cancer*. (2023) 18(12):1703–13. doi: 10.1016/j.jtho.2023.06.017

138. Nishino M, Soejima K, Mitsudomi T. Brain metastases in oncogene-driven non-small cell lung cancer. *Transl Lung Cancer Res*. (2019) 8:S298–307. doi: 10.21037/tlcr.2019.05.15

139. Patil T, Smith DE, Bunn PA, Aisner DL, Le AT, Hancock M, et al. The incidence of brain metastases in stage IV ROS1-rearranged non-small cell lung cancer and rate of central nervous system progression on crizotinib. *J Thorac Oncol Off Publ Int Assoc Study Lung Cancer*. (2018) 13:1717–26. doi: 10.1016/j.jtho.2018.07.001

140. Steindl A, Brastianos PK, Preusser M, Berghoff AS. Precision medicine biomarkers in brain metastases: applications, discordances, and obstacles. *Neuro Oncol Adv*. (2021) 3:v35–42. doi: 10.1093/noajnl/vdab105

141. Lee K, Choi YJ, Kim JS, Kim DS, Lee SY, Shin BK, et al. Association between PD-L1 expression and initial brain metastasis in patients with non-small cell lung cancer and its clinical implications. *Thorac Cancer*. (2021) 12:2143–50. doi: 10.1111/1759-7714.14006

142. Tonse R, Rubens M, Appel H, Tom MC, Hall MD, Odia Y, et al. Systematic review and meta-analysis of PD-L1 expression discordance between primary tumor and lung cancer brain metastasis. *Neuro Oncol Adv*. (2021) 3:vdab166. doi: 10.1093/noajnl/vdab166

143. *Cancer Clinical Trial Eligibility Criteria: Brain Metastases*. FDA. Available at: https://www.fda.gov/media/121317/download.

144. Angeli E, Nguyen TT, Janin A, Bousquet G. How to make anticancer drugs cross the blood–brain barrier to treat brain metastases. *Int J Mol Sci*. (2019) 21:22. doi: 10.3390/ijms21010022

145. Zhang C, Zhou W, Zhang D, Ma S, Wang X, Jia W, et al. Treatments for brain metastases from EGFR/ALK-negative/unselected NSCLC: A network meta-analysis. *Open Med*. (2023) 18:20220574. doi: 10.1515/med-2022-0574

146. Dong K, Liang W, Zhao S, Guo M, He Q, Li C, et al. EGFR-TKI plus brain radiotherapy versus EGFR-TKI alone in the management of EGFR-mutated NSCLC patients with brain metastases. *Transl Lung Cancer Res*. (2019) 8:268–79. doi: 10.21037/tlcr.2019.06.12

147. Vansteenkiste J, Reungwetwattana T, Nakagawa K, Cho BC, Dols MAC, Cho EK, et al. CNS response to osimertinib vs standard of care (SoC) EGFR-TKI as first-line therapy in patients (pts) with EGFR-TKI sensitising mutation (EGFRm)-positive advanced non-small cell lung cancer (NSCLC): Data from the FLAURA study. *Ann Oncol*. (2017) 28:x189. doi: 10.1093/annonc/mdx729.007

148. Jänne PA, Riely GJ, Gadgeel SM, Heist RS, Ou SHI, Pacheco JM, et al. Adagrasib in non–small-cell lung cancer harboring a KRASG12C mutation. *N Engl J Med*. (2022) 387:120–31. doi: 10.1056/NEJMoa2204619

149. Wolf J, Seto T, Han JY, Reguart N, Garon EB, Groen HJM, et al. Capmatinib in MET exon 14–mutated or MET-amplified non–small-cell lung cancer. *N Engl J Med*. (2020) 383:944–57. doi: 10.1056/NEJMoa2002787

150. Le X, Sakai H, Felip E, Veillon R, Garassino MC, Raskin J, et al. Tepotinib efficacy and safety in patients with MET exon 14 skipping NSCLC: outcomes in patient subgroups from the VISION study with relevance for clinical practice. *Clin Cancer Res*. (2022) 28:1117–26. doi: 10.1158/1078-0432.CCR-21-2733

151. Subbiah V, Gainor JF, Oxnard GR, Tan DSW, Owen DH, Cho BC, et al. Intracranial efficacy of selpercatinib in RET fusion-positive non–small cell lung cancers on the LIBRETTO-001 trial. *Clin Cancer Res*. (2021) 27:4160–7. doi: 10.1158/1078-0432.CCR-21-0800

152. Kim DW, Tiseo M, Ahn MJ, Reckamp KL, Hansen KH, Kim SW, et al. Brigatinib in patients with crizotinib-refractory anaplastic lymphoma kinase–positive non–small-cell lung cancer: A randomized, multicenter phase II trial. *JCO*. (2017) 35:2490–8. doi: 10.1200/JCO.2016.71.5904

153. Peters S, Camidge DR, Shaw AT, Gadgeel S, Ahn JS, Kim DW, et al. Alectinib versus crizotinib in untreated ALK-positive non–small-cell lung cancer. *N Engl J Med*. (2017) 377:829–38. doi: 10.1056/NEJMoa1704795

154. Gandhi L, Ou SHI, Shaw AT, Barlesi F, Dingemans AMC, Kim DW, et al. Efficacy of alectinib in central nervous system metastases in crizotinib-resistant ALK-positive non–small-cell lung cancer: Comparison of RECIST 1.1 and RANO-HGG criteria. *Eur J Cancer*. (2017) 82:27–33. doi: 10.1016/j.ejca.2017.05.019

155. Kim DW, Mehra R, Tan DSW, Felip E, Chow LQM, Camidge DR, et al. Activity and safety of ceritinib in patients with ALK-rearranged non-small-cell lung cancer (ASCEND-1): updated results from the multicentre, open-label, phase 1 trial. *Lancet Oncol*. (2016) 17:452–63. doi: 10.1016/S1470-2045(15)00614-2

156. Dziadziuszko R, Krebs MG, Braud FD, Siena S, Drilon A, Doebele RC, et al. Updated integrated analysis of the efficacy and safety of entrectinib in locally advanced or metastatic ROS1 fusion–positive non–small-cell lung cancer. *JCO*. (2021) 39:1253–63. doi: 10.1200/JCO.20.03025

frontiers | Frontiers in Oncology

TYPE Case Report
PUBLISHED 23 December 2024
DOI 10.3389/fonc.2024.1476205

OPEN ACCESS

EDITED BY
Lin Zhou,
Sichuan University, China

REVIEWED BY
Fei Song,
Affiliated Hospital of Nantong University, China
Tengfei Liu,
Shanghai Jiao Tong University, China

*CORRESPONDENCE
Xinju Xu
13569183612@163.com

RECEIVED 05 August 2024
ACCEPTED 04 December 2024
PUBLISHED 23 December 2024

CITATION
Xie M, Zhao Y, Hou X, Li N, Niu S and Xu X (2024) Penpulimab and Anlotinib in PDL1 high-expression pulmonary giant cell carcinoma with cerebral metastases: case report and review.
Front. Oncol. 14:1476205.
doi: 10.3389/fonc.2024.1476205

Penpulimab and Anlotinib in PDL1 high-expression pulmonary giant cell carcinoma with cerebral metastases: case report and review

Minghong Xie[1], Yunlong Zhao[2], Xiaohua Hou[1], Ning Li[1], Sha Niu[1] and Xinju Xu[1]*

[1]Department of Respiratory and Critical Care Medicine, First Affiliated Hospital of Henan Polytechnic University, Jiaozuo Second People's Hospital, Jiaozuo, China, [2]Department of Pathology, First Affiliated Hospital of Henan Polytechnic University, Jiaozuo Second People's Hospital, Jiaozuo, Henan, China

Pulmonary giant cell carcinoma (PGCC) is a rare subtype of non-small cell lung cancer (NSCLC) characterized by complex pathology, high rates of misdiagnosis or missed diagnosis, an aggressive clinical course, rapid progression, and poor prognosis. This case report describes a 67-year-old Chinese male with a left upper lobe lung mass, diagnosed *via* CT-guided lung biopsy as PGCC with symptomatic multiple cerebral metastases. The tumor showed strong PD-L1 positivity, and genetic testing revealed a TP53 exon 4 c.313G mutation. Treatment involved first-line therapy with Penpulimab injection combined with Anlotinib and concurrent cranial radiotherapy. Significant reduction in both the pulmonary and cerebral metastatic lesions was observed, with notable efficacy. As of June 2024, there has been no disease progression for 26 months, with the patient currently maintained on Anlotinib monotherapy. This case demonstrates the favorable efficacy of Penpulimab injection combined with Anlotinib in treating advanced PGCC. These findings indicate that this combination therapy may offer a promising new therapeutic option for this rare type of lung cancer.

KEYWORDS

pulmonary giant cell carcinoma, Penpulimab injection, Anlotinib, cerebral metastases, PD-L1 positivity

Introduction

PGCC presents clinically in a manner similar to other non-small cell lung cancers (NSCLC), yet it is distinguished by rapid proliferation and robust invasive behavior, leading to extensive multi-organ metastasis. The primary treatment for PGCC typically involves surgical intervention; however, due to the aggressive nature of the disease, surgery alone is often insufficient. PGCC exhibits high malignancy and poor prognosis, with most patients

experiencing recurrence or death within 16-18 months post-surgery, and an average survival time approximating 12 months (1, 2).

Immunotherapy endeavors to reinvigorate antitumor immune cells and overcome tumor immune evasion mechanisms. Penpulimab, a novel IgG1 subtype monoclonal antibody targeting programmed cell death protein 1 (PD-1), has been exclusively approved in China. By binding to the PD-1 receptor, it blocks its interaction with programmed death-ligand 1(PD-L1) and PD-L2, thereby preventing immune cell phagocytosis and cytotoxicity through structural modifications in the Fc segment, and thwarting tumor immune evasion. Anlotinib is a multi-targeted tyrosine kinase inhibitor (TKI) known for its broad-spectrum inhibition of tumor angiogenesis and growth.

In recent years, combined immunotherapy and anti-angiogenic targeted strategies have shown promising outcomes. Previous studies have demonstrated that the combination of Anlotinib and Penpulimab as first-line treatment for hepatocellular carcinoma achieved an overall response rate (ORR) of 31%, a disease control rate (DCR) of nearly 83%, and a median progression-free survival (PFS) of 8.8 months, showing comparable efficacy to similar anti-angiogenic and immunotherapeutic combinations. Adverse events were manageable, with a satisfactory safety profile (3). In an Ib/II phase study of Penpulimab in 65 patients with advanced solid tumors, a median PFS of 12.6 months was reported, with an ORR of 12.3% (95% confidence interval [CI], 5.5%-22.8%). Complete response was achieved in 3 cases (4.6%) and partial response in 5 cases (7.7%) (4). A retrospective study evaluating the efficacy of Anlotinib combined with immunotherapy in 101 patients with advanced NSCLC found a partial response in 19 patients (18.8%), disease stabilization in 61 patients (60.4%), an ORR of 18.8% and a DCR of 79.2% (5).

Cerebral metastases remain a critical challenge in the management of NSCLC due to its high incidence and poor prognosis, with survival rates typically limited to just a few months. For patients with multiple cerebral metastases or those for whom stereotactic radiosurgery (SRS) is not feasible, radiotherapy is still considered the gold standard treatment (6). A retrospective analysis indicated that the median overall survival (OS) was 7.0 months (n=435) after stereotactic radiotherapy (SRT) and 3.0 months (n=1705) after whole-brain radiotherapy (WBRT). Additionally, 27% of SRT patients and 50% of WBRT patients died within 90 days of initiating radiotherapy (7). Reviews have suggested that immunotherapy and anti-angiogenic combination therapies might exhibit significant activity against cerebral metastases (8). Recently, in the era of immunotherapy, the use of PD-1 or PD-L1 inhibitors, either alone or in combination with chemotherapeutic agents, has demonstrated therapeutic activity against cerebral metastases in both NSCLC and SCLC patients (9, 10).

This case report presents a 67-year-old male with advanced PGCC and cerebral metastases who achieved remarkable clinical efficacy with a combined treatment of Penpulimab and Anlotinib, providing valuable insights for clinical management.

Case presentation

On April 22, 2022, a 67-year-old Chinese male presented with intermittent coughing for over 10 days underwent a chest X-ray at a local health clinic, revealing a lesion in the left lung. A subsequent chest computed tomography (CT) scan at a county-level hospital confirmed the presence of the lesion. The patient was then admitted to the First Affiliated Hospital of Henan Polytechnic University, where an enhanced chest CT scan showed an irregular soft tissue mass in the left lung with heterogeneous enhancement, measuring approximately 49mm x 50mm x 55mm. Multiple moderately enhanced nodular soft tissue density shadows were observed in the mediastinum, with some showing fusion (Figure 1A). The biomarker cytokeratin-19 fragment (CYFRA21-1) was elevated to 41.12 ng/ml (normal reference range <2.37 ng/ml). In adddition, the levels of biomarkers such as neuron-specific enolase (NSE) 、squamous cell carcinoma(SCC)、progastrin-releasing peptide(PROGRP)、carbohydrate antigen 242(CA24-4)、and carcinoembryonic antigen (CEA) were within the normal range throughout the disease and treatment course of the patients. The patient's medical history included over 10 years of hypertension, a past case of hyperthyroidism which had been cured, and a 40-year smoking history of 20 cigarettes per day, with no family history of lung cancer.

Pathological examination of a CT-guided biopsy from the right upper lobe of the lung indicated NSCLC, immunohistochemically confirmed to be of lung origin. Microscopically, the tumor cells were characterized by eosinophilic cytoplasm, poor adhesion, loose arrangement, large and irregular nuclei, prominent nucleoli, multiple multinucleated giant cells, and infiltration neutrophils. Immunohistochemistry results showed high Ki-67 expression, and variable expression of Napsin A, TTF-1, P40, and CK5/6. In this case, focal weak positivity for CgA, focal positivity for CK5/6, and negative expression for Napsin A, TTF-1, P40, and Vimentin were observed, with high Ki-67 expression (70%) (Figure 2). These findings, combined with the morphological and immunohistochemical findings, supported the diagnosis of giant cell carcinoma.

Enhanced brain MRI indicated abnormal signals in the right frontal-parietal lobes, left parietal lobe, left thalamus, and right cerebellar hemisphere, showing nodular and ring-like enhancement with clear boundaries. The largest lesion was located in the right frontal lobe, measuring approximately 11mm in its longest diameter, with surrounding patchy edema, suggestive of multiple metastases (Figure 3A). Bone scans revealed no bone metastases, and enhanced abdominal CT scans showed no signs of metastasis. Based on the comprehensive evaluation of clinical and examination results, the patient was diagnosed with stage IV PGCC (T4N2M1a according to the TNM staging system).

Due to the patient's symptoms of headache and nausea, priority was given to whole-brain radiotherapy (WBRT) at a dose of 40Gy/23f and a local lesion dose of 50Gy/23f, over 23 sessions. High-throughput sequencing of lung tissue specimens was performed to evaluate genes associated with lung cancer, revealing a TP53 exon 4 c.313G mutation. PD-L1 expression (TPS) was 75%. Based on the guidelines from NMPA, NCCN, and ASCO, and a review of public databases, the patient was subsequently given Anlotinib at 12mg daily, administered for 2 weeks and 1-week off, constituting a 3-week (21 days) cycle. This was combined with Penpulimab injection at 200mg, administered every 3 weeks (21 days), as a first-line treatment regimen. Excitingly, after two cycles of combined treatment, a follow-up chest CT scan showed a significant reduction in the size of the tumor in the left upper lobe of the lung (30x32x34mm) and the mediastinal lymph nodes

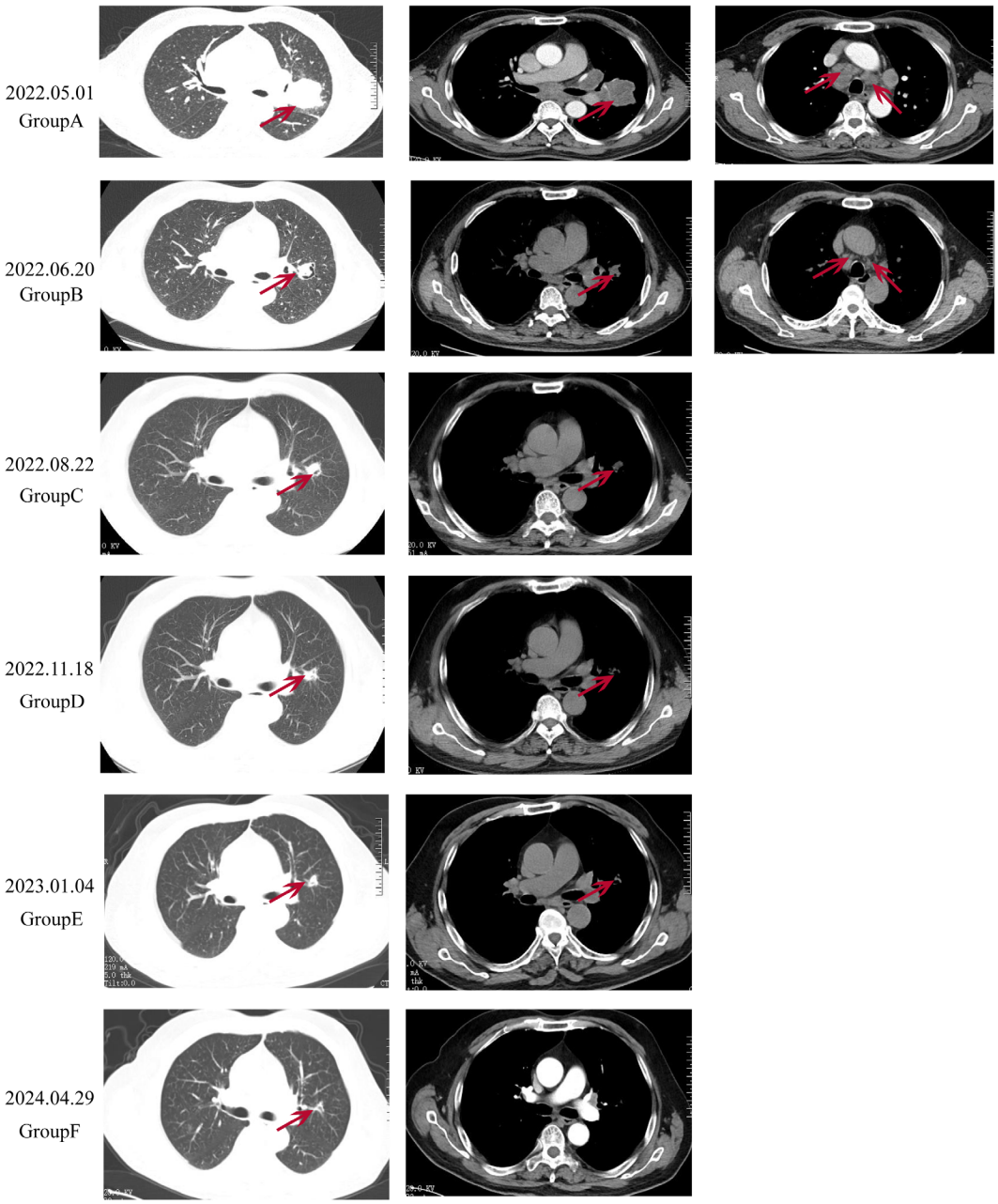

FIGURE 1
Radiological changes in the patient's lung before and after treatment. **(A)**: Pre-treatment imaging showing a pulmonary mass measured approximately 49x50x55mm in size, with multiple enlarged and partially fused lymph nodes. **(B)**: After 2 cycles of treatment, the tumor size reduced to approximately 30x32x34 mm, and the mediastinal lymph nodes significantly decreased in size. **(C, D)**: Throughout the treatment, the lung tumor continued to shrink, and the mediastinal lymph nodes continues to decrease in size, with no mediastinal lymph nodes visible in **(E)**. **(F)**: During treatment, the tumor size was approximately 12x18x15 mm, with no significant enlargement of the mediastinal lymph nodes.

(Figure 1B). A follow-up enhanced brain MRI indicated that the abnormal signals in the right frontal-parietal lobe, left parietal lobe, left thalamus, and right cerebellar hemisphere appeared as spot-like and ring-like enhancements with clear boundaries. The brain metastases had significantly reduced in size, with the largest lesion in the right frontal lobe now measuring approximately 7mm in its longest diameter (Figure 3B). The patient's clinical symptoms of brain metastases were remarkadly relieved, and the quality of life improved significantly.

Two months later, a follow-up examination showed that the tumor had shrunk to 21x29x22mm, and the mediastinal lymph nodes had also significantly reduced in size (Figure 1C). Subsequent bi-monthly chest CT scans showed continued tumor shrinkage. By November 18, 2022, a follow-up chest CT scan showed that the tumor had significantly reduced to 12x19x17mm, with no significant enlargement of the mediastinal lymph nodes (Figure 1D). Follow-up enhanced brain MRI indicated that the metastases in the left parietal lobe, left thalamus, and right cerebellar hemisphere had disappeared,

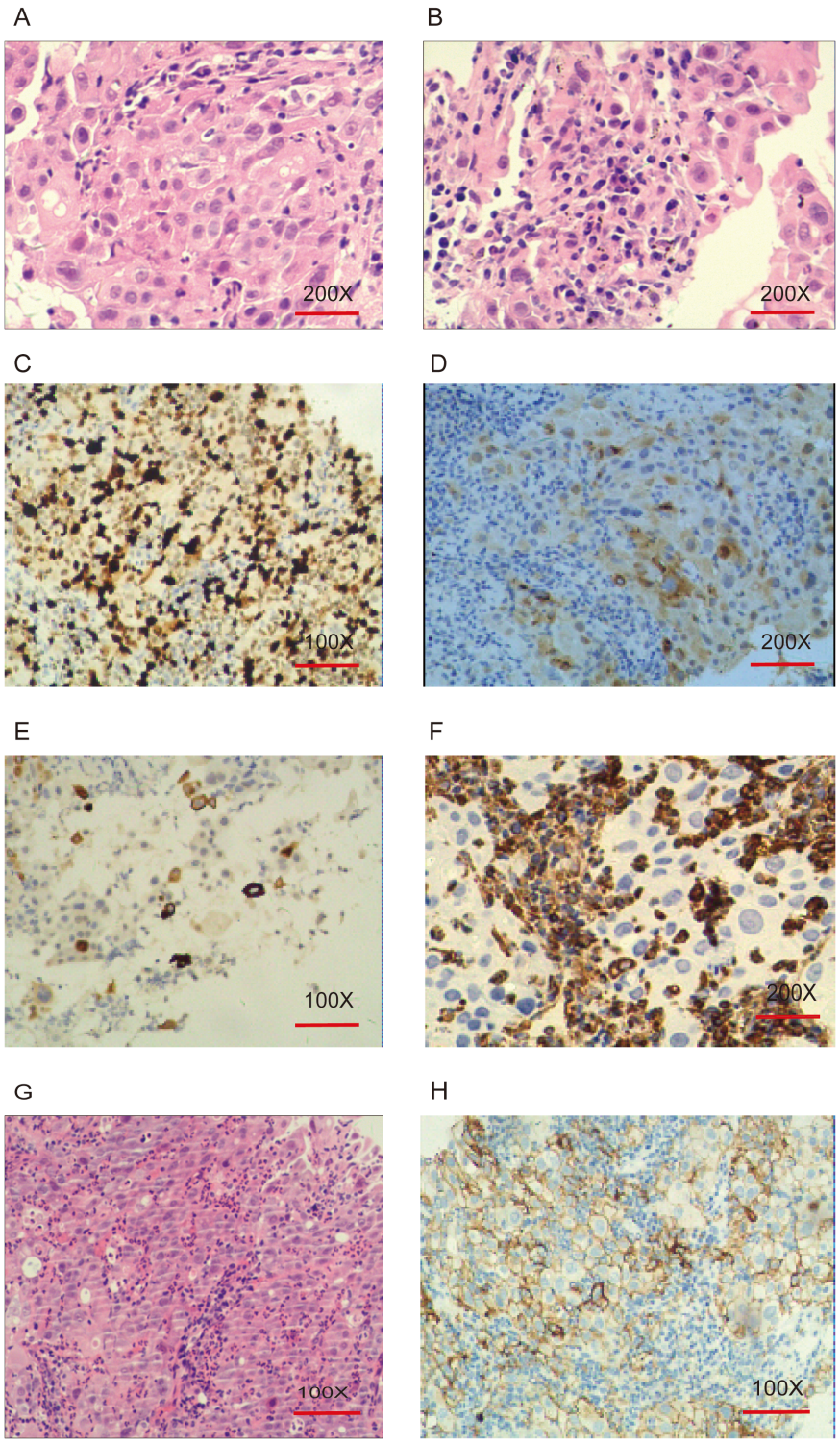

FIGURE 2
Pathological and immunohistochemical features of pulmonary giant cell carcinoma. **(A, B)**: Hematoxylin and eosin (H&E) staining, original magnification ×200. Tumor giant cells exhibit eosinophilic cytoplasm, poor cohesion, loose arrangement, large and irregular nuclei, prominent nucleoli, multinucleated giant cells, and neutrophilic infiltration. **(C)**: Ki-67 (70%+), original magnification ×100. **(D)**: CgA (+), original magnification ×200. **(E)**: CK5/6 (+), original magnification ×100. **(F)**: Vimentin (-), original magnification ×200. **(G)**: H&E staining, original magnification ×100. **(H)**: PD-L1 IHC, original magnification ×100. Tumor Proportion Score (TPS): 75% (TPS is defined as the percentage of at least 100 viable tumor cells showing partial or complete membrane staining for PD-L1).

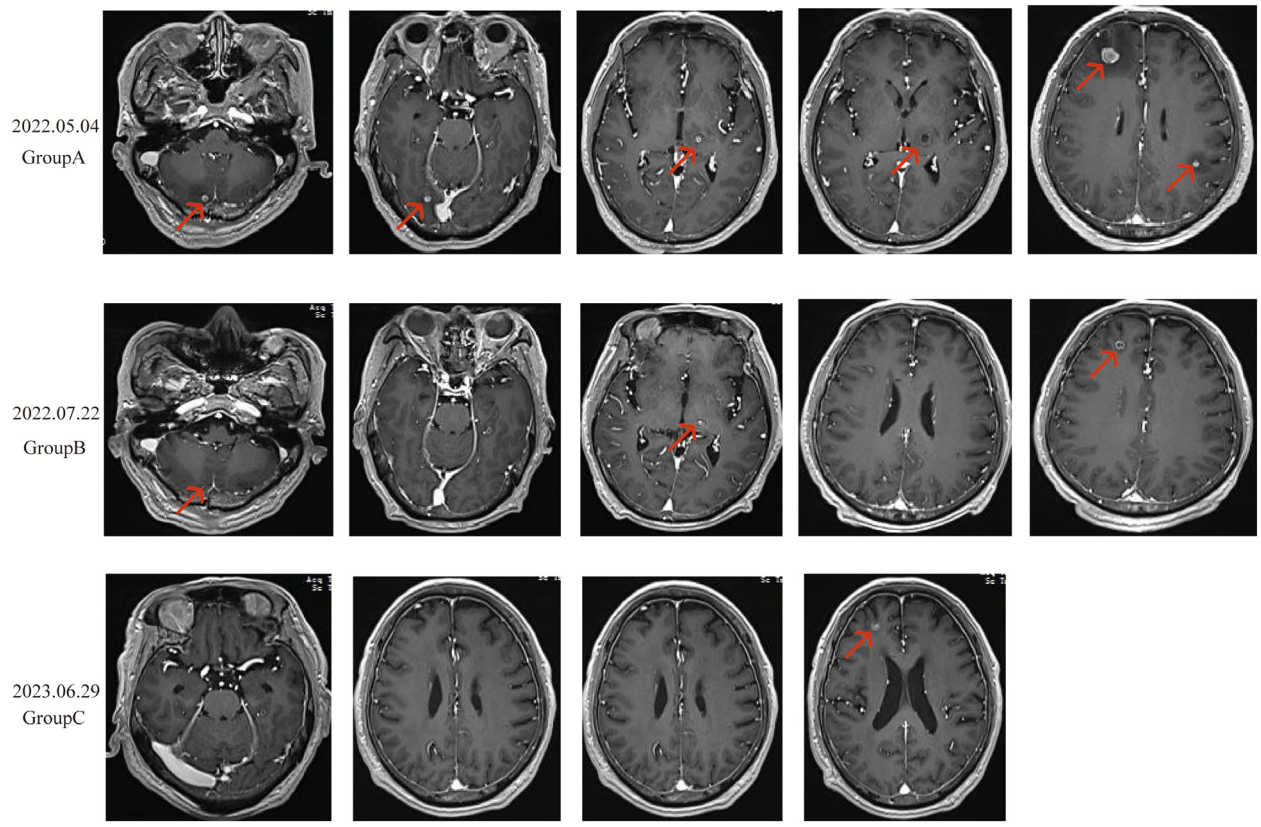

FIGURE 3
Radiological changes in brain metastases before and after treatment. **(A)**: Nodular and ring-enhanced abnormal signals in the right frontal-parietal lobe, left parietal lobe, left thalamus, and right cerebellar hemisphere. Multiple metastases are observed, with the largest lesion in the right frontal lobe, measuring approximately 11 mm in length, surrounded by small patches of edema. **(B)**: The brain metastases in the same locations showed significant shrinkage, with most lesions showing reduced enhancement. The largest lesion in the right frontal lobe measured approximately 7 mm in length. **(C)**: The metastases in the left parietal lobe, left thalamus, and right cerebellar hemisphere disappeared. The largest lesion, located in the right frontal lobe, measured approximately 7 mm in length.

with the largest lesion in the right frontal lobe remaining at approximately 7mm (Figure 3C). According to the RECIST 1.1 criteria, the patient's condition was classified as partial response (PR).

During follow-up chest CT scans. the tumor size remained stable, and on January 4, 2023, a chest CT scan showed the tumor remained at 12x19x17mm, with no significant enlargement of the mediastinal lymph nodes (Figure 1E). On April 29, 2024, a follow-up enhanced chest CT scan showed the tumor size was 12x18x15mm, with no significant enlargement of the mediastinal lymph nodes (Figure 1F). The CYFRA21-1 level had decreased to 2.61 ng/ml (normal range <2.37 ng/ml). According to RECIST 1.1 criteria, the patient's condition was classified as stable disease (SD). The patient's CYFRA21-1 level has stabilized between 2 and 3 ng/ml (Figure 4). Considering the sustained disease stability and the patient's good tolerance, the Penpulimab treatment was lasted for two years and has now ended. The patient continues with maintenance therapy using Anlotinib monotherapy and is currently under regular monitoring and ongoing treatment.

Discussion

According to the 2021 World Health Organization classification criteria, pulmonary sarcomatoid carcinoma (PSC) is a subset of NSCLC characterized by spindle or giant cell components. PSC can be classified into five subtypes: pleomorphic carcinoma, spindle cell carcinoma, carcinosarcoma, pulmonary blastoma, and pulmonary giant cell carcinoma (PGCC). These tumors, particularly those with

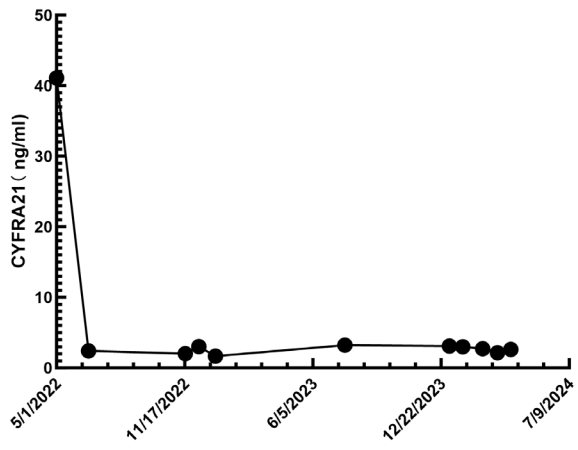

FIGURE 4
Changes in cytokeratin-19 fragment levels during treatment (normal reference range <2.37 ng/ml).

spindle and giant cells, are highly aggressive and resistant to conventional treatments (11). PSC accounts for approximately 0.3%-0.4% of all pulmonary malignancies, with an incidence rate of three new cases per million annually. The disease predominantly affects male smokers, with a male-to-female ratio of about 5:1. Although PSC can occur at any age, the average onset age is between 50 and 60 years, which is younger than the average age for other NSCLC patients. PSC constitutes less than 1% of all lung cancers (12). Due to its rarity, data on treatment strategies and prognosis are significantly lacking (1), particularly for advanced PGCC, where randomized controlled trials and long-term follow-up data are scarce. This patient's presentation with advanced disease and multiple metastases underscores the highly invasive and metastatic nature of PGCC.

Anlotinib is a multi-targeted anti-angiogenic agent that inhibits tumor growth by suppressing angiogenesis and inhibiting tumor cell proliferation and metastasis (13). The ALTER-0303 clinical trial demonstrated that Anlotinib is more effective than a placebo in the third-line treatment of advanced NSCLC patients. Compared to the placebo group, the Anlotinib group showed improved ORR and disease control rate (DCR) (ORR 9.18% vs 0.7%, P<0.0001; DCR 80.95% vs 37.06%, P<0.0001). Furthermore, Anlotinib significantly extended median PFS and OS compared to placebo (14).

Tumor immunotherapy, particularly immune checkpoint blockade, has achieved significant clinical success by inducing long-term regression in cases resistant to all other treatments. PD-1/PD-L1 inhibitors have shown promising therapeutic effects in various malignancies. PD-L1 expression is the only FDA-approved biomarker for guiding immunotherapy in lung adenocarcinoma patients. Results from the KEYNOTE-042 study indicated that first-line Pembrolizumab monotherapy continues to show long-term OS benefits and durable responses compared to chemotherapy, regardless of PD-L1 TPS, in PD-L1-positive locally advanced/metastatic NSCLC patients without EGFR/ALK alterations. The 5-year OS rate reached 22%, supporting the continued use of Pembrolizumab monotherapy as the standard treatment for previously untreated PD-L1-positive advanced/metastatic NSCLC (15). In patients with high PD-L1 expression (at least 50% of tumor cells) and advanced NSCLC, Pembrolizumab has demonstrated longer PFS, OS, and fewer adverse events compared to platinum-based chemotherapy (16). Retrospective studies and case reports have found that PD-1/PD-L1 inhibitors exhibit significant efficacy in PSC patients with high PD-L1 expression (17, 18). The high expression of PD-L1 provides a biological basis for the use of immunotherapy in PGCC patients.

Taking the tumor het erogeneity in human cancers into account, meticulous combined-modality treatment may be necessary to achieve breakthroughs in current cancer therapy for advanced refractory tumors.Clinical trials and studies have demonstrated that the synergistic antitumor activity of anti-angiogenesis combined with immune checkpoint blockade can enhance the treatment outcomes in various solid tumors (19–22). Anti-angiogenesis therapy can inhibit negative immune signals by increasing the ratio of antitumor/pro-tumor immune cells and reducing the expression of multiple immune checkpoints. Concurrently, immunotherapy can restore the immune-supportive microenvironment and promote vascular normalization (23). Therefore, the combination of anti-angiogenesis therapy and immunotherapy can synergize, improving therapeutic efficacy (24). The patient in this case achieved significant clinical benefits from the combination of immunotherapy and Anlotinib, consistent with previous study findings.

Brain metastases (BM) represent the most common form of intracranial malignancies in adults and are associated with poor prognosis (25). Lung cancer is the most frequent primary tumor leading to brain metastases (26). Increasing preclinical and clinical research indicates that combination therapies have significant antitumor activity; however, the efficacy against brain metastases remains unclear due to the stringent selection criteria in most clinical trials. In the era of immunotherapy, accumulating evidence supports using immune checkpoint inhibitors (ICIs) for treating NSCLC brain metastases in the absence of actionable driver mutations (27). In a multicohort study (NCT02039674) involving 25 patients, 4 (16%) had brain metastases, with an ORR of 56%, including 1 (4%) complete response and 13 (52%) partial responses. The median PFS was 7.1 months, and the median OS was 16.7 months (28). A retrospective analysis suggested that Pembrolizumab is effective in previously untreated NSCLC brain metastases patients with high tumor PD-L1 expression (29). The ARIO study assessed the outcomes of radiotherapy in NSCLC patients with brain metastases receiving ICIs (n=100) versus those not receiving ICIs (n=50). The study found that patients undergoing combined treatment had longer intracranial PFS (p=0.007) (30). Patients receiving radiotherapy (SRS/SRT) concurrently or after the initiation of ICIs achieved the greatest benefits, with most studies indicating that concurrent treatment improves OS (31).

In this study, a TP53 mutation was identified. TP53 mutations are the most common genetic alterations in PSC, with approximately three-quarters of patients harboring it. P53R2, a downstream target gene of TP53, comprises 9 exons and 1 intron and shares sequence homology with TP53. It plays a dual role in cancer regulation, including tumor suppression by promoting apoptosis and inhibiting cell proliferation; these pathways depend on the P21 signaling pathway. High levels of P53R2 protein are associated with poor OS. The presence of P53R2 is a significant factor associated with poor prognosis in PSC patients, and its expression is closely related to the occurrence, development, and progression of PSC (32).Generally, mutant TP53-carrying tumors reveal poorer sensitivity to conventional chemotherapy and have worse prognosis than wild-type tumors. This is a possible reason for chemotherapy resistance of PGCC (33).TP53 mutation-reversing drugs may be an effective option for the treatment of this disease in the future. However, currently targeted drugs for TP53 mutation have not been marketed. Although several drugs have shown significant efficacy in clinical trials, more trials are needed to verify. Basic studies have shown that TP53 mutations transmit signals conducive to tumor growth by promoting VEGF-mediated cell migration, angiogenesis, and metastasis or by overcoming ETS1 regulation (34). Therefore, VEGF pathway blockade may be effective in the treatment of this mutant tumor.

Tumor mutational burden (TMB) is also a useful biomarker for ICI response in advanced NSCLC (35). However, its value in brain metastases remains unclear. A retrospective study found that PSC patients with high TMB and TP53 mutations who received ICIs exhibited a longer survival trend compared to those with low TMB (18 months vs. 1.84 months) (23). This observation, however, has not yet been evaluated in advanced PGCC. The patient in this case has been treated for over two years, with follow-up enhanced brain MRI showing stable disease, suggesting that the combination of Penpulimab and Anlotinib may be effective against brain metastases. This indicates that the integration of immunotherapy, anti-angiogenic therapy, and cranial radiotherapy could provide additional benefits for patients. Further investigation is warranted to substantiate these findings.

In this study, the combination of Anlotinib, Penpulimab, and cranial radiotherapy was employed as a first-line treatment, resulting in long-term disease stability and significant efficacy. Therefore, Penpulimab combined with Anlotinib offers a promising new treatment option for untreated advanced PGCC or those with concurrent brain metastases, improving prognosis.

The patient, diagnosed with advanced PGCC, was confirmed *via* a small biopsy specimen from a lung puncture. Literature review indicates that small biopsy specimens are acceptable for diagnosing advanced NSCLC in clinical practice (36).

The primary adverse effect observed in this patient was Grade 1 hypothyroidism, which was attributed to Anlotinib. Despite this, thyroid function remained within normal reference ranges and was effectively managed with oral levothyroxine. No Grade 3-4 adverse events were observed. The optimal duration of maintenance therapy with Penpulimab remains undetermined, although clinical studies typically recommend a period of two years. Currently, the patient maintains a good quality of life, with continuous partial response (PR) and a survival period exceeding 26 months. Ongoing Follow-up will continue to monitor the patient's condition.

To our knowledge, this is the first report demonstrating the efficacy of Penpulimab combined with Anlotinib in the treatment of advanced PGCC with brain metastases, high PD-L1 expression, and TP53 mutation. The combination of immunotherapy and anti-angiogenic agents presents a potentially promising strategy for treating PGCC. However, further studies are required to validate the efficacy and safety of this treatment approach.

Data availability statement

The original contributions presented in the study are included in the article/supplementary material. Further inquiries can be directed to the corresponding author.

Ethics statement

The studies involving humans were approved by Medical Ethics Review Committee of Jiaozuo City Second People's Hospital, The second people's Hospital of Jiaozuo. The studies were conducted in accordance with the local legislation and institutional requirements. The participants provided their written informed consent to participate in this study. Written informed consent was obtained from the individual(s) for the publication of any potentially identifiable images or data included in this article.

Author contributions

MX: Data curation, Funding acquisition, Writing – original draft, Writing – review & editing, Formal analysis, Investigation, Validation. YZ: Investigation, Writing – review & editing. XH: Investigation, Validation, Visualization, Writing – original draft. HL: Formal analysis, Investigation, Software, Writing – review & editing. NL: Methodology, Supervision, Validation, Writing – review & editing. SN: Formal analysis, Writing – review & editing, Investigation, Methodology. XX: Conceptualization, Project administration, Supervision, Validation, Writing – review & editing, Writing – original draft.

Funding

The author(s) declare financial support was received for the research, authorship, and/or publication of this article. Henan Province Medical Science and Technology Research Program (Joint Construction) Project, Funding number: LHGJ20191352.

Conflict of interest

The authors declare that the research was conducted in the absence of any commercial or financial relationships that could be construed as a potential conflict of interest.

Publisher's note

References

1. Vieira T, Girard N, Ung M, Monnet I, Cazes A, Bonnette P, et al. Efficacy of first-line chemotherapy in patients with advanced lung sarcomatoid carcinoma. *J Thorac Oncol*. (2013) 8:1574–7. doi: 10.1097/01.JTO.0000437008.00554.90

2. Xia C, Dong X, Li H, Cao M, Sun D, He S, et al. Cancer statistics in China and United States, 2022: profiles, trends, and determinants. *Chin Med J (Engl)*. (2022) 135:584–90. doi: 10.1097/CM9.0000000000002108

3. Han C, Ye S, Hu C, Shen L, Qin Q, Bai Y, et al. Clinical activity and safety of penpulimab (Anti-PD-1) with anlotinib as first-line therapy for unresectable hepatocellular carcinoma: an open-label, multicenter, phase ib/II trial (AK105-203). *Front Oncol*. (2021) 11:684867. doi: 10.3389/fonc.2021.684867

4. Zheng Y, Zhu J, Xiong J, Jiang O, Wang H, Xie Y, et al. Phase 1b/2 study of penpulimab (AK105), an antiprogrammed cell death-1 immunoglobulin G1 antibody, in advanced or metastatic solid tumors (AK105-204). *Cancer*. (2024) 130:2180–90. doi: 10.1002/cncr.35259

5. Yang S, Zhang W, Chen Q, Guo Q. Clinical investigation of the efficacy and safety of anlotinib with immunotherapy in advanced non-small cell lung cancer as third-line therapy: A retrospective study. *Cancer Manag Res*. (2020) 12:10333–40. doi: 10.2147/CMAR.S280096

6. Li W, Yu H. Separating or combining immune checkpoint inhibitors (ICIs) and radiotherapy in the treatment of NSCLC brain metastases. *J Cancer Res Clin Oncol*. (2020) 146:137–52. doi: 10.1007/s00432-019-03094-9

7. Karlsson AT, Hjermstad MJ, Omdahl T, Aass N, Skovlund E, Hellebust TP, et al. Overall survival after initial radiotherapy for brain metastases; a population based study of 2140 patients with non-small cell lung cancer. *Acta Oncol (Madr)*. (2021) 60:1054–60. doi: 10.1080/0284186X.2021.1924399

8. Fang L, Zhao W, Ye B, Chen D. Combination of immune checkpoint inhibitors and anti-angiogenic agents in brain metastases from non-small cell lung cancer. *Front Oncol*. (2021) 11:670313. doi: 10.3389/fonc.2021.670313

9. Hu H, Xu Z-Y, Zhu Q, Liu X, Jiang S-C, Zheng J-H. Brain metastases status and immunotherapy efficacy in advanced lung cancer: A systematic review and meta-analysis. *Front Immunol*. (2021) 12:669398. doi: 10.3389/fimmu.2021.669398

10. Crinò L, Bronte G, Bidoli P, Cravero P, Minenza E, Cortesi E, et al. Nivolumab and brain metastases in patients with advanced non-squamous non-small cell lung cancer. *Lung Cancer*. (2019) 129:35–40. doi: 10.1016/j.lungcan.2018.12.025

11. Maneenil K, Xue Z, Liu M, Boland J, Wu F, Stoddard SM, et al. Sarcomatoid carcinoma of the lung: the mayo clinic experience in 127 patients. *Clin Lung Cancer*. (2018) 19:e323–33. doi: 10.1016/j.cllc.2017.12.008

12. Yendamuri S, Caty L, Pine M, Adem S, Bogner P, Miller A, et al. Outcomes of sarcomatoid carcinoma of the lung: A Surveillance, Epidemiology, and End Results database analysis. *Surgery*. (2012) 152:397–402. doi: 10.1016/j.surg.2012.05.007

13. Shen G, Zheng F, Ren D, Du F, Dong Q, Wang Z, et al. Anlotinib: a novel multi-targeting tyrosine kinase inhibitor in clinical development. *J Hematol Oncol*. (2018) 11:120. doi: 10.1186/s13045-018-0664-7

14. Han B, Li K, Wang Q, Zhao Y, Zhang L, Shi J, et al. Third-line treatment: A randomized, double-blind, placebo-controlled phase III ALTER-0303 study—Efficacy and safety of anlotinib treatment in patients with refractory advanced NSCLC. *J Clin Oncol*. (2017) 35:9053–3. doi: 10.1200/JCO.2017.35.15_suppl.9053

15. de Castro G Jr., Kudaba I, Wu YL, Lopes G, Kowalski DM, Turna HZ, et al. Five-year outcomes with pembrolizumab versus chemotherapy as first-line therapy in patients with non–small-cell lung cancer and programmed death ligand-1 tumor proportion score ≥ 1% in the KEYNOTE-042 study. *J Clin Oncol*. (2023) 41:1986–91. doi: 10.1200/JCO.21.02885

16. Reck M, Rodríguez-Abreu D, Robinson AG, Hui R, Csőszi T, Fülöp A, et al. Pembrolizumab versus chemotherapy for PD-L1–positive non–small-cell lung cancer. *New Engl J Med*. (2016) 375:1823–33. doi: 10.1056/NEJMoa1606774

17. Lee J, Choi Y, Jung HA, Lee SH, Ahn JS, Ahn MJ, et al. Outstanding clinical efficacy of PD-1/PD-L1 inhibitors for pulmonary pleomorphic carcinoma. *Eur J Cancer*. (2020) 132:150–8. doi: 10.1016/j.ejca.2020.03.029

18. Wu S, Wu S, Liao X, Zhou C, Qiu F, Wang C, et al. Pembrolizumab combined with anlotinib improves therapeutic efficacy in pulmonary sarcomatoid carcinoma with TMB-H and PD-L1 expression: a case report and literature review. *Front Immunol*. (2023) 14:1274937. doi: 10.3389/fimmu.2023.1274937

19. Yu L, Xu J, Qiao R, Han B, Zhong H, Zhong R. Efficacy and safety of anlotinib combined with PD -1/ PD-L1 inhibitors as second-line and subsequent therapy in advanced small-cell lung cancer. *Cancer Med*. (2023) 12:5372–83. doi: 10.1002/cam4.5360

20. Rini BI, Plimack ER, Stus V, Gafanov R, Hawkins R, Nosov D, et al. Pembrolizumab plus Axitinib versus Sunitinib for Advanced Renal-Cell Carcinoma. *New Engl J Med*. (2019) 380:1116–27. doi: 10.1056/NEJMoa1816714

21. Xie L, Xu J, Sun X, Guo W, Gu J, Liu K, et al. Apatinib plus camrelizumab (anti-PD1 therapy, SHR-1210) for advanced osteosarcoma (APFAO) progressing after chemotherapy: a single-arm, open-label, phase 2 trial. *J Immunother Cancer*. (2020) 8:e000798. doi: 10.1136/jitc-2020-000798

22. Chu T, Zhong R, Zhong H, Zhang B, Zhang W, Shi C, et al. Phase 1b study of sintilimab plus anlotinib as first-line therapy in patients with advanced NSCLC. *J Thorac Oncol*. (2021) 16:643–52. doi: 10.1016/j.jtho.2020.11.026

23. Yi M, Jiao D, Qin S, Chu Q, Wu K, Li A. Synergistic effect of immune checkpoint blockade and anti-angiogenesis in cancer treatment. *Mol Cancer*. (2019) 18:60. doi: 10.1186/s12943-019-0974-6

24. Huang Y, Kim BYS, Chan CK, Hahn SM, Weissman IL, Jiang W. Improving immune–vascular crosstalk for cancer immunotherapy. *Nat Rev Immunol*. (2018) 18:195–203. doi: 10.1038/nri.2017.145

25. Achrol AS, Rennert RC, Anders C, Soffietti R, Ahluwalia MS, Nayak L, et al. Brain metastases. *Nat Rev Dis Primers*. (2019) 5:5. doi: 10.1038/s41572-018-0055-y

26. Le Rhun E, Guckenberger M, Smits M, Dummer R, Bachelot T, Sahm F, et al. EANO–ESMO Clinical Practice Guidelines for diagnosis, treatment and follow-up of patients with brain metastasis from solid tumours. *Ann Oncol*. (2021) 32:1332–47. doi: 10.1016/j.annonc.2021.07.016

27. Wang S, Hu C, Xie F, Liu Y. Use of programmed death receptor-1 and/or programmed death ligand 1 inhibitors for the treatment of brain metastasis of lung cancer. *Onco Targets Ther*. (2020) 13:667–83. doi: 10.2147/OTT.S235714

28. Gadgeel SM, Stevenson JP, Langer CJ, Gandhi L, Borghaei H, Patnaik A, et al. Pembrolizumab and platinum-based chemotherapy as first-line therapy for advanced non–small-cell lung cancer: Phase 1 cohorts from the KEYNOTE-021 study. *Lung Cancer*. (2018) 125:273–81. doi: 10.1016/j.lungcan.2018.08.019

29. Wakuda K, Yabe M, Kodama H, Nishioka N, Miyawaki T, Miyawaki E, et al. Efficacy of pembrolizumab in patients with brain metastasis caused by previously untreated non-small cell lung cancer with high tumor PD-L1 expression. *Lung Cancer*. (2021) 151:60–8. doi: 10.1016/j.lungcan.2020.11.009

30. Scoccianti S, Olmetto E, Pinzi V, Osti MF, Di Franco R, Caini S, et al. Immunotherapy in association with stereotactic radiotherapy for non-small cell lung cancer brain metastases: results from a multicentric retrospective study on behalf of AIRO. *Neuro Oncol*. (2021) 23:1750–64. doi: 10.1093/neuonc/noab129

31. Rios-Hoyo A, Arriola E. Immunotherapy and brain metastasis in lung cancer: connecting bench side science to the clinic. *Front Immunol*. (2023) 14:1221097. doi: 10.3389/fimmu.2023.1221097

32. Chen J, Xiao Y, Cai X, Liu J, Chen K, Zhang X. Overexpression of p53R2 is associated with poor prognosis in lung sarcomatoid carcinoma. *BMC Cancer*. (2017) 17:855. doi: 10.1186/s12885-017-3811-6

33. Li X, Zhang Z, Liu J, Wang D, Wei S, Chen J. Molecular features of giant-cell carcinoma of the lung: a case report and literature review. *Onco Targets Ther*. (2018) 11:751–6. doi: 10.2147/OTT.S150124

34. Joshi H, Bhanot G, Børresen-Dale A-L, Kristensen V. Potential tumorigenic programs associated with TP53 mutation status reveal role of VEGF pathway. *Br J Cancer*. (2012) 107:1722–8. doi: 10.1038/bjc.2012.461

35. Marabelle A, Fakih M, Lopez J, Shah M, Shapira-Frommer R, Nakagawa K, et al. Association of tumour mutational burden with outcomes in patients with advanced solid tumours treated with pembrolizumab: prospective biomarker analysis of the multicohort, open-label, phase 2 KEYNOTE-158 study. *Lancet Oncol*. (2020) 21:1353–65. doi: 10.1016/S1470-2045(20)30445-9

36. Chang C-L, Hsieh M-S, Shih J-Y, Lee Y-H, Liao W-Y, Yang C-Y. Real-world treatment patterns and outcomes among patients with advanced non-small-cell lung cancer with spindle cell and/or giant cell carcinoma. *Ther Adv Med Oncol*. (2022) 14:175883592211338. doi: 10.1177/17588359221133889

frontiers | Frontiers in Oncology

TYPE Case Report
PUBLISHED 30 January 2025
DOI 10.3389/fonc.2025.1502934

OPEN ACCESS

EDITED BY
Jianxin Xue,
Sichuan University, China

REVIEWED BY
Jisheng Li,
Shandong University, China
Hesong Wang,
Fourth Hospital of Hebei Medical University, China

*CORRESPONDENCE
Wei Wang
wangwei929@cqu.edu.cn
Xiaoping Huang
626951237@qq.com
Yi Liu
liuyi_leo@hotmail.com

RECEIVED 27 September 2024
ACCEPTED 06 January 2025
PUBLISHED 30 January 2025

CITATION
Zhong M, Zhou L, Guo J, Chen C, Wang W, Huang X and Liu Y (2025) Case report: A case report and literature review on the efficacy of high-dose aumolertinib combined intrathecal pemetrexed by Ommaya reservoir for EGFR-mutated NSCLC with leptomeningeal metastasis as the initial symptoms.
Front. Oncol. 15:1502934.
doi: 10.3389/fonc.2025.1502934

Case report: A case report and literature review on the efficacy of high-dose aumolertinib combined intrathecal pemetrexed by Ommaya reservoir for EGFR-mutated NSCLC with leptomeningeal metastasis as the initial symptoms

Maoxi Zhong[1,2,3], Li Zhou[1,2,3], Jing Guo[1,2,3], Chuan Chen[1,2,3], Wei Wang[1,2,3]*, Xiaoping Huang[1,2,3]* and Yi Liu[2,3,4]*

[1]Department of Cancer Center, Chongqing University Three Gorges Hospital, Chongqing, China, [2]School of Medicine, Chongqing University, Chongqing, China, [3]Chongqing Municipality Clinical Research Center for Geriatric Diseases, Chongqing, China, [4]Department of Thoracic Surgery, Chongqing University Three Gorges Hospital, Chongqing, China

Leptomeningeal metastasis (LM) is a significant complication of advanced non-small cell lung cancer (NSCLC), occurring in only 3-5% of patients and exceedingly rare in newly diagnosed NSCLC patients. This also indicates that the tumor is highly malignant and aggressive, which brings great challenges to treatment. Here we present a case report of an EGFR-mutated NSCLC patient who presented with LM as the primary clinical manifestation, and review the latest advances in existing studies on LM-related treatment. The patient underwent multiple cycles of high-dose aumolertinib in combination with intrathecal pemetrexed administered via Ommaya reservoir. As of the submission date, the patient achieved significant remission and a LM Progression-Free Survival (PFS) exceeding 20 months. This case highlights the positive impact of high-dose aumolertinib combined with intrathecal pemetrexed on NSCLC patients presenting with severe meningeal symptoms as the initial manifestation, offering a viable therapeutic approach for managing severe meningeal symptoms associated with LM, such as headache, nausea, neck stiffness, and vomiting.

KEYWORDS

high-dose aumolertinib, intrathecal chemotherapy, leptomeningeal metastasis, NSCLC, case report

1 Introduction

LMoccurs when tumor cells spread into the leptomeninges, subarachnoid space, and other cerebrospinal fluid (CSF) chambers. NSCLC is one of the most common solid tumors with LM. Clinical manifestations are diverse and non-specific, primarily including neurological symptoms in three aspects, increased intracranial pressure (dizziness, headache, vomiting, and optic neuroid edema), meninges irritation (cervical stiffness, Kernig's sign, and Brudzinski's sign), and cerebral neuropathy (1). The diagnosis of LM is based on clinical findings, head MRI, and CSF cytology. Once LM develops, the patient may rapidly progress toward death. Modern treatments have increased the OS from 1-3 months to 3-11 months (1, 2), but treatment remains extremely challenging. LM patients are heterogeneous due to complex etiology and molecular characteristics. The optimal approach remains uncertain, particularly for those with driver gene mutations, leaving many questions about precise and personalized treatment decisions.

2 Case description

In December 2022, a 52-year-old female patient was admitted to the Neurology Department of Chongqing University Affiliated Three Gorges Hospital, presenting with an acute "thunderclap" headache and vomiting. The patient had no history of smoking and maintained good overall health prior to admission.

Upon presentation, her Eastern Cooperative Oncology Group Performance Status (ECOG PS) score was assessed at 4, with signs of elevated intracranial pressure. Following symptomatic management, a lumbar puncture was performed, revealing CSF pressure measured at 370 mmH2O and atypical cells within the CSF. Subsequent imaging studies revealed abnormal signals in the frontal, parietal, and occipital sulci of the cerebrum on head MRI, with widening noted in the right frontal lobe (Figure 1). Chest CT revealed increased scattered streaky density in the right lung with partial consolidation, suggestive of infectious lesions, and associated pleural effusion in the right thoracic cavity and interlobar fissure (Figure 1). Further positron emission tomography-computed tomography (PET-CT) scan showed increased tracer uptake of multiple tumor nodules localized in the right lower lobe (SUVmax 6.0) and extensive metastasis (SUVmax 7.3) (Supplementary Figure 1). In terms of pathological diagnosis, atypical cells were only detected in CSF (Supplementary Figure 2), but not in the right pleural effusion. Due to the patient's poor condition, further tissue biopsy could not be performed, resulting in a lack of histopathological evidence for diagnosis. As the disease progresses, the patient experienced

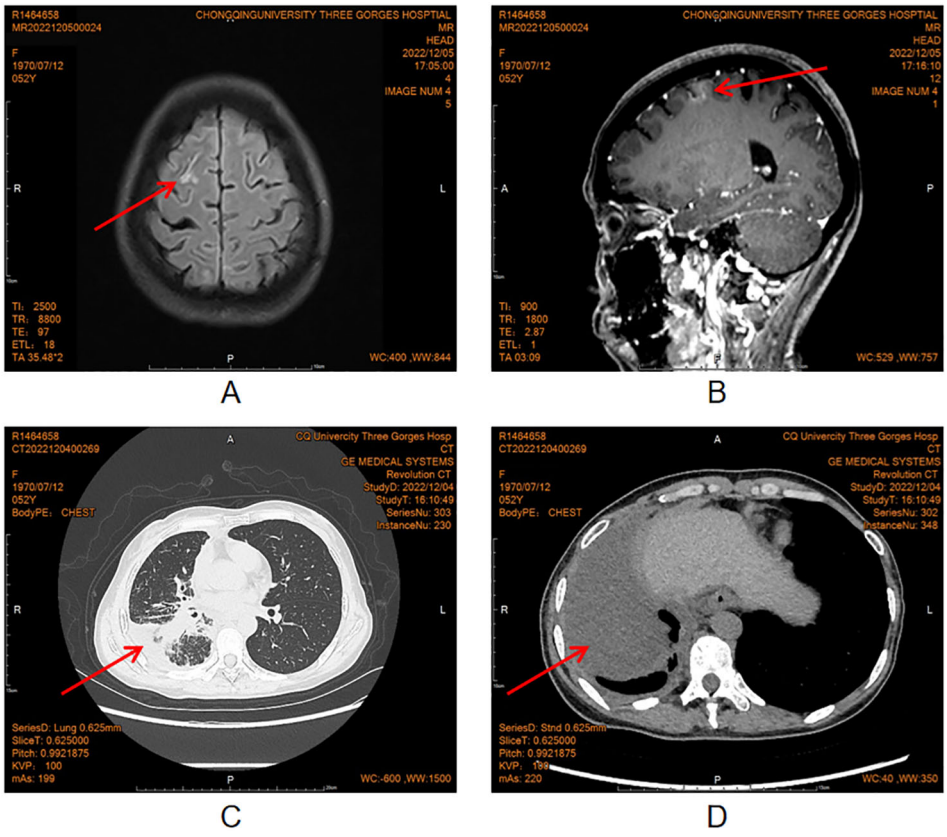

FIGURE 1
Head MRI and chest CT in December, 2022.

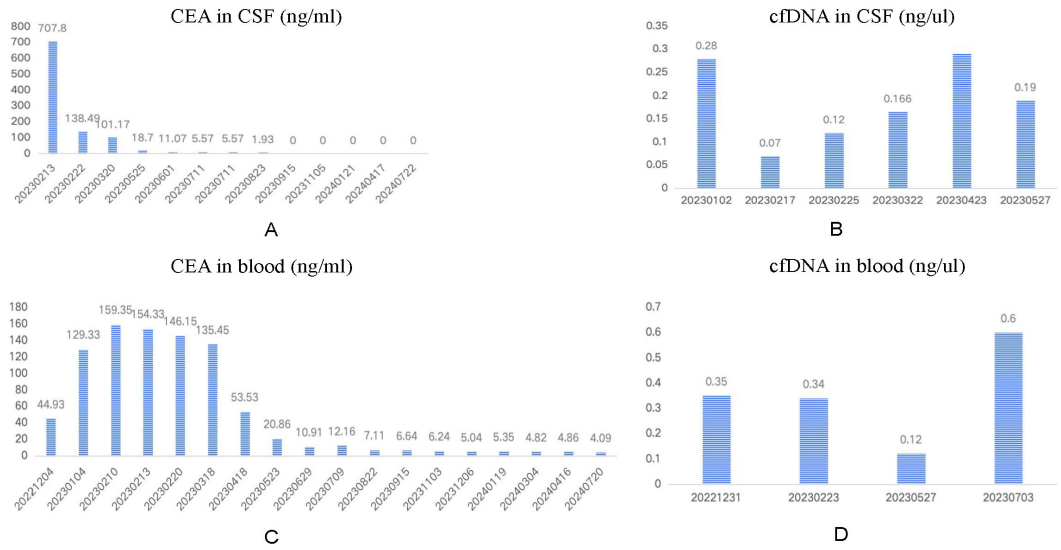

FIGURE 2
Dynamic monitoring of CEA and cfDNA in the CSF and in the blood.

paroxysmal severe headaches, intermittent seizures accompanied by nausea and vomiting. Additionally, there was a gradual onset of blurred vision in the left eye and significant visual decline leading to blindness in the right eye.

Due to the patient's critical condition and lack of sufficient pathological diagnosis, a multidisciplinary consultation (MDT) was conducted within the hospital. After MDT discussion, the patient was clinically diagnosed with a malignant tumor in the right lower lobe of the lung, which is highly likely to be NSCLC, and the tumor had spread to the right hilar lymph node, mediastinal lymph node, right pleura, multiple bones, and leptomeninges. Subsequently, the patient was transferred to the oncology department for further treatment. To enhance diagnostic accuracy and alleviate symptoms associated with elevated intracranial pressure, it was advised to implant an Ommaya reservoir for CSF drainage followed by subsequent ITC. On December 8, 2022, the patient underwent a ventriculostomy followed by the implantation of an Ommaya reservoir. The patient, a non-smoking Asian woman with lung cancer, had a higher probability of testing positive for the driver gene. Because of the critical condition, despite the unknown genetic mutation, she still bravely tried the third generation of epidermal growth factor receptor (EGFR) tyrosine kinase inhibitor (TKI). In light of evident LM symptoms requiring enhanced disease management measures; high-dose aumolertinib (165 mg/day) was initiated on December 29th 2022 as targeted therapy regimen. Fortunately after one week since treatment initiation, significant improvement was observed regarding "lightning strike" headache episodes along with alleviation in nausea/vomiting, and slight relief from blurred vision, and the ECOG PS dropped to 2 points, indicating that the general condition of the patient was significantly improved. Genetic testing results obtained on January 9, 2023 confirmed the presence of an EGFR-sensitive mutation in the patient. Specifically, EGFR exon 21 p.L858R was detected in both CSF and blood with mutation abundance of 41.15% and 0.78%, respectively.

February 10, 2023, CT examination showed pleural effusion were mostly absorbed, partial remission of lung lesions, complete remission of LM lesions. In addition, the intracranial pressure decreased significantly in retesting (370mmH2O before treatment vs. 220mmH2O after treatment). However, she performed an elevated carcinoembryonic antigen (CEA) level (707.8 ng/mL) in CSF. To further enhance the local control of LM, in the next two weeks, the patient received ITC with pemetrexed (30mg) via the Ommaya reservoir, 30mg on day 1 and day 8, with a cycle every 3 weeks. On February 21, 2023, the patient underwent a single cycle of systemic chemotherapy involving pemetrexed and carboplatin at dosages of 600mg and 300mg, respectively. Subsequently, we found that the CEA level in CSF dropped to 138.5 ng/mL. However, the patient developed severe myelosuppression (grade IV) with fever after chemotherapy, so systemic chemotherapy was discontinued in subsequent treatment, and targeted therapy combined with ITC by Ommaya reservoir was continued. Reexamination of imaging on April 19, 2023 showed a significant reduction in the lesions of pulmonary and intracranial tumors, but an expansion of bone metastasis and the emergence of significant lower back pain symptoms in the patient. In order to alleviate the lower back pain and reduce the risk of pathological fractures, the patient underwent palliative radiotherapy for some thoracolumbar vertebral metastases in May 2023.

Subsequently, considering the patient's tolerance, the ITC of pemetrexed regimen via Ommaya reservoir was adjusted to 30 mg every 4 weeks starting July 2023, with the last chemotherapy on January 20, 2024. The patient continued oral high-dose aumolertinib (165 mg/day) during this period. Imaging showed improvement in lung and brain tumors while bone metastases remained stable; overall efficacy was evaluated as PR.

Additionally, CEA levels in blood and CSF gradually normalized during follow-up (Figure 2), and no atypical cells were found in CSF after repeated examinations. cfDNA concentration in CSF significantly decreased early in treatment but slowly increased at 3 months before decreasing again at 5 months. In contrast, cfDNA levels in blood gradually decreased over the first 6 months of treatment followed by a rebound at month 7 (Figure 2).

During the single-dose ITC administered every 4 weeks, the patient's adverse reactions resolved. The main treatment-related adverse reactions (TRAEs) were grade II myelosuppression and grade I gastrointestinal issues (nausea, vomiting, and oral ulcers), which improved with symptomatic treatment (specific TRAEs are listed in Table 1). The patient has an ECOG PS score of 1 and significant relief from headache, nausea, and vomiting. Her left eye vision notably improved while her right eye progressed from blindness to blurriness. Due to this positive response to treatment, she has been on a chemotherapy hiatus since February 2024 and is now receiving high-dose aumolertinib. The latest follow-up was on July 20, 2024. We have documented changes in clinical manifestations, imaging exams, and genetic testing via next-generation sequencing (NGS) throughout the treatment process (see Table 2, Figure 3, Supplementary Table 1).

3 Discussion

LM is a devastating complication of NSCLC, with a low rate of early diagnosis and limited treatment options, resulting in poor prognosis. The incidence of LM in NSCLC without driver genes is 3.8%, while it can reach 9% in patients with EGFR mutations (3). Due to the low incidence rate, the rapid progress of the disease, and the heterogeneity of the LM population, there is currently no standard treatment protocol. In addition to symptomatic supportive therapy, active treatment strategies include systemic chemotherapy, ITC, whole brain radiation therapy (WBRT) and/or spinal axis radiation, as well as the EGFR-TKI for EGFR-positive patients. Radiotherapy is mainly used to alleviate symptoms from brain edema or focal lesion, however, there is limited evidence of its effectiveness in improving survival, and it increases the risk of toxicity (4–7). Some researchers suggest selecting suitable candidates for radiotherapy, noting that WBRT may benefit EGFR wild-type, nodular LM patients (8).

Systemic chemotherapy has limited efficacy for LM because it cannot achieve effective blood-brain barrier (BBB) penetration (1). However, ITC can bypass the BBB, achieving high CSF concentrations with low drug doses (9), enhancing local control of LM. Two main ITC methods exist: lumbar puncture and Ommaya reservoir. The Ommaya reservoir is more convenient and safer for CSF sampling and ITC. Emerging technologies like the Lumbar Intrathecal Port (LIP) are also becoming prominent in ITC (10). Due to dose-limiting toxicity and related complications, there is no consensus on the optimal dose, frequency, and duration of ITC. Classic ITC drugs include: thiotepa, methotrexate, (liposomal) cytarabine (3). Recently, pemetrexed has emerged as an important ITC agent. However, there is currently no consensus on the optimal dosage, administration frequency, and treatment duration. A phase I clinical study (11) showed that intrathecal injection of 10mg pemetrexed once or twice weekly resulted in favorable therapeutic effects and manageable toxicity in patients with LM. The response rate was 31% (4/13), with a disease control rate (DCR) of 54% (7/13). The most common AEs included bone marrow suppression, elevated liver transaminases, and neuritis. A single-arm phase 1/2 clinical trial (12) utilized ITC of 50 mg pemetrexed as the recommended dosage (RD). The regimen involved 50 mg on day 1 and 5 of the first week, followed by every three weeks for four cycles, then monthly until disease progression or intolerance. The mOS was 9.0 months. Primary AEs included nausea, vomiting, myelosuppression, and neurotoxicity (grade 1 or grade 2). Researchers have suggested administering 30 mg of pemetrexed on days 1 and 8 every three weeks, which has demonstrated positive effects in clinical practice (13). In this case, the patient initially received a 3-week pemetrexed regimen (30mg, D1, D8, q3W) for 4

TABLE 1 TRAEs.

Event	CTCAE 5.0	Possibility factor	Drug treatment/ self remission
WBC count decrease	4	Systemic chemotherapy, ITC or Aumolertinib	Drug treatment
Platelet count decrease	2	Systemic chemotherapy, ITC or Aumolertinib	Drug treatment
Anemia	2	Systemic chemotherapy, ITC or Aumolertinib	Drug treatment
Nausea	2	ITC	Drug treatment
Vomiting	2	ITC	Drug treatment
Oral ulcers	2	Aumolertinib or ITC	Drug treatment
Decreased appetite	2	Systemic chemotherapy, ITC or Aumolertinib	Drug treatment
Fatigue	2	Systemic chemotherapy, ITC or Aumolertinib	Self remission
ALT increase	1	Aumolertinib or ITC	Drug treatment
AST increase	1	Aumolertinib or ITC	Drug treatment

TRAEs, treatment-related adverse reactions; CTCAE 5.0, the common terminology criteria for adverse events version 5.0; ITC, intrathecal chemotherapy.

TABLE 2 Records of important clinical manifestations of the patient.

Date	ECOG PS (0-4)	NRS of pain (0-10)	Nausea and vomiting (CTCAE 5.0) (1-5)	Pupil size (mm) and light reflex (sensitive +, slow -)	Eyesight
2022-12-09	4	6-7	4	Left: 3, +; Right: 6, -	Left: fuzzy; Right: blindness
2023-02-15	3	3-5	2	Left: 3, +; Right: 6, -	Left: light sense; Right: blindness
2023-04-16	2	1-2	1	Left: 3, +; Right: 5, -	Left: <4.0; Right: light sense
2023-06-20	1	1	1	Left: 3, +; Right: 5, -	Left: <4.0; Right: light sense
2023-09-25	1	0	1	Left: 3, +; Right: 4, -	Left: 4.0; Right: light sense
2023-12-30	1	0	1	Left: 3, +; Right: 4, -	Left: 4.0; Right: light sense
2024-03-28	1	0	0	Left: 3, +; Right: 4, -	Left: 4.0; Right: light sense
2024-06-25	1	0	0	Left: 3, +; Right: 4, -	Left: 4.0; Right: light sense
2024-07-20	1	0	0	Left: 3, +; Right: 4, -	Left: 4.0; Right: light sense

ECOG PS, eastern cooperative oncology group performance status; NRS, numerical rating scale; CTCAE 5.0, the common terminology criteria for adverse events version 5.0.

cycles. In the maintenance stage, pemetrexed was adjusted to a 4-week schedule (30 mg, D1, D8, q4W) for 5 cycles. The 3-week regimen had a higher risk of myelosuppression, while the 4-week regimen was better tolerated. Therefore, prophylactic leukocyte-count support is crucial, especially for patients with multiple bone metastases. Folic acid and vitamin B12 supplementation should also be regularly administered to reduce AEs (11, 12).

For LM patients with EGFR-positive, third-generation TKIs have demonstrated superior efficacy compared to first- and second-generation TKIs. Small sample studies have reported LM-PFS of 2.0

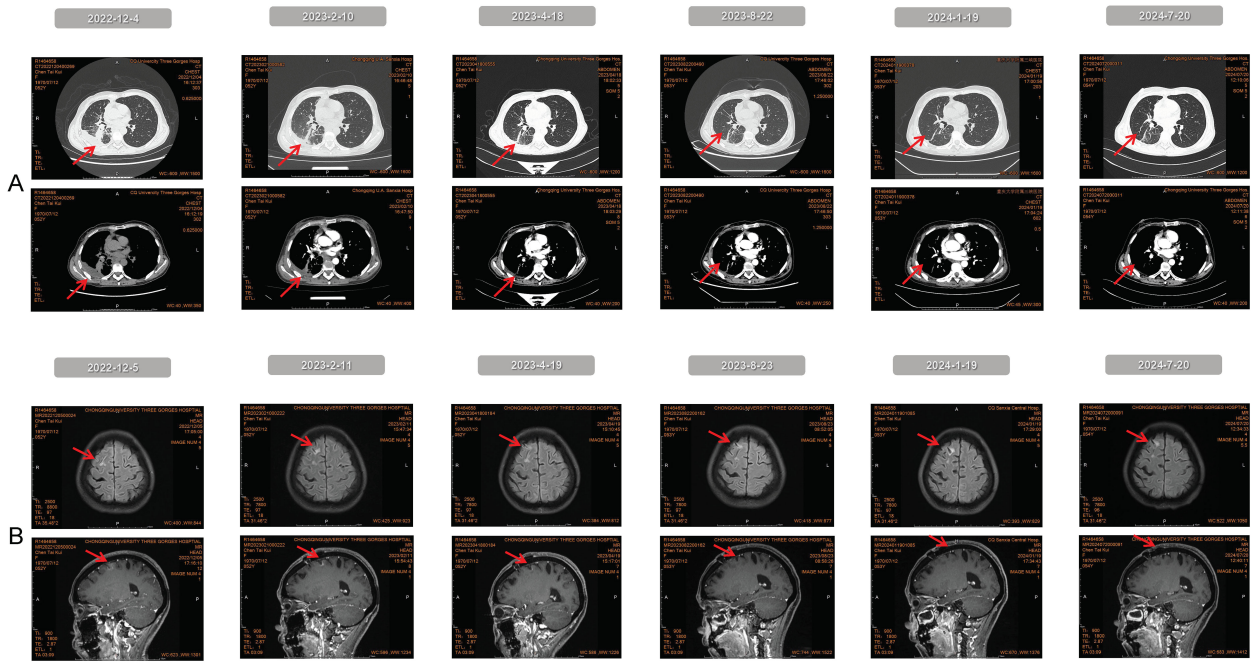

FIGURE 3
The imaging results obtained from the continuous follow-up.

to 2.3 months and mOS of 3.4 to 3.8 months for gefitinib, erlotinib, and afatinib (14–16). Third-generation EGFR-TKIs exhibit superior penetration through the BBB, making them more suitable for treating LM (3, 17). A retrospective study compared clinical outcomes of standard-dose osimertinib to first-generation TKIs in untreated EGFR-positive NSCLC with LM, showing superior mPFS (16.9 months vs. 8.6 months) and mOS (26.6 months vs. 20.0 months) in the osimertinib group (18). Researchers are attempting to improve disease management by increasing the concentration of EGFR TKI in CSF. A phase II study showed that osimertinib (160 mg/day) achieved an objective response rate (ORR) of 27.5% and a DCR of 82.5% in EGFR T790M-positive NSCLC with BM/LM, the mPFS was 5.7 months, and the common AEs included decreased appetite, diarrhea, and skin rash, most grade 1 or 2 levels (19). In a Phase I study (BLOOM) (6), osimertinib (160 mg/day) achieved an LM-ORR of 62% in EGFRm NSCLC patients with LM who had progressed on TKIs (n=41). The mPFS and mOS were 8.6 and 11.0 months. 24% of patients experienced ≥3 grade AEs, leading to discontinuation in 9 and dose reduction in 5 patients. A real-world study (n=48) showed that high-dose furmonertinib (240 mg/day) achieved an LM-ORR of 50.0%, an LM-DCR of 92.1%, and a mOS of 8.43 months in EGFR-mutated LM. 22 patients (45.8%) experienced TRAEs, and 3 (6.3%) had grade 3 AEs, leading to a dose reduction to 160 mg/day (20). Related studies indicate that aumolertinib is effective in controlling CNS metastasis, particularly at higher doses, although there is currently limited data on LM. In the AENEAS study (21), aumolertinib (110 mg/day) demonstrated significant improvement in CNS PFS compared to gefitinib when used as a first-line treatment for advanced NSCLC. The median CNS PFS was 29.0 months for aumolertinib and 8.3 months for gefitinib (HR=0.31; 95% CI, 0.17-0.56; P<0.001). The 12-month CNS PFS rates were 72.5% for aumolertinib and 30.4% for gefitinib. The ACHIEVE study (22) showed that high-dose aumolertinib (165 mg/day) administered as first-line treatment to patients with EGFR-positive NSCLC with BM resulted in a 12-month intracranial PFS (iPFS) rate of 75.0%, with the miPFS not reached. The ARTISTRY study (23) cohort 2 is currently enrolling 10 newly diagnosed patients with LM-NSCLC, with the initial treatment dose of aumolertinib set at 110mg/day. Patients will undergo efficacy assessments every 4 weeks until they progress, and if there are no PDs in two consecutive assessments, the dose can be gradually increased to 165/220mg/day ± radiation therapy. It is worth noting that,patients with the exon 19 mutation have a relatively better prognosis than those with the L858R mutation (4, 18). Based on these studies, third-generation EGFR-TKIs show superior efficacy and safety in patients with brain/meningeal metastases from EGFR-mutated NSCLC, and dose escalation may be a better treatment strategy. Further research is required to determine the optimal selection of TKIs, the best drug dosage, and the impact of different mutation types on TKIs efficacy in LM.

Monotherapy has a limited effect on improving the prognosis of LM, while a combination treatment model may provide greater benefit. Retrospective studies show that the use of ITC and EGFR-TKI are important predictors of good survival prognosis (7, 24). A retrospective analysis (9) showed that combining osimertinib (80mg/day) with ITC of methotrexate resulted in a mPFS of 10.8 months for LM patients who progressed after EGFR-TKI. This is comparable to the efficacy observed with 160 mg/day osimertinib in the BLOOM study, suggesting that combination therapy may offer better outcomes. Another retrospective analysis showed that in NSCLC patients who progressed to LM after osimertinib treatment (n=9), the combination of high-dose aumolertinib (220 mg/day) with ITC of pemetrexed, combined or not combined with bevacizumab resulted in a mPFS of 11 months and a mOS of 14 months (25). Additionally, relevant studies have shown that TKIs combined with anti-angiogenic drugs has better efficacy in LM. A retrospective real-world study (26) indicated that compared with EGFR-TKI alone, TKI combined with anti-angiogenic therapy (bevacizumab) experienced a delayed onset of LM (mOS1: 19.4 months vs. 13.9 months) and an extended survival after LM (mOS2: 14.5 months vs. 10.0 months). However, EGFR-TKI combined with systemic chemotherapy did not show a survival benefit advantage. A phase II prospective clinical trial (27) using osimertinib (80mg/day) plus bevacizumab (7.5mg/kg, q3W) for EGFRm NSCLC with LM (n=14) showed mLM-PFS of 9.3 months, LM-ORR of 50%, mOS of 12.6 months, and 1-year OS rate of 35.7%. Common AEs included leukopenia, thrombocytopenia, anemia, rash, anorexia, fatigue, ingrown toenail, hemoptysis/rhinorrhea, creatinine elevation, hypertension, and proteinuria. Grade 3 AEs were rare (one case of creatinine elevation, two cases of hypertension). Therefore, a combination of TKI with ITC or anti-angiogenesis therapy may be a more optimal treatment strategy for LM.

The diagnosis and prognosis of LM are crucial, but the unique nature of LM presents challenges for assessment. The Response Assessment in Neuro-Oncology (RANO) group has proposed a composite evaluation that includes three elements: standardized neurological examination, CSF cytology or flow cytometry, and radiographic evaluation (28, 29). However, the assessment criteria still lack clinical universality. Several studies show that tumor markers in CSF assist in diagnosing LM (1, 30, 31). In this case, a significant increase in CEA levels in CSF was noted at initial diagnosis. Moreover, the detection of cfDNA in CSF was crucial since the patient could not provide pathological tissue at that time. Studies indicate that liquid biopsy technology can achieve sensitivity as high as 93% (32). In our patient group, EGFR exon 21 mutations were detected in the CSF, with a significantly higher mutation load than in the blood. During treatment, two co-mutations were detected in CSF but not in blood. A small prospective study (n=21) indicated that the detection rate of EGFR mutations in CSF circulating tumor DNA (ctDNA) was about 2.4 times higher than that in blood (33). CSF testing more accurately reflects molecular changes associated with meningeal metastasis and offers better prognostic value than blood tests. For a thorough evaluation of patients with LM, combined CSF and blood tests are recommended. A significant correlation exists between tumor cell clearance in CSF and dynamic changes in CEA levels, which are key indicators for monitoring treatment efficacy and prognosis. While dynamic changes in cfDNA concentration in CSF were not significantly linked, studies suggest its potential prognostic

value (34). Furthermore, circulating tumor cells (CTCs) and pro-inflammatory cytokines in CSF also correlated with LM patient prognosis (34, 35). Thus, alongside CSF cytology and tumor markers, csfDNA testing can be an essential diagnostic and management tool for LM.

Patients with NSCLC and LM exhibit significant heterogeneity, leading to varied clinical outcomes. In this case, the patient was diagnosed with LM initially, indicating high malignancy and aggressive tumor behavior that complicate treatment. However, after targeted therapy and ITC, the patient experienced prolonged PFS. A retrospective Korean study found that NSCLC patients with initial LM do not always have a poor prognosis; some achieved OS exceeding 12 months (36). Future research should further investigate the clinical and molecular characteristics of this subgroup. Patients with targetable mutations presenting with initial LM may be suitable candidates for aggressive therapeutic interventions.

In summary, LM is a hidden and dangerous disease, making early identification and intervention essential. Treatment presents both challenges and opportunities, and molecularly stratified treatment is recommended for NSCLC patients. We are currently conducting a prospective, open-label clinical trial titled "Aumolertinib Combined Intrathecal Chemotherapy for Leptomeningeal Metastasis From EGFR-Mutated NSCLC and Prognostic Value of Dynamic Changes in cfDNA Profiles " (NCT05810350). Preliminary results have been presented at the 2023 and 2024 WCLC, and look forward to the future results. This case is one of our trial participants. Our findings suggest that combining high-dose amorafenib with intrathecal chemotherapy via the Ommaya reservoir may be a promising treatment for EGFR-positive NSCLC patients with LM. Monitoring CSF cfDNA using NGS technology aids in the diagnosis and treatment of LM patients. More randomized controlled trials are needed to further explore TKI drug selection, dosage, combination strategies, and achieve an appropriate balance between efficacy, quality of life, and cost-effectiveness.

Data availability statement

The original contributions presented in the study are included in the article/Supplementary Material. Further inquiries can be directed to the corresponding authors.

Ethics statement

The studies involving humans were approved by Scientific research Ethics Committee of Chongqing University Three Gorges Hospital. The studies were conducted in accordance with the local legislation and institutional requirements. The participants provided their written informed consent to participate in this study. Written informed consent was obtained from the individual(s) for the publication of any potentially identifiable images or data included in this article.

Author contributions

MZ: Data curation, Formal analysis, Project administration, Visualization, Writing – original draft. LZ: Data curation, Formal analysis, Writing – original draft. JG: Data curation, Visualization, Writing – original draft. CC: Data curation, Writing – original draft, Methodology. WW: Conceptualization, Funding acquisition, Resources, Supervision, Writing – review & editing. XH: Conceptualization, Resources, Supervision, Writing – review & editing. YL: Methodology, Project administration, Supervision, Visualization, Writing – review & editing.

Funding

The author(s) declare financial support was received for the research, authorship, and/or publication of this article. This study was supported by the Science and Health Joint Research Project in Wanzhou District, Chongqing (Project No. wzstc-kw2022017), the hospital-level Chongqing University Three Gorges Hospital (Project No. 2022YJKYXM-010), the Fundamental Research Funds for the Central Universities Project (Project No. 2023CDJYGRH-YB07), and the CSCO Haosen Cancer Research Fund Project (Project No. Y-HS202301-0093).

Conflict of interest

The authors declare that the research was conducted in the absence of any commercial or financial relationships that could be construed as a potential conflict of interest.

Generative AI statement

The author(s) declare that no Generative AI was used in the creation of this manuscript.

Publisher's note

Supplementary material

The Supplementary Material for this article can be found online at: https://www.frontiersin.org/articles/10.3389/fonc.2025.1502934/full#supplementary-material

References

1. Zhao Y. The riddle of the sphinx: progress in leptomeningeal metastasis of non-small cell lung cancer. *Clin Med Insights Oncol*. (2023) 17:11795549231205206. doi: 10.1177/11795549231205206

2. Li YS, Jiang BY, Yang JJ, Tu HY, Zhou Q, Guo WB, et al. Leptomeningeal metastases in patients with Nsclc with Egfr mutations. *J Thorac Oncol*. (2016) 11:1962–9. doi: 10.1016/j.jtho.2016.06.029

3. Remon J, Le Rhun E, Besse B. Leptomeningeal carcinomatosis in non-small cell lung cancer patients: A continuing challenge in the personalized treatment era. *Cancer Treat Rev*. (2017) 53:128–37. doi: 10.1016/j.ctrv.2016.12.006

4. Umemura S, Tsubouchi K, Yoshioka H, Hotta K, Takigawa N, Fujiwara K, et al. Clinical outcome in patients with leptomeningeal metastasis from non-small cell lung cancer: Okayama lung cancer study group. *Lung Cancer (Amsterdam Netherlands)*. (2012) 77:134–9. doi: 10.1016/j.lungcan.2012.03.002

5. Yan W, Liu Y, Li J, Han A, Kong L, Yu J, et al. Whole brain radiation therapy does not improve the overall survival of Egfr-mutant Nsclc patients with leptomeningeal metastasis. *Radiat Oncol (London England)*. (2019) 14:168. doi: 10.1186/s13014-019-1376-z

6. Yang JCH, Kim SW, Kim DW, Lee JS, Cho BC, Ahn JS, et al. Osimertinib in patients with epidermal growth factor receptor mutation-positive non-small-cell lung cancer and leptomeningeal metastases: the bloom study. *J Clin Oncol*. (2020) 38:538–47. doi: 10.1200/jco.19.00457

7. Morris PG, Reiner AS, Szenberg OR, Clarke JL, Panageas KS, Perez HR, et al. Leptomeningeal metastasis from non-small cell lung cancer: survival and the impact of whole brain radiotherapy. *J Thorac Oncol*. (2012) 7:382–5. doi: 10.1097/JTO.0b013e3182398e4f

8. Zhen J, Wen L. Whole brain radiotherapy (Wbrt) for leptomeningeal metastasis from nsclc in the era of targeted therapy: A retrospective study. *Radiat Oncol (London England)*. (2020) 15:185. doi: 10.1186/s13014-020-01627-y

9. Xu H, Chen H, Kong J, Zhang Y, Liu S, Yang G, et al. Survival analysis of different kinds of tyrosine kinase inhibitors in the treatment of patients with epidermal growth factor receptor mutated non-small cell lung cancer and leptomeningeal metastasis. *Chin Med J*. (2022) 102:7. doi: 10.3760/cma.j.cn112137-20211009-02231

10. Comlek S, Saglam S. A new approach for leptomeningeal metastases: chemotherapy administered through lumbar intrathecal port. *Arquivos neuro-psiquiatria*. (2021) 79:816–23. doi: 10.1590/0004-282x-anp-2020-0554

11. Pan Z, Yang G, Cui J, Li W, Li Y, Gao P, et al. A pilot phase 1 study of intrathecal pemetrexed for refractory leptomeningeal metastases from non-small-cell lung cancer. *Front Oncol*. (2019) 9:838. doi: 10.3389/fonc.2019.00838

12. Fan C, Zhao Q, Li L, Shen W, Du Y, Teng C, et al. Efficacy and safety of intrathecal pemetrexed combined with dexamethasone for treating tyrosine kinase inhibitor-failed leptomeningeal metastases from Egfr-mutant Nsclc-a prospective, open-label, single-arm phase 1/2 clinical trial (Unique identifier: chictr1800016615). *J Thorac Oncol*. (2021) 16:1359–68. doi: 10.1016/j.jtho.2021.04.018

13. Li H, Lin Y, Yu T, Xie Y, Feng J, Huang M, et al. Treatment response to intrathecal chemotherapy with pemetrexed via an ommaya reservoir in Egfr-mutated leptomeningeal metastases from non-small cell lung cancer: A case report. *Ann palliative Med*. (2020) 9:2341–6. doi: 10.21037/apm-19-521

14. Jackman DM, Cioffredi LA, Jacobs L, Sharmeen F, Morse LK, Lucca J, et al. A phase I trial of high dose gefitinib for patients with leptomeningeal metastases from non-small cell lung cancer. *Oncotarget*. (2015) 6:4527–36. doi: 10.18632/oncotarget.2886

15. Nosaki K, Yamanaka T, Hamada A, Shiraishi Y, Harada T, Himeji D, et al. Erlotinib for non-small cell lung cancer with leptomeningeal metastases: A phase ii study (Logik1101). *oncologist*. (2020) 25:e1869–e78. doi: 10.1634/theoncologist.2020-0640

16. Tamiya A, Tamiya M, Nishihara T, Shiroyama T, Nakao K, Tsuji T, et al. Cerebrospinal fluid penetration rate and efficacy of Afatinib in patients with Egfr mutation-positive non-small cell lung cancer with leptomeningeal carcinomatosis: A multicenter prospective study. *Anticancer Res*. (2017) 37:4177–82. doi: 10.21873/anticanres.11806

17. Patil S, Rathnum KK. Management of leptomeningeal metastases in non-small cell lung cancer. *Indian J Cancer*. (2019) 56:S1–s9. doi: 10.4103/ijc.IJC_74_19

18. Tamura K, Yoshida T, Masuda K, Matsumoto Y, Shinno Y, Okuma Y, et al. Comparison of clinical outcomes of osimertinib and first-generation Egfr-tyrosine kinase inhibitors (Tkis) in tki-untreated Egfr-mutated non-small-cell lung cancer with leptomeningeal metastases. *ESMO Open*. (2023) 8:101594. doi: 10.1016/j.esmoop.2023.101594

19. Park S, Lee MH, Seong M, Kim ST, Kang JH, Cho BC, et al. A phase ii, multicenter, two cohort study of 160 Mg osimertinib in Egfr T790m-positive non-small-cell lung cancer patients with brain metastases or leptomeningeal disease who progressed on prior Egfr Tki therapy. *Ann Oncol*. (2020) 31:1397–404. doi: 10.1016/j.annonc.2020.06.017

20. Chen H, Wang L, Wu Y, Wu Y, Ma S , Yang S, et al. High-dose furmonertinib in patients with Egfr-mutated non-small cell lung cancer and leptomeningeal metastases: a real-world study. *J Clin Oncol*. (2024) 42:16_suppl:8587–7. doi: 10.1200/JCO.2024.42.16_suppl.8587

21. Lu S, Dong X, Jian H, Chen J, Chen G, Sun Y, et al. Central nervous system efficacy of aumolertinib versus gefitinib in patients with untreated, Egfr-mutated, advanced non-small cell lung cancer: data from a randomized phase iii trial (Aeneas). *Cancer Commun (London England)*. (2024) 44:1005–17. doi: 10.1002/cac2.12594

22. Fan Y, Zhu J, He J, Zhou R, Chen J, Han G, et al. 367p high-dose aumolertinib in Egfr-mutant Nsclc patients with brain metastases: primary data from achieve. *Ann Oncol*. (2022) 33:S1585. doi: 10.1016/j.annonc.2022.10.405

23. Zhang X, Zhang M, Wei C, Du X, Zhang G, Niu Y, et al. P1.12a.05 aumolertinib in treatment-naïve Egfr-mutant Nsclc patients with brain metastases : efficacy and safety data from the artistry. *J Thorac Oncol*. (2024) 19:S194. doi: 10.1016/j.jtho.2024.09.351

24. Lee SJ, Lee JI, Nam DH, Ahn YC, Han JH, Sun JM, et al. Leptomeningeal carcinomatosis in non-small-cell lung cancer patients: impact on survival and correlated prognostic factors. *J Thorac Oncol*. (2013) 8:185–91. doi: 10.1097/JTO.0b013e3182773f21

25. Ding H, Xu T, Wang X, Cheng W, Fang S. Aumolertinib combination therapy for EGFR-mutant NSCLC patients with refractory leptomeningeal metastasis following osimertinib failure. *J Thorac Oncol*. (2023) 18:11_suppl:S670–1. doi: 10.1016/j.jtho.2023.09.1287

26. Wu Y, Zhao Y, Wu Y, Chen H, Ma S, Wang Q. A retrospective real-world study of prognostic factors associated with Egfr mutated lung cancer with leptomeningeal metastasis. *Clin Lung Cancer*. (2024) 25:347–53.e1. doi: 10.1016/j.cllc.2024.02.001

27. Lu ZQ, Cai J, Wang X. Osimertinib combined with bevacizumab for leptomeningeal metastasis from Egfr-mutation non-small cell lung cancer: A phase ii single-arm prospective clinical trial. *Thorac Cancer*. (2021) 12:172–80. doi: 10.1111/1759-7714.13738

28. Chamberlain M, Junck L, Brandsma D, Soffietti R, Rudà R, Raizer J, et al. Leptomeningeal metastases: A rano proposal for response criteria. *Neuro-oncology*. (2017) 19:484–92. doi: 10.1093/neuonc/now183

29. Le Rhun E, Devos P, Boulanger T, Smits M, Brandsma D, Rudà R, et al. The rano leptomeningeal metastasis group proposal to assess response to treatment: lack of feasibility and clinical utility and a revised proposal. *Neuro-oncology*. (2019) 21:648–58. doi: 10.1093/neuonc/noz024

30. Sasaki S, Yoshioka Y, Ko R, Katsura Y, Namba Y, Shukuya T, et al. Diagnostic significance of cerebrospinal fluid Egfr mutation analysis for leptomeningeal metastasis in non-small-cell lung cancer patients harboring an active Egfr mutation following gefitinib therapy failure. *Respir Invest*. (2016) 54:14–9. doi: 10.1016/j.resinv.2015.07.001

31. Wang X, Tang X, Gu J, Sun Z. Ceacam6 serves as a biomarker for leptomeningeal metastasis in lung adenocarcinoma. *Cancer Med*. (2023) 12:4521–9. doi: 10.1002/cam4.5221

32. Lin X, Fleisher M, Rosenblum M, Lin O, Boire A, Briggs S, et al. Cerebrospinal fluid circulating tumor cells: A novel tool to diagnose leptomeningeal metastases from epithelial tumors. *Neuro-oncology*. (2017) 19:1248–54. doi: 10.1093/neuonc/nox066

33. Ma C, Yang X. Detection of circulating tumor DNA from non-small cell lung cancer brain metastasis in cerebrospinal fluid samples. *Thorac Cancer*. (2020) 11:588–93. doi: 10.1111/1759-7714.13300

34. Nevel KS, DiStefano N, Lin X, Skakodub A, Ogilvie SQ, Reiner AS, et al. A retrospective, quantitative assessment of disease burden in patients with leptomeningeal metastases from non-small-cell lung cancer. *Neuro-oncology*. (2020) 22:675–83. doi: 10.1093/neuonc/noz208

35. Naidoo J, Schreck KC, Fu W, Hu C, Carvajal-Gonzalez A, Connolly RM, et al. Pembrolizumab for patients with leptomeningeal metastasis from solid tumors: efficacy, safety, and cerebrospinal fluid biomarkers. *J Immunother Cancer*. (2021) 9(8):e002473. doi: 10.1136/jitc-2021-002473

36. Park JH, Kim YJ, Lee JO, Lee KW, Kim JH, Bang SM, et al. Clinical outcomes of leptomeningeal metastasis in patients with non-small cell lung cancer in the modern chemotherapy era. *Lung Cancer (Amsterdam Netherlands)*. (2012) 76:387–92. doi: 10.1016/j.lungcan.2011.11.022

Frontiers in Oncology

Advances knowledge of carcinogenesis and tumor progression for better treatment and management

The third most-cited oncology journal, which highlights research in carcinogenesis and tumor progression, bridging the gap between basic research and applications to imrpove diagnosis, therapeutics and management strategies.

Discover the latest Research Topics

See more →

Frontiers

Avenue du Tribunal-Fédéral 34
1005 Lausanne, Switzerland
frontiersin.org

Contact us

+41 (0)21 510 17 00
frontiersin.org/about/contact